

# Polymers of Intrinsic Microporosity for Heterogeneous Base Catalysis



---

Natasha Hawkins

School of Chemistry

Swansea University

---

A thesis submitted to Swansea University in fulfilment of the requirements for the  
Degree of Doctor of Philosophy

2022

Supervisor: Dr Mariolino Carta

## Abstract

The climate crisis is the greatest challenge facing this generation, and in order to meet ambitious targets set by global leaders, great advancements in sustainable technologies are needed. This thesis work aimed to develop a new series of polymers of intrinsic microporosity (PIMs) for catalytic applications. PIMs have been of great interest within materials chemistry since their development in the early 2000s, they are purely organic materials that have a lower environmental impact than competing materials and can be synthesised under relatively mild conditions.

More specifically, Tröger's' base (TB) PIMs are materials that, along with the typical high porosity of PIMs, possess two bridgehead nitrogens that can be used to tune the polarity of the final material. In this work, we have synthesised a series of novel TB-PIMs which can act as basic catalysts because of the basicity of the bridgehead nitrogens. We have demonstrated that by increasing the degree of flexibility in the polymers, we can induce a "swelling" effect that facilitates the accessibility of the catalytic sites and allows the use of larger substrates, thus increasing the catalytic performance. We have also shown that new functionalities can very easily be incorporated into PIM structures, meaning that these materials can be tailor made for specific applications. We have demonstrated that by increasing the number of basic nitrogen sites in a repeated unit, we can further increase the rate of a reaction. Finally, we have shown that post-functionalised PIMs can successfully catalyse a range of environmentally important reactions. For instance, quaternised TB polymers were successfully used to catalyse the cycloaddition of CO<sub>2</sub> into epoxides, to form cyclic carbonates that can be employed as sustainable solvents, and sulfonated PIMs have been successful in the transesterification of oils for biodiesel synthesis.

We believe that this work lays a foundation for future research into PIM catalysts, as they are a versatile, facile, robust, and efficient catalytic technology.

## Declarations

This work has not previously been accepted in substance for any degree and is not being concurrently submitted in candidature for any degree.

Signed

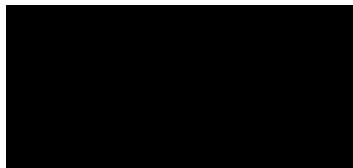


Date

19/11/2022

This thesis is the result of my own investigations, except where otherwise stated. Other sources are acknowledged by footnotes giving explicit references. A bibliography is appended.

Signed



Date

19/11/2022

I hereby give consent for my thesis, if accepted, to be available for electronic sharing

Signed

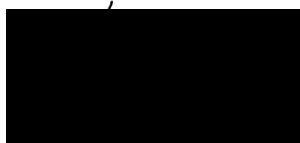


Date

19/11/2022

The University's ethical procedures have been followed and, where appropriate, that ethical approval has been granted.

Signed



Date

19/11/2022

# Table of Contents

Abstract .....	i
Declarations .....	ii
Acknowledgements .....	vii
Abbreviations.....	viii
Chapter 1 – Introduction.....	1
Measuring the Catalytic Ability .....	3
Porous Materials in Catalysis .....	5
Crystalline Materials .....	6
Zeolites .....	6
Metal-Organic Frameworks .....	10
Amorphous Materials.....	16
Hyper Cross-Linked Polymers.....	17
Conjugated Microporous Polymers .....	19
Covalent Triazine Frameworks.....	21
Porous Aromatic Frameworks .....	26
Polymers of Intrinsic Microporosity.....	28
Aims of the project.....	33
Chapter 2 - Novel PIM Copolymers for Catalysis .....	34
Introduction .....	34
Synthesis of monomers .....	35
Results and Discussion .....	40

Confirmation of Copolymerisation .....	40
BET Surface Areas of Polymers.....	42
Knoevenagel Reaction and Catalytic Testing .....	44
Conclusion .....	48
Chapter 3 - Increasing Flexibility in PIM-Catalysts .....	50
Introduction .....	50
Synthesis.....	50
BET Surface Areas and Characterisation.....	54
Results and Discussion .....	55
Addition of a solvent.....	57
Knoevenagel reaction with larger benzaldehydes .....	58
Knoevenagel reaction with even larger benzaldehydes.....	63
Recyclability Tests .....	65
Computational Study.....	66
Conclusion .....	67
Chapter 4 - Nitrogen-rich PIM catalysts.....	69
Introduction .....	69
Synthesis.....	69
BET Surface Areas and Characterisation.....	74
Results and Discussion .....	75
Catalytic tests .....	75
Changing the methylene species .....	78
pH and the Henry Reaction.....	84

Conclusion .....	88
Chapter 5 - CO <sub>2</sub> Utilisation Reactions .....	89
Introduction .....	89
Initial Experiments .....	89
Synthesis.....	92
TGA of Quaternised Polymers .....	93
BET surface areas of Quaternised Polymers .....	94
Catalysis with quaternised TB-PIMs .....	95
Conclusion .....	97
Chapter 6 - Biodiesel Reactions.....	98
Introduction .....	98
Synthesis.....	99
Results and Discussion .....	101
Esterification of Acids.....	101
Transesterification of Esters with PIMs .....	104
Transesterification of Oils.....	105
Conclusion .....	108
Chapter 7 – Future Work and Conclusions.....	110
Chapter 8 – Experimental Section.....	114
Monomer Synthesis.....	115
Polymer Synthesis.....	129
General Procedure A of Ladder Homopolymer Synthesis .....	129
General Procedure B of Network Homopolymer Synthesis .....	130

General Procedure C of Copolymer Synthesis.....	130
Chapter 9 – References.....	148

## Acknowledgements

First and foremost, a huge thank you to my supervisor Lino. I am very grateful for giving me the opportunity to work with you, and especially grateful for your guidance, patience, support, and friendship throughout.

Next, thank you to all members of the Carta group past and present – Rhodri, Haoli, Yue and Susana, as well as all the Swansea Chemistry research family.

Two particular mentions to two excellent women: Kadie, my gal, thank you for your love and support, for always having a shoulder to cry on, and for dropping anything at the drop of a hat for a coffee and a gossip – it has meant the world to me to have met you! And Ariana, who has not only academically helped tremendously throughout my PhD but has also been such a supportive friend through what have been a tough few years – I will be forever grateful!

Thank you to our collaborators, particularly to Elena, Alessio and Chiara at ITM CNR for your work on modelling our flexible polymers.

A huge thank you to my friends, especially to Gregor, thank you for all the wise words, love, and support – I hope I get a London 2012 breakfast set as a graduation present! And to Amy, Della, and Rachel – it has been King of the Mountense, but hopefully it will all be fishing rod and chicken from now on – see you in the hot tub, you bring the quadvods and I'll bring the hobnobs.

A big thank you to my family: To my mum, my biggest role model, the strongest woman I know. It is hard to put it into words, but it is all because of you. To my grandparents, you are inspirational, and I am so lucky to have you! To Mark and Iain, for being there when they didn't have to be.

Finally, to Steven, for moving for me, for supporting me, for believing in me when I did not believe in myself, for doing more than his fair share so that I could get through, for everything. It's a cliché, but I could not have done it without you. I love you.

Dedicated to Richard Pele Edwards – Who would not have cared. We miss you every day.

Thank you to EPSRC for funding this research.





## Abbreviations

**BET** – Brunauer–Emmett–Teller

**CMP** – Conjugated microporous polymers

**CTF** – Covalent triazine frameworks

**DABMA** – Diaminobenzomethanoanthracene

**DAT** – Diaminotriptycene

**DCM** – Dichloromethane

**DMF** – Dimethylformamide

**DMM** – Dimethoxymethane

**EA** – Ethanoanthracene

**FAME** – Fatty acid methyl esters

**HCP** – Hyper cross-linked polymers

**IR** – Infrared

**MOF** – Metal-Organic Framework

**MP** – Melting point

**NLDFT** – Non-local density functional theory

**NMR** – Nuclear Magnetic Resonance

**PAF** – Porous aromatic frameworks

**PIM** – Polymers of intrinsic microporosity

**POP** – Porous Organic Polymer

**TAPA** – Tri(aminophenyl)amine

**TAPAT** – Tri(aminophenyl)aminotriazine

**TAPB** – Triaminophenylbenzene

**TAPBext** – Triamino(biphenyl)benzene

**TAPT** – Tri(aminophenyl)triazine

**TAT** – Triaminotriptycene

**TB** – Tröger's Base

**TBAB** – Tetrabutylammonium bromide

**TB-NH<sub>2</sub>** – 4,10-dimethyl-6H,12H-5,11-methanodibenzo[b,f][1,5]diazocine-2,8-diamine

**TB-NO<sub>2</sub>** – 4,10-dimethyl-2,8-dinitro-6H,12H-5,11-methanodibenzo[b,f][1,5] diazocine (TB-NO<sub>2</sub>)

**TBPB** – 1,3,5-tris(4-bromophenyl)benzene

**TFA** – Trifluoroacetic acid

**TFAA** – Trifluoroacetic anhydride

**TGA** – Thermogravimetric analysis

**THF** – Tetrahydrofuran

**TNPAT** – Tri(nitrophenyl)aminobenzene

**TNPB** – Tris(nitrophenyl)benzene

**TOF** – Turnover Frequency

**Tol** – Tolidine

**TON** – Turnover Number

**Trip** – Triptycene

# Chapter 1 – Introduction

With an ever-increasing population and global warming at an all-time high,<sup>1</sup> there has never been a more important time for environmental and sustainable chemistry research. In 1998 *Anastas and Warner* published 'The 12 Principles of Green Chemistry' - a list of research priorities and practical changes that synthetic chemists should aim to make in order to reduce environmental damage (**Figure 1.1a**).<sup>2, 3</sup> This list includes Catalysis, a process that has a crucial importance on a global scale. A catalyst can be described as a species that increases the rate of a reaction, which itself is not used up in the overall synthesis.<sup>4</sup> Catalysts achieve this by providing an alternative reaction pathway that has a lower activation energy (**Figure 1.1b**).<sup>5</sup>

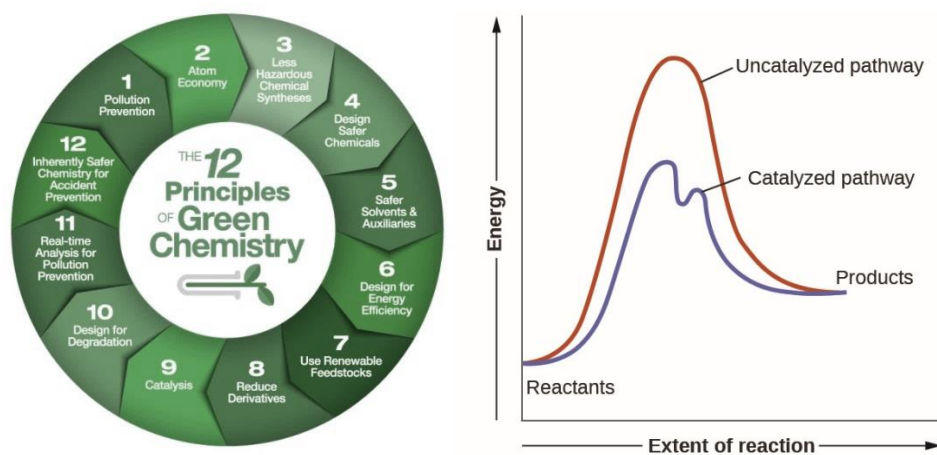


**Figure 1.1:** a) 12 Principles of Green Chemistry<sup>3</sup>; b) Different energy profiles with and without a catalyst<sup>5</sup>

Catalysts were first studied in chemistry by Elizabeth Fulhame in the late 18<sup>th</sup> century, where she considered their use in oxidation and reduction reactions,<sup>6</sup> though catalysis has existed in nature for millions of years most commonly in the form of enzymes. Since then, they have become a major area of research in the field of chemistry. Catalysts allow otherwise kinetically unfavourable reactions to take place, as well as allowing reactions to happen at lower temperatures and pressures, therefore reducing the energy usage of a reaction. In these two

respects it is clear how environmentally important catalysts are, particularly in an industrial setting. It is estimated that around 90% of chemical processes use catalysts.<sup>7</sup> One key example is the production of ammonia, which is responsible for around 2% of energy consumption globally,<sup>8</sup> largely due to its use as a feedstock for fertilizers in the food industry. Early methods of ammonia production were complex, slow, and gave poor yields.<sup>9</sup> But in the early 20<sup>th</sup> Century Haber and Bosch developed a much simpler method where efficiency was hugely improved due to a metal catalyst.<sup>10</sup> Without this, the energy output would be far greater. There are many examples of desirable reactions that are possible with the right catalyst (see later).

Catalysts can be divided into two main types: homogeneous and heterogeneous, and each have their benefits and drawbacks.<sup>11, 12</sup> A homogeneous catalyst is one which exists in the same phase as the reactants. As the catalyst has high diffusivity in the reaction media, all sites are available for reaction. This increases the selectivity and performance of these catalysts.<sup>13</sup> The reaction mechanism of homogeneous catalysts can be monitored and studied in detail, which makes modification easier, leading to highly selective materials.<sup>14</sup> On the other hand, they are typically sensitive to high temperatures and pressures, limiting their use in organic reactions. They are also extremely difficult to separate once a reaction is complete, and this typically leads to high costs and large amounts of waste materials and solvents needed for their purification and recycling. Heterogeneous catalysts exist in a different phase to the reaction media, making removal and recycling much easier, cheaper, and more sustainable. Their typical stability in harsh conditions makes them desirable in a broad range of reactions, however traditional heterogeneous catalysts are typically harder to modify than their homogeneous counterpart. In addition, they often perform less well than homogeneous ones due to the relative lack of accessible catalytic sites, affecting the selectivity and activity.

It is generally accepted that catalysis occurs via one of two main pathways.<sup>13</sup> A catalyst can take part in the reaction and later be reformed, therefore not appearing in the overall chemical equation (**Figure 1.2a**). This pathway is typical of homogeneous catalysts.

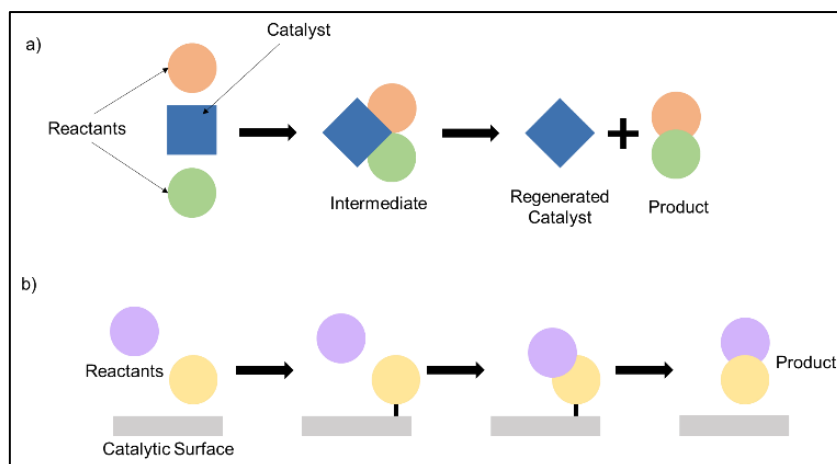


**Figure 1.2:** Two typical reaction pathways for catalysis

The second is typical of heterogeneous catalysis, which can provide a surface for the reactants to adsorb onto, weakening the bonds in the reactant molecule and making it easier for other species to react with it (**Figure 1.2b**).

Heterogeneous catalysts are generally preferred, especially in industry, because of the ease of removal and the lower costs associated with them. It is clear though that their performance (activity and selectivity) must be improved, and this corresponds to one of the major research focuses within the field.

## Measuring the Catalytic Ability

There are a number of factors that are important in determining a good catalyst, but one of the most important, especially from an industrial point of view, is the catalytic activity.<sup>12</sup> This is defined as the rate of consumption of a reactant, not to be confused with selectivity, which is a percentage of the desired product over all products. Heterogeneous catalysts typically have good activities, due to the large number of available sites, but low selectivities. Homogeneous catalysts, on the other hand, have high selectivities, but typically only moderate activity.<sup>15</sup> Activity is measured by monitoring a reaction periodically, most commonly via NMR spectroscopy, though sometimes other analytical techniques may be more appropriate such as gas chromatography. Selectivity is calculated after the reaction is completed and final products have been separated. It is also important to quote the reaction conditions under

which these figures are calculated, as well as the mass/molarity of catalyst used, in order to make these results reproducible and comparable.

Another key measure of a successful catalyst is its reusability. Over time catalysts lose their activity for a number of reasons: Active sites can become blocked over time, catalytic moieties can sinter (see later), or the sites can be poisoned. A long-lasting catalyst is essential for many industrial processes, as this keeps costs low but also allows reactions to run back-to-back. Turnover number (TON) is a measure of catalytic activity that factors in the longevity of the material. TON is a unitless measure of the number of moles of substrate that can be transformed by a number of moles of catalyst until it has been completely deactivated.<sup>16</sup>

$$TON = \frac{n^{\circ} \text{ moles reactant}}{n^{\circ} \text{ moles catalyst}}$$

**Equation 1.1:** Turnover Number

In simpler terms, TON is a measure of the number of cycles a catalyst can survive. Turnover frequency (TOF) gives a measure of how quickly a catalyst can perform a cycle, and can be calculated using the TON.<sup>17</sup>

$$TOF = \frac{TON}{\text{time taken}}$$

**Equation 1.2:** Turnover Frequency ( $s^{-1}$ )

Whilst these are both useful metrics, TON (and therefore TOF) are hard to calculate for a heterogeneous catalyst as it is very difficult to accurately distinguish the number of active sites per mole.<sup>18</sup> As such, they are often not included in the literature for heterogeneous catalysis. In general, a good heterogeneous catalyst will allow molecules to adsorb strongly enough that the molecule is weakened, but not so strongly that it prevents reaction with other molecules.<sup>13</sup> This is particularly true of amorphous materials, where the number of catalytic sites per repeating unit can be difficult to define.

Common catalytic sites are transition metal centres, as these are good for coordination chemistry, and so therefore have the space and valency to accommodate the reactants.<sup>19</sup> It is

also common for catalytic moieties to be contained in a support frame made of a porous material.

## Porous Materials in Catalysis

Porous materials are solids containing penetrable channels and cavities, which can be exploited for a variety of applications.<sup>20</sup> Porous materials can be divided into three different types depending on pore size: microporous (<2 nm diameter), mesoporous (2-50 nm diameter) and macroporous (>50 nm diameter).<sup>20</sup> Altogether, these pores make up the internal free volume (IFV) of the material, which can be determined using isothermal gas adsorption. This works by placing the sample material in a closed space where it is heated and degassed.<sup>21</sup> The material is then exposed to a known quantity of gas (usually N<sub>2</sub>) starting from a high vacuum, initially calculated by the instrument (P), monitoring the increase of the pressure needed to adsorb any extra amount of N<sub>2</sub> until we reach atmospheric pressure (P<sub>0</sub>). In this way we will be able to see how much gas is eventually adsorbed onto the surface. The higher the adsorption at low partial pressure (i.e., without the need of increasing the pressure), the higher the surface area.

Catalytic species such as transition metal cations often use porous materials as supports.<sup>13</sup> Over time catalysts lose activity, often because of sintering – whereby catalyst particles merge together, reducing the number of available active sites. A porous support allows the catalytic material to spread throughout a network, which reduces the risk of sintering, and therefore can increase the efficiency and the longevity of the catalyst. Not only do support materials maintain the integrity of the catalysts, but they force the reactions to take place in confined pore spaces, which increases the frequency of collisions between reagents and catalytic sites, meaning that the overall activity increases.<sup>22</sup>

Of growing interest in the field of catalysis is the production of porous materials that have catalytic sites merged into their backbone, as opposed to only hosting/embedding catalytic moieties in their structures.

## Crystalline Materials

### Zeolites

Having been discovered in the mid-18<sup>th</sup> century, zeolites are one of the most extensively researched species in the field of porous materials.<sup>23</sup> Although they occur naturally, they can also be synthesised successfully and to date there are over 200 known structures.<sup>24</sup> Zeolites are crystalline aluminosilicate materials, consisting of  $\text{SiO}_4$  and  $\text{AlO}_4$  tetrahedra connected by oxygen bridges. These negatively charged frameworks have open pores and channels, which host cationic species such as metal ions.<sup>25</sup> Like all porous materials, the accessible space in zeolites has been exploited for numerous applications including gas separation, gas storage, ion exchange, and of course catalysis.<sup>26, 27</sup>

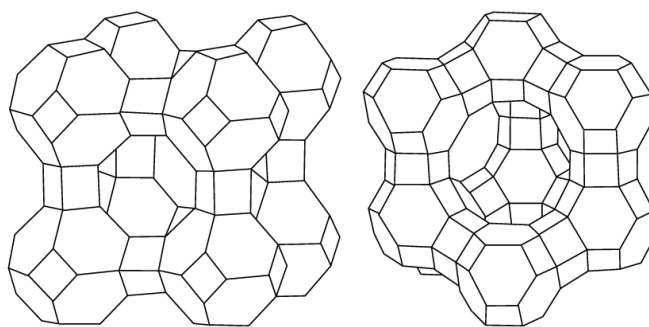


**Figure 1.3:** Framework structure of Zeolite X and Y respectively

Zeolites have been widely used as catalysts in industry for several decades.<sup>27-31</sup> In 1962 synthetic zeolite X and zeolite Y (**Figure 1.3**) were implemented in industrial fluid catalytic cracking (FCC), processing hydrocarbons into useful compounds for fuels.<sup>32, 33</sup> These new catalysts were found to be more active than their competitors, and they helped increase the production of gasoline – one of the most useful fuels worldwide.<sup>34</sup> This selectivity towards certain compounds can be associated with the uniform nature of the zeolite cavities. This is an example of shape selective catalysis. ZSM-20 and ITQ-21 have similar cavity sizes to zeolite Y, but have a selectivity towards diesel production because of the more open structure of the framework.<sup>35</sup> The stability of zeolite Y in hydrothermal conditions was shown to be improved by tuning the acid site density (Si/Al ratio), showing the adaptability of these

materials.<sup>33</sup> All of the aforementioned zeolites can also be described as acid catalysts – that is the catalytic activity of these materials is due to the acidic sites in the structures. Within zeolites there are two types of acid sites: Brønsted acid sites (H atoms coordinated to bridging oxygens) and Lewis acid sites (Al in the framework and cationic species in the pores). It is believed that the Brønsted acid sites are usually responsible for the catalytic activity in zeolites,<sup>29, 36</sup> though it is also thought that the Lewis acid sites may have a secondary influence.<sup>34, 37</sup>

Following the success of zeolites X and Y, there have been many more examples of zeolites being used as acid catalysts in industrial processes.<sup>29-31</sup>

### **Acid Catalysis with zeolites**

Zeolite ZSM-5 was discovered in the 1970s which acts as a shape-selective acidic catalyst for gas-phase alkylation reactions,<sup>38</sup> showing particular efficiency in ethylbenzene processing.<sup>39</sup> Zeolite MCM-22 was also selectively produced ethylbenzene from benzene and ethylene, in this case decreasing the molar ratio of benzene to ethylene, and therefore lowering the E-factor of the reaction.<sup>38</sup>

Zeolites have been used in Friedel-Crafts acylation reactions, an important set of reactions in fine industrial chemistry.<sup>40, 41</sup> Historically these reactions have been catalysed by strong Lewis acid catalysts.<sup>42</sup> Zeolite beta and zeolite Y have a high concentration of acid sites within the crystalline channels, improving activity whilst also giving some shape selectivity to the final products. These catalysts were shown to be highly selective when reacting xylenes with benzoyl chloride.<sup>40</sup> Both zeolites beta and Y have also been successful in the reaction between anisole and veratrole, though the catalysts are readily deactivated.<sup>43</sup>

Oligomerization of alkenes is another key type of reactions in the petrochemical industry, specifically in oil refinery. For this purpose, zeolite HZSM-5 has been studied as a catalyst for the oligomerization of many alkenes including ethylene and propene.<sup>44</sup> Interestingly, it was found that the nature of the oligomers formed depended on where in the



zeolitic framework the reactions take place. Highly branched oligomers are preferentially formed via reactions with acidic sites on the edges of the frameworks, whereas linear oligomers are formed favourably in the zeolite channels. This is another example of shape selectivity - by deactivating acidic sites either on the edges or in the framework cavities, HZSM-5 can be tuned towards products with specific geometries.<sup>45</sup> Inactivation of catalytic sites during oligomerisation reactions represents an issue, as the large product molecules can block the channels. Therefore for these reactions it is essential for reactions to take place under milder conditions, and zeolites with larger pores are preferred.<sup>46</sup>

Zeolite NaY has been studied as catalysts for ring opening of epoxides, and found to give high yields and 100% selectivity towards the  $\beta$ -amino alcohol.<sup>47</sup> It was found that its high performance was due to both the high aluminium content in the framework and the high surface area. The same reaction can also be achieved in just 3 minutes under microwave conditions.<sup>48</sup> Zeolite beta was also found to be an effective catalyst for epoxide hydration when metal ions were incorporated into the framework. The catalytic activity in this case correlated to the Lewis acid strength of the added metal ( $\text{Sn}^{4+} > \text{Zr}^{4+} > \text{Ti}^{4+}$ ).<sup>49</sup>

### **Hierarchical zeolites**

We have seen the impact that zeolites have had, however there are also drawbacks. The majority of the industrial processes that use zeolitic acid catalysts take place with reagents in the gas phase.<sup>29</sup> Zeolites are very good for gas phase reactions because of their high thermal and chemical stability, and can withstand the flow of gas through the pores without limiting mass transport, and the reagents can diffuse well.<sup>36, 50</sup> However for liquid phase reactions the channels are too small for steady mass transport, and therefore they do not allow efficient diffusion onto the active sites.<sup>50</sup> It is also of note that catalytic activity is proportional to the number of active sites, but too many active sites can block channels and limit diffusion of reagents through the materials. In response to this, research has looked into synthesising hierarchical zeolites, or zeolites that contain both micropores and mesopores.<sup>50</sup>

An example of this is using hierarchical zeolites as catalysts for the conversion of methanol to hydrocarbons.<sup>30</sup> Although it has been found that H-ZSM-5 can successfully convert methanol to certain hydrocarbons with relatively little loss of activity due to coke formation,<sup>51</sup> it has been found that zeolites with mesopores perform better in this type of reaction.<sup>30, 51, 52</sup> In addition, there is a positive correlation between mesoporosity and catalytic lifetime when studying mesoporosity in MFI zeolites.<sup>53</sup>

The catalytic conversion of biomass to fuels over zeolites has been suggested due to the similarity of this reaction to crude oil refining.<sup>54</sup> However, as this reaction takes place in condensed phase it is not favourable for standard zeolites.<sup>54</sup> Moreover, the stability of the zeolites in these conditions is low. Mesoporous zeolites are typically more stable than generic zeolites,<sup>55, 56</sup> and as previously mentioned they are better equipped to cope with liquid phase mass transport.<sup>57, 58</sup> H-ZSM-5 shows selectivity towards the production of aromatics from biomass.<sup>59</sup> Also, there is positive correlation between pore size and aromatic yield.<sup>60</sup> A range of hierarchical faujasite zeolites have shown promise for future work, however there are still issues surrounding selectivity and diffusion.<sup>61</sup> In addition, there are some issues surrounding the hydrothermal stability of mesoporous zeolites, which is a major factor in an industrial setting.<sup>62, 63</sup>

An increasingly important reaction in chemistry is the utilisation of CO<sub>2</sub>, with one of the most common examples in the literature being the cycloaddition of CO<sub>2</sub> into epoxides.<sup>64, 65</sup> Both acidic and basic sites are necessary in this reaction, as the CO<sub>2</sub>, being a Lewis acid, is initially activated at the basic sites forming a carbamate, while the epoxides are adsorbed on the acid sites. These activated species can then readily react with one another.<sup>66</sup> Although zeolites have an abundance of acidic sites, the only basic sites are the oxygen bridges in the framework,<sup>36</sup> which generally limits their use in base catalysis. There are examples of zeolites modified with alkali metals which increased the basicity and therefore the catalytic activity of these materials.<sup>67</sup> Other cases show that the addition of ammonium salts to the channels of MFI zeolites increased the activity towards CO<sub>2</sub> cycloaddition.<sup>68</sup>

## Base Catalysis with zeolites

Zeolites are seldom used as base catalysts due to the relative lack of basic sites, and the cheap alternative base catalysts available, such as NaOH and KOH.<sup>29</sup> Basic groups, such as amines, can be added pendant to the zeolite frameworks to improve the basicity of the materials, but the addition of groups limits mass transport.<sup>36</sup> Despite these limitations, there are some examples of zeolites in base catalysis. Zeolites X and Y containing alkali metals have been shown to be active in the Knoevenagel condensation reaction.<sup>69</sup> Similarly, Zeolite CsX shows high basicity and good performance, as well as Zeolite Zn-beta.<sup>70</sup> Further studies have looked into base catalysis in a wide array of reactions, but they have not performed well, at least in comparison to more commercially viable options.<sup>71, 72</sup>

## Metal-Organic Frameworks

Metal-organic frameworks (MOFs) are a species of 3D porous materials consisting of inorganic templates connected through organic linkers to form large crystalline frameworks (**Figure 1.4**).<sup>73, 74</sup> The inorganic parts can simply be composed of metal ions, though more recently, MOFs have been built using secondary building units (SBUs) which can be metal clusters or metal complexes.<sup>73</sup>

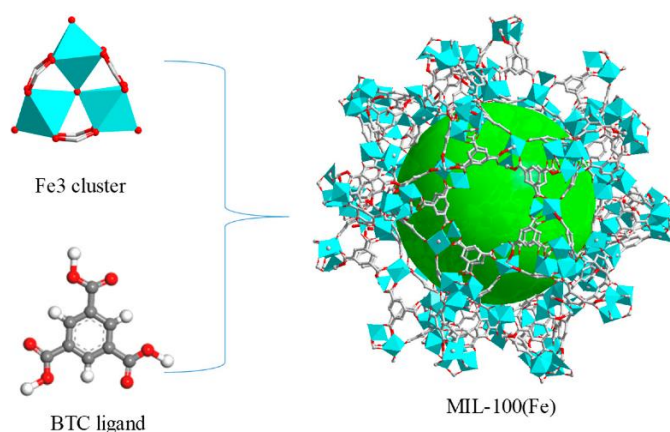


**Figure 1.4:** Structure of the MOF MIL-100(Fe)

The first MOFs were reported in the late 1990s as an extension of the preparation of synthetic zeolites.<sup>75</sup> Where zeolites have limited permutations – less than 300 have been successfully synthesised despite numerous simulations,<sup>76</sup> the number of MOFs is vast, with thousands of structures already registered in the Cambridge Crystallographic Data Centre. The possibility of using different combinations of organic and inorganic linkers makes it possible to fine tune the materials for specific needs, causing the rapid increase of research interest into the preparation of new MOFs for a number of different applications. For example, in the case of catalysis, MOFs can be designed to contain pores large enough to aide mass transport, but small enough to induce a confinement effect.<sup>77</sup> In addition, several MOFs have been shown to have incredibly high surface areas, many exceeding  $6000 \text{ m}^2 \text{ g}^{-1}$ .<sup>78</sup> This high porosity helps with diffusion of catalytic sites and can aid mass transport through the materials.<sup>79</sup> There are, however, a number of issues with MOFs for catalytic applications. Typically, they have low structural, thermal, and hydrothermal stability, vastly limiting their potential in catalysis.<sup>80</sup> Also, due to the nature of many MOF structures, the catalytic metal ions are often surrounded by a coordination centre which prevents the adsorption of substrates.<sup>80</sup> Despite these issues, there has been much research into MOFs for catalysis. Herein we discuss some key examples in the field.

### **Acid Catalysis with MOFs**

Metal-Organic Frameworks have been of particular interest as acid catalysts, in particular as Lewis acids, with their acidity stemming from the metal centres.<sup>29, 79, 81-85</sup> Brønsted acidity can also be introduced with the addition of functional groups to the framework, such as carboxylic or sulfonic acids,<sup>80</sup> though this requires the preparation of a very stable platform.<sup>86</sup> This leads to a limited number of examples of Brønsted acid MOF catalysts compared to their Lewis acid counterparts. As previously mentioned, MOFs typically show low stability under harsh conditions (e.g., high temperatures and pressures) and in aqueous conditions, due to the easy hydrolysis of the metal cluster. To avoid this problem, the use of tri- and tetra-valent metal centred MOFs is normally preferred, as they are known to be more stable in harsh

conditions and, therefore, the vast majority of MOFs for catalysis present these structure desig.<sup>79, 86</sup>

The Materials Institut Lavoisier (MILs) represent a series of MOFs that all feature trivalent metal centres, and have been extensively studied for catalysis.<sup>87</sup> For instance, MIL-100(Fe) (**Figure 1.4**) was investigated for the catalysis of *p*-xylene acylation with benzoyl chloride,<sup>40</sup> and it was reported having a fast conversion rate (100% in 15 minutes), most likely due to the numerous unsaturated iron sites and the relatively wide pores (0.47 × 0.55 nm) By removing the coordinated water molecules from terminal sites of MIL-100(Fe), catalytically active Lewis acid sites can be created that are useful for reactions such as Friedel-Crafts,<sup>88</sup> Claisen-Schmidt condensations,<sup>89</sup> and ring-opening of epoxides.<sup>90</sup> MIL-100(Sc) proved to be an effective catalyst for reactions involving C-C and C=N bond formations, such as Michael additions and imine formations.<sup>91</sup> High conversion and recyclability were also reported for these materials. For instance, MIL-100 (Al, Fe, and Cr) were shown to selectively catalyse the rearrangement of  $\alpha$ -pinene oxide (PO) to campholenic aldehyde (CA), and all three showed PO conversion over 95%, and CA selectivity ranging between 51 and 61%, with MIL-100(Al) performing best. MIL-101(Cr) can be functionalised with sulfonic acid groups to provide Brønsted acid sites for epoxide ring opening reactions. MIL-101(Cr)-SO<sub>3</sub>H, for instance, proved to catalyse the ring opening of styrene oxides with methanol at the (sulfonic acid groups) with 100% selectivity and conversion.<sup>92</sup> When functionalised with basic *n*-Pr<sub>4</sub>NBr, MIL-101(Fe and Cr) can both catalyse CO<sub>2</sub> cycloaddition,<sup>93, 94</sup> which, as previously mentioned, requires both acidic and basic sites in close proximity for the catalyst to be effective. MIL-101(Cr) and MIL-53(Cr) functionalised with sulfonic acid groups, instead, showed good catalytic behaviour for the esterification of *n*-butanol with acetic acid, with MIL-53(Cr) showing a turnover frequency (TOF) of 0.72 min<sup>-1</sup>.<sup>95</sup>

Other MOF types have also seen success in CO<sub>2</sub> cycloaddition. Cu<sub>4</sub>[(C<sub>57</sub>H<sub>32</sub>N<sub>12</sub>)(COO)<sub>8</sub>] demonstrated a high CO<sub>2</sub> uptake due to the presence of the nitrogen containing triazole groups, which assists in high yields for a number of small epoxides such as 2-

methyloxirane (96%), 2-ethyloxirane (83%), 2-(chloromethyl)oxirane (85%), and 2-(bromomethyl)oxirane (88%).<sup>96</sup> MIL-101(Cr) also proved to be an efficient catalyst in cyanosilylation of benzaldehyde,<sup>97</sup> and the Baeyer condensation of benzaldehyde.<sup>98</sup> Several  $\text{Cu}^{2+}$  trinuclear MOFs, with a  $\text{Cu}_3(\mu_3\text{-OH})(\mu\text{-pyrazole})$  SBU, have been studied as catalysts in the peroxidative oxidation of cycloalkanes.<sup>83</sup> Preparation of the MOF in ethanol and water gave slightly different structures both with good catalytic activity and stability.  $[\text{Cu}_3(\mu_3\text{-OH})(\mu\text{-pz})_3(\text{EtCOO})_2(\text{EtOH})]$  showed top yields of 32%, and a top TON of 43, and  $[\text{Cu}_3(\mu_3\text{-OH})(\mu\text{-pz})_3(\text{EtCOO})_2(\text{H}_2\text{O})]$  showed a slightly higher TON of 44, both competitive with other catalysts for this reaction type.

In terms of tetravalent metal centred MOFs, zirconium-based frameworks have been of particular interest in catalysis due to their relatively high chemical stability. UiO-66 has been studied in a variety of reactions including aldol condensations.<sup>99</sup> However, the catalytic activity can be increased by introducing defects into the materials, which expands the number of open Lewis acid sites in the materials.<sup>100</sup>

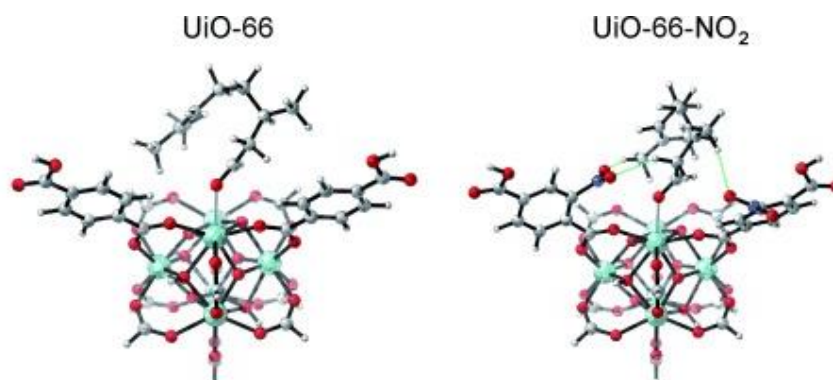


**Figure 1.5:** UiO-66 and its functionalised counterpart

Vermoortele *et al.* also successfully boosted the activity of UiO-66 through functionalisation, by introducing  $\text{NO}_2$  substituted BDC ligands (**Figure 1.5**), leading to an improved rate in the cyclization of citronellal to isopulegol.<sup>101</sup> Another example of a Zr-MOF for catalysis is provided by the preparation of PCN-223(Fe), which includes Fe(III)-porphyrin centres. The addition of Lewis acid sites in its structure helped to catalyse the hetero-Diels Alder reaction between aldehydes and dienes.<sup>102</sup>

Another MOF that has frequently been tested for acid catalysis is  $\text{Cu}_3(\text{btc})_2$ , also known as HKUST-1, containing  $\text{Cu}^{2+}$  ions connected through organic BTC (benzene-1,3,5-tricarboxylic acid) ligands with water molecules coordinated to the metal centres.<sup>103</sup> By removing the water ligands, the Cu centres become accessible Lewis acidic sites. HKUST-1 proved to be selective for a number of reactions, for example to catalyse the acylation of *p*-xylene with benzoyl chloride.<sup>40</sup> Although the conversion rate was low (37%), it still performed better than zeolites beta and Y for this reaction. Other reactions successfully catalysed by HKUST-1 include benzaldehyde cyanosilylation,<sup>104</sup>  $\text{CO}_2$  conversion,<sup>105</sup> and citronellal cyclization.<sup>106</sup> It should be noted that strongly coordinating solvents, such as THF, cannot be used in reactions with HKUST-1 as a catalyst, as they can bond to the Cu sites and therefore block reagent adsorption. It is also worth reporting that HKUST-1 does not generally display high reusability, as the activity deteriorated over time in several of the reported reactions.

MOFs typically have a very large amount of acid sites per gram. For example, Ni-MOF-74, containing unsaturated nickel ions on the nodes of the framework, can be efficiently used to catalyse propene oligomerisation.<sup>107</sup> Compared to other materials, the Ni sites in the MOF proved to be less active, but due to the high number of sites, this material was found to be competitive with other catalysts.

MOFs have also been considered for the cycloaddition of  $\text{CO}_2$  to epoxides. Zeolitic-imidazolate frameworks (ZIFs) have shown promise in these reactions due to the presence of both acidic and basic sites. ZIFs are a subspecies of MOFs with tetrahedrally coordinated metal centres connected by imidazolate linkers. Their name derives from the similar topologies to zeolites, due to the bond angles about the metal centres being similar to the Si-O-Si bonds in zeolites. ZIF-8 has shown to catalyse the conversion of epichlorohydrin to chloropropylene carbonate with a 44% yield and a 52% selectivity for the cyclic product.<sup>108</sup> The addition of ethylene diamine groups to ZIF-8 increased the number of basic sites and therefore the adsorption of  $\text{CO}_2$ , leading to an increase in both the selectivity and the yield to 73%.

Despite the versatility of the MOF synthesis, there are some practical problems, which are mainly connected to their limited thermal and physical stability. In fact, very few MOFs can compete with zeolites in a number of gas-phase reactions, which typically operate under harsh conditions. However, they seem better suited to liquid-phase reactions because of the relative ease of tuning pore sizes (as previously mentioned, liquid-phase reactions generally require wider channels to allow for good mass transport).<sup>109</sup> These conditions are typical of fine chemical production and, therefore, MOFs are seen as desirable catalysts in these industries.

### Base Catalysis with MOFs

There are far fewer examples of MOFs used for base catalysis, though there are some key cases. Basicity can be introduced to MOF frameworks through post-synthetic functionalisation using groups such as amines, amides and pyridyls attached to the organic linkers or to the metal nodes.<sup>29</sup> For instance, a number of studies on base catalysis involving amine-functionalised IRMOF-3 have been reported.<sup>110, 111</sup> It is shown that IRMOF-3 is extremely effective at catalysing the Knoevenagel condensation of benzaldehyde, with a 99% yield and 100% selectivity towards the desired product. However, as previously mentioned, MOFs are often sensitive to hydrolysis,<sup>112, 113</sup> and the Knoevenagel reaction releases water. This raises questions about the reusability of IRMOF-3 and similar MOFs for this reaction. MIL-101(Cr) functionalised with amine groups gives extremely high conversion and selectivity towards the desired ethyl trans- $\alpha$ -cyanocinnamate product. The functionalised MIL-101(Cr) gave 98% conversion, which is a massive improvement in comparison to 32% conversion for the unfunctionalized form.<sup>114</sup> A 2009 paper by Savonnet *et al.* reported that IRMOF-3 and [ZnF(Am<sub>2</sub>Taz)] are both effective catalysts for Aza-Michael condensation reactions, showing good turnover numbers in mild conditions.<sup>115</sup> They also tested these materials for catalysing transesterification, and although they performed reasonably well at high temperatures, they had very low conversions under mild conditions, attributing the relatively weak basicity of the amine functional groups. Typically, stronger bases are required to catalyse transesterifications such as guanidines.<sup>116</sup> However, this is a problem for MOF base catalysts, as strongly basic



functionalities lead to structural collapse of the framework, which vastly limits their use in this field.<sup>29</sup>

On the surface, MOFs appear to be a competitive material for catalysis over their predecessor zeolites, as they are far more versatile in design and therefore can be finetuned for individual purposes. However, there are a number of major disadvantages in action that prevent their efficient use and commercialisation. The water sensitivity of MOFs seems the major limiting factor for their industrial catalytic applications, as many reactions take part in aqueous conditions.<sup>117</sup> In addition, MOFs are also unstable under harsh conditions which further limits the scope for catalysis, typically only finding a good use for them in the production of fine chemicals.<sup>118</sup> Although a number of MOFs have been reported for successful catalysis, there are questions over the validity of much of the data with regards to the reported TGA data, and the recyclability of the MOFs.<sup>119</sup>

## Amorphous Materials

A common disadvantage among certain synthetic crystalline materials is related to their stability. Although they have high surface areas and open pore structures, this often makes them vulnerable to high pressures and temperatures. Furthermore, crystalline materials can be highly sensitive to common solvents and reagents, with water stability being a major concern in this area. For these reasons there is growing interest in substituting them with amorphous materials in the field of heterogeneous catalysis.<sup>120</sup> Porous organic polymers (POPs) are a broad range of relatively new amorphous materials, with unique and favourable properties that makes them valuable in catalysis.<sup>121</sup> They have incredibly high stability in a broad range of conditions including wet environments and acidic and basic conditions, and they are most commonly made via irreversible reactions made with strong covalent bonds.<sup>122</sup> Although their amorphous nature makes them harder to model or characterise than their crystalline counterparts, it also brings several advantages, for example the synthesis of POPs

is typically simpler and faster than MOFs or other crystalline porous compounds. In addition, these materials can often be synthesised in milder conditions, which is beneficial from the environmental and the industrial point of view.<sup>123</sup> Furthermore, they are not confined to a crystalline framework, so it is easier to introduce functionalities into the materials. There are several different amorphous materials that exist under the title of porous organic polymers including hypercrosslinked polymers, conjugated microporous polymers, porous aromatic frameworks, covalent triazine frameworks, and polymers of intrinsic microporosity.

## Hyper Cross-Linked Polymers

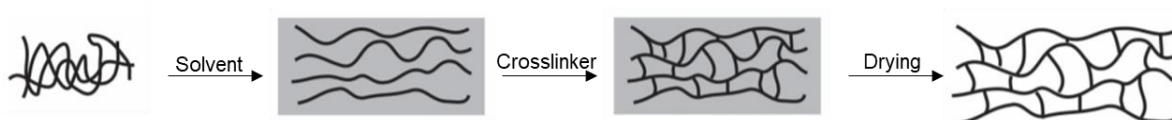


**Figure 1.6:** Formation of Hyper Cross-Linked Polymers

Hyper cross-linked polymers (HCPs) are a category of POP most commonly created by post-polymerisation cross-linking. A polymer is swollen in a solvent and an additional Lewis acid or another cross-linker is added, to create “bridges” between polymer chains (**Figure 1.6**).<sup>124</sup> This spaces the chains apart, and creates pores which can be fine-tuned for a variety of applications, most commonly gas storage and separation.<sup>125</sup> Within the field of heterogeneous catalysis, HCPs have been studied as supports for catalytic species, predominantly metals.<sup>126, 127</sup> However, there have been recent advances in functionalised HCPs as heterogeneous catalysts in their own right.<sup>128</sup>

A number of hyper cross-linked polymers have been sulfonated for a variety of acid catalyst reactions. HBS and HDS are synthesised via the post-sulfonation of the self-cross linked polymer HB and HD respectively, and was shown to catalyse Friedel-Crafts (FC) reactions and Beckmann rearrangements.<sup>129</sup> Several permutations of HDS and HBS were shown to have excellent catalytic abilities and high recyclability. The best performing resulted HBS-4 (HD treated with 4 mL of  $\text{ClSO}_3\text{H}$  per gram of polymer), which showed a 99%

conversion and 100% selectivity in the FC reaction of anisole and benzyl alcohol. HDS-4 was also shown to give a 99% conversion and an 83% selectivity for the rearrangement of cyclohexanone oxime. Polymers P(1,3-DEB)-SO<sub>3</sub>H and P(1,4-DEB)-SO<sub>3</sub>H are both synthesised from commercial monomers (**Figure 1.7**) and performed the catalysis of a number of reactions.<sup>130</sup> They are efficient catalysts for the esterification of fatty acids (TON ~400 mol.mol<sup>-1</sup>) and Prins cyclization reactions (TON ~90 mol.mol<sup>-1</sup>), also demonstrating good recyclability. Most importantly, they are shown to have a higher turnover than commercial polymer-based catalyst such as Amberlyst 15.

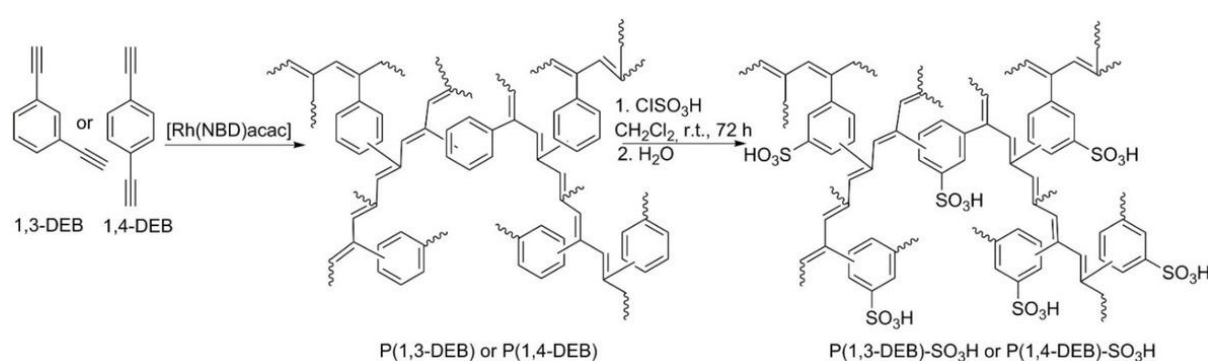


**Figure 1.7:** Synthesis of P(1,3-DEB)-SO<sub>3</sub>H and P(1,4-DEB)-SO<sub>3</sub>H

Sulfonated hyper cross-linked polystyrene has also been reported as a successful catalyst for a transesterification reaction, in this case the transesterification of fatty acids.<sup>131</sup> It was found to be more catalytically active than both Amberlysts 15 and 35, despite having a lower concentration of sulfonic acid sites, and this was attributed to the accessibility of the sites in the polystyrene HCP. The polymer showed good recyclability with only a minor loss of activity on repeated reactions.

Sulfonated hyper cross-linked poly(2-naphthol) also proved to successfully catalyse a variety of acylation reactions.<sup>132</sup> Kalla *et al.* tested the polymer catalyst for the acylation of a broad range of organic compounds, showing good activity in mild conditions. Of particular interest is the high selectivity in the acylation of phenols and alcohols. The material also showed excellent reusability, with only a small drop in performance over 10 cycles.

HCPs bearing basic functionalities were also successfully used for interesting catalytic applications. For instance, a group of imidazolium functionalised HCPs effectively catalysed the CO<sub>2</sub> cycloaddition with epoxides.<sup>133</sup> Several combinations of monomers were tested, the best performing was I<sub>C2</sub>HCP-5b, with a yield of 90%, a selectivity of 99% and a TON of 840. This result was obtained over 4h at 120 °C. In addition, there was no loss of activity over 5 cycles.

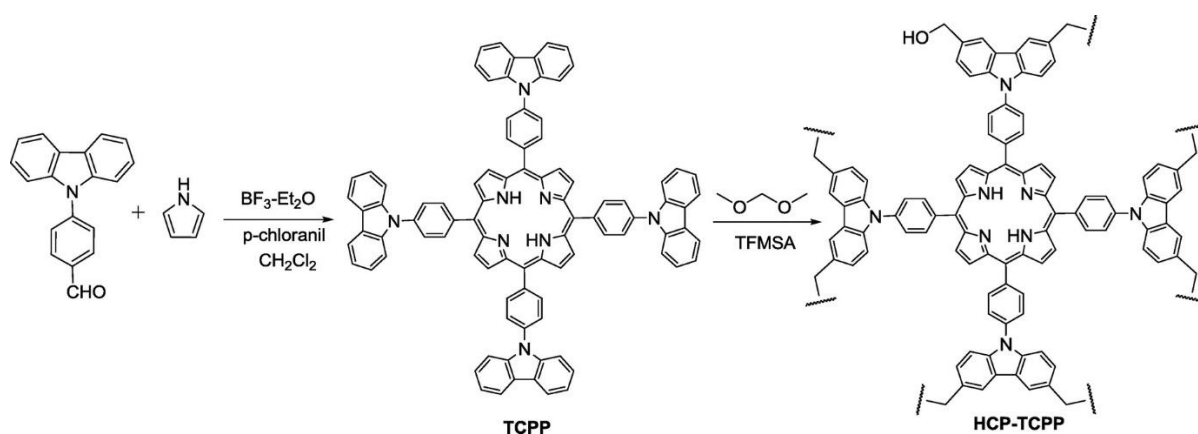


**Figure 1.8:** Synthesis of HCP-TCPP

The hyper cross-linked polyporphyrin HCP-TCPP with its basic nitrogen sites in the centre (**Figure 1.8**) has been reported as an efficient catalyst for the Knoevenagel condensation.<sup>134</sup> Feng *et al.* reported excellent yields for a number of different condensations, using a variety of aromatic aldehydes as reagents. They also reported good recyclability, with no significant loss of performance or mass over 6 runs.

## Conjugated Microporous Polymers

Conjugated microporous polymers (CMPs) are another type of crosslinked porous polymers, but unlike HCPs they feature  $\pi$ -conjugated skeletons in their 3D networks.<sup>135</sup> Like most POPs they possess high chemical and thermal stability, which combined with the versatile design make them good candidates for heterogeneous catalysis. CMPs are most commonly prepared via metal-catalysed cross-coupling reactions, combining monomers such as halogenated and alkyne bearing aromatics, to create extended conjugated networks.<sup>136, 137</sup> Catalytic functional groups can be added pre-polymerisation using functionalised monomers,

though the conjugated frameworks make also post synthetic additions relatively easy.<sup>138</sup> Their unique electronic properties have made these materials of particular interest in photocatalysis and electrocatalysis,<sup>136, 139</sup> there are numerous examples that demonstrate their application in heterogeneous conditions.

Many examples of CMPs in heterogeneous catalysis feature metal loading,<sup>140, 141</sup> or metal centres.<sup>142-144</sup> But, there are some examples of efficient organocatalysts within this field too. For instance, CMP-12, a thiophene polymer, was shown to be an effective catalyst in a number of reactions.<sup>145</sup> The monomer unit is based on the commercially available BNPPA, ((R)-3,3'-bis(9-anthracenyl)-1,1'-binaphthyl-2,2'-diyl hydrogenphosphate), with additional thiophene functionalities on the anthracene units becoming the sites of polymerisation (**Figure 1.9**).

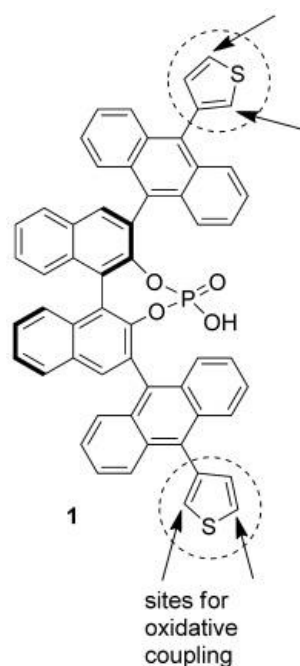


**Figure 1.9:** Structure of CMP-12

The polymer was shown to successfully catalyse transfer hydrogenations, *aza-ene* type reactions, and the asymmetric Friedel-Crafts alkylation of pyrrole, all with high conversions and selectivity, and with minimal loss of performance during several cycles. Moreover, the polymer performs just as well in the transfer hydrogenation as the monomer and the

commercial catalyst BNPPA, but with the added benefits of a heterogeneous catalyst, such as high recyclability and easier purification of the products.

Zhang *et al.* tested a nanoporous conjugated polymer, DMAP-NCP, for the catalytic acylation of alcohols and phenols.<sup>146</sup> The polymer is the product of the Sonogashira-Hagihara coupling of DMAP (3,5-dibromo-*N,N*-dimethylpyridin-4-amine) and 1,3,5-triethylpyridin-4-amine. Various alcohols were converted with high conversion and yields (92-99%), with very little loss in performance over 14 cycles.

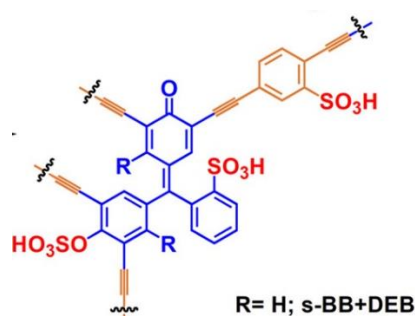


**Figure 1.10:** Structure of *s*-BB+DEB

Tantisriyanurak *et al.* synthesised a series of sulfonated CMPs which could catalyse the transesterification of oils into fatty acid methyl esters (FAMES), a common source of biodiesel.<sup>147</sup> In their study, the best performing polymer resulted *s*-BB + DEB (**Figure 1.10**), which could catalyse the transesterification of coconut oil at 60 °C in 24 hours, though this did require an over 80 wt% catalyst loading to achieve.

Only one example of CMPs as basic organocatalysts could be found in the literature: a pyrrole-base CMP which was able to catalyse the Knoevenagel reaction, synthesised by Gao *et al.*<sup>148</sup> 1 mol% of both TrPB-CMP and TePB-CMP gave a 100% conversion between nitrobenzaldehyde and malononitrile at 40 °C in 6 hours. There are a number of base-functionalised CMPs which could be tested in the future.<sup>138, 149, 150</sup>

## Covalent Triazine Frameworks

Covalent triazine frameworks (CTFs) are a species of POP defined by the aromatic C=N linkages (triazines), which are often formed during polymerisation.<sup>151</sup> This highly stable

core contributes to the overall strength of the material, allowing for their application also in harsh conditions. By design they may appear crystalline, as they look similar to MOFs and COFs but, in practice, the vast majority of reported CTFs are amorphous due to the flexibility and stability of the polymers.<sup>152</sup> There are limitations in the design of CTFs due to the nature of the linking unit. Most reported CTFs have been synthesised via the trimerization of nitrile-containing monomers.<sup>153</sup> There are some examples of CTFs made from the trimerization of amide-containing monomers, or the copolymerisation of aldehyde and amidine monomers.<sup>154</sup> In addition, there are only a handful of successful synthetic routes known. The first reported CTF used nitrile monomers in ionothermal conditions at 400 °C.<sup>155</sup> Not only is this counterintuitive from an environmental point of view, it is also not feasible for large scale production. However, there are some examples of CTFs synthesised in mild conditions.<sup>154, 156</sup> In their short history, CTFs have been tested for a number of different applications including gas storage, gas separations, electrocatalysis, photocatalysis, and heterogeneous catalysis.<sup>157</sup>

Covalent triazine frameworks are alkaline due to their high nitrogen content, which not only makes them ideal candidates for base catalysis, but also as supports for including metal centres post-polymerisation.<sup>158</sup> For example, a CTF formed with 1,4-dicyanobenzene monomers has been tested as a support for different reactions including oxidation,<sup>159, 160</sup> hydroformylation of 1-octene,<sup>161</sup> and hydrogenation of N-heterocycles,<sup>162</sup> showing moderate TOFs, but typically high selectivities and recyclability. Bavykina *et al.* synthesised a CTF with Ir<sup>III</sup>Cp\* centres attached to the nitrogen which showed great success in catalysing the formation of hydrogen from formic acid.<sup>163</sup> With 0.2 wt% loading of the Ir centre, a TOF of 27,000 h<sup>-1</sup> was reported at 80 °C. The reaction was successful at lower temperatures, but with much lower turnover frequencies. The material also was easy to recover and showed good recyclability. It is worth noting the harsh conditions required to make this CTF – an ionothermal synthesis at 500 °C,<sup>155</sup> and the high costs associated with the iridium complex. A cheaper alternative using Ru<sup>II</sup>( $\eta_6$ -C<sub>6</sub>H<sub>6</sub>) was also tested but reported a much lower TOF of 4020 h<sup>-1</sup> with

2.7 wt% loading at the same temperature. Bavykina *et al.* improved on their findings by using the CTF as a coating for cordierite monoliths, leading to TOFs in excess of 200,000 h<sup>-1</sup> for the same conditions but with a lower wt% of the iridium centre.<sup>164</sup>

There are also examples of covalent triazine frameworks used as organocatalysts. Several CTFs have been tested as catalysts for the cycloaddition of CO<sub>2</sub> into epoxides. An imidazolium-based CTF synthesised at varying temperatures was shown to give high conversions and selectivity towards the chloropropene carbonate product.<sup>165</sup> The best performing polymer was CCTF-350, that is CCTF synthesised at 350 °C, with very little loss in activity over 5 cycles. HB-CTP was synthesised from cyanuric chloride and 2,4,6-trihydrazinyl-1,3,5-triazine monomers, giving a hydrazine-bridged copolymer.<sup>166</sup> The polymer was tested for CO<sub>2</sub> insertion into a variety of epoxides with varying functional groups, at 80 °C temperatures and over 12 hours reaction times. The yields varied between 67% and 99%, though the majority of results were above 90%, and with minimal loss of activity over several cycles.

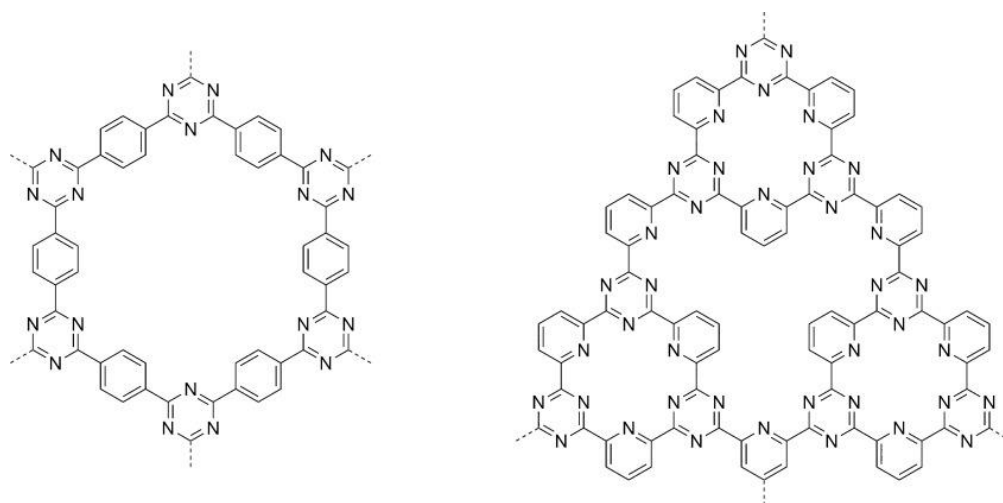


**Figure 1.11:** Structure of CTF-1

Roeser *et al.* tested two polymers for CO<sub>2</sub> cycloaddition (**Figure 1.11**).<sup>167</sup> CTF-1 is a crystalline material, however an amorphous analogue can be synthesised (CTF-P-HSA). It can be made using the same monomer as CTF-1 but polymerised at higher temperatures. Both materials gave complete conversions and high selectivity for the formation of chloropropene carbonate



from epichlorohydrin. In addition, they showed good recyclability over 6 runs. Other epoxides were tested, but epichlorohydrin was considerably more successful.

Tuci *et al.* studied CTF-1 (CTF-ph), as well as a pyridine-centred CTF, as a catalyst for the conversion of ethylbenzene to styrene.<sup>168</sup> Both polymers were synthesised using the established ionothermal method at temperatures varying between 400 and 600 °C. CTF-1 was shown to be less selective towards the styrene product than the industrial K-Fe catalyst, with 90% compared to 97%. However, the ethylbenzene conversion proved almost three times higher than the current industrial catalyst, therefore outperforming the current technology. CTF-py gave similar selectivity to CTF-1, with a lower conversion rate for ethylbenzene, although still higher than K-Fe. CTF-1 maintains a steady conversion for 50 hours on the stream, but CTF-py shows a drop in performance over time.

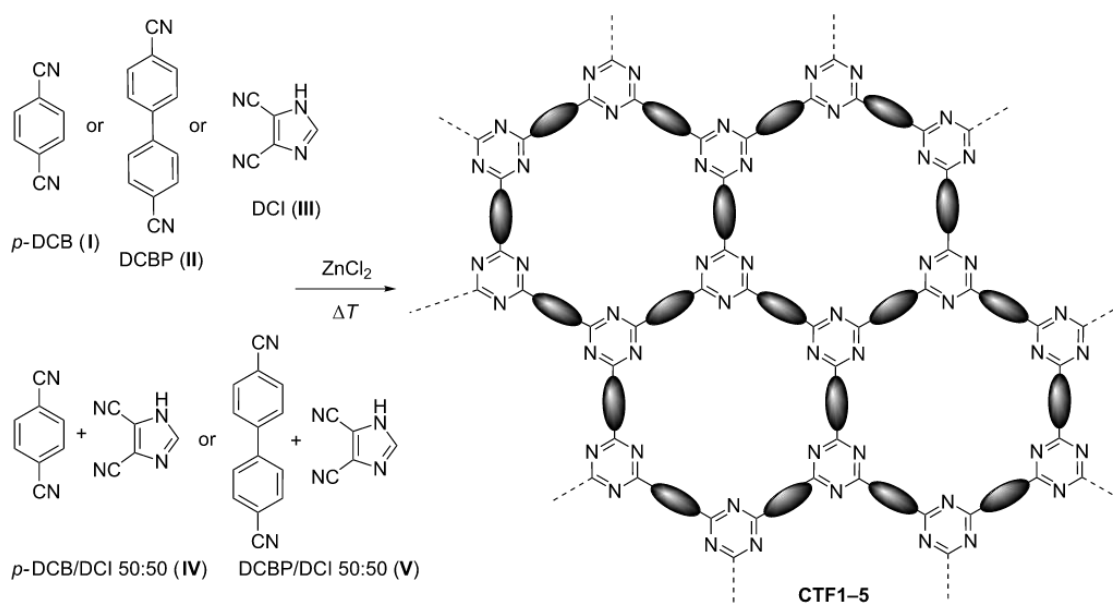


**Figure 1.12:** Syntheses of CTFs 1-5

The same group, in subsequent work, studied a number of other CTFs for the same reaction (**Figure 1.12**).<sup>169</sup> The most successful result was CTF-5 – a copolymer made of 4,4'-dicyanobiphenyl and 4,5-dicyanoimidazole, which performed better than CTF-1 and CTF-py. Not only was the ethylbenzene conversion higher (around 50%), but also the styrene selectivity proved higher, at around 98%. CTF-4, a copolymer composed of dicyanobenzene and 4,5-dicyanoimidazole, showed the highest selectivity at 99%, but the ethylbenzene

conversion resulted lower than the industrial catalyst counterpart. These catalysts, in particular CTF-1 and CTF-5, are of particular interest due to the high performance in steam- and oxygen-free conditions, which are relatively less studied in the current research and of interest in sustainable chemistry. However, considering the harsh conditions required to synthesise the catalysts, the environmental benefits are somewhat questionable. Jena *et al.* have synthesised a number of CTFs for the catalytic dimerization of benzylamine to N-benzyl-1-phenylmethanimine.<sup>170</sup> Isox (4,4'-(isoxazole-3,5-diyl)dibenzonitrile) was used as a monomer at 400 °C using 5 equivalents of ZnCl<sub>2</sub>, giving a polymer capable of 100% conversion and 98% selectivity. Similar results were achieved using pyz (4,4'-(1H-pyrazole-3,5-diyl)dibenzo-nitrile) as a monomer, though the selectivity was slightly lower at 92%. The materials also showed high recyclability over five cycles.

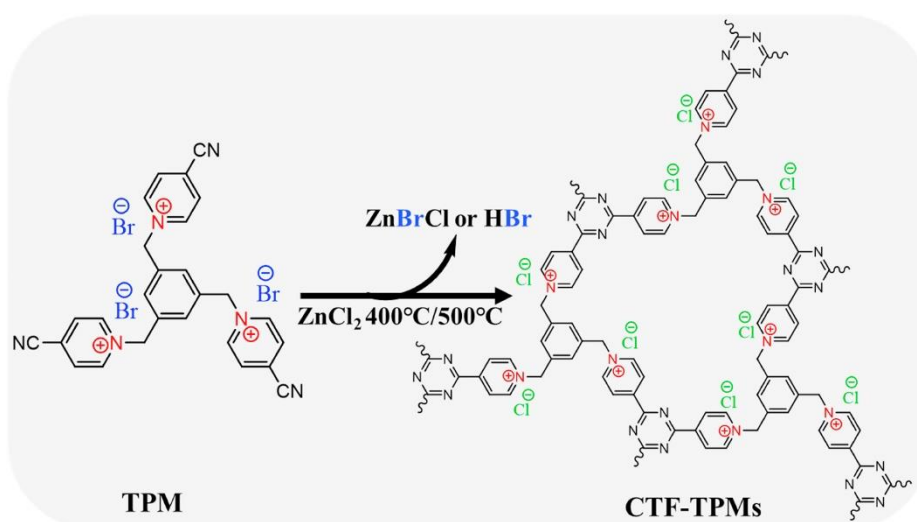


**Figure 1.13:** Synthesis of CTF-TPMs

Zhao *et al.* synthesised a CTF which could catalyse the cycloaddition of CO<sub>2</sub> into various epoxides (**Figure 1.13**).<sup>171</sup> In this case, the nitrogen centres of CTF-TPM-400 and CTF-TPM-500 do not act as the basic sites – they are positively charged with Cl<sup>-</sup> counterions. These two sites work together to catalyse the cycloaddition of CO<sub>2</sub> into epoxides, with epichlorohydrin, epibromohydrin, and epoxypropyl phenyl ether showing 100% conversion in 24 hours at 100 °C and 0.7 MPa pressure.

## Porous Aromatic Frameworks

Porous aromatic frameworks (PAFs) are another sub-category of porous organic framework, which differ from other POFs as they are constructed from purely aromatic linkers.<sup>172</sup> PAFs are typically self-assembled through covalent coupling reactions in catalysed solvothermal conditions.<sup>173</sup> They show excellent stabilities due to the robust frameworks and strong bonds. They are amorphous because of the high degree of free rotation around the polymer chains, however they typically remain highly porous because of the bulky nature of the monomers they are made from.<sup>174</sup> Most PAFs are insoluble and, since they can withstand harsh conditions, they are highly desirable to be used as heterogeneous catalysts. Many PAFs have been used as supports,<sup>175-181</sup> but there are some that have been designed purposely for catalysis.

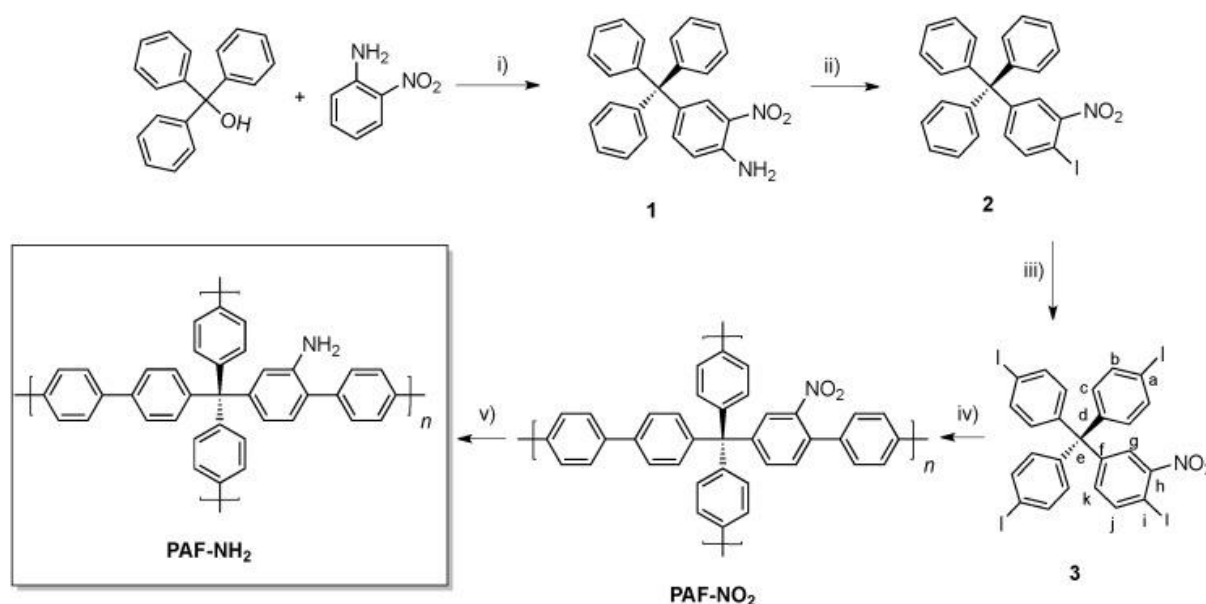


Figure 1.14: Synthesis of PAF-NH<sub>2</sub>

Verde-Sesto *et al.* synthesised pre-functionalised PAFs that supported transition metals as catalysts for a number of cyclopropanation reactions.<sup>177</sup> 4,4',4''-[(4-Iodo-3-nitrophenyl)methanetriyl]tris(iodobenzene) was polymerised via a Suzuki coupling reaction and then reduced to give PAF-NH<sub>2</sub> (**Figure 1.14**). In order to incorporate the transition metals, PAF-NH<sub>2</sub> was modified with picolinaldehyde to yield PAF-NPy, and with N<sup>t</sup>Boc-L-proline, isopropyl chloroformate and triethyl-amine followed by trifluoroacetic acid to yield PAF-NPro. The PAFs

complexed with copper were compared with their corresponding monomers for catalysis of cyclopropanation reactions. PAF-NH<sub>2</sub> and PAF-NPy were both considerably outperformed by their corresponding monomers. But PAF-NPro-Cu achieved better results than its monomeric counterpart as gave higher conversions and selectivity towards cyclised products, with all of tested substrates. For example, with the substrate prop-1-en-2-ylbenzene the PAF gives a conversion of 96% and a selectivity of 99%, whereas the monomer achieves 72% and 97% respectively. PAF-NPro-Cu also out-performed more established catalysts such as the MOF Cu<sub>3</sub>BTC<sub>2</sub>, MCM-41-Cu, and a number of Schiff bases. The same group tested several modified PAFs as supports for Ir and Ru centred complexes for the *N*-alkylation of amines with alcohols.<sup>175</sup> PAF<sub>spf</sub>, based on 9,9'-spirobisfluorene, was synthesised via a Suzuki-Miyaura coupling reaction, and post-functionalised with 1-mesityl-1H-imidazole (IMes) or 2-(1H-imidazol-1-yl)pyridine (IPy). These sites then reacted with metal complexes to form the supported catalyst. When used for the alkylation of anilines with benzyl alcohol, PAF<sub>spf</sub>-IPyIr showed 100% conversions, and a high selectivity towards the desired secondary amine products – varying between 80-96% depending on the aniline. Secondary amines are desirable for many important reactions, including the synthesis of pharmaceuticals, and without a catalyst the reaction completely favours the imine product. PAF<sub>spf</sub>-IMesIr, PAF<sub>C</sub>-IPyIr and PAF<sub>C</sub>-IMesIr all also gave 100% conversions of aniline with selectivities towards the secondary amine product. Cheaper ruthenium complexes were also synthesised, but they did not perform as well as the iridium complexes.

There are only a limited number of PAFs as organocatalysts to date. Yang *et al.* synthesised a fluorinated PAF for the catalytic halogenation of aryl compounds.<sup>182</sup> Cyclodextrins can be added to PAF-63 to create size selective pores that favour the formation of *para*-halo compounds.  $\alpha$ -CD-PAF-63 in particular gives strong preference for *para*-substituted products with several aryl compounds. In addition, the material has high recyclability with only a minor loss of performance over 10 cycles. Merino *et al.* functionalised a PAF similar to the aforementioned PAF<sub>spf</sub> which, functionalised with amino groups and

sulfonic acid groups, are efficient catalysts for a number of cascade reactions.<sup>183</sup> PPAF-SO<sub>3</sub>H-NH<sub>2</sub> was shown to catalyse the Knoevenagel reaction with 100% conversion and 100% yield for the dicyano product. This was higher than a mixture of both PPAF-SO<sub>3</sub>H and PPAF-NH<sub>2</sub>, which only gave a 91% yield, though this was still better than the commercial catalyst Amberlyst which only gave a 33% conversion and yield. PPAF-SO<sub>3</sub>H-NH<sub>2</sub> also showed good recyclability over 8 cycles.

### Polymers of Intrinsic Microporosity

Polymers of intrinsic microporosity (PIMs) are a unique class of organic porous material which differ previously discussed ones.<sup>184</sup> Generally, polymers comprise of long chains of connected monomers and are generally very strong, stable materials. Their strength is in part due to the way the long chains stack together, bending and conforming to efficiently pack together and therefore minimising electronic interactions. Because of this, polymers are not normally considered to be porous, as there is no free space.



**Figure 1.15:** Illustration of inefficient packing

PIMs, however, are built on the idea of intrinsic microporosity, which can be defined as “a continuous network of interconnected intermolecular voids within the polymer, which forms as a direct consequence of the shape and rigidity of the component macromolecules”.<sup>125</sup> PIMs are designed to contain rigid, contorted chains that are unable to pack efficiently, leaving accessible pores whilst still remaining stable (**Figure 1.15**). This is quite different to other porous polymers, where typically the porosity is designed by having long interconnected monomers that leave large spaces in between.<sup>185</sup>

PIM porosity is said to be intrinsic as the void space is present without the need for post-polymerisation modification. PIM monomers are also designed to contain rigid linkers that increase the pore sizes whilst maintaining rigidity.<sup>125</sup>

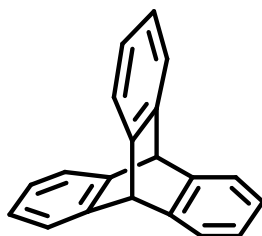


**Figure 1.16:** Triptycene

Different functionalities can be incorporated into PIMs monomers to increase the void space. A common example throughout PIM design is the use of triptycene, which is the simplest of the iptycene family of hydrocarbons, and consists of three aromatic rings arranged in a three dimensional paddlewheel structure with bond angles of  $120^\circ$  (**Figure 1.16**).<sup>186</sup> Its structure is ideal for making PIMs, as the large areas of free volume in the paddlewheel shape do not allow efficient packing. Triptycene is a commercial compound, though it can also be synthesised from anthracene via a Diels-Alder reaction.<sup>187</sup> Derivatives of triptycene can also be synthesised via the same mechanism.

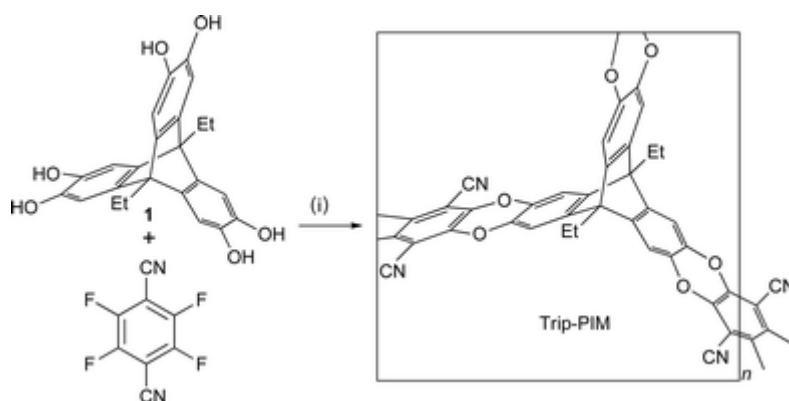


**Figure 1.17:** Synthesis of Trip-PIM

Trip-PIM was the first PIM synthesised using triptycene units, forming a polymer through all three of the aromatic rings (**Figure 1.17**).<sup>188</sup> This is an example of a network polymer, whereby the polymer forms in multiple directions, as opposed to a ladder polymer

which forms in a linear chain. Trip-PIM has an impressive surface area of  $1065 \text{ m}^2\text{g}^{-1}$ , indicative of the effect bulky functionalities can have.

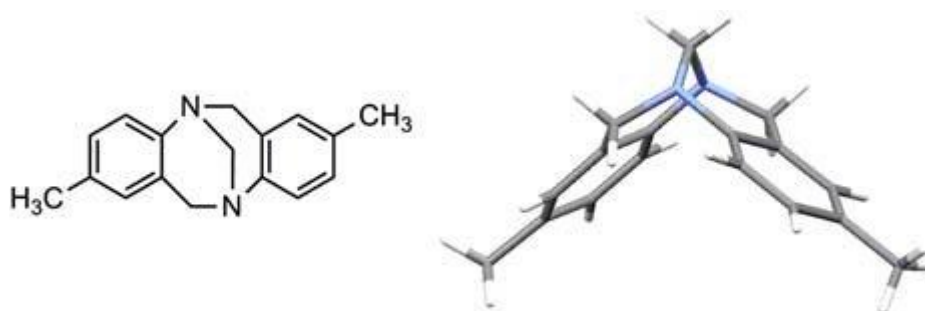


**Figure 1.18:** Structure of Tröger's Base

Functionalities can not only be included in the monomers but can also be formed along the polymer chain as linkers. A good example of this is the use of Tröger's base as a polymer linker. Julius Tröger first synthesised Tröger's Base (TB) from 4-methylaniline and formaldehyde (**Figure 1.18**),<sup>189</sup> although its unique structure was not confirmed until almost 50 years later.<sup>190</sup> Tröger's base is a chiral aromatic diamine with bridged nitrogen atoms. The nitrogen bridge prevents rotation which means this compound is very rigid. It was initially thought that TB was only weakly basic,<sup>191</sup> but recent studies show it is in fact more basic than anticipated.<sup>192</sup> This is because of the geometry of the bridged nitrogens, which leaves the lone pairs highly exposed. In 2013, Carta *et al.* first synthesised a Tröger's base polymer, PIM-EA-TB (**Figure 1.19**).<sup>193</sup>

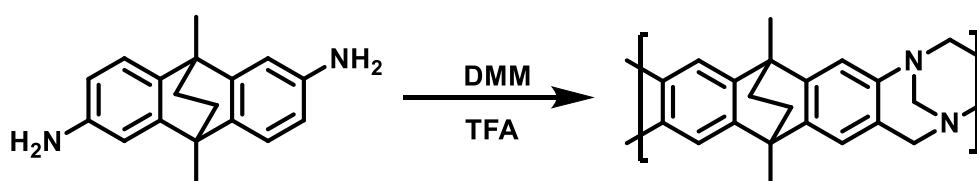


**Figure 1.19:** Synthesis of PIM-EA-TB

Not only did this polymer have a high surface area of  $1028 \text{ m}^2\text{g}^{-1}$ , but there was also a high selectivity for  $\text{CO}_2$ . This is a common feature of Tröger's base PIMs, as  $\text{CO}_2$  is a Lewis acid and therefore is attracted to the basic sites. Other functionalities have been added to PIMs to increase selectivity towards other gases, making PIMs great materials for gas separations.<sup>194</sup> To date, most PIM research has focussed on their use as gas storage and gas separation

materials due to their remarkable surface areas, and the ease of fine-tuning.<sup>195</sup> However, PIMs were initially developed as potential materials for heterogeneous catalysis.

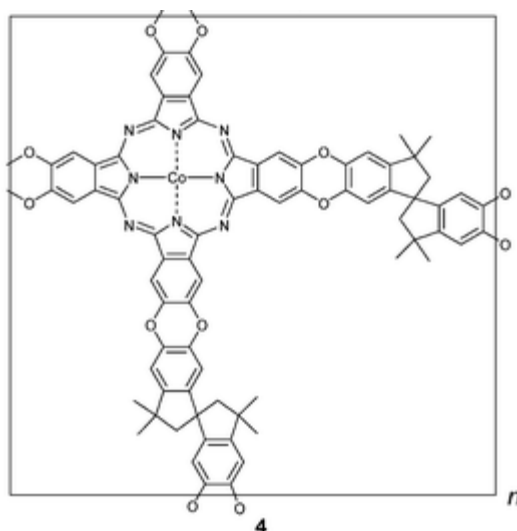


**Figure 1.20:** Synthesis of CoPc-PIM-A

In 2003, McKeown *et al.* synthesised a porphyrin-based PIM for heterogeneous catalysis.<sup>196</sup> Spirobisindane units were incorporated as rigid linkers to aid with the intrinsic microporosity (**Figure 1.20**). Cobalt was added into the PIMs in varying ratios and via a variety of synthetic routes and each tested in a number of catalytic reactions.<sup>197</sup> The polymers were found to show catalytic activity for the decomposition of hydrogen peroxide, as well as the oxidation of both cyclohexene and hydroquinone. In particular, these polymers gave superior results to the low molecular mass oligomeric versions of the same materials.<sup>198</sup>

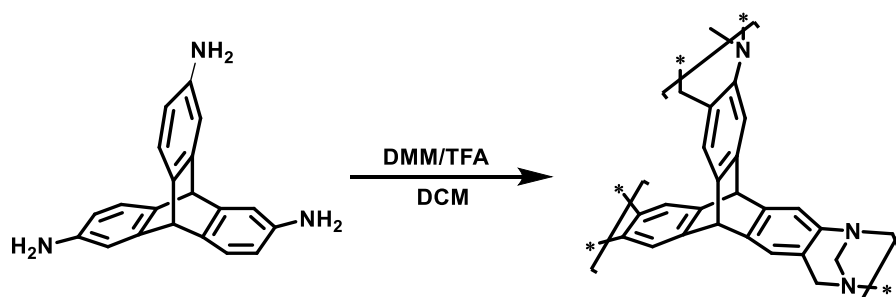


**Figure 1.21:** Synthesis of PIM-TB-Trip-1

In 2014, Carta *et al.* first demonstrated the potential of PIMs as basic catalysts, using polymers containing triptycene and Tröger's base functionalities to catalyse the Knoevenagel reaction (**Figure 1.21**).<sup>199</sup> The polymers increased the reaction rate significantly, the best



performing, PIM-TB-Trip-1 (1.7%), giving a 100% conversion over 2 hours, with a TON of 37 and a TOF of 2.5. Furthermore, these results proved to be better than using Tröger's base as a homogeneous catalyst, further proving the benefits of the use of a porous network. TB polymers present the potential for a novel type of catalyst that is not only metal free but is its own porous support. This is beneficial for a variety of reasons: by having active sites in the polymer chain itself, leaching of active sites is minimised, which increases the recovery and reusability of the catalyst. Also, the available reaction space is increased as there are not catalytic moieties filling the pores. However, despite these positive results, very little work on PIMs as catalysts has been done since.

## Aims of the project

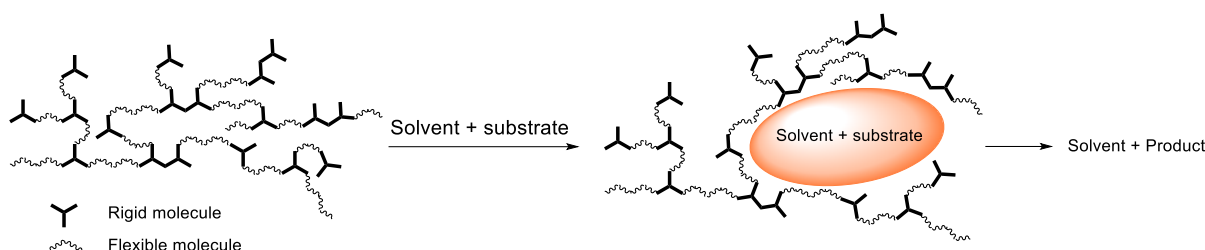


**Figure 1.22:** Swellability of polymers

One of the problems for PIMs as catalysts is that the high internal surface areas is largely due to the high proportion of small micropores. Therefore, in order to access all catalytic sites, reagents need to be able to access these small pores, which greatly limits the size of substrates, the range of reactions and the applications. We hypothesised that introducing a degree of flexibility to the polymers could induce a “swelling” effect in the polymers – whereby the polymer chains are able to move apart in the presence of solvent, meaning that more active sites become accessible, and that larger reagents can be incorporated (**Figure 1.22**). This was expected to lead to a reduction of the overall porosity, but the synergy of the enlarged pores and the number of catalytic sites per repeated unit could compensate it, increasing the conversions and allowing for larger substrates to be used.

In this work, we looked at the design and synthesis of a series of polymers and copolymers that incorporate the traditional rigid elements of PIMs with more flexible components, to create highly active metal-free polymer catalysts for a range of applications. We had the ambition and the aim to show that PIMs can be easily adapted for various applications by fine-tuning and incorporating new functionalities. We tested our polymers in a series of reactions, including Knoevenagel condensation, CO<sub>2</sub> utilisation reactions and biodiesel synthesis, which have growing global appeal in the efforts to prevent climate change.

# Chapter 2 - Novel PIM Copolymers for Catalysis

The combined outcomes of chapter 2 and 3 were published in the paper:

**Tröger's Base Network Polymers of Intrinsic Microporosity (TB-PIMs) with Tunable Pore Size for Heterogeneous Catalysis** A.R. Antonangelo, N. Hawkins, E. Tocci, C. Muzzi, A. Fuoco, M. Carta. *Journal of the American Chemical Society*, **2022**, 144 (34), 15581-15594

## Introduction

Following on from its initial success in the Knoevenagel condensation reaction between benzaldehyde and malononitrile,<sup>199</sup> a series of polymers and copolymers were designed inspired by PIM-TAT-TB. Due to the high surface area resulting from the inefficient packing of the very rigid, contorted polymer chains that is typical of high performing PIMs, triaminotriptycene (**TAT**), diaminotriptycene (**DAT**), and diaminobenzomethanoanthracene (**DABMA**) were initially selected as monomers (**Figure 2.1**).

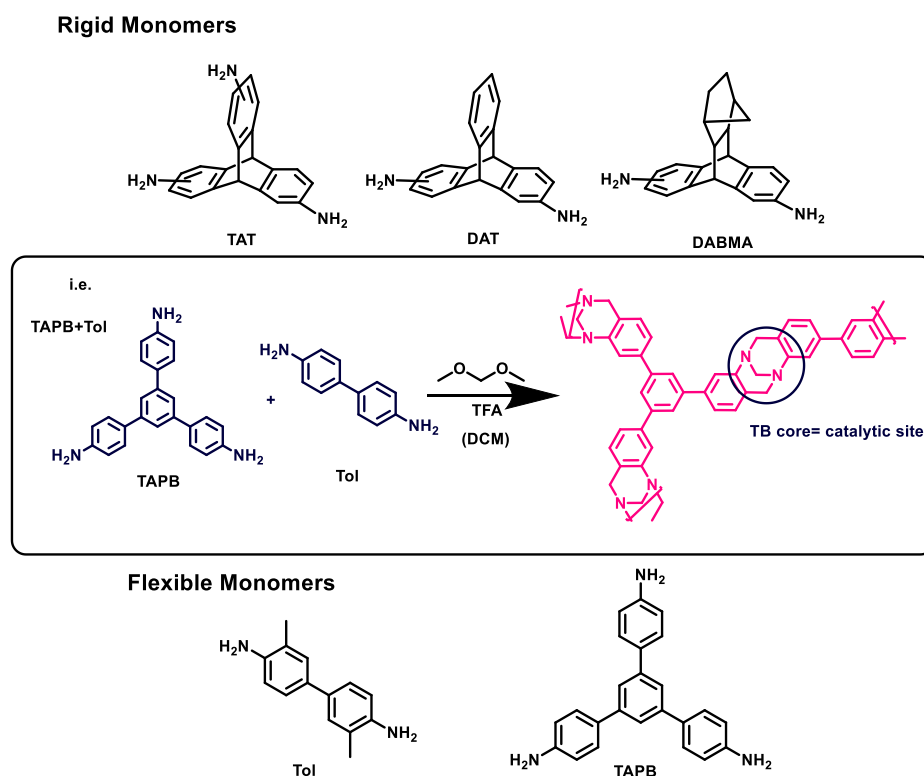


**Figure 2.1:** Monomers used in chapter 2 and polymerisation method used

All these monomers have previously been used to create homopolymers-PIMs. Whilst not strictly “homopolymers,” as they rely on the reaction with dimethoxymethane (DMM) to create the polymer chain, and which influences the repeating unit, they will be referred to as such to distinguish them from the copolymers, where two unique monomers are combined.

Tri- and disubstituted triptycenes have both already been used in PIM research,<sup>199, 200</sup> whilst DABMA is relatively new. The latter is an important core, as its synthesis is easier and cheaper than that of DAT, and its structure allows a minimal loss in surface area, compared to related triptycenes.<sup>201</sup> Triaminophenylbenzene (**TAPB**) has a similar size and shape to TAT, with three anilines connected to a central unit, though TAPB provides higher flexibility, due to the free rotation around the single bonds that connect the aromatic moieties. Whilst this increased flexibility will reduce the surface area of the polymer, this should increase its swellability, as discussed previously, which may aid the catalysis. To further explore this theory, tolidine (Tol) was also selected as a monomer. Tolidine (**Tol**) is a commercially available dianiline which has free rotation about the single bond connecting the rings, making it very flexible.

## Synthesis of monomers

Triaminotriptycene was synthesised as a mixture of isomers, according to literature procedures (**Figure 2.2**).<sup>188</sup> The presence of isomers does not influence the porosity or other properties of the final material, so the different isomers were not separated. Commercially produced triptycene was stirred in nitric acid and sulfuric acid overnight at 80 °C.

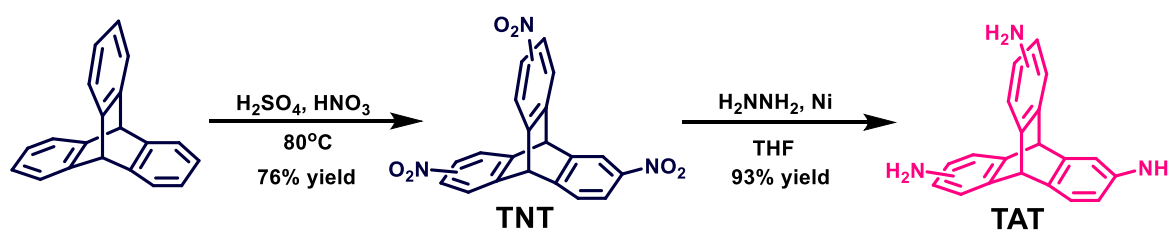


**Figure 2.2:** Synthesis of TAT

The crude product was purified by column chromatography, giving pale yellow crystals in a 76% yield. The isolated product was reduced by refluxing in THF with hydrazine monohydrate and Raney<sup>®</sup> Nickel for 16 hours, to afford a 90% yield of off-white crystals.

Diaminotriptycene similarly was made as a mixture of isomers, according to a previously published procedure (**Figure 2.3**).<sup>200</sup> Again, commercial triptycene was used, this time reacting with potassium nitrate and trifluoroacetic anhydride (TFAA), at room temperature and left to stir for 16 hours.

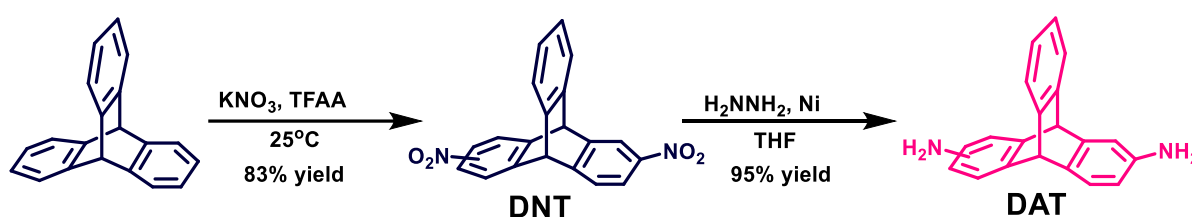


**Figure 2.3:** Synthesis of DAT

These milder reaction conditions are preferred over the nitric acid method seen previously when one wants to add a specific amount of nitro groups in the molecule, as it reduces the likelihood of over-nitration - in this case the formation of trinitrotriptycene. These conditions prevent the formation of a large amount of trinitrotriptycene, which simplifies the purification of the desired product, and also improves the atom economy of the reaction. In fact, although some trinitrotriptycene is produced as a by-product, the crude product was purified by column chromatography to yield an excellent 83% of pale-yellow crystals. The product was again reduced by refluxing in THF for 16 hours with hydrazine monohydrate and Raney<sup>®</sup> Nickel, giving a 95% yield of pale-yellow product.

Benzomethanoanthracene was synthesised via the Diels-Alder reaction of anthracene and norbornene at  $250^\circ\text{C}$  for 1 hour in a microwave reactor (**Figure 2.4**). The use of a microwave reactor greatly improves the yield of this reaction, whilst also vastly reducing the time the reaction takes to complete, and therefore the sustainability of the reaction is also improved.

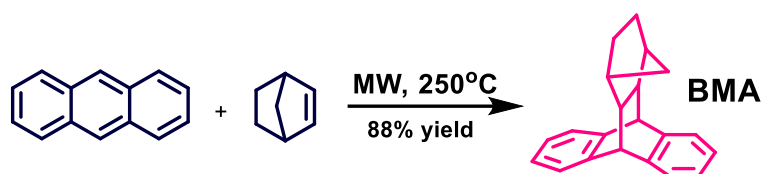


Figure 2.4: Synthesis of BMA

The crude product was refluxed in THF and maleic anhydride overnight, then precipitated in water, and washed with methanol to give the benzomethanoanthracene as an off-white powder in an 88% yield. DABMA was then synthesised from benzomethanoanthracene using the same method as that of DAT. Benzomethanoanthracene was nitrated using potassium nitrate and TFAA, and stirred in acetonitrile overnight, following the same procedure used for the triptycene.

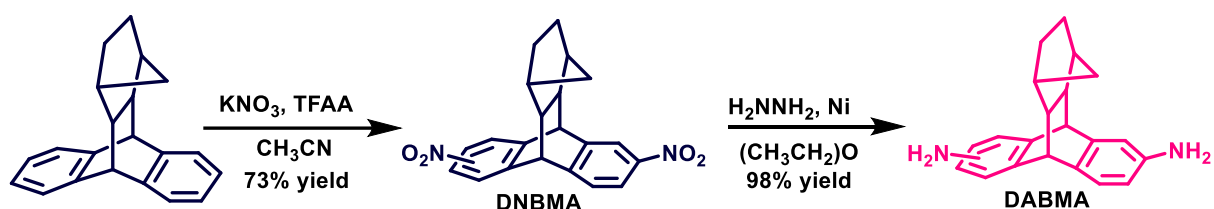


Figure 2.5: Synthesis of DABMA

The impure product was purified through silica with chloroform as an eluent to give a 73% yield of off-white crystals. This was then reduced once again using hydrazine monohydrate and Raney<sup>®</sup> Nickel, this time refluxing in diethyl ether to give a 98% yield of beige crystals (Figure 2.6).

For TAPB, it was initially thought the best synthetic route would be the direct nitration of 1,3,5-triphenylbenzene, to form the related tris(nitrophenyl)benzene (TNPB), and then to reduce this down to TAPB (Figure 2.6) similarly to how TAT is synthesised.

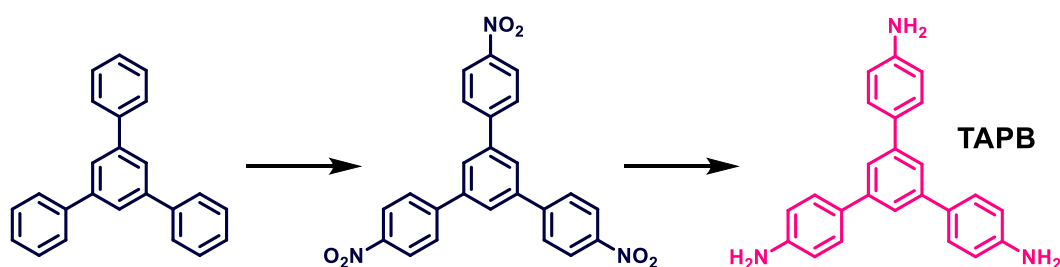
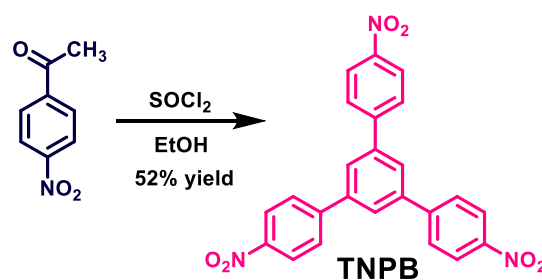


Figure 2.6: Proposed synthesis of TAPB

So, 1,3,5-triphenylbenzene was reacted with nitric acid and sulphuric acid and refluxed for 24 hours at 80 °C. However, the NMR showed a mixture of products difficult to separate, instead of the clean product that we expected. It was hypothesised that the highly acidic conditions may have been too harsh, and therefore the reaction was tried again in weaker conditions. It was tried using potassium nitrate and TFAA in acetonitrile, in the attempt to insert exactly three nitro groups, but also this method proved unsuccessful, so we considered an alternative reaction pathway. A search of the literature showed that this monomer could be formed starting from nitroacetophenone, a cheap commercial compound that can undergo a cyclisation reaction to form tri(nitrophenyl)benzene. This can then be reduced to form TAPB.<sup>202</sup> Using  $\text{SiCl}_4$  as a catalyst, in ethanol as the solvent, nitroacetophenone was refluxed overnight, and the reaction was worked up according to the literature.



**Figure 2.7:** Synthesis of TNPB

However, once again the NMR showed this to also to be unsuccessful, so the cyclisation reaction was repeated using thionyl chloride in ethanol (**Figure 2.7**).<sup>203</sup> This was left to reflux for 4 hours, followed by a recrystallisation in dimethylformamide (DMF) which yielded the desired TNPB as a yellow powder in a 52% yield.

The nitro monomer was then reduced following the method employed in the same paper, using hydrazine monohydrate and nickel in ethanol. The reaction was monitored by TLC and seemed successful, though neither the reagent nor product were found to be soluble in ethanol. This therefore made the removal of the catalyst difficult as, given the volatile nature of Raney<sup>®</sup> Nickel, traditional filtration methods are not safe to perform. A similar method using Pd/C as a catalyst was then utilised,<sup>204</sup> which allowed an easier removal of the catalysts

reaction by hot filtration. The resulting product was stirred in water, the mixture brought to neutral pH, and the solid filtered off, to afford a pale grey product in a 75% yield.

Given the cyclotrimerisation reaction to form TNPB, it was considered that a similar approach could be used to form TAPB in a one-step synthesis. An alternative method was found to produce TAPB in a one-step synthesis (**Figure 2.8**).<sup>205</sup>

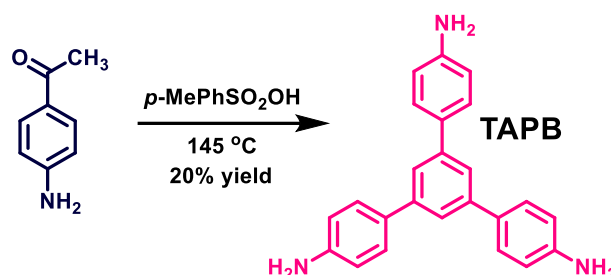


**Figure 2.8:** One-step synthesis of TAPB

Aminoacetophenone can, in fact, undergo a cyclisation reaction in the presence of *p*-toluenesulfonic acid at 145 °C after 16 hours. However, the purification of the product proved rather difficult – requiring quite a long column chromatography, and the final product was collected only in a 20% yield. For this reason, the 2-step synthesis was finally preferred.



**Figure 2.9:** Tolidine structure

The commercially available tolidine (**Figure 2.9**) was used as a second flexible monomer. This compound has a single bond connecting the two aromatic moieties and is linear, which partially allows free rotation, so we imagined would make the entire polymeric chain more flexible, especially compared to the more rigid TAPB.

With these five monomers, a series of copolymers was synthesised (**Figure 2.1**). All of them were prepared according to the well-established TB-PIM synthesis method,<sup>188</sup> where monomers are stirred with dimethoxymethane, TFA and DCM, and left for ~16 hours. The resulting jelly-like polymers were precipitated in ice and aqueous ammonia, washed with



acetone, THF, DCM and methanol, to remove eventual oligomers, before being dried in a vacuum oven. All copolymers are produced as A-B random polymers, which means that it is impossible to know whether the structure is regular or not, but on average, two or more similar cores would result one next to the other. To guarantee that all polymerisation sites are engaged, the equivalent ratio of monomers was varied depending on the number of substitution sites in each compound. For instance, copolymers featuring monomers with the same number of amino-sites were mixed in a 1:1 ratio, but for those featuring one tri-substituted and one di-substituted, we used 2 equivalents of the trisubstituted and 3 equivalents of the disubstituted monomers, respectively.

## Results and Discussion

### Confirmation of Copolymerisation

The complete polymerisation can be confirmed using FT-IR, where there is a clear disappearance of  $\text{-NH}_2$  peaks from the monomer to the polymers (**Figure 2.10a**). For example, from TAPB to TB-TAPB-PIM, there is a loss of peaks at 3430, 3360 and 3200  $\text{cm}^{-1}$ . This same pattern is observed across all polymers and copolymers. Furthermore, the formation of TB binding units can be confirmed using solid state  $^{13}\text{C}$  NMR. The peak at 50-70 ppm is associated with the methylene carbon on the TB bridge, and the peaks at 120-160 ppm are associated with the aromatic carbons (**Figure 2.10b**). This is in agreement with previously reported TB-PIMs.<sup>206</sup>

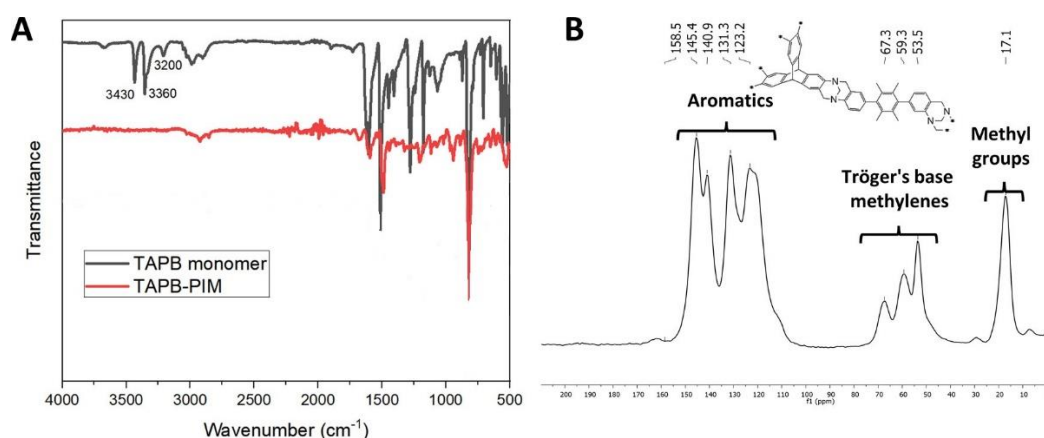


**Figure 2.10:** a) IR of TAPB monomer vs polymer; b)  $^{13}\text{C}$  NMR of PIM-TAT-TB

Elemental analysis was performed in an attempt to further confirm the composition of the polymers; however, the measured values were found to be significantly different from the calculated ones. This is actually common in porous materials because of their tendency to absorb atmospheric gases and compounds (e.g., CO<sub>2</sub> and moisture), which then affect the elemental analysis.<sup>207, 208, 209</sup>

TGA analysis instead proved very useful to confirm the composition and, therefore, the completion of the polymerisation. TGA monitors the thermal degradation of materials and allows the relative (or %) mass loss versus the increase of the temperature to be plotted. From this, it is possible to ascertain when thermally vulnerable bonds are broken, quantify the mass lost at this point and compare it to the calculated value of a polymer's repeated unit. Thus, for this experiment, we synthesised a copolymer of TAPB and ethanoanthracene (EA) in accordance with the method described above. The EA was used because its ethylene bridge is thermally labile, breaking at about 250 °C, which differs from the thermal decomposition of the average TB-PIM backbone, which typically begins at around 440 °C.

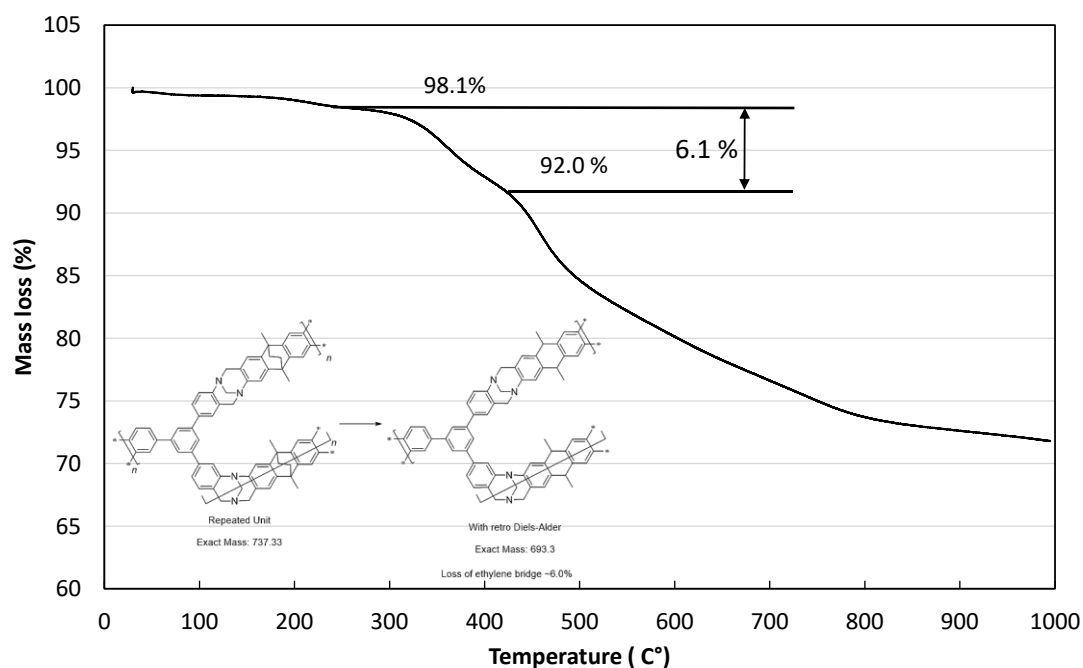


**Figure 2.11:** TGA of PIM-TAPB+EA-TB

This method has been used before to successfully confirm the PIM composition of some homopolymers.<sup>210, 211</sup> The TGA of PIM-TAPB+EA-TB showed around a 6% mass loss between

250-400 °C (**Figure 2.11**), which matches perfectly with the calculated elemental breakdown of the polymer, and therefore complete polymerisation is proven. We further assume complete polymerisation of the other copolymers, given the same method is used, the monomers are all similarly reactive, and the achieved yields were also very similar. TGA analysis also demonstrated the high thermal stability of this series of polymers, with degradation occurring over 400 °C in all polymers.

## BET Surface Areas of Polymers

**Table 2.1:** Surface areas of PIMs in varying adsorbate gases

Entry	Monomer 1	Monomer 2	Adsorbate Gas	
			N <sub>2</sub> 77K	CO <sub>2</sub> 273K
1	DABMA	TAPB	10	575
2	DAT	TAPB	1	410
3	TAT	TOLIDINE	20	430
4	TAT	TAPB	380	430
5	TOLIDINE	TAPB	5	360
6	PIM-TAPB-TB		500	
7	PIM-TAT-TB		900	

The surface area of each polymer was measured via the BET calculation (**Table 2.1**). Typically, surface areas are measured using nitrogen gas as an adsorbate at the temperature of 77K. The homopolymer PIM-TAT-TB gave a surface area of  $\sim 900 \text{ m}^2 \text{ g}^{-1}$ , which is very close to the one previously reported ( $1035 \text{ m}^2 \text{ g}^{-1}$ ).<sup>206</sup> PIM-TAPB-TB was found to have a surface area of  $\sim 500 \text{ m}^2 \text{ g}^{-1}$ , which is lower than PIM-TAT-TB, but that was expected given the increased level of flexibility of the monomer, which reduces the free volume. Several copolymers, though, particularly those with a combination of di- and tri- substituted monomers, gave very low BET surface areas when measured by N<sub>2</sub> adsorption at 77 K, often lower than  $10 \text{ m}^2 \text{ g}^{-1}$ . This was somewhat unexpected, as we knew that the increased flexibility of the chains would have led to a loss of porosity, but not to this extent. However, we also speculated that this could be due to slow adsorption kinetics, especially at such a low temperature, rather than because of a lack of porosity. The increased flexibility of these polymers allows for a more efficient packing of the chains in the solid state, which means that N<sub>2</sub> molecules cannot

penetrate the pores as easily in the solid state. Furthermore, in cold conditions there is far less kinetic energy, and the more flexible chains will compact in order to maximise intermolecular forces, even when the adsorbate gas is introduced. With that in mind, we repeated the measurement using CO<sub>2</sub> as the probe gas, as not only is it smaller than N<sub>2</sub> (3.3 vs 3.64 Å), and therefore can penetrate the pores more easily, but the measurement takes place at a higher temperature. CO<sub>2</sub> adsorption is measured at 273 K, and these warmer conditions generate more energy, allowing the chains to move more freely to accommodate the gas molecules. The change of adsorbate, in combination with the higher temperature, afforded BET surface areas in the range of 350-600 m<sup>2</sup> g<sup>-1</sup>.

It is worth noting that the change in partial pressure, necessary to calculate the BET values from CO<sub>2</sub> at 273 K, is approximated. To do the calculation properly, the probe gas should reach saturation pressure ( $p_0$ ), which for CO<sub>2</sub> at 273 K is ~ 35 bar. Since our instrument allows a maximum final pressure of 1 bar (which would correspond to ~ 0.03  $p/p_0$ , if we reached saturation), the calculation of the BET surface areas at 273 K is performed between 0 and 0.03  $p/p_0$ . Considering that the BET calculation is always done at very low  $p/p_0$ , the error is minimised. The values may prove more accurate when measured at 195 K as, at this temperature, the saturation pressure of CO<sub>2</sub> is exactly 1 bar (same as N<sub>2</sub> at 77 K). Nevertheless, our measurements and BET calculation performed at this temperature showed similar values to the ones obtained at 273 K, so we decided to keep the latter as a standard, since the analyses are faster and consumes less energy.

The surface areas of all five copolymers are relatively similar, and all surface areas are considerably lower than that of PIM-TAT-TB, which was reported to have a surface area of 1035 m<sup>2</sup> g<sup>-1</sup>. However, a high surface area is not necessarily indicative of high catalytic performance.<sup>120</sup> Whilst clearly there needs to be enough space to accommodate the reagents, larger surface areas are usually associated with a high concentration of small micropores. These more flexible polymers are designed to allow more space for the reagents to enter, whilst still providing a confinement effect to promote the catalytic activity.

For additional comparison, a homopolymer of TAPB, PIM-TAPB-TB was synthesised using the same polymerisation method as that of the copolymers. The surface area was found to be  $500 \text{ m}^2 \text{ g}^{-1}$ . Furthermore, PIM-TAT-TB was resynthesised according to the same literature procedure,<sup>199</sup> with the resulting polymer giving a surface area of  $900 \text{ m}^2 \text{ g}^{-1}$ . This is lower than the reported surface area, but within an acceptable range (and within the margin of error typical of this method). An initial test was done on this new PIM-TAT-TB to compare the results to the published data.

### Knoevenagel Reaction and Catalytic Testing

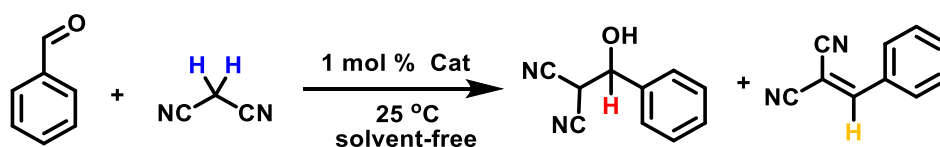


**Figure 2.12:** Knoevenagel reaction

The simple Knoevenagel condensation reaction (**Figure 2.12**) between benzaldehyde and malononitrile is frequently used as a starting point to test acid and base catalysts (**Figure 2.13**).<sup>29, 71</sup> We used the same conditions as the paper published in 2014, as it represents the ideal starting point for the comparison of the results of our polymer. That is 1 mol% catalyst with a 3:1 ratio of benzaldehyde to malononitrile under solvent free conditions at room temperature (25 °C). The 1 mol% is based on the repeating unit of the polymer.

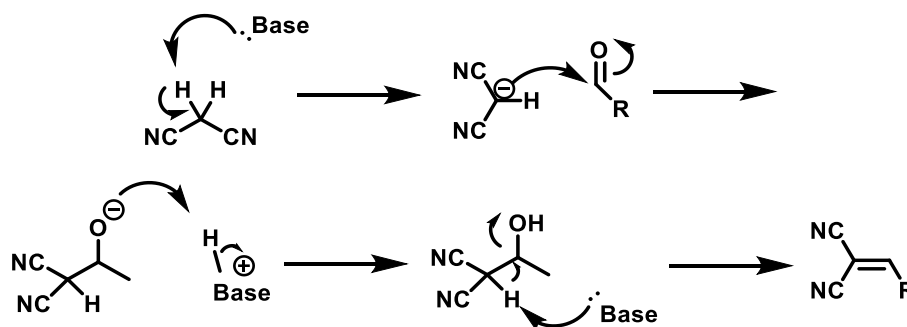


**Figure 2.13:** Mechanism of Knoevenagel reaction with a base catalyst

In a typical experiment, benzaldehyde and malononitrile were stirred in a vial until all the malononitrile had dissolved. Then, the catalyst was added to the vial, and the timer was started. Every 10 minutes, a 10  $\mu\text{l}$  sample was taken for a total of 2 hours, then adjusted

according to the conversion rates recorded. The samples were then analysed by  $^1\text{H}$  NMR. The peak at 3.66 ppm (circled blue) is associated with the two protons on the malononitrile starting material, and we can integrate that relative to the peaks associated with the alcohol (5.2 ppm) (circled yellow) and the alkene (7.8 ppm) (circled red) products (**Figure 2.14**).

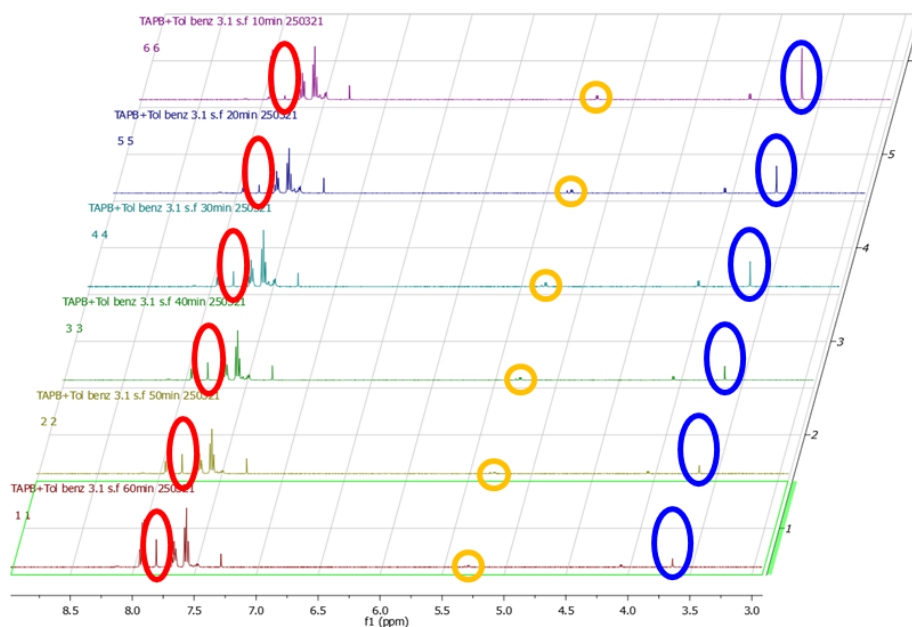


**Figure 2.14:** NMRs monitoring the formation of products and loss of reagents over time

These ratios from each time point can then be plotted on a graph to show the consumption of malononitrile and the formation of the two products (**Figure 2.15a**). Since both the alcohol and the alkene represent the product of the catalysis, to avoid confusion and not to have too many lines in the plots, the graphs herein will be presented to show the formation of combined products over time (i.e., combining the yellow and red lines, as demonstrated in **Figure 2.15b**).

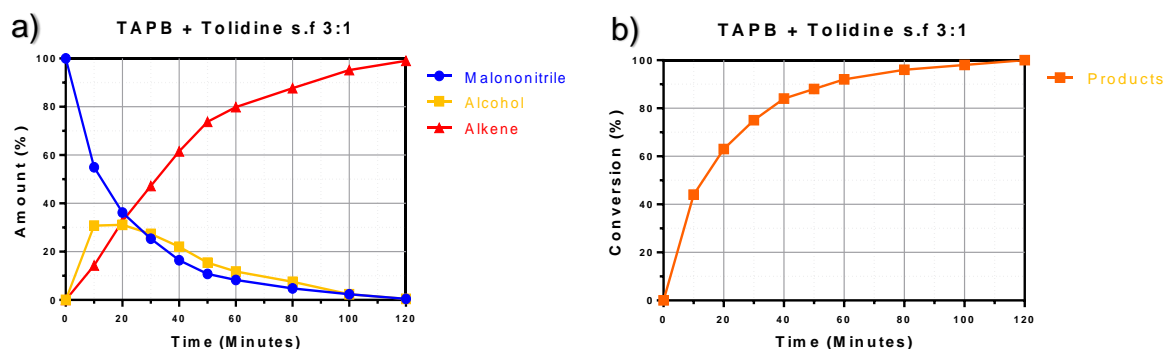


**Figure 2.15:** a) Percentage amount of malononitrile and products over time; b) Combined products

**Figure 2.16** shows a comparison of the two PIM-TAT-TB results, the one from this study and one from the literature,<sup>199</sup> proving that they are very similar, which validates our testing method and also the quality of the polymer.

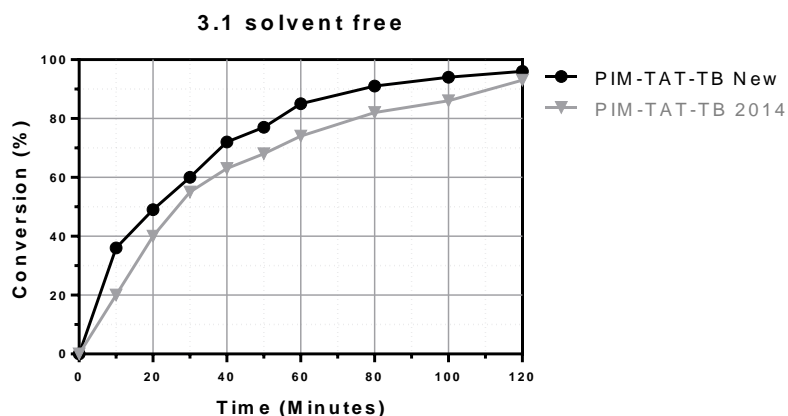


**Figure 2.16:** Comparing PIM-TAT-TB from the literature<sup>199</sup> and resynthesized

All synthesised polymers were tested as catalysts for the Knoevenagel reaction under the same conditions, to guarantee reproducibility (**Figure 2.17**).

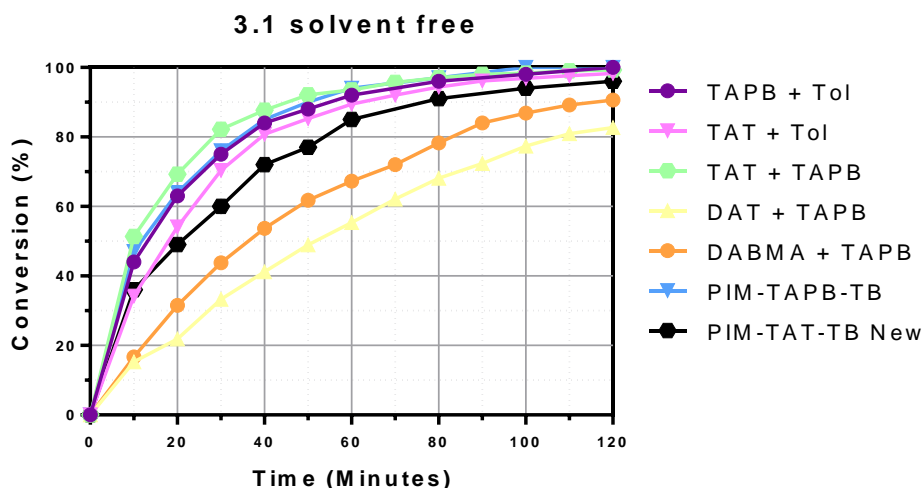


**Figure 2.17:** All solvent free reaction results, showing PIM-TAT+TAPB-TB as the best performing polymer.

The conversion results of the copolymers were generally very positive, with four of the polymers outperforming PIM-TAT-TB, reaching over 95% conversion in just 80 minutes. However, very little could separate their performance. Two polymers, DAT + TAPB and DABMA + TAPB did not perform as well as the other polymers. This was somewhat

unexpected as it was thought that these two polymers would give similar results to TAT + TAPB, if not better due their increased flexibility. It was considered that there was an issue with the polymerisation reaction. In fact, all other polymers were produced as a powder or fine solid, but these last two outliers were produced as much larger “particles” (to the naked eye, the pieces appeared larger). This clearly could have an effect on the dispersion of the particles throughout the reaction and therefore would have an effect on the activity. The polymers were resynthesised, this time using additional DCM to aid the stirring for longer. After 16 hours, the reaction showed a jelly-like consistency, but much looser than previously seen. The jelly-like polymer was reduced to fine particles, before adding it to ice and ammonia to prevent larger parts hardening quickly. After washing, the resulting polymers appeared much more similar to the rest of the polymer series. The catalysis experiment was repeated with these new polymers and the results were much closer to the other values. In fact, following these adjustments, all polymers outperformed PIM-TAT-TB.

This early result showed that there was great promise for these types of PIMs in catalysis, and that introducing flexibility into the polymers’ chains could significantly improve the catalytic activity. Given their enhanced flexibility, it was also thought that they could “swell” in the presence of a solvent, opening the polymer chains even more, and making more active sites accessible to reagents. With that in mind, the catalysis was attempted with the aid of DCM as both starting materials are very soluble in it, still using a 3:1 ratio of benzaldehyde to malononitrile, but we did not notice a clear improvement in the catalytic performance (**Figure 2.18**). In fact, in some cases the reaction occurred slower, suggesting the solvent had hindered the reaction somewhat, perhaps diluting it too much. Next, the same reactions were repeated in ethanol, as Knoevenagel reactions had been reported to work well with ethanol as a solvent, most likely as it helps stabilising the charged intermediate.<sup>212, 213</sup> In addition, ethanol is a greener solvent than the halogenated DCM, which makes the reaction more sustainable for the environment. In this case, we noticed a slight improvement in the performance, but typically the reactions still required 2 hours to reach completion.



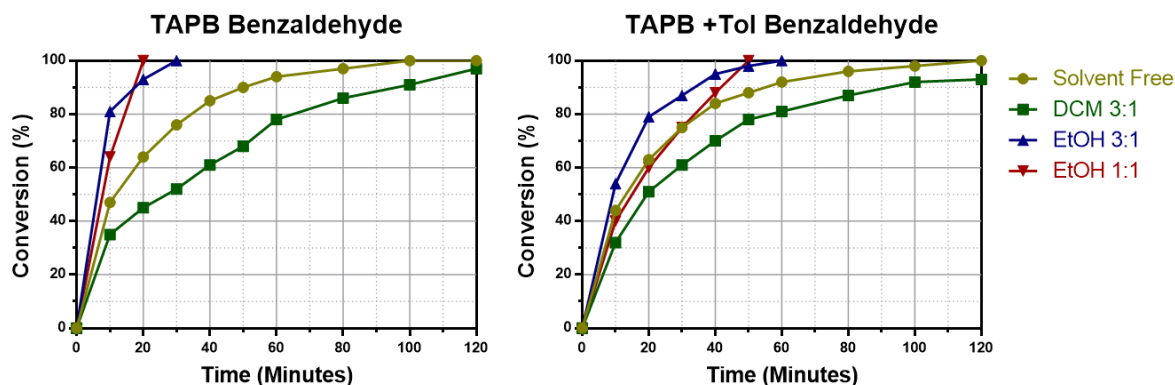


**Figure 2.18:** Catalyst performance in varying solvent conditions

The reaction was again repeated in ethanol, but this time a 1:1 ratio between the reagents was used. Under these conditions, the catalytic performance proved to be much higher than the previous experiments. Now, the conversion typically reached 95% completion within an hour, a substantial improvement compared to solvent free conditions. This set of results are of great excitement for a number of reasons. Firstly, the catalysts perform better using a green solvent, than they do with an environmentally unfriendly solvent such as DCM. Secondly, the reaction proved to be better using a 1:1 ratio, which improves the atom economy of the reaction, as all reactants are converted into products and there is no need of purify or separate them from unreacted starting materials. Both of these factors improve the overall sustainability of the reactions, which is of great importance when considering procedures for industrial applications.

## Conclusion

In this initial section of work, we have established a reproducible catalytic testing method as well as accurate ways to measure the characteristics of the polymers. Seven polymers, one novel homopolymer, one homopolymer from the literature, and five novel copolymers, were synthesised, and their catalytic performances tested. The two homopolymers, PIM-TAT-TB and PIM-TAPB-TB, have very different degrees of rigidity, which is confirmed when comparing the surface areas. PIM-TAT-TB has almost double the surface area of PIM-TAPB-TB but, despite that, both polymers perform very similarly as catalysts in

the Knoevenagel reaction. The five copolymers were designed to show varying levels of flexibility, but the surface area measurements did not reflect this, with all measurements in the same region. Likewise, all five copolymers performed very similarly as catalysts. Catalysis results across all polymers improved when ethanol was introduced, which begins to prove the benefits of “swellable” polymers for catalysis. Furthermore, we were delighted to find that when using ethanol, the reaction still worked efficiently using a 1:1 ratio of benzaldehyde to malononitrile, which improves the atom economy of the reaction.

These initial results suggest that flexibility does not hinder the catalysis - if anything it improves it. But the degree of flexibility we introduced to these initial polymers was not enough to explore the true effect that flexibility has on these systems.

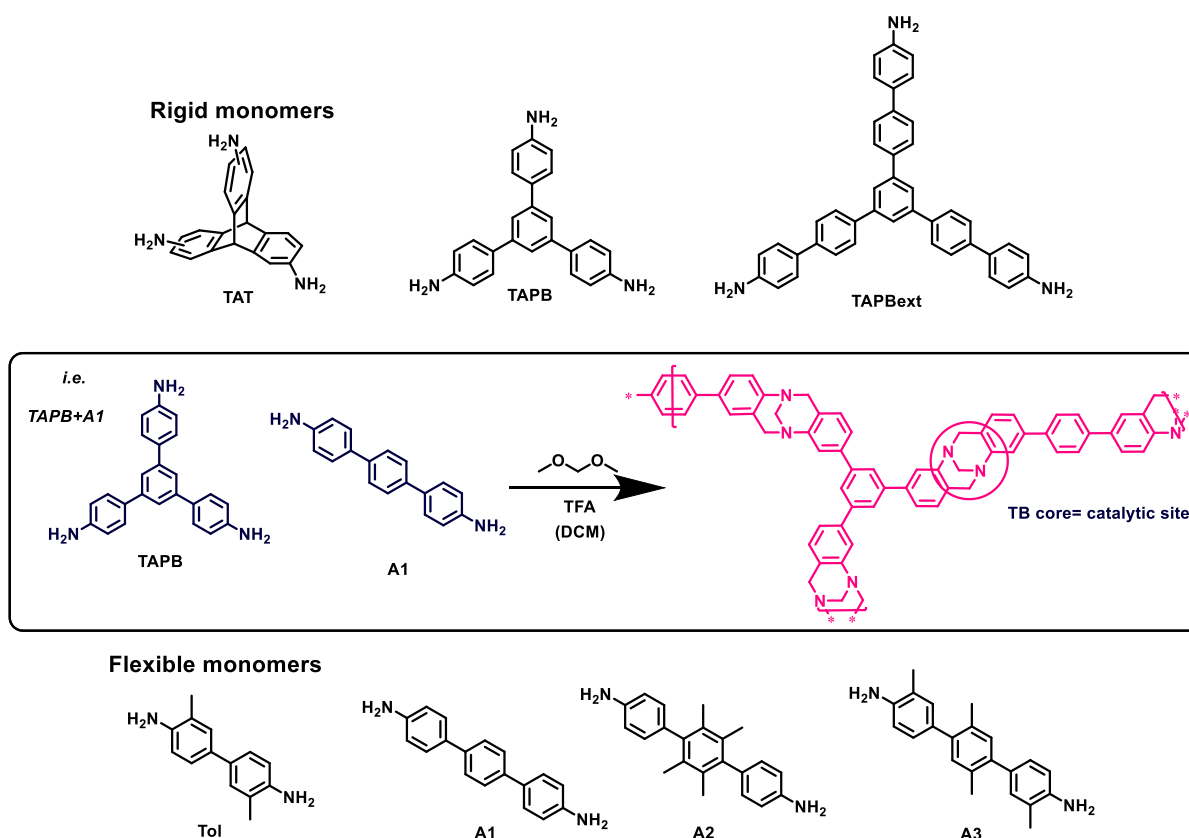
# Chapter 3 - Increasing Flexibility in PIM-Catalysts

## Introduction

Whilst the results obtained from the first series of copolymers presented in chapter 2 proved to be very positive, and outperformed those of the 2014 paper, they all looked very similar to one another, so we aimed to test if the system could be further improved. There was little difference in the surface areas, and from the repeated units the geometries were actually quite similar, and so it was hard to gather information about trends, particularly in relation to flexibility. Despite having half the surface area of PIM-Trip-TB, PIM-TAPB-TB outperformed it in each catalytic test in chapter 2, which demonstrated that the increased flexibility could be beneficial. Combined with the fact that TAPB is quicker, easier, and cheaper to synthesise than TAT, TAPB was chosen as a starting point for this series. It was therefore decided to create a series of polymers with increasing levels of flexibility, to better gauge whether there is a correlation between flexibility of the polymers and activity of the catalysts.

## Synthesis

A series of novel polymers and copolymers was designed for this chapter (**Figure 3.1**), which aimed to extend the geometries – making the arms of the monomer units longer, as well as increasing the degree of free rotation in the polymer units. It was hoped that these additions would further increase the flexibility of the materials and, therefore, the catalytic performance.



In order to continue a coherent comparison with the 2014 paper,<sup>199</sup> PIM-Trip-TB was used, as well as TAT + Tol and TAT + TAPB. These are ideal to compare with their TAPB-containing counterparts. In the previous chapter, TAPB proved to be more rigid than anticipated, and therefore in this chapter it was combined with even more flexible monomers. Tolidine was also used again as a flexible monomer. As a linear monomer with aromatic groups connected by only single bonds, it creates increased flexibility of the chains between the larger rigid monomers, basically acting as a “spacer.”

Inspired by this role of the tolidine, three further flexible linear monomers were also chosen to incorporate into the copolymers. Extended anilines 1, 2, 3 (**A1**, **A2**, **A3**) all feature three benzene rings connected by single bonds, with each featuring unique methyl groups that, typically, create some extra free volume between one chain and the next (**Figure 3.2**). As seen in the previous chapter, we want to optimise between porosity and swellability of the molecular chains (as one will lead to a decrease in the other). The elongation of the chains

and additional free rotation were, consequently, of great interest for the flexibility/swellability theory, and how it improves the catalytic conversions.

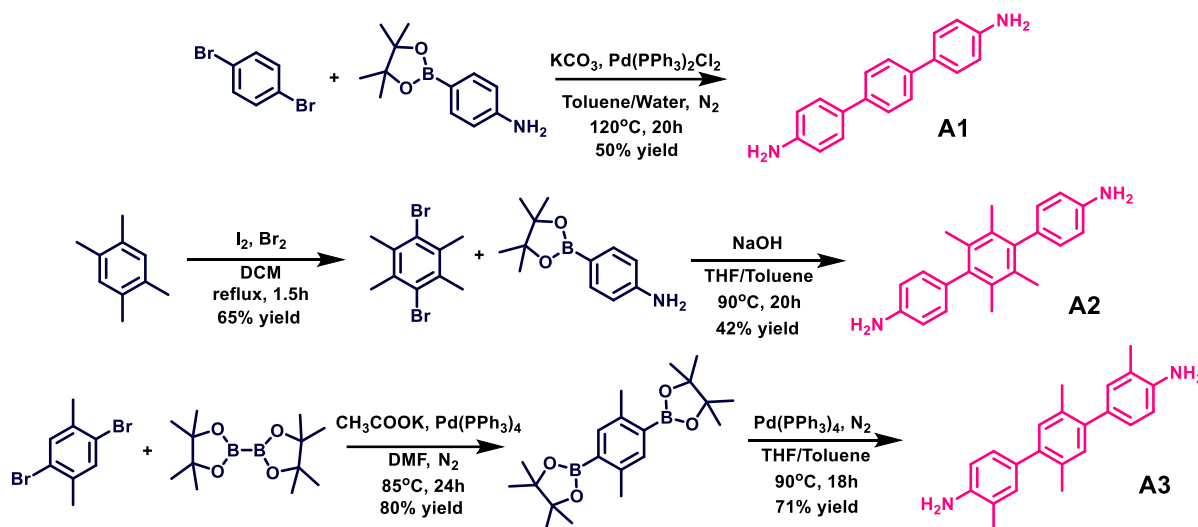


**Figure 3.2:** Synthesis of A1, A2, A3

A1 was synthesised according to a literature procedure, via a one-step Suzuki coupling reaction between 1,4-dibromobenzene and 4-aminophenylboronic pinacolboronate, in the presence of potassium carbonate and  $\text{Pd}(\text{PPh}_3)_2\text{Cl}_2$  as a catalyst.<sup>214</sup> The crude product was purified via column chromatography to give A1 as a brown powder in a 50% yield. A2 was made in a two-step synthesis.<sup>215</sup> 1,4-dibromo-2,3,5,6-tetramethylbenzene was prepared via the simple bromination of tetramethylbenzene using  $\text{Br}_2$ . The crude product was recrystallised to give a white solid in a 65% yield. This then underwent a Suzuki coupling reaction, similar to A1, using 4-aminophenylboronic pinacolboronate, before it was purified by column chromatography and recrystallised to give A2 as a light brown powder in a 42% yield. The synthesis of A3 is a two-step process, this time featuring two separate Suzuki-coupling reactions. The first is between 1,4-dibromo-2,5-dimethylbenzene and bis(pinacolato)diboron using  $\text{Pd}(\text{PPh}_3)_4$  as a catalyst, and potassium acetate as a reagent.<sup>216</sup> The crude product is purified via column chromatography giving 1,4-bis(pinacolatoboronyl)-2,5-dimethylbenzene as a white solid, in an 80% yield. This product then undergoes another Suzuki coupling reaction with 4-bromo-2-methyl aniline in the presence of sodium hydroxide and  $\text{Pd}(\text{PPh}_3)_4$ . The product was purified by chromatography to give A3 as a light brown solid in a 71% yield. Monomers A1-3 were

combined with TAT as well as TAPB to see comparisons of the more rigid triptycene centre versus the more flexible TAPB monomer.

Additionally, triamino(biphenyl)benzene (**TAPBext**) was chosen as another rigid monomer (**Figure 3.3**). The extra benzene groups on the arms of the trigonal structure aim, again, to increase the degree of free rotation, but also help to create larger pore space.

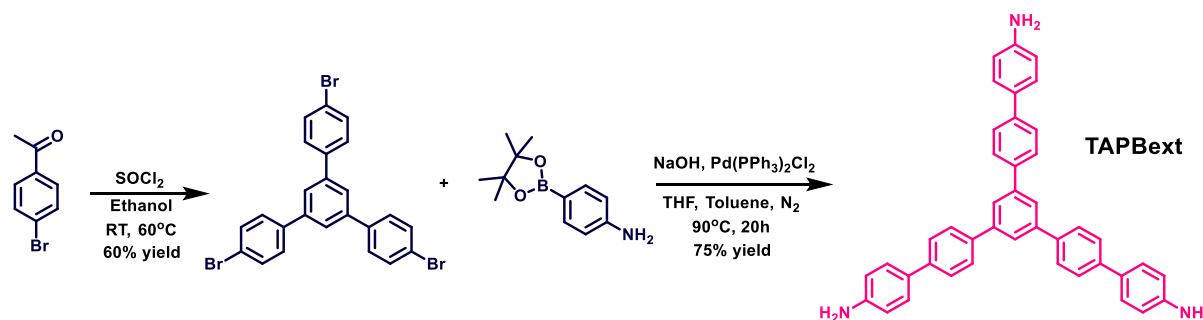


**Figure 3.3:** Synthesis of TAPBext

TAPBext can be synthesised via a two-step synthesis.<sup>217</sup> 4-bromoacetophenone undergoes a cyclisation reaction, similar to those seen in chapter 1 for the formation of TNPB and TAPB. Thionyl chloride was then added to 4-bromoacetophenone and ethanol over ice and then refluxed for 16 hours.<sup>204</sup> Following a simple work up, 1,3,5-tris(4-bromophenyl)benzene (TBPB) was collected as a pale yellow solid in a 60% yield. TBPB then undergoes a Suzuki coupling reaction with 4-aminophenylboronic pinacolyl ester, in the presence of sodium hydroxide and the catalyst  $\text{Pd}(\text{PPh}_3)_2\text{Cl}_2$ . TAPBext was hence obtained as a pale-yellow powder in a 75% yield. TAPBext was combined with Tol and A1 to complete a series of gradually extending polymers that can be utilised to see any trends in the catalytic performance.

All TB polymers were made via the same method used for the other TB-PIM synthesised in chapter 2.

## BET Surface Areas and Characterisation

Based on the findings in chapter 2 surrounding surface area measurements with more flexible polymers, the BET surface areas of this series of polymers were all measured using CO<sub>2</sub> as an adsorbate gas, due to the expected flexibility of the polymers, and the warmer measurement temperature of 273K. **Table 3.1** shows that generally the polymers designed to be more flexible gave lower surface areas (as expected), with the lowest surface area in the series coming from the most flexible PIM-TAPBext+A1-TB, with a value of 250 m<sup>2</sup>g<sup>-1</sup>.

**Table 3.1:** Surface area of chapter 3 polymers

Entry	Monomer 1	Monomer 2	Surface Area in CO <sub>2</sub> (273K)
1	TAPB	-	500
2	TAPBext	-	350
3	TAPB	Tol	360
4	TAPB	A1	470
5	TAPB	A2	370
6	TAPB	A3	350
7	TAPB	TAT	545
8	TAT	Tol	430
9	TAT	A1	520
10	TAT	A2	600
11	TAT	A3	500
12	TAPBext	Tol	395
13	TAPBext	A1	250

Analysis of the morphology of the polymers' particle size were also compared by taking SEM images of three chosen polymers, with varying degrees of flexibility (**Figure 3.4**). The more rigid polymer, PIM-TAPB-TB, exhibited rod-like aggregates, consistent with a more regular, rigid morphology, whereas the more flexible polymer, PIM-TAPBext+A1-TB, showed more globular, spherical particles which is consistent with more free movement in the polymer chains.

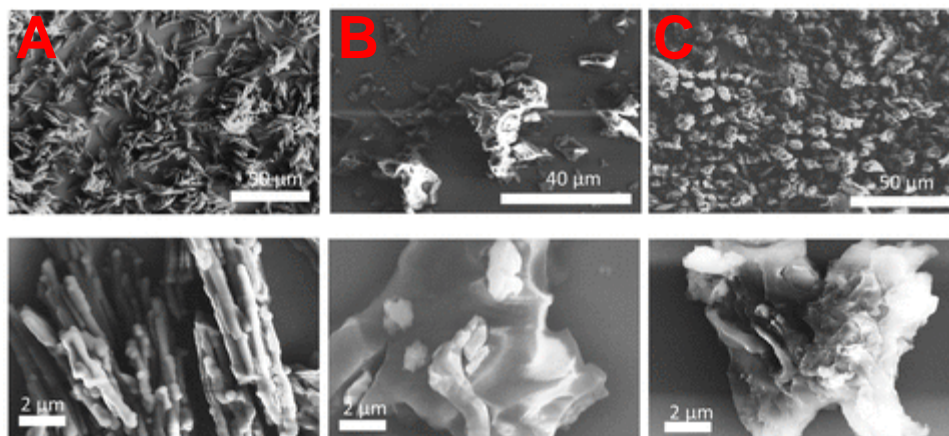


**Figure 3.4:** SEM images of: **A)** PIM-TAPB-TB; **B)** PIM-TAPB+A1-TB; **C)** PIM-TAPBext+A1-TB

## Results and Discussion

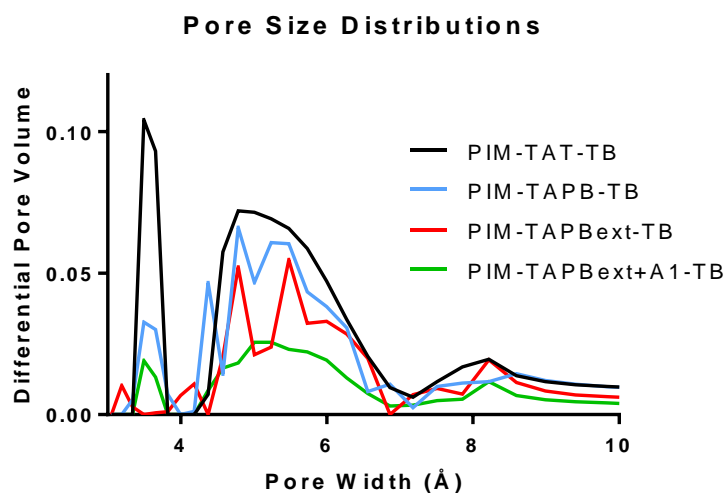
The catalysis with the new polymers was initially tested under the same starting conditions as the previous chapter, which is with a 3:1 ratio of benzaldehyde to malononitrile and under solvent free conditions. As **Table 3.2** shows, all polymers in this series outperformed the published PIM-TAT-TB, with some of the best performing polymers giving a 95% conversion in 30 minutes. All of the copolymers featuring TAT were outperformed or matched by their TAPB-containing counterparts. This is a great improvement because, as mentioned in chapter 2, TAPB is easier and cheaper to synthesise than TAT. The best performing polymer of the series was PIM-TAPBext+A1-TB, which reached 95% completion in only 20 minutes. When this is compared to literature results, where typically higher temperatures and/or higher catalytic loading is required to get this kind of percent completion (and most often with metals included in the backbone), it shows that our materials are very competitive. Furthermore, PIM-TAPBext+A1-TB was the polymer in this series designed to have the highest degree of flexibility and is the best performing. If our theory is correct, there should be an upper bound of flexibility, where there is not enough rigidity to cause a confinement effect. This result shows that we have not yet reached that upper limit.



**Table 3.2:** Conversions in Knoevenagel reaction - 3:1 benzaldehyde:malononitrile in solvent free conditions

Entry	Catalyst	Conversion (%) at varying times (mins)				
		20	30	60	80	120
1	PIM-TAT-TB	45	55	74	80	93
2	PIM-TAPB-PIM	64	76	94	97	
3	PIM-TAPB+Tol-TB	63	75	92	96	
4	PIM-TAPB+A1-TB	86	97			
5	PIM-TAPB+A2-TB	64	74	92	98	
6	PIM-TAPB+A3-TB	76	87	98		
7	PIM-TAT+TAPB-TB	69	82	94	97	
8	PIM-TAT+Tol-TB	54	70	90	94	98
9	PIM-TAT+A1-TB	63	78	95	97	
10	PIM-TAT+A2-TB	75	85	98		
11	PIM-TAT+A3-TB	79	85	96	98	
12	PIM-TAPBext-TB	78	87	98		
13	PIM-TAPBext+Tol-TB	83	89	96		
14	PIM-TAPBext+A1-TB	95	100			
15	No catalyst				30	
16	TB homogeneous	25	35	54	65	85

As we had anticipated, there is a general increase in performance as the polymers became more flexible, and we actually see an inverse correlation between the conversion rates and the pore size distribution, according to the NLDFT from CO<sub>2</sub> adsorption (**Figure 3.5**).

**Figure 3.5:** Pore size distributions of increasingly flexible polymers

It is worth noting that this method of pore size distribution analysis is not quantitative,<sup>218</sup> but still we can see a trend amongst these polymers from the same family. The increased flexibility, in fact, results in a lower proportion of ultra-micropores but a higher proportion of larger ones, meaning that reagents can enter the pore space more easily, whilst still remaining in a confined pore. This is desirable as it keeps the reagents in a small space which maximise collisions.

### Addition of a solvent

As shown in Chapter 2, the theory that flexible and more swellable polymers was further put to the test by performing the Knoevenagel reaction in the presence of a solvent. This should allow for more movement of the polymer chains, therefore facilitating the access of reagents into the pores. The reaction was first performed in DCM, and it demonstrated a minor improvement, but not a significant difference (**Table 3.3**). Given the negative environmental impact of DCM, it was not work pursuing with this solvent for only a small change. Ethanol was then used in the reaction, and we noticed a considerable increase in the performance of the catalyst, with all polymers leading the reaction to completion in an hour or less. In this case, not only is the ethanol allowing the polymer chains to swell, but we also speculate that the protic solvent aides the reaction, as already shown in previous works that studied the behaviour of materials towards the Knoevenagel condensation.<sup>213, 219</sup> This is most likely due to the polarity of ethanol, which helps to stabilise the charged intermediate. Furthermore, when the ratio of reagents was adjusted to 1:1 in ethanol, the performance of all the polymers improved further, with some polymers reaching 100% completion in only 20 minutes. We arrive at the conclusion that, in the 3:1 system, the excess benzaldehyde combined with the ethanol was diluting the reaction too much, and the 1:1 molar ratio made optimum collisions more frequent. As already discussed in chapter 2, this is highly favourable as it improves the atom economy of the of the reaction and allows the use of a relatively “green” solvent. With the 1:1 in ethanol reactions, we did not see a clear correlation between flexibility and catalytic performance, though the results were all similar. But, in comparison to

the 3:1 reaction in ethanol, it is the more rigid polymer catalysts that see the most significant improvement when using the simplest benzaldehyde and malononitrile. Since the two substrates are rather small, there is very little change for the flexible polymers. This arguably is because there was less room for improvement with the more flexible polymers as they already showed excellent conversions.

**Table 3.3:** Conversions of the Knoevenagel reaction between benzaldehyde and malononitrile in varying ratios with varying solvents.

Entry	Catalyst (1mol%)	Ratio of reagents	Solvent	Conversion (%) at varying times (mins)					
				10	20	40	60	80	120
1	PIM-TAPB-PIM	3:1	DCM	35	35	61	78	86	97
		3:1	EtOH	81	93	100			
		1:1	EtOH	64	95	100			
2	PIM-TAPB+Tol-TB	3:1	DCM	32	51	70	81	87	93
		3:1	EtOH	54	79	95	100		
		1:1	EtOH	40	60	88	100		
3	PIM-TAPB+A1-TB	3:1	DCM	38	66	79	92	95	100
		3:1	EtOH	84	100				
		1:1	EtOH	64	87	100			
4	PIM-TAPBext-TB	3:1	DCM	72	84	93	98	100	
		3:1	EtOH	80	100				
		1:1	EtOH	86	100				
5	PIM-TAPBext+Tol-TB	3:1	DCM	50	62	74	87	92	100
		3:1	EtOH	70	84	96	100		
		1:1	EtOH	63	78	100			
6	PIM-TAPBext+A1-TB	3:1	DCM	46	70	86	100		
		3:1	EtOH	85	100				
		1:1	EtOH	88	100				

### Knoevenagel reaction with larger benzaldehydes

At the beginning of this study, it was hypothesised that more flexible polymers would create a larger catalytic environment that would allow better access to pore space. With 1:1 benzaldehyde to malononitrile in ethanol, all polymers performed excellently, despite the clear difference in flexibility between the polymers. It was thought that the relatively small substrates

did not pose a challenge to the more rigid polymers, and therefore to test the theory it was important to use larger molecules in the reaction.

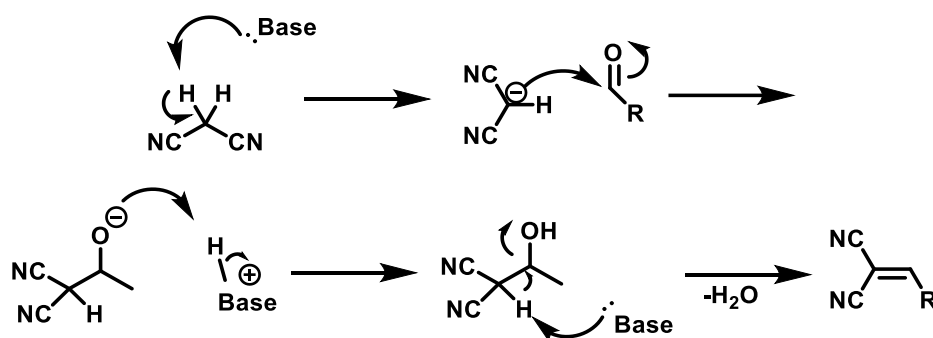


**Figure 3.6:** Knoevenagel mechanism

In the Knoevenagel reaction, it is the malononitrile molecule that interacts directly with the base catalyst, creating an intermediate which the aldehyde then reacts with (**Figure 3.6**). In this chapter we want to understand the steric effects of larger substrates in the polymers, and whilst it is essential that both reagents can easily enter the pore space, by changing the aldehyde as opposed to the malononitrile we aimed to minimise any additional electronic effects. Because of that, a series of increasingly larger benzaldehydes were selected. To accomplish this task, 4-fluoro, 4-methoxy and 4-<sup>t</sup>Bu benzaldehyde were initially chosen (**Figure 3.7**). Apart from being larger than the original benzaldehyde, we selected them as they are all liquids at room temperature, and therefore solubility issues would not need to be considered.

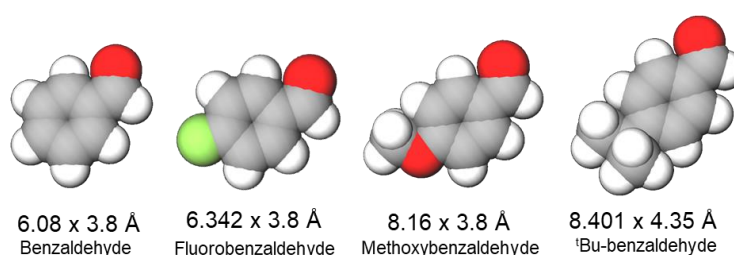


**Figure 3.7:** Model structures of varying benzaldehydes used

It is worth noting that, clearly, we expected that the electronic effect of each R group on the benzene ring would play a role in the reaction, with the electron-withdrawing fluoride likely to increase the performance of the carbonyl in comparison to the more electron-donating

methoxy and tert-butyl groups. We therefore made sure to not only compare a single polymer against all four benzaldehydes, but to test all polymers against each single benzaldehyde, and therefore we can notice trends between the increasingly flexible polymers as well as the increasingly large benzaldehydes. All materials were initially tested with these new benzaldehydes in the typical solvent free 3:1 ratio (benzaldehyde to malononitrile) to allow for direct comparisons with benzaldehyde and the previous part of this work (**Figure 3.8**). As expected, we noticed that in solvent free conditions, the larger the benzaldehyde, the lower the catalytic conversion. This was anticipated as the larger, bulkier benzaldehydes are likely to have more difficulty entering the pores and therefore have reduced contact with the catalytic TB sites.

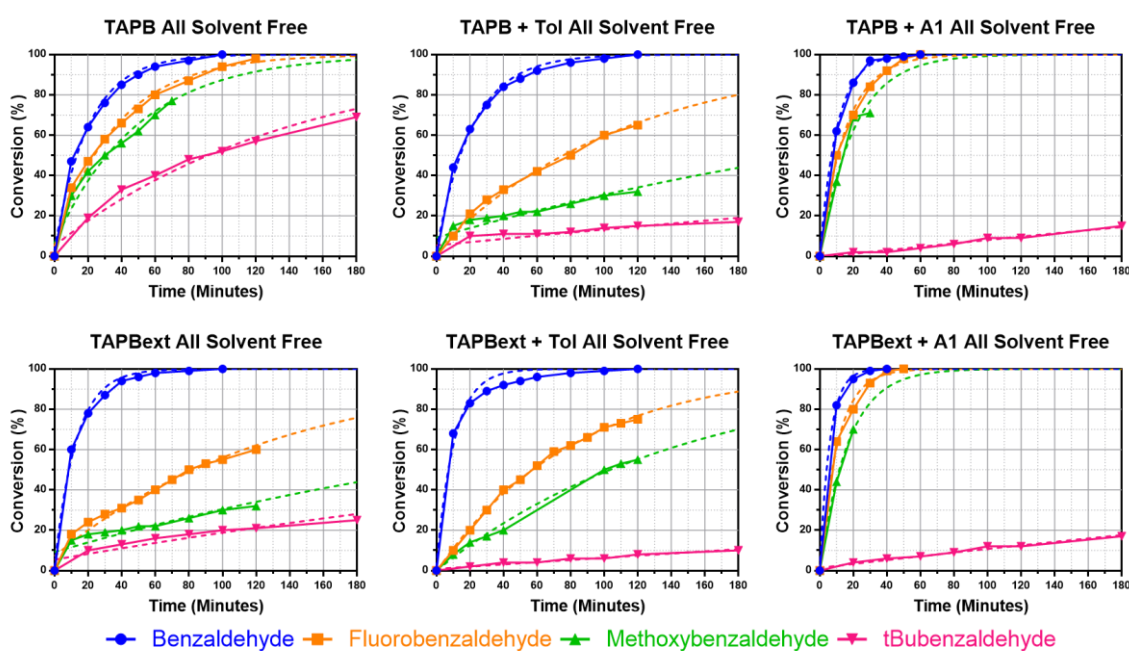


**Figure 3.8:** Catalytic performance using varying benzaldehydes in solvent free conditions

Furthermore, for 4-fluoro and 4-methoxybenzaldehyde, it is possible to see a clear trend of increasing catalytic performance as the polymers became more flexible. In fact, there is minimal difference between the substituted benzaldehydes and normal benzaldehyde for the three most flexible polymers, PIM-TAPB+A1-TB. It is worth mentioning that, under the solvent free conditions, the stirring was impeded as the reaction reached completion due to the lower melting point of the product in comparison to the starting materials. This meant that the

reaction could not reach completion as we expected, not because of the size of the reagents and the hindered accessibility to the pores, but because the reaction environment is not necessarily the most appropriate. Instead of changing these conditions, which have thus far remained consistent to indicate reproducibility and a fair comparison, it was decided to extrapolate the data for these reactions, following the trend of the curve and hypothesising completion. To validate our assumption, we can observe that the extrapolation for the benzaldehyde and *tert*-butylbenzaldehyde, which did not have these stirring issues, showed almost an exact overlap. We can then safely assume that the extrapolated values can be considered reliable. We did not notice much difference between the performance using the fluorinated benzaldehyde and 4-methoxybenzaldehyde, which is noteworthy considering the anticipated electronic differences of the R groups. This would suggest that the electronic effect at play is minimal in these reactions, and it is clear that the polymer catalysts are able to accommodate these larger substrates without much difficulty. To carry on with our test, we aimed to find the best reaction conditions also with bulkier substrates, the reaction was tested in the presence of ethanol using a 1:1 molar ratio of reagents, which are the optimised conditions found using the simplest benzaldehyde (**Figure 3.9**).

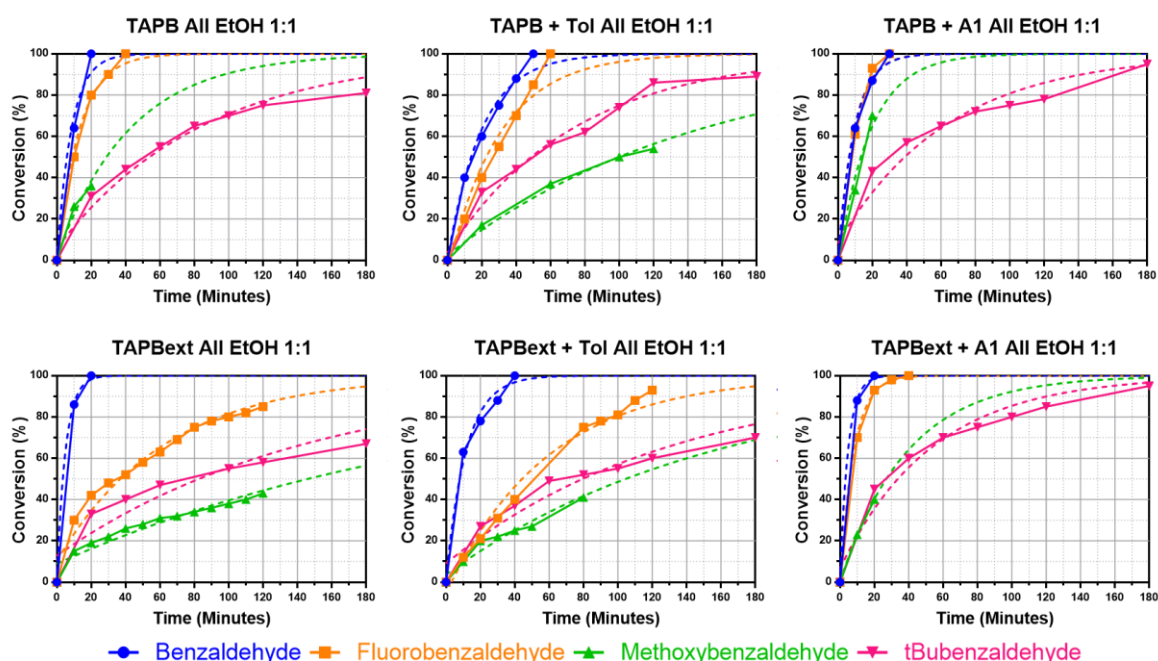


**Figure 3.9:** Catalytic performance using varying benzaldehydes in ethanol

We can see that all catalytic performance improved with the addition of solvent, for both F-benzaldehyde and MeO-benzaldehyde. The solvent also aided the stirring of the fluorobenzaldehyde reaction, though that was still an issue for the methoxybenzaldehyde.

The bulkiest of the four benzaldehydes, 4-<sup>t</sup>Bu benzaldehyde, proved the most difficult to convert, giving low turnovers under solvent free conditions. This was expected, given the size of the substrate and the lack of solvent to facilitate the expansion of the polymer chains. PIM-TAPB-TB, though, was an outlier, giving an impressive 69% conversion after 3 hours, compared to the other polymers which only reached 10-25% completion in the same time frame. This test was repeated, and concurrent results were recorded. It is thought that this may be due to the catalysis happening mostly on the surface of the polymer. As this is the most rigid polymer of the series, it has the highest number of catalytic sites accessible on the outside, as it is less able to compact. In contrast, in the absence of a solvent that increases the swelling ability of the polymer, the more flexible material will naturally compress in on itself to maximise intramolecular forces, meaning that many of the catalytic sites are inaccessible without the aid of a solvent.

To confirm this assumption, we can see from **Figure 3.10** that of all the benzaldehydes tested, the change in performance when the solvent was added was most dramatic when 4-<sup>t</sup>Bu-benzaldehyde was used. Using DCM and a 3:1 ratio, all polymer catalysts achieved >60% conversion, and in ethanol at a 3:1 ratio, all polymers catalysed the reaction to over 80%.

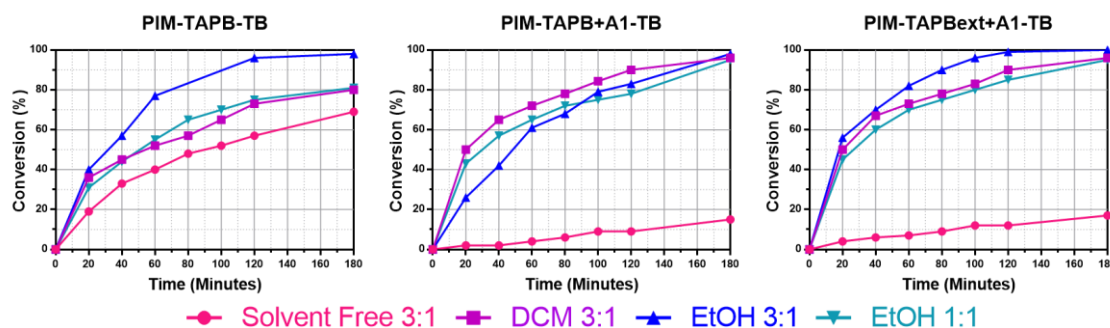


**Figure 3.10:** <sup>t</sup>Bu-benzaldehyde and malononitrile reaction in varying solvent conditions

All polymers performed less well using a 1:1 ratio in ethanol, which would suggest that the larger benzaldehydes may need additional solvation to maximise catalyst potential. To summarise this part, the performance of the most rigid polymer (PIM-TAPB-TB), proved better under solvent free conditions, but the most flexible polymers outperformed it in the presence of a solvent. This further adds to our swellability theory, as the more rigid polymers would be expected to have a smaller change in performance in the presence of solvent, as the solvent will have a lesser impact on the polymer chains. On the other hand, the more flexible chains will be free to move and expand in the presence of a solvent, allowing for an easier access to all catalytic sites.

Looking closely at literature results, there is evidence that ethanol can improve catalysis rates, and we have already confirmed that for our polymers with simple benzaldehyde. It is clear now that ethanol helps the formation and dissolution of the intermediate of the reaction, which improves the final steps of the reaction. In fact, the Knoevenagel reaction between malononitrile and 4-<sup>t</sup>Bu-benzaldehyde in ethanol alone (so, catalysts free) gave around a 10% conversion. This shows that this solvent massively helps the conversion, but it is clearly not enough, as the presence of the catalyst shows a much larger influence on the reaction rates. Whilst we cannot ignore the effect of the ethanol in the Knoevenagel condensation, we can safely assume that it will have the same affect across all the tested substrates, and therefore we can still draw reasonable conclusions from all of our results. It is also clear that the introduction of a solvent to polymers designed to have a degree of flexibility, induces a swelling effect that opens up a large, previously buried, proportion of catalytic sites, which obviously increases the rate of reaction.

### Knoevenagel reaction with even larger benzaldehydes

To further test the size-selective nature of the catalysts, the bulkier 2-naphthaldehyde, biphenyl-4-carboxaldehyde and 9-anthracenecarboxaldehyde were also studied (**Figure 3.11**). All three of these substrates are solid at room temperature, unlike all the previous



benzaldehydes used which are liquid. Therefore, these benzaldehydes could only be tested in solvent conditions.

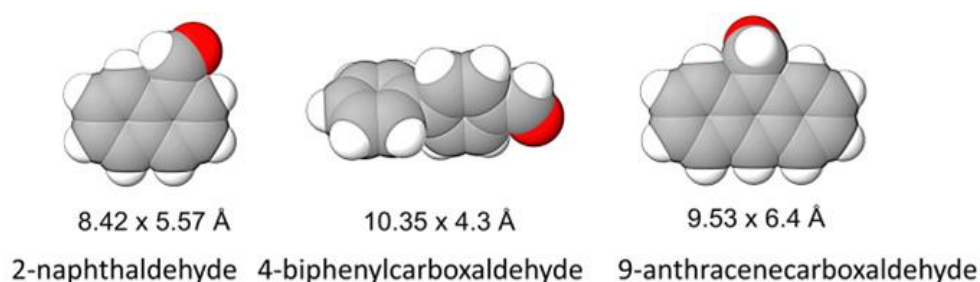


**Figure 3.11:** Larger benzaldehydes

DCM was the only solvent we could use, in this case, as the new substrates are completely insoluble in ethanol. Since we wanted to test the two extremes in terms of swellability, the more rigid, PIM-TAPB-TB and the more flexible PIM-TAPBext+A1-TB were assessed with these larger benzaldehydes, for a direct comparison (**Table 3.4**). PIM-TAPBext+A1-TB gave the best results as follows: benzaldehyde > 2-naphthaldehyde > 4-biphenylcarboxaldehyde > 9-anthracenecarboxaldehyde > 4-tert-butylbenzaldehyde. This shows a general trend of increased catalytic activity with decreased aldehyde size, though clearly there are outliers to this.

**Table 3.4:** Knoevenagel condensation using larger aldehydes, all in DCM

Catalyst (1mol%)	Aldehyde used	Conversion (%) at varying times (mins)			
		30	60	120	180
<b>PIM-TAPB-PIM</b>	Benzaldehyde	20	40	50	55
	t'bu-benzaldehyde	18	29	38	40
	2-naphthaldehyde	18	37	53	60
	4-biphenylcarboxaldehyde	17	29	44	50
	9-anthracenecarboxaldehyde	7	15	23	27
<b>PIM-TAPBext+A1-TB</b>	Benzaldehyde	30	45	73	80
	t'bu-benzaldehyde	18	29	47	60
	2-naphthaldehyde	30	46	74	77
	4-biphenylcarboxaldehyde	22	39	66	70
	9-anthracenecarboxaldehyde	15	26	47	57

For at least two of the benzaldehydes, namely benzaldehyde and tBu-benzaldehyde, DCM is not the best solvent for the reaction (as seen in chapter 2), and this may have a negative

effect. What is clear, though, is that all reactions were far more successful with the more flexible polymer than with the rigid one. The largest substrate tested, 9-anthracenecarboxaldehyde demonstrated a 60% conversion with PIM-TAPBext+A1-TB whereas PIM-TAPB-TB reached only 30%. This, once more, confirms that the opening of pore space in solvent conditions is possible only for more flexible polymers.

### Recyclability Tests

One of the major advantages of heterogeneous catalysis is the relative ease of removal from a reaction, which makes recycling catalysts easier, and therefore improves the sustainability and the economics of a chemical reaction. It is important that a catalyst does not lose performance over time, or at least that it does not show a fast drop. Recyclability tests were performed to assess this potential issue. PIM-TAPBext+A1-TB was studied, as being the most flexible polymer, it was thought it would prove the most difficult to clean and recycle. Similarly, 4-<sup>t</sup>Bu-benzaldehyde was used, as this larger benzaldehyde and the product would be the most difficult to be removed from the pores. The tests were run in the optimised conditions of 1:1 aldehyde to malononitrile in ethanol. After 3 hours, the catalyst was filtered, washed with aqueous ammonia, THF, DCM, and methanol, before drying in a vacuum oven overnight.

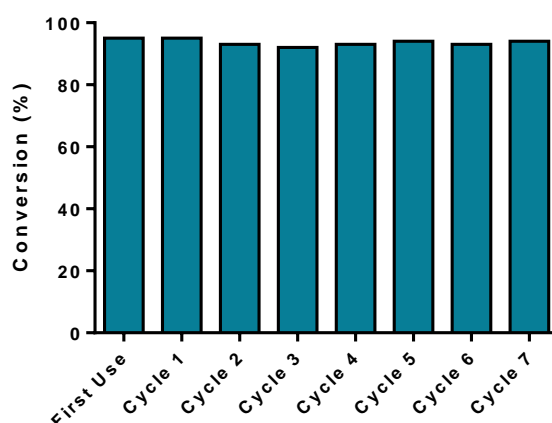


**Figure 3.12:** Conversion of Knoevenagel reaction between <sup>t</sup>Bu-benzaldehyde and malononitrile after multiple cycles using PIM-TAPBext+A1-TB

This procedure was repeated in total 8 times, with no apparent loss in activity – each reaction gave a product yield in the range 89-93%, with the final run giving a 92% turnover (**Figure 3.12**). Washing the catalyst with ammonia is an important step for regenerating the catalysts, as it removes any protons that may stick to the basic TB sites. But even so, this is a very simple and effective workup which demonstrates the stability of these catalysts and their suitability in larger scale settings such as industry.

### Computational Study

To further support the concept of the enhanced swellability of these polymers, and its effect on the catalytic conversions, collaborators from the Institute on Membrane Technology (CNR-ITM) modelled two polymers with varying flexibility and simulated their interactions in the presence of the reagents and the solvent. PIM-TAPB+A1-TB and PIM-TAPBext+A1-TB were modelled as A-B random copolymers, with crosslinking to simulate the networks and pores formed in the physical structures. Solvent molecules and reagents were added to the models to give an increasing level of swelling. 4-<sup>i</sup>Bu-benzaldehyde and malononitrile in a 1:1 ratio was used, as we saw them as the optimum reaction conditions to display the polymer behaviour with this bulky reagent. The study reported a clear trend between the radii of gyration ( $R_g$ , a measure of the degree of polymer chain compacting) and the amount of solvent in the system.

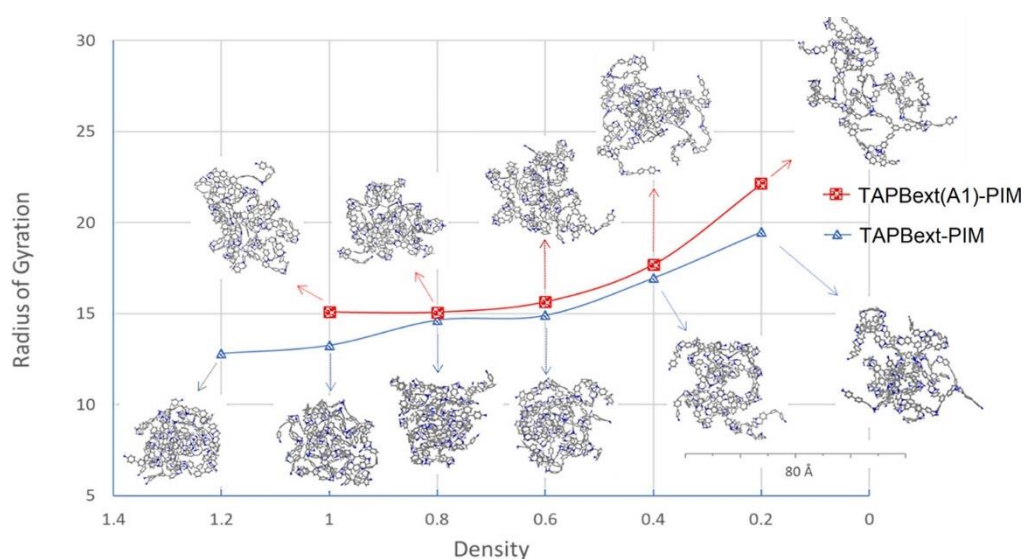


**Figure 3.13:** Changing rate of gyration as solvent is added

The more solvent they added to the calculation, the higher the  $R_g$  value was found to be, and therefore the more open the chains were. This is a clear indication that the solvent and reagents induce a swelling effect in the polymer chains (**Figure 3.13**). Furthermore, it was clear that whilst there is some swelling from the reagents alone, the addition of solvent to the system increases the  $R_g$  value greatly, showing that polymer swelling is particularly favourable in solvent conditions. The computational study was also able to demonstrate that the more flexible polymer, PIM-TAPBext+A1-TB, swells even more than the less flexible PIM-TAPB+A1-TB. Not only is the more flexible polymer consistently less compact than the other in the presence of solvent and reagents, but there is a much larger increase in  $R_g$  values when more solvent is included. The increased free rotation in PIM-TAPBext+A1-TB in comparison to PIM-TAPB+A1-TB, combined with the elongated aromatic geometries, demonstrates that the polymer chains are able to move in the presence of solvent, but also do not completely compact in on themselves without it. This is a very important finding, as we need to reach an optimum between the increase of flexibility and the retention of some porosity.

## Conclusion

In this chapter, the concept of swellability was tested by synthesising a series of increasingly flexible polymers and testing their catalytic performance with a series of increasingly bulky reagents. Firstly, it was shown that the polymers designed to be more flexible had a smaller proportion of micropores, in comparison to the more rigid polymers, which was both anticipated and desired. This resulted in a general decrease in surface area as the flexibility increased, which was also anticipated. All polymers performed better in the presence of ethanol than under solvent free conditions, and whilst this is partly due to the solvation effects of the ethanol alone, it is clear that the polymers themselves change in solvent conditions, and that the enhancement of the conversion rates is predominantly due to the catalyst design. The remarkable results of the more flexible polymers in ethanol versus solvent free using even the bulkiest benzaldehydes is testament to the swellability of the polymer chains. This concept was further proven using computational studies, which

highlighted the link between increased flexibility and a swelling factor. The experimental data then shows the correlation between flexibility and increased catalytic performance. Finally, the recyclability of the polymers was also found to be excellent.

# Chapter 4 - Nitrogen-rich PIM catalysts

## Introduction

So far, we have demonstrated how increasing the degree of flexibility in polymer catalysts can lead to a significant improvement in the rates of the reaction in the presence of a solvent. This was particularly noticeable when using larger reagents, which benefit from swellability of the more flexible polymer chains, as the additional movement allows access to otherwise hidden active sites. We also demonstrated that this increase in flexibility was relatively straightforward to achieve - it is simply a case of synthesising elongated monomers with some degree of flexibility or rotation. By this same process, it is possible to adapt PIM catalysts in other ways. This chapter looks at increasing the number of active sites in a repeating unit by synthesising monomers with multiple nitrogen environments and exploring the effect that this has on the rates of reactions.

## Synthesis

A new selection of polymers was designed for this chapter (**Figure 4.1**). Knowing the effect that the geometry of monomers and co-monomers has in tuning the pore size, we decided to keep the same structural backbone used in previous chapters but, in this instance, we included more basic nitrogen sites, rather than the simple Tröger's base core formed during the polymerisation.

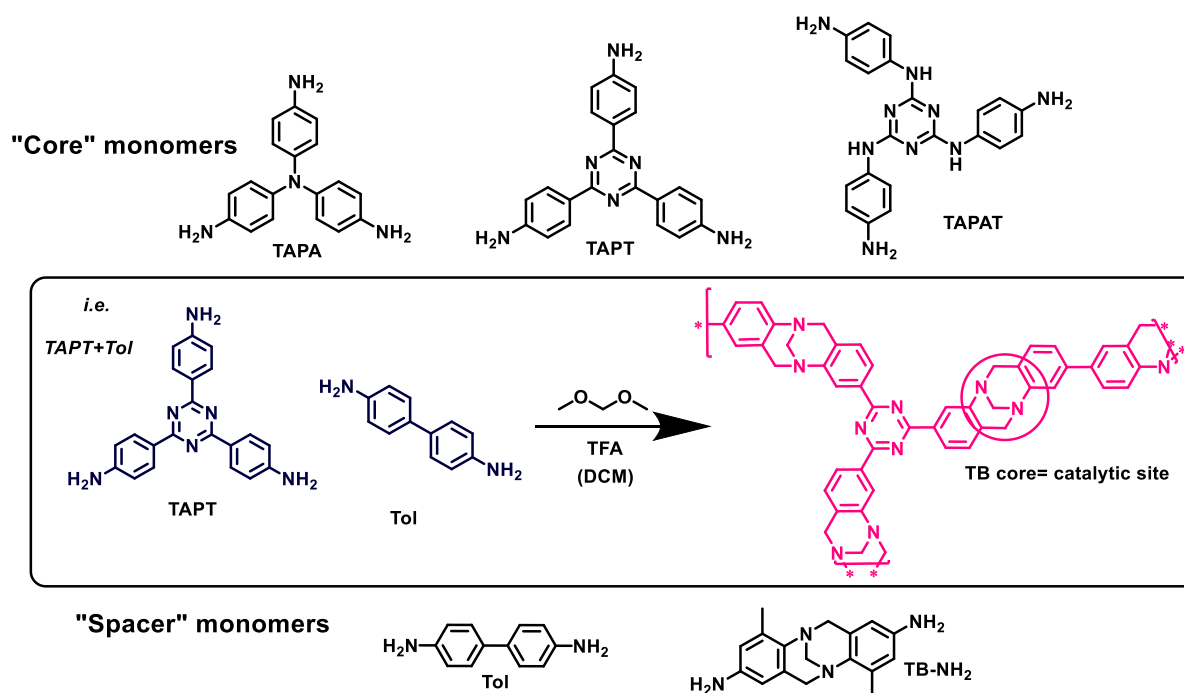


Figure 4.1: Monomers used in chapter 4

The first core monomer chosen was tri(aminophenyl)triazine (**TAPT**), which is structurally very similar to the previously used TAPB but featuring a triazine centre, which therefore introduces extra nitrogen into the structure (**Figure 4.2**). We thought this would allow for an interesting comparison, as there would be relatively little change in the geometry of the polymer, and therefore we can focus more on how the additional basic sites influence the reaction.

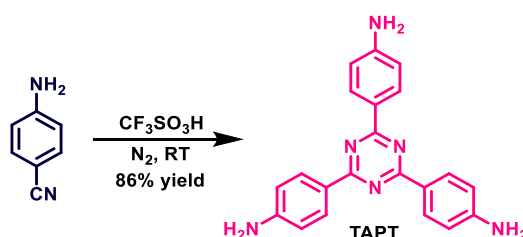
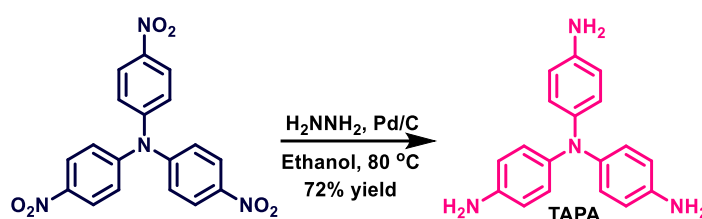


Figure 4.2: Synthesis of TAPT

TAPT was synthesised according to a literature procedure via the one one-step cyclisation reaction of 4-aminobenzonitrile in trifluoromethanesulfonic acid and ethanol under nitrogen.<sup>220</sup> After stirring at room temperature for 24 hours, the neutralised crude product was washed with portions of water to give the desired TAPT as a bright yellow powder in an 86% yield.

Tri(aminophenyl)amine (**TAPA**) was also selected as core monomer as, whilst it is smaller than the aforementioned TAPB and TAPT, the tertiary amine centre provides a different kind of basic site compared to TAPT that we aimed to explore (**Figure 4.3**). In fact, the basic sites at the centre of TAPT are partially stabilised by resonance, which may not confer extra basicity to the system, whereas TAPA has a proper tertiary amine centre that may impart a more significant impact to the catalysis. The trigonal structure is similar to those of TAPB and TAPT, but the geometry around the central nitrogen is likely to provide easier access to the lone pair.



**Figure 4.3:** Synthesis of TAPA

TAPA was synthesised following a literature procedure, where the commercial tris(nitrophenyl)amine was stirred in ethanol in the presence of Pd/C catalyst.<sup>221</sup> To help the reduction of the nitro groups, hydrazine monohydrate was added dropwise and the reaction refluxed overnight. The crude product was recrystallised in ethanol to give blue-grey crystals in a 72% yield.

The final core monomer chosen for this chapter was tri(aminophenyl)aminotriazine (**TAPAT**) which features different nitrogen hybridisation states, so it represents a sort of compromise between the two previous structures (**Figure 4.4**). This monomer bears both the triazine centre, which features in TAPT, as well as additional secondary amine sites linking the triazine to the benzene groups, which is similar to TAPA. These secondary amine sites are expected to provide interesting results, as they typically are more basic than tertiary ones.



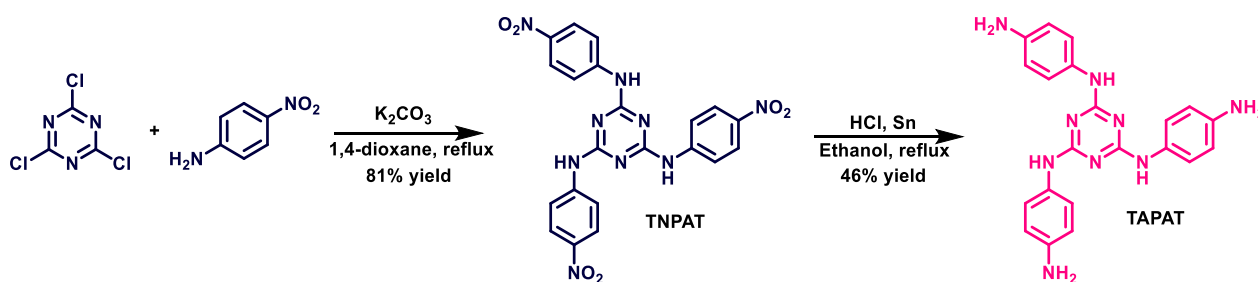


Figure 4.4: Synthesis of TAPAT

The intermediate tri(nitrophenyl)aminobenzene (**TNPAT**) can be synthesised according to a literature procedure via a substitution reaction, where the chlorine groups in cyanuric chloride are replaced with anilines by reacting it with *p*-nitroaniline.<sup>222</sup> The two reagents were stirred in 1,4-dioxane and  $K_2CO_3$  before refluxing at 100 °C for 24 hours. The crude product was washed with water and methanol to give a pale-yellow solid in an 81% yield. TNPAT can then be reduced to form the desired monomer. At first, the method from the paper used to synthesis TNPAT was considered, but the reported yield proved to be rather low, and required a 900% molar equivalent of  $SnCl_2$ , which was not feasible on the scale we required.<sup>222</sup> It was thought that the same method used to synthesise both TAPA and TAPB could be used, whereby the nitrated reagent is stirred in ethanol and Pd/C catalyst, followed by the addition of hydrazine monohydrate, before leaving to reflux. The reaction was monitored by TLC, and after only 3 hours there appeared to be product. However, the desired product of the reaction proved difficult to isolate from the mixture. Another similar method was found that used the same catalysts and reagents but with DMF instead of ethanol, however this also proved unsuccessful.<sup>223</sup> It was then thought to try another reduction method that is commonly used to synthesise anilines. TNPAT was stirred in ethanol and hydrochloric acid in the presence of Sn (0).<sup>224, 225</sup> The reaction was left to reflux for 48 hours. The reaction was filtered and the solid dissolved in hot water, before filtering off the catalyst. The solution was then neutralised, and the crude product collected and washed with water and methanol to give a pale-yellow powder in a 46% yield.

We have already established that flexibility is a great benefit to catalysis, particularly when using larger substrates. In this chapter we chose not to play with this aspect too much,

as we specifically wanted to explore the effects that additional and varied basic sites would have in a catalytic reaction. Spacer monomers are still useful additions to these polymers, to allow easier access to the catalytic sites, so we kept the tolidine co-monomer, but it was decided at this stage to not use the longer A1 (**Figure 3.1, page 51**).

Instead, a second spacer monomer was chosen, 4,10-dimethyl-6H,12H-5,11-methanodibenzo[b,f][1,5]diazocine-2,8-diamine (**TB-NH<sub>2</sub>**) which features a Tröger's base functionality in the molecule, as well as amine sites to further polymerise (**Figure 4.5**). TB-NH<sub>2</sub> is a similar size to that of tolidine, and so it provides a good comparison, and allows us to see the effect that an additional TB site may have on the catalysis performance.

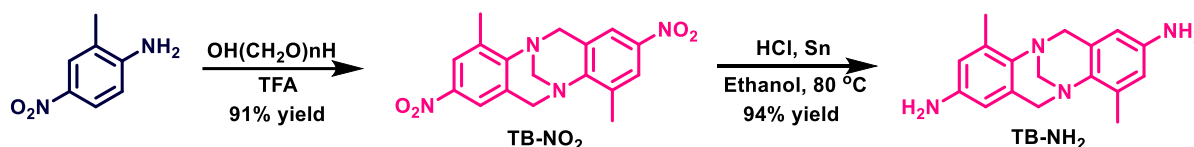


**Figure 4.5:** Synthesis of TB-NH<sub>2</sub>

TB-NH<sub>2</sub> was made according to a literature procedure via a two-step method.<sup>226</sup> First, 2-methyl-4-nitroaniline was stirred in TFA at 0 °C, and paraformaldehyde was gradually added. The presence of the strongly electron-withdrawing nitro group makes the aniline far less reactive towards the formation of the Tröger's base, and for this reason the reaction was left to stir at room temperature for a total of 14 days, until completion. The crude product was recrystallised in acetone to give a yellow powder in a 91% yield. This was then reduced by stirring in ethanol, HCl and Sn, before it was left to reflux at 80 °C for 24 hours to give the final product as a yellow powder in a 94% yield.

These monomers were then combined to make homopolymers and copolymers using the same method used throughout this work and outlined in chapter 2.

## BET Surface Areas and Characterisation

As seen in the previous chapters, all BET surface areas were measured by isothermal adsorption at 273 K using CO<sub>2</sub> as the probe gas (**Table 4.1**).

**Table 4.1:** Surface areas of chapter 4 polymers

Entry	Monomer 1	Monomer 2	Surface Area in CO <sub>2</sub> (273K)
1	TAPT	-	312
2	TAPA	-	420
3	TAPAT	-	160
4	TAPT	Tol	220
5	TAPT	TB	150
6	TAPA	Tol	260
7	TAPA	TB	170
8	TAPAT	TB	285

The surface areas of this series of monomers are all somewhat lower than those seen in the previous chapters. However, as demonstrated throughout this work so far, there is not a strict correlation between surface area and catalytic performance, so it was not cause for concern.

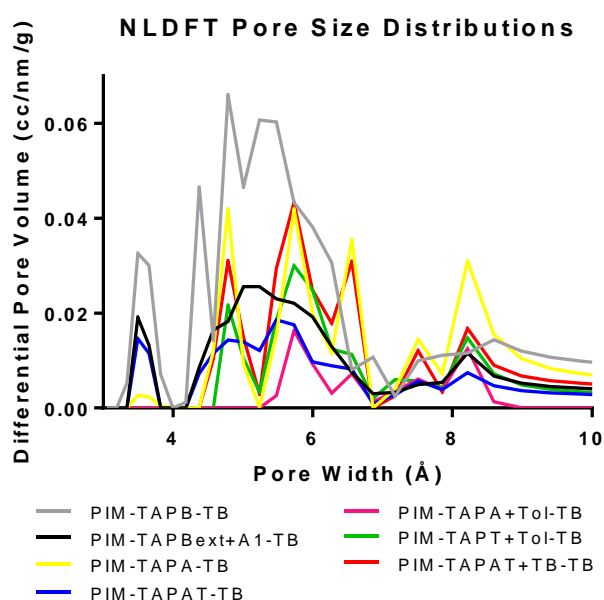


**Figure 4.6:** Pore size distributions

Regarding the pore size distributions (**Figure 4.6**), we can see that this new series of polymers featuring additional basic sites have a much lower proportion of small micropores, even lower

than the most flexible polymer from chapter 3, which means that the portion of ultra-micropores should not negatively influence the catalysis. This could be explained by considering that the basic nature of nitrogens leads to strong intramolecular attraction with hydrogen atoms, meaning that nitrogen-rich polymers often have reduced surface areas as the chains compact together to maximise these forces.<sup>227</sup> Since the selection of monomers feature numerous nitrogen sites with varying hybridisations, it was expected that it would have an impact in the textural properties of the related polymers.

## Results and Discussion

### Catalytic tests

The Knoevenagel reaction was again used to test this new series of polymer catalysts, starting with the solvent free reaction between benzaldehyde and malononitrile in a 3:1 ratio, as we showed in the previous chapters. As **Table 4.2** shows, this new series of polymers did not typically perform as well in solvent free conditions as those from the previous chapter, with the best performance coming from PIM-TAPA+TB-TB, with an over 95% conversion in 1 hour.

**Table 4.2:** Conversions in Knoevenagel reaction - 3:1 benzaldehyde:malononitrile in solvent free conditions

Entry	Catalyst	Conversion (%) at varying times (mins)				
		20	40	60	80	120
<b>1</b>	PIM-TAPA-TB	44	70	83	86	90
<b>2</b>	PIM-TAPA+Tol-PIM	63	84	92	<b>96</b>	<b>100</b>
<b>3</b>	PIM-TAPA+TB-TB	69	92	<b>97</b>	<b>99</b>	
<b>4</b>	PIM-TAPT-TB	51	66	76	85	93
<b>5</b>	PIM-TAPT+Tol-TB	22	56	72	82	89
<b>6</b>	PIM-TAPT+TB-TB	77	88	92	93	<b>96</b>
<b>7</b>	PIM-TAPAT-TB	58	72	84	90	<b>98</b>
<b>8</b>	PIM-TAPAT+TB-TB	22	38	49	60	77
<b>9</b>	PIM-TAT-TB	45	63	74	80	93
<b>10</b>	PIM-TAPB-TB	64	85	94	<b>97</b>	
<b>11</b>	PIM-TAPB+A1-TB	86	<b>100</b>			
<b>12</b>	PIM-TAPBext+A1-TB	<b>95</b>	<b>100</b>			
<b>13</b>	No catalyst				30	
<b>14</b>	TB homogeneous	25	35	54	65	85

Despite the extra basic sites, these polymers provided lower surface areas than previous ones, so this could have had a major influence in the solvent-free performance. We have previously noted how the more flexible polymers can have lower catalytic turnovers without the aid of solvent, as the chains compact in on themselves preventing access to all “buried” catalytic sites and allowing the catalysis to happen only on the exposed surface of the material. Unsurprisingly, a large increase in performance was observed when the reaction was performed in ethanol using a 1:1 ratio of malononitrile:benzaldehyde (**Table 4.3**). Many of the polymers in this series gave results that are comparable to those seen in chapter 3, with the best performing polymers reaching 100% completion in only 20 minutes. Generally, this series of polymers proved to be very similarly to those in chapter 3 although, considering the already excellent performance, we can say that there was not all that much room for improvement.

**Table 4.3:** Conversions in Knoevenagel reaction - 1:1 benzaldehyde:malononitrile in ethanol

Entry	Catalyst	Conversion (%) at varying times (mins)				
		10	20	30	40	60
1	PIM-TAPA-TB	46	66	74	<b>100</b>	
2	PIM-TAPA+Tol-PIM	7	15	23	31	41
3	PIM-TAPA+TB-TB	70	92	<b>100</b>		
4	PIM-TAPT-TB	48	65	80	<b>100</b>	
5	PIM-TAPT+Tol-TB	17	33	44	61	73
6	PIM-TAPT+TB-TB	80	<b>100</b>			
7	PIM-TAPAT-TB	71	<b>100</b>			
8	PIM-TAPAT+TB-TB	75	94	100		
10	PIM-TAPB-TB	64	<b>95</b>	<b>98</b>	<b>100</b>	
11	PIM-TAPB+A1-TB	64	87	<b>95</b>	<b>100</b>	
12	PIM-TAPBext+A1-TB	88	<b>100</b>			

It is noteworthy that those polymers containing the TB monomer (**Table 4.3 entry 3 and 6**) outperform their corresponding tolidine-containing polymers (**entry 2 and 5**). This is an early indication of the increased performance from additional base sites. Next, the polymers were used to catalyse the reaction between <sup>t</sup>Bu-benzaldehyde and malononitrile in a 1:1 ratio in

ethanol (**Figure 4.7**). Impressively, a number of catalysts achieved over 95% conversion in 90 minutes or less, which is roughly half the time it took the best performing polymers in chapter 3. Whilst on one hand this is to be expected, given the higher number of catalytic sites in this new series, these polymers were not necessarily designed to have an increased level of flexibility to accommodate larger substrates. However, from the BET surface area measurements and the pore size distribution graphs, it is clear that a reasonable degree of flexibility in these polymers was still achieved, probably due to the increase in free rotation around some bonds.

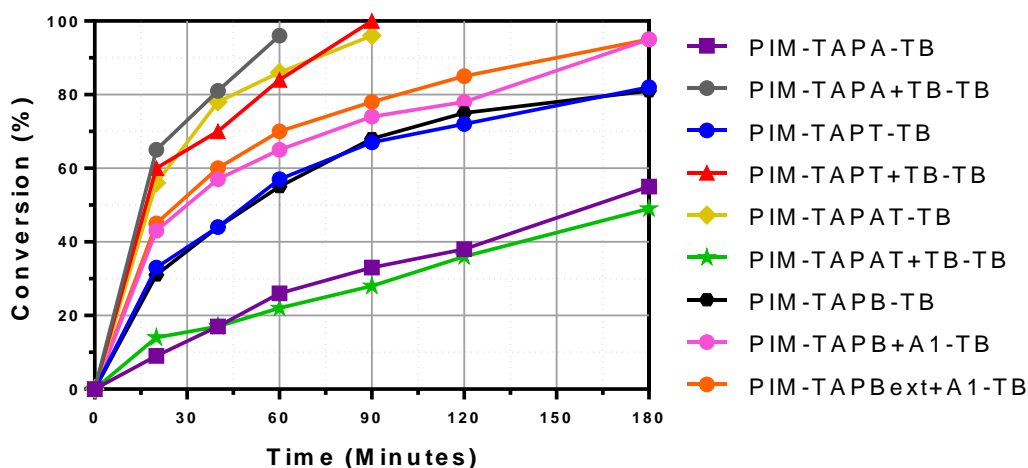


**Figure 4.7:** Conversions in Knoevenagel reaction - 1:1 <sup>t</sup>Bu-benzaldehyde:malononitrile in ethanol

PIM-TAPA+TB-TB and PIM-TAPAT-TB perform best in solvent free conditions with <sup>t</sup>Bu-benzaldehyde, reaching a 32 and 28% conversion respectively (**Figure 4.8**), but there is a huge improvement in the turnover when solvent is introduced into the system.

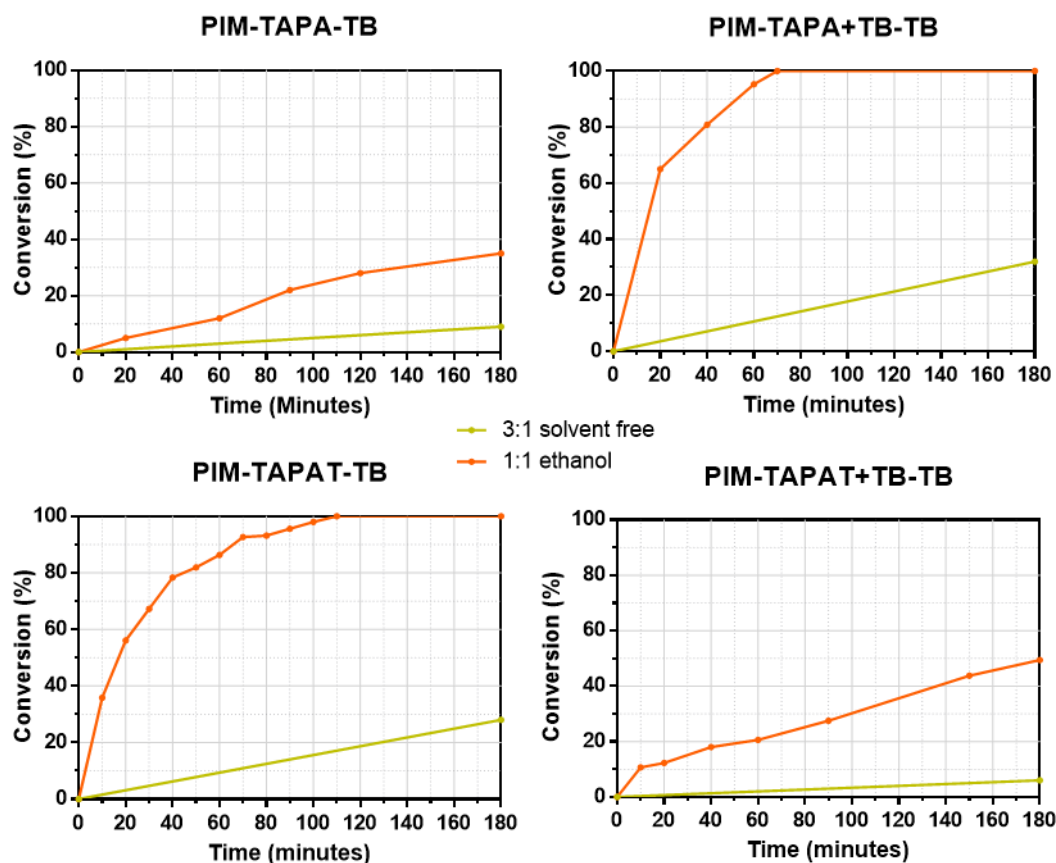


**Figure 4.8:** Performance of polymers with *t*Bu benzaldehyde in solvent free and ethanol conditions

From these findings, it is apparent that the additional nitrogen sites have led to an increased catalytic performance. This is demonstrated by the fact that all polymers containing TB-NH<sub>2</sub> outperform their tolidine counterparts in each reaction.

### Changing the methylene species

As mentioned in chapter 3, in the mechanism of the Knoevenagel reaction between malononitrile and benzaldehyde, it is the malononitrile that interacts with the base catalyst creating a carbanion intermediate that attacks the carbonyl of the aldehyde. Up until now, we have only changed the aldehyde species, to test the flexibility of the polymer catalysts and the size of one of the reagents. With this set of nitrogen-rich polymers, however, it is also very important to understand the effect of the increased basicity of the polymers, and whether this method could be used to design stronger basic catalysts for future catalytic reactions. By altering the methylene species involved in the Knoevenagel reaction, we change the species

that interacts with the catalyst, and therefore we aim for a better understanding of its relative reactivity.

### Methyl Cyanoacetate

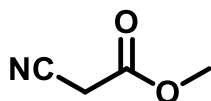


**Figure 4.9:** Methyl cyanoacetate

The first new methylene source chosen was methyl cyanoacetate (**Figure 4.9**), inspired by its use in the literature for similar catalysts.<sup>71, 228</sup> PIM-TAPA-TB was employed to optimise the conditions for this reaction, as it was one of the more mid-range performing catalysts in the previous tests.

**Table 4.4:** Optimising conditions for the reaction between benzaldehyde (A) and methyl cyanoacetate (B) using 1 mol% of PIM-TAPA-TB as a catalyst

Entry	Molar Ratio of Reagents (A:B)	Solvent	Temperature (°C)	Conversion (%)	
				6h	18h
1	3:1	-	25	7	
2	1:1	EtOH (2ml)	25	30	72
3	1:1	EtOH (2ml)	50	45	80
4	1:1	Water (2ml)	50	43	84
5	1:1	EtOH (4ml)	50		84
6	3:1	EtOH (2ml)	50	83	<b>100</b>
7	3:1	EtOH (2ml)	25	52	86

First, benzaldehyde and methyl cyanoacetate were combined in a 3:1 ratio in solvent free conditions and left to stir at room temperature with 1 mol% of PIM-TAPA-TB catalyst. After 6 hours, the reaction had only reached a 7% conversion (**Table 4.4**). The reaction was repeated using a 1:1 ratio of methyl cyanoacetate to benzaldehyde, this time in ethanol. After 6 hours, the reaction had reached 30% conversion, so it was left to stir overnight, whereupon it reached a 72% conversion. Other conditions were tried using the 1:1 molar ratio (**Table 4.4 entries 3-5**), and whilst this led to a slight improvement, the reaction still did not reach completion. It



was decided to try the reaction with an excess of benzaldehyde, as is often done in the literature. With this excess, and heating up to 50 °C, it reached completion in 18 hours. The reaction was repeated under these conditions, sampling every hour, and it was found that it actually reached completion in only 10 hours and not in 18, with an excellent 83% conversion after only 6 hours. The reaction was then repeated using the excess of benzaldehyde, but this time keeping it at room temperature. Whilst an improvement was noted, compared to the 1:1 room temperature reaction, it only reached an 86% conversion after 18 hours, and 52% conversion after 6 hours. Therefore, it was decided that the optimised conditions were those found in **entry 6** of **Table 4.4**. These were then used to test the new nitrogen-enriched PIM catalysts (**Figure 4.10**).

### 3.1 benzaldehyde + methyl cyanoacetate (ethanol, 50 °C)

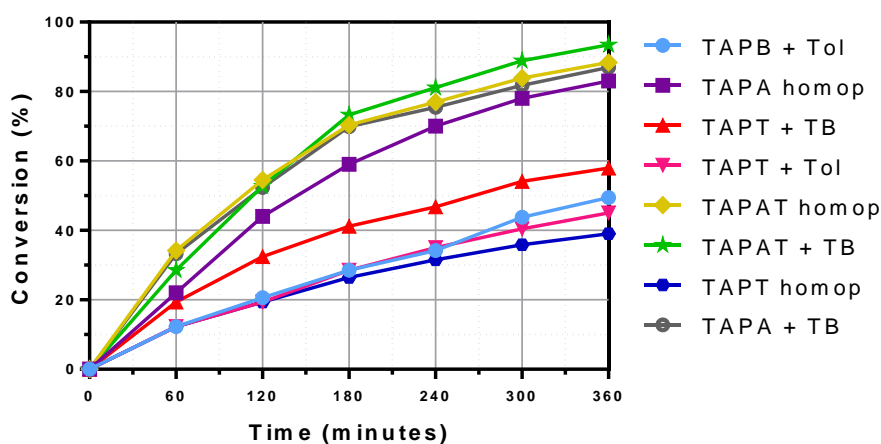
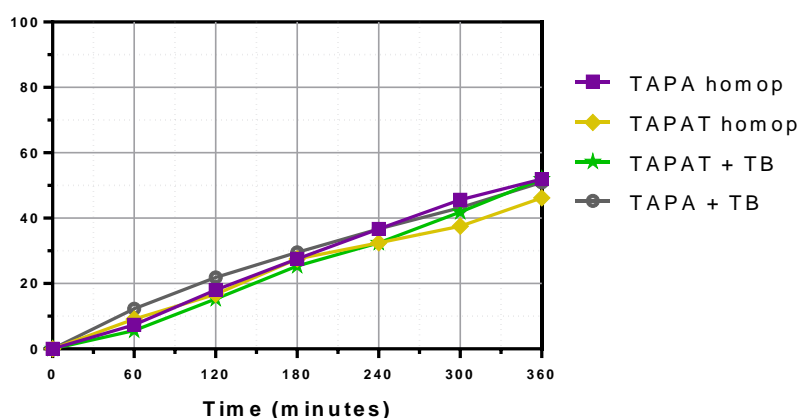


**Figure 4.10:** Performance of polymers in the reaction between benzaldehyde and methyl cyanoacetate at 50 °C

In each instance, once again, the tolidine-containing copolymers are outperformed by their TB counterparts, proving the effectiveness of the extra nitrogen-rich polymers. The best performing material proved to be PIM-TAPAT+TB-PIM, with a conversion of 93% in 6 hours, which is perhaps unsurprising, considering it is the polymer with the most basic sites in its repeating unit. PIM-TAPA-TB, PIM-TAPA+TB-TB and PIM-TAPAT-TB, achieved over 80% conversion in 6 hours. PIM-TAPB+Tol-TB from chapter 3 performed marginally better than PIM-TAPT+Tol-TB, which was a surprising result. These two polymers have very similar geometries, but it was thought that the triazine core would improve the catalytic performance.

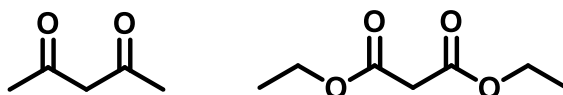
In fact, all three polymers featuring TAPT cores did not perform as well as the others in this series. The triazine core is only weakly basic, and the entire core is actually very electron-withdrawing, this could lead to partial stabilisation of intermediates with loss of activity.<sup>229</sup> The top four polymers were tested at room temperature over the same time frame (**Figure 4.11**), and all of them performed very similarly, achieving around a 50% conversion in 6 hours.

### 3.1 benzaldehyde + methyl cyanoacetate (ethanol, 25 °C)



**Figure 4.11:** Performance of polymers in the reaction between benzaldehyde and methyl cyanoacetate at 25 °C

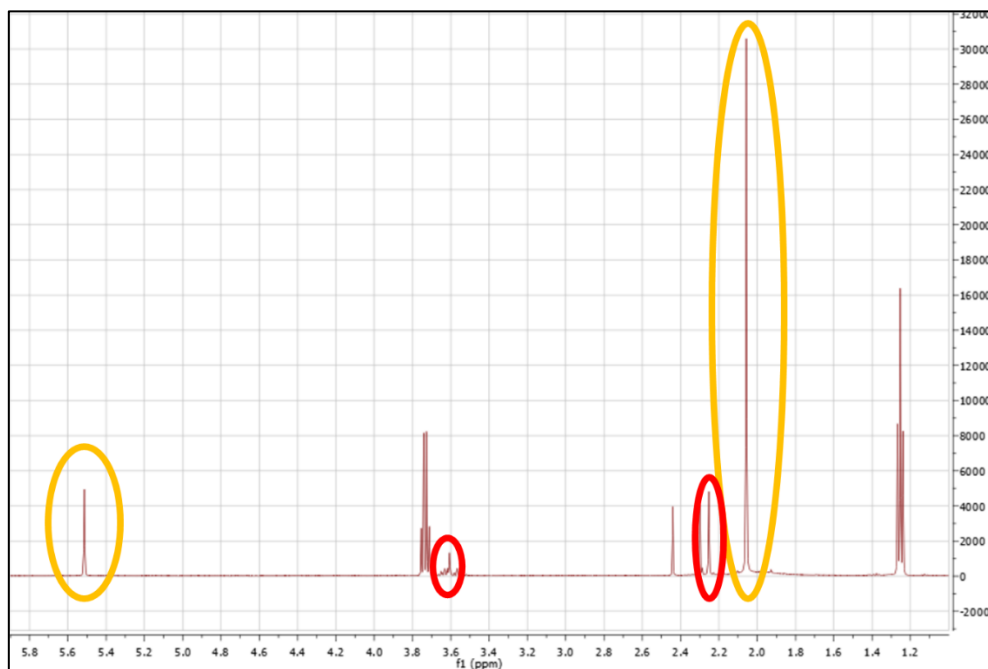
### Acetylacetone and Diethyl Malonate



**Figure 4.12:** Acetylacetone and diethyl malonate

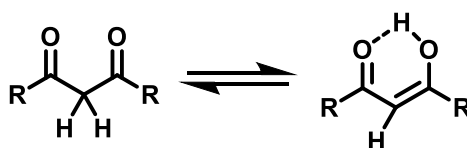
Following on from the success with methyl cyanoacetate, more methylene species were tested in the Knoevenagel reaction. Acetylacetone and diethyl malonate (**Figure 4.12**) were chosen due to the more acidic nature of the methylene protons.<sup>230</sup> The optimised conditions found for the reaction with methyl cyanoacetate were first used with both reagents (**Table 4.5 entries 1 and 2**). However, both these reactions proved to be unsuccessful, as there was no evidence of desired product according to the <sup>1</sup>H NMR analysis. Strangely, though, only a very small peak in both spectra was connected to the methylene starting materials. Whilst the benzaldehyde is in excess in the reaction, previous <sup>1</sup>H NMR analysis

have always shown a significant peak associated with the methylene protons around 3.6 ppm when the reaction was not completed. However, for example with acetylacetone in **Figure 4.13**, there is only a small peak around this area (highlighted in red). There is also a large, unexpected peak at around 2.05 ppm.



**Figure 4.13:** NMR of reaction between benzaldehyde and acetylacetone

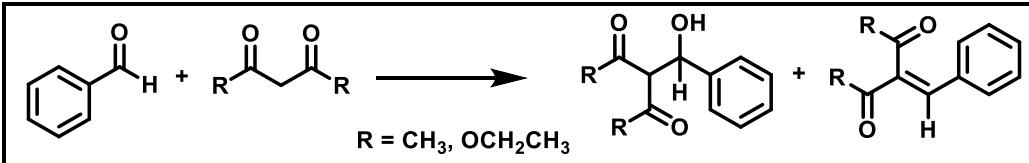
Due to the presence of two carbonyl separated by a methylene, it is obvious to expect that the methylene may tautomerise. A quick search of the literature that tackled the same reactions, confirmed that both acetylacetone and diethyl malonate undergo tautomerisation, and they can also exist as the related enols (**Figure 4.14**).<sup>231, 232</sup> Although under basic conditions the enol should be as nucleophilic as the related methylene, it is clear that in this case it prevents the reaction with benzaldehyde. It is plausible that the pseudo-six-member ring, formed by the hydrogen bonding of the proton of one enol and the neighbouring carbonyl, as shown in **Figure 4.14**, may stabilise the intermediate making it less reactive in our conditions.



**Figure 4.14:** Tautomerisation of methylene species

There was also a concern that the reaction conditions were not entirely appropriate for these reagents, and so it was next decided to follow a method from the literature.<sup>230</sup> The reactions were then attempted at room temperature in DCM, hoping that the aprotic solvent would reduce the tautomerism, but this had no effect. It was then noted that more polar solvents would promote the keto form.<sup>233, 234</sup> Up until this point, all <sup>1</sup>H NMR samples had been taken in chloroform, and so the deuterated solvent was changed to DMSO-d<sub>6</sub>. Whilst there was a small increase in the keto-peak, the enol peak was still dominant. The reaction was repeated in water at 50 °C, but this was unsuccessful, and there was still clearly a majority of enol-product. The temperature was decreased to room temperature, but this also had no effect.

**Table 4.5:** Conditions tested for the reaction between benzaldehyde (A) and methylene species (B) – either acetylacetone (R=CH<sub>3</sub>) or diethyl malonate (R=OCH<sub>2</sub>CH<sub>3</sub>), using 1 mol% of PIM-TAPAT+TB-TB as a catalyst

				
Entry	R group	Molar Ratio of Reagents (A:B)	Solvent (2ml)	Temperature (°C)
1	CH <sub>3</sub>	3:1	EtOH	50
2	OCH <sub>2</sub> CH <sub>3</sub>	3:1	EtOH	50
3	CH <sub>3</sub>	3:1	DCM	25
4	OCH <sub>2</sub> CH <sub>3</sub>	3:1	DCM	25
5	CH <sub>3</sub>	3:1	Water	50
6	OCH <sub>2</sub> CH <sub>3</sub>	3:1	Water	50
7	CH <sub>3</sub>	3:1	Water	25
8	OCH <sub>2</sub> CH <sub>3</sub>	3:1	Water	25
9	CH <sub>3</sub>	3:1	MeOH	25

These results were difficult to explain – the series of polymers tested were all proven to be catalytically active in similar reactions, and yet here they were proving unsuccessful. It has widely been understood that Tröger's base is a strong enough base, and therefore it should not have difficulty attracting the acidic methylene protons. According to Liu *et al.*, strong bases can lead to reactions at the methyl sites of acetylacetone,<sup>235</sup> but there was no evidence

of this product in the spectra either. These results led us to further explore the basicity of this series of polymers.

### pH and the Henry Reaction

An indication of the degree of basicity was key to understanding the reactivity of these polymers and therefore gauge the types of reactions that would be successful in the future. The polymers were stirred in methanol and then tested using a pH meter, but unfortunately the readings read around 4.5, which is the expected pKa of TB-PIMs,<sup>236, 237</sup> but it is also the same as pure methanol. A back titration experiment was then set up, whereby a known amount of polymer was stirred in a 1 molar solution of hydrochloric acid for 5 minutes. This mixture was then titrated against a 1 molar sodium hydroxide solution, but this experiment was also unsuccessful. As all our polymers are heterogeneous and insoluble, it makes measuring the pH and therefore pKa of these materials particularly difficult, and specialist techniques are required. We have submitted samples to collaborators who specialise in electrochemistry, who will be able to accurately measure the pKa of these materials. Instead, we hoped to get a qualitative measure of basicity – how basic each polymer in this series was in relation to one another. The Henry reaction between nitromethane and benzaldehyde was used to try and measure this relative basicity (**Figure 4.15**).

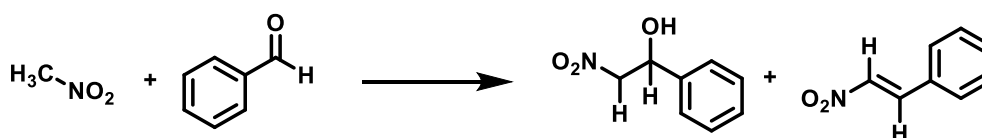


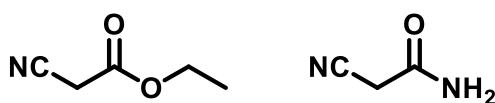
**Figure 4.15:** Henry reaction between nitromethane and benzaldehyde

The Henry reaction follows the same mechanism as the Knoevenagel reaction, and is still base-catalysed, but specifically between nitroalkanes and carbonyl compounds,<sup>238</sup> though it follows the same mechanism as the Knoevenagel reaction. PIM-TAPA+TB-TB was tested as a catalyst in the reaction between benzaldehyde and nitromethane, using similar optimised conditions to those used for methyl cyanoacetate – using 1 mol% of catalyst with a 3:1 ratio of benzaldehyde to nitromethane, in ethanol and heating to 50 °C. There was no reaction after

24 hours, so the reaction was repeated at 75 °C, but this also had no effect. The solvent was changed to water to increase the polarity,<sup>239</sup> and the temperature increased to 95 °C, but there was still no improvement. It was thought that the addition of an electron withdrawing group in the para position of the benzaldehyde would improve the reactivity of the species and help drive the reaction. Nitrobenzaldehyde and nitromethane were combined in a 5:1 ratio using ethanol as a solvent at 70 °C, but after 24 hours there was still no effect. The reaction was tried using 10 mol % catalyst and a 10:1 ratio of nitrobenzaldehyde to nitromethane, and a 10:1 ratio of nitromethane to nitrobenzaldehyde, but none of these changes had any effect on the result.

The question at this point of the study was why is it that certain reagents work, and others do not? It cannot simply be the case that these materials are not catalytic enough, because we have seen such positive results in other similar reactions. We are also confident that it cannot be a steric problem, given our findings in chapter 3. Looking at those that worked - malononitrile and methyl cyanoacetate, both contain cyano groups adjacent to the methylene protons. So, other reagents with this functionality were tested.

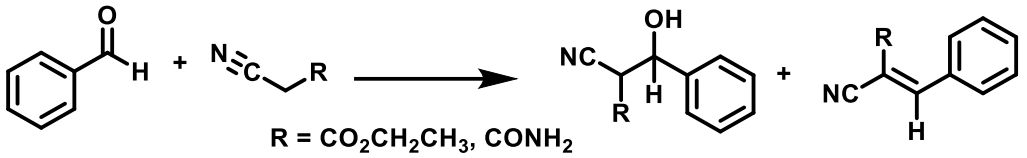
### Ethyl Cyanoacetate and Cyanoacetamide



*Figure 4.16: Ethyl cyanoacetate and cyanoacetamide*

Both of the new reagents chosen to test the Knoevenagel reaction were selected based on their use in the literature,<sup>240, 241</sup> but predominantly because of the presence of the cyano group (**Figure 4.16**). Both new reagents were tested under the optimised conditions found with methyl cyanoacetate and using the best performing polymers from this test. As **Table 4.6** shows, the reaction was successful with both species.

**Table 4.6:** Results of the Knoevenagel reaction between benzaldehyde and varying methylene species (3:1) at 50 °C in ethanol

					
Methyl Species	Catalyst (1 mol%)	% Conversion after x time			
		2h	4h	6h	24h
<b>Ethyl Cyanoacetate</b>	PIM-TAPA-TB	29	53	65	94
	PIM-TAPA+TB-TB	32	44	60	90
	PIM-TAPAT-TB	32	58	70	<b>97</b>
	PIM-TAPAT+TB-TB	23	44	61	<b>98</b>
<b>Cyanoacetamide</b>	PIM-TAPA-TB	23	40	50	78
	PIM-TAPA+TB-TB	32	44	57	74
	PIM-TAPAT-TB	40	59	71	89
	PIM-TAPAT+TB-TB	27	52	63	82

Each polymer tested reached at least a 50% conversion after 6 hours with both methylene species, which is lower than we saw for methyl cyanoacetate, though this was somewhat expected given the relative sizes of these molecules (**Figure 4.17**).

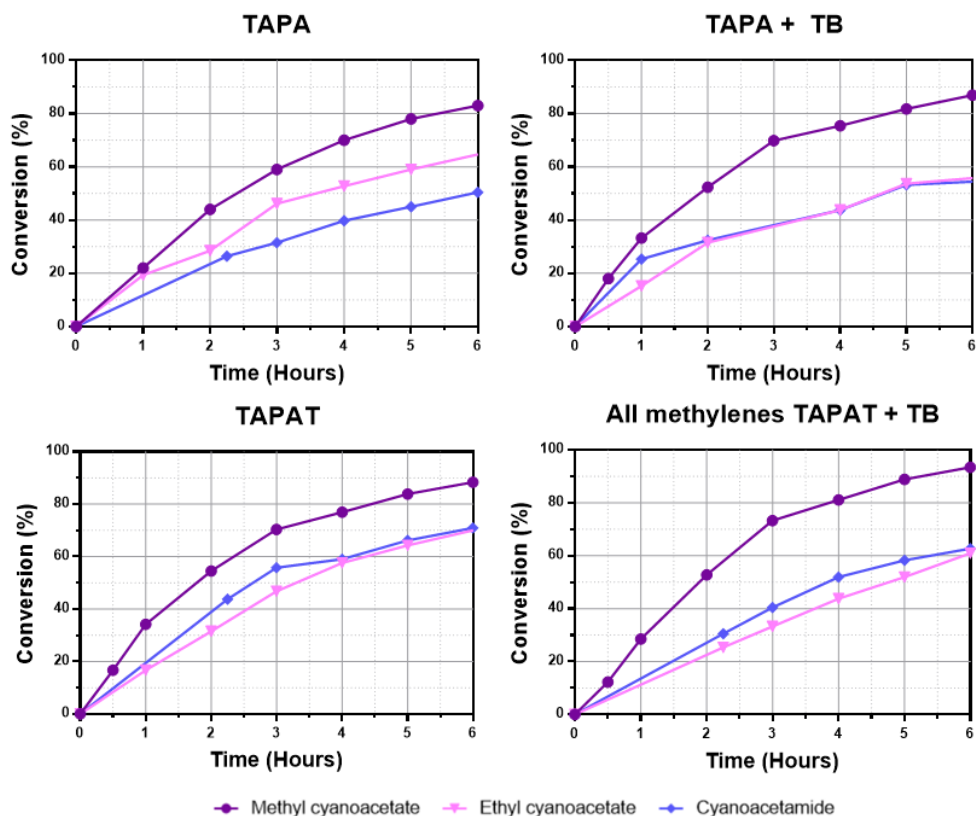


**Figure 4.17:** Performance comparisons with varying methylene species

Each polymer showed little difference between ethyl cyanoacetate and cyanoacetamide over a 6-hour time period, but over 24 hours, ethyl cyanoacetate proved a better reagent. That the acetoamide is the least reactive is not surprising, since it is well known that the nitrogen next to the carbonyl stabilises it by resonance, making it less electrophilic. This, in turn, makes the alpha protons less acidic and, so, less available to be removed by the base catalyst to initiate the reaction. This means that overall, the conversion for methylenes by this series of polymers was: malononitrile > methyl cyanoacetate > ethyl cyanoacetate > cyanoacetamide.

These results are positive demonstrations of the potential of these catalysts, but there is still uncertainty around why these cyano-containing reagents work and the other methylenes tested do not. A search of the literature did find some other cases where only cyano-containing methylenes were successful.<sup>242, 243</sup> Yadav *et al.* suggest an alternative mechanism to the reaction which supports these findings (**Figure 4.18**).

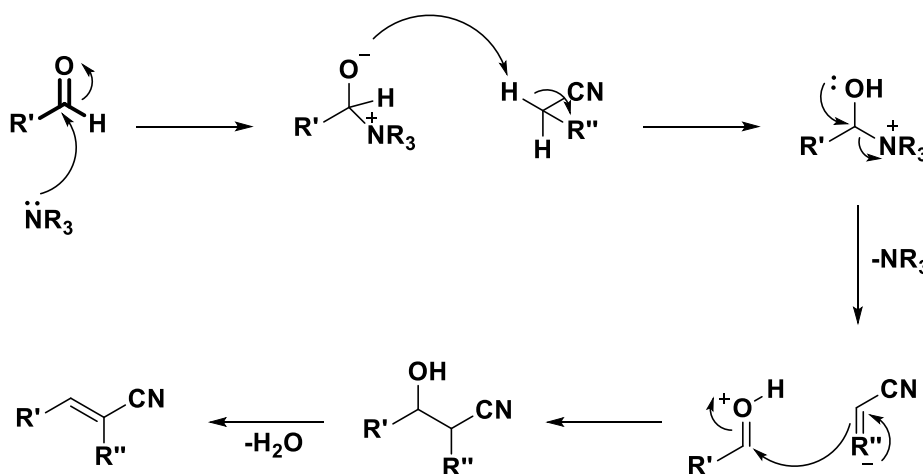


**Figure 4.18:** Proposed mechanism

Up until now, it was assumed that the base catalyst deprotonates the methylene, which subsequently reacts with the aldehyde (**Figure 3.6, page 59**).<sup>244</sup> This led to confusion when the results with acetylacetone and diethyl malonate did not work, as the methylene protons should be as acidic, if not more, than those of malononitrile. It is understood that this reaction is possible with even weakly basic catalysts, which can cause the formation of the enolate on the methylene species. This mechanism is unlikely, given it would take a very strong base to



enolise the benzaldehyde,<sup>245</sup> given its lack of alpha protons, but it is noteworthy that others have found similar issues.

## Conclusion

In this chapter, we have demonstrated the ease with which new functionalities can be added to polymers, and the positive impact these can have on the catalytic performance. The presence of additional catalytic sites leads to an increase performance in the Knoevenagel reaction between malononitrile and substituted benzaldehydes. The polymer catalysts were also tested with various methylene species, and we found that the polymers with the TAPAT cores performed best. This was to be expected, as they were the most nitrogen rich of the entire set and featured secondary amine sites, which are thought to be more basic. TAPA-cored polymers also performed very well, whilst TAPT polymers underperformed in comparison to their TAPB counterparts. Whilst there were some successful results, there were also some conflicting and confusing findings, with many methylene species not reacting at all with the aldehyde. Particularly strange was that the reagents that did not work are those we considered to contain the most acidic methylenes. The reason for this is still not fully understood, we suspect there is a problem with the tautomerism of the reagents, and there is also a possibility that the reaction may take place via a different mechanism altogether. We anticipate that the additional nitrogen sites have increased the basicity of the polymers, though we were unable to establish pKa values for the polymers because of their insoluble nature. We have sent samples to collaborators to establish their pH values, and we hope this will lead to further explanation of the results from this chapter.

# Chapter 5 - CO<sub>2</sub> Utilisation Reactions

## Introduction

In previous chapters, novel PIM catalysts have exclusively been used for the Knoevenagel reaction. Whilst this is an excellent starting point for testing base catalysts, the scope of this reaction has limited industrial applications.<sup>228</sup> In the final parts of this thesis, a series of PIMs will be tested in reactions which have real industrial potential.

In line with the Paris Agreement, the UK government has set a target of reaching 'Net Zero' by 2050.<sup>246</sup> This refers to achieving a perfect balance of greenhouse gas emissions – so for every amount of greenhouse gas emitted, an equal amount is removed from the atmosphere, which aims to slow down global warming. This target is very ambitious and requires huge advancements in the carbon capture technology in a short space of time. This clearly would lead to the accumulation of the excess of captured CO<sub>2</sub> gas and, whilst storage technologies already exist, they are costly and wasteful. Therefore, the reutilisation of CO<sub>2</sub> represents an equally important technology to develop and an increasingly interesting research field. Because of that, we decided to test our polymers as catalysts for CO<sub>2</sub> conversion/utilisation reactions.

## Initial Experiments

One of the most popular CO<sub>2</sub> utilisation reactions, showed in previous works, is the cycloaddition of CO<sub>2</sub> into epoxides to make cyclic carbonates (**Figure 5.1**). This reaction can be used to create valuable feedstocks for a variety of reactions including pharmaceuticals, fuels, and industrial chemicals, all whilst reusing capture greenhouse gases that otherwise

would be wasted.<sup>247</sup> As with the Knoevenagel condensation, this reaction is often base catalysed so our TB polymers could prove good materials for this application.

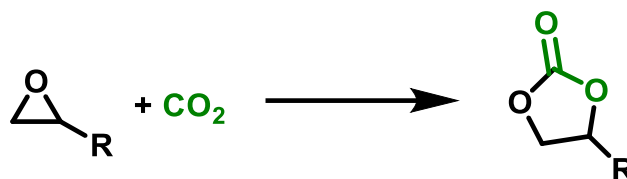


**Figure 5.1:** CO<sub>2</sub> cyclisation reaction

The first experiment that we decided to test was the cycloaddition of CO<sub>2</sub> into epichlorohydrin (where R = CH<sub>2</sub>Cl), as it is a common procedure found in the literature. When looking at the previous works, the majority of CO<sub>2</sub> utilisation reactions take place in a reactor, where a stoichiometric amount of CO<sub>2</sub> can be used in a pressurised and controlled environment. Unfortunately, those resources were not directly available in our lab, and so an alternative method was needed to test the reaction. We therefore set up the reaction using a balloon inflated with pure CO<sub>2</sub>, and a needle and septum to transfer the gas into the reaction.<sup>248, 249</sup> To increase the efficiency of the reaction, in combination with a porous polymer that helps the trapping of the CO<sub>2</sub>, a co-catalyst is commonly used in these experiments.<sup>250</sup> Probably the most widely used is the tetrabutylammonium bromide (TBAB), which helps in the ring opening of the epoxide which starts the formation of the cyclic carbonate (**Figure 5.2**).

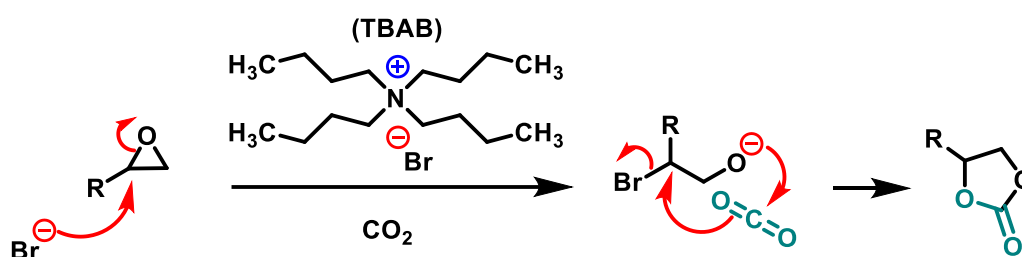


**Figure 5.2:** Tetrabutylammonium bromide and the formation of cyclic carbonate

In our experiments, 0.5 mol% of TBAB was used, as well as 1 mol% of the best performing polymer from previous chapters, PIM-TAPAT+TB-TB, to test the performance of the neutral TB core. The catalysts were stirred in epichlorohydrin and ethanol in a narrow test tube with a

rubber septum. The tube was purged with CO<sub>2</sub> for five minutes, and then held in a CO<sub>2</sub> atmosphere for 3 hours at 70 °C (**Figure 5.3**).



**Figure 5.3:** Reaction set up for CO<sub>2</sub> cyclisation reactions

Unfortunately, the reaction proved to be unsuccessful. The solvent was then changed to water, to increase the polarity of the reaction, and the temperature increased to 90 °C, but there was still no effect. We wanted to use a solvent as we know this improves the performance of our catalysts (chapters 2-4), but this clearly limited the temperature range of the reaction. We therefore chose to try the reaction solvent-free at 120 °C, which was reported in several literature procedures.<sup>251</sup> Using this temperature, and bubbling CO<sub>2</sub> directly into the reaction mixture, we managed to achieve an 85% conversion in 3 hours (**Table 5.1**). For comparison, PIM-TAT-TB was also tested in this reaction. As this is the least flexible polymer prepared in this project, it was thought it may perform well in solvent free conditions as has been noted throughout this work thus far. Again using 1 mol% of PIM-TAT-TB with 0.5 mol% TBAB, the reaction reached 80% conversion in solvent free conditions. These results were initially very positive, though they were both in the presence of the cocatalyst. The reaction was then tested using only 0.5 mol% of TBAB, which gave a 61% conversion in 3 hours. This demonstrates that whilst the polymer catalysts did improve the conversion, the increase was only in a 20-25% range. Nevertheless, this represents an encouraging result, as the reaction with TBAB

alone requires a further two hours to reach a similar conversion, which on a small scale may seem insignificant but on an industrial scale would amount to a large energy saving.

**Table 5.1:** Results of the cycloaddition of CO<sub>2</sub> into epichlorohydrin at 120 °C

Entry	Catalyst Used (1 mol%)	Cocatalyst (0.5 mol%)	Percentage Conversion (%)	
			3h	5h
1	-	-		0
2	-	TBAB	61	79
3	PIM-TAT-TB	-		5
4	PIM-TAT-TB	TBAB	80	
5	PIM-TAPAT+TB-TB	-		6
6	PIM-TAPAT+TB-TB	TBAB	85	
7	PIM-TAPBext+A1-TB	-		0

The reaction was repeated using only the polymer catalysts and was also tested using the most flexible polymer PIM-TAPBext+A1-TB without TBAB present in the reaction environment. Unfortunately, this polymer only achieved a 0-6% conversion over a 5-hour period. It is thought that a porous framework may act as a supporting material, aiding the reaction of the TBAB catalyst by providing enclosed pore space to increase collisions, but that the TB catalytic sites themselves are perhaps not active enough to act alone. We then considered altering the structure of our polymers by making it similar to the structure of TBAB, which features a quaternised ammonium. In fact, it would be possible to achieve the quaternisation of the Tröger's base core of our polymers, and this could lead to the desired enhancement of the catalytic activity.

## Synthesis

Through post-polymerisation functionalisation, we looked to quaternise the TB sites of PIM-TAT-TB. This polymer was chosen as it is the most rigid polymer of the series with the highest surface area and the most well-defined pore space. This is crucial and yet in contrast with what we wanted to achieve in the Knoevenagel condensation. In fact, in this case, the different reagents are all small in size, and the CO<sub>2</sub> is a gas, so we preferred to use the polymers which showed the highest amount of ultra-micropores over the ones with enhanced

flexibility and larger pore size. These features were considered advantageous to hosting anions, especially when the reaction takes place in solvent free conditions.

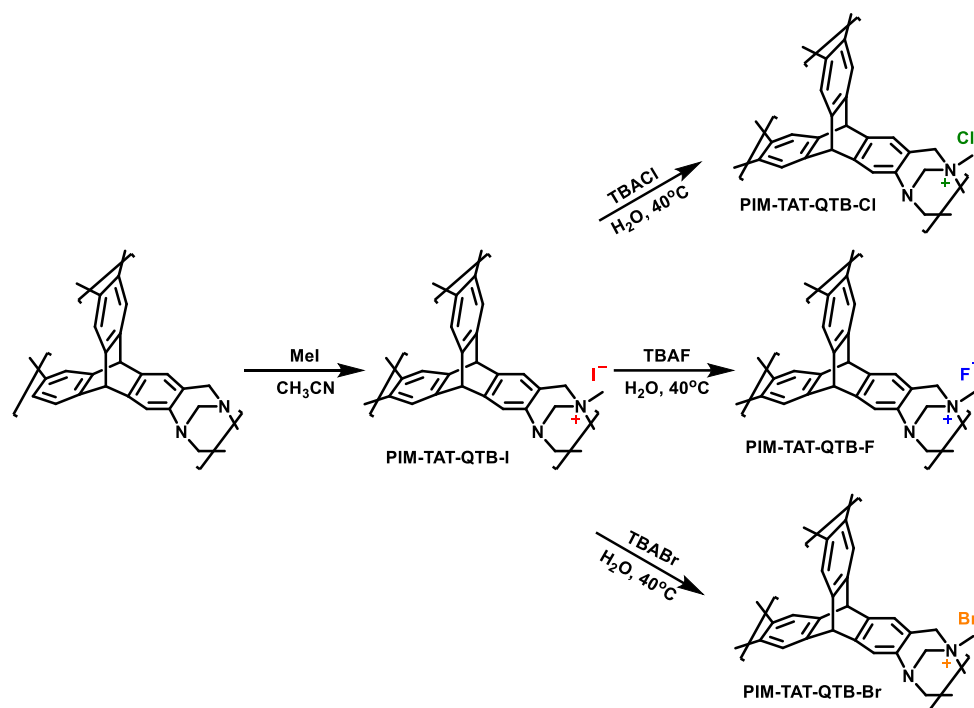


**Figure 5.4:** Synthesis of quaternised PIM-TAT-TB, and ion exchanges

PIM-TAT-TB was stirred in an excess of methyl iodide in acetonitrile for 72 hours at room temperature to give PIM-TAT-QTB-I (**Figure 5.4**). In order to compare the performance with different counterions, ion exchange reactions were performed on PIM-TAT-QTB-I. This could reveal important considering that the iodide is a very large counterion and this would lead to loss of porosity, whereas a smaller anion may help retaining part of it. The quaternised polymer was stirred in deionised water and the respective tetrabutylammonium halide (-Cl, -F, -Br) was added in excess. Each mixture was stirred at 40 °C for a week providing PIM-TAT-QTB-Cl, PIM-TAT-QTB-F, and PIM-TAT-QTB-Br.

### TGA of Quaternised Polymers

To confirm the complete ion-exchange, we performed TGA analysis on the new materials. Each quaternised polymer showed a mass loss starting around 150 °C, which we related to the loss of the counterion. By measuring the percentage of the mass loss against

the original weight of the repeated unit, it is possible to see whether the ion exchange has been successful and quantify it.

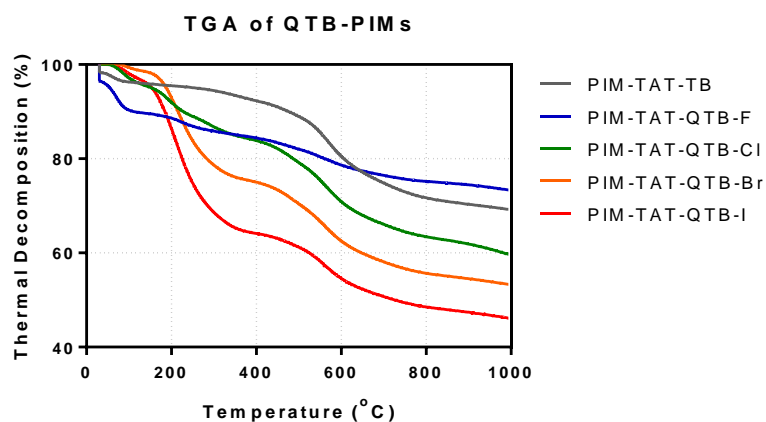


**Figure 5.5:** Thermal decomposition of PIM-TAT-TB and the related quaternised polymers

**Figure 5.5** shows the thermal decomposition of all the quaternised polymers, as well as PIM-TAT-TB for comparison. For QT B-TAT-PIM-I, we recorded a 28% mass loss in the range of 150-350 °C, which corresponds to the 28% by mass of iodine in the repeated unit of the polymer that we expected for a full quaternisation. Similarly, a 5% mass loss was noticed for QT B-TAT-PIM-F, a 10% mass loss for QT B-TAT-PIM-Cl, and a 20% mass loss for QT B-TAT-PIM-Br. We were pleased to confirm that, for all of the attempted experiments, we could match the expected percentage of halogen species in each polymer's repeated unit. Therefore, it is clear that the ion exchanges were highly successful for all TB-PIMs.

### BET surface areas of Quaternised Polymers

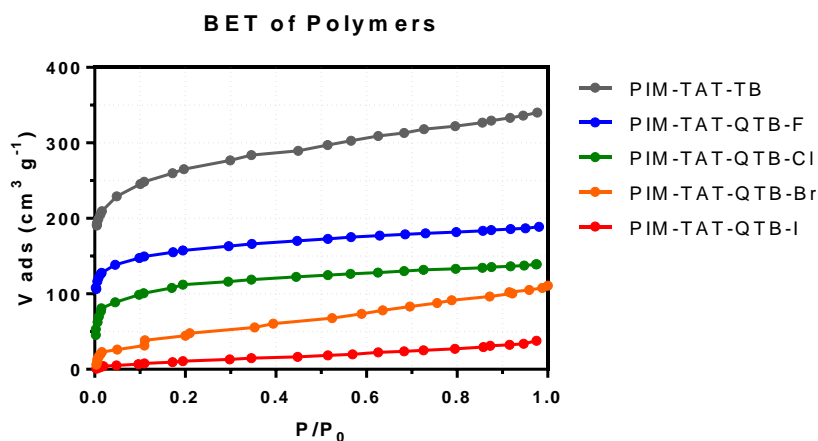


**Figure 5.6:** BET graphs of PIM-TAT-TB and related quaternised polymers

Surface area measurements were also taken for all the quaternised polymers, to test how the different ions would influence the porosity of the final materials. As expected, as the counterions become larger, the surface area decreases, because the larger ions block the pore space. This is clearly seen in the measurements taken using N<sub>2</sub> as an adsorbate gas at 77K (**Figure 5.6**).

**Table 5.2:** BET surface areas of QTB PIMs

Entry	Polymer	BET Surface Area (N <sub>2</sub> 77K) m <sup>2</sup> g <sup>-1</sup>
1	PIM-TAT-TB	950
2	PIM-TAT-QTB-F	560
3	PIM-TAT-QTB-Cl	397
4	PIM-TAT-QTB-Br	165
5	PIM-TAT-QTB-I	40

We noticed an almost total loss of BET with PIM-TAT-QTB-I, which only showed a 40 m<sup>2</sup> g<sup>-1</sup> surface area in comparison to PIM-TAT-TB which has a surface area of almost 1000 m<sup>2</sup> g<sup>-1</sup>. Then, following ion exchanges, the surface area increases as the smaller ions take up less room (**Table 5.2**).

## Catalysis with quaternised TB-PIMs

This new series of quaternised polymers were then tested as catalysts in the CO<sub>2</sub> cycloaddition reaction with epichlorohydrin using the same optimised conditions previously discussed. PIM-TAT-QTB-I demonstrated a moderate improvement in the presence of co-catalyst TBAB in comparison to the non-quaternised polymer, achieving an 90% conversion in 3 hours in comparison to the 80% by PIM-TAT-TB. But the most significant results came when the co-catalyst was removed - all quaternised polymers were all able to catalyse the reaction between CO<sub>2</sub> and epichlorohydrin without the aid of TBAB (**Table 5.3**). These results are not only far better than the previously tested TB polymers, but several of the quaternised



polymers outperform the TBAB itself. This is a very important achievement, as the TBAB is a homogeneous catalyst, and it needs to be chemically separated from the products, whereas our TB-PIMs can be simply removed by filtration and reutilised immediately with no energy penalty.

**Table 5.3:** Quaternised polymer performances in CO<sub>2</sub> cyclisation reactions

Entry	Catalyst Used (1 mol%)	Cocatalyst (0.5 mol%)	R =	Percentage Conversion*	
				3h	5h
1	-	TBAB	-CH <sub>2</sub> -Cl	61	79
2	PIM-TAT-TB	TBAB	-CH <sub>2</sub> -Cl	80	
3	PIM-TAT-QTB-I	TBAB	-CH <sub>2</sub> -Cl	90	95
4	PIM-TAT-QTB-I	-	-CH <sub>2</sub> -Cl	56	85
5	PIM-TAT-QTB-F	-	-CH <sub>2</sub> -Cl		50
6	PIM-TAT-QTB-I		-Ph		16
7	PIM-TAT-QTB-F		-Ph		3
8		TBAB	-Ph	24	

Surprisingly, PIM-TAT-QTB-I achieved a much higher performance than PIM-TAT-QTB-F, which only reached 50% conversion in 3 hours, though these are very much preliminary results. Another epoxide, this time styrene oxide, was used to test the catalysts.<sup>252</sup> This epoxide is much bulkier because of the phenyl group, and therefore it is unsurprising that the results were not as good, with the best performance coming from PIM-TAT-QTB-I with a 16% conversion in 5 hours. This is in line with results obtained with TBAB, which achieved a 24% conversion in 3 hours. These initial results from the quaternised polymers are very promising.

Because of these limitations in the method, it was decided to send the polymers to a collaborator who specialises in catalysis and has access to reactors. This will not only allow us to repeat the above tests to obtain more reliable results which we can confidently compare to the literature, but it will also allow us to test other factors. As the reactors create a closed environment, low boiling point epoxides can be tested, and solvents can be introduced to see if they improve the reactions. Furthermore, a stoichiometric amount of CO<sub>2</sub> can be used, which will vastly improve the atom economy of the reaction.

## Conclusion

In this chapter, we have looked to expand the potential applications of PIM catalysts by testing their performance in a CO<sub>2</sub> utilisation reaction, which has increasing global importance. Whilst the series of polymers that we had previously synthesised proved ineffective, in this particular reaction, we have herein demonstrated how straightforward it is to adapt our polymeric materials to specific needs. By performing a simple post-functionalisation quaternisation of the neutral polymers, we were able to synthesise quaternised polymers which bear a permanent positive charge in the main backbone, which can then undergo ion exchange reactions to further adapt the materials. We have shown a promising set of results using a simple set up, showing good catalytic performance without the need for a cocatalyst. We greatly look forward to the results we receive from our collaborators and anticipate a promising future of PIM catalysts in CO<sub>2</sub> utilisation reactions.

# Chapter 6 - Biodiesel Reactions

In this chapter the polymers used come from a paper published in parallel to the catalysis one:

**Adjustable Functionalization of Hyper-Cross-Linked Polymers of Intrinsic Microporosity for Enhanced CO<sub>2</sub> Adsorption and Selectivity over N<sub>2</sub> and CH<sub>4</sub>** H. Zhou, C. Rayer, A.R. Antonangelo, N. Hawkins, M Carta. *ACS Applied Materials & Interfaces*. **2022**, 14 (18), 20997–21006

## Introduction

Reaching net zero is an admirable global target, and one that would have a long-term positive impact on the planet. However, not only is there a huge amount of research and development still needed in the production and storage of renewable energies, but a world-wide retrofitting programme would be necessary which is complex and costly. This is because the vast majority of renewable energies have an electricity output instead of a physical fuel (coal, petrol, gas, etc.), and so all the technologies that rely on physical fuels are expected to become obsolete, and new electrical alternatives will be needed.<sup>253</sup> Retrofitting is likely to be a rate determining step in the net zero target, and therefore an interim solution is needed. Biofuels are physical fuels that are derived from biological matter, mainly plants. They are a desirable short-term answer to the climate crisis because they are more sustainable than traditional fuels, but can be used in existing technologies. Biodiesels are a subgroup of biofuels that are predominantly made of fatty acid methyl esters (FAMEs).<sup>254</sup> As the name suggests, they are similar to fossil fuel derived diesel, and can be used in existing diesel engines. FAMEs are synthesised from lipids – long chained fatty acids that are typically derived from plant oils via a transesterification reaction. This can be aided with either an acid or base catalyst, though base catalysis is thought to be a more effective method, in some cases reported to be 4000 times faster.<sup>255</sup> In industrial applications, bases such as sodium hydroxide and potassium hydroxide are used as homogeneous base catalysts, but these are undesirable not only

because of the drawbacks associated with homogeneous catalysis (i.e., expensive separation of products from catalysts, unreacted materials, and by-products), but also because the strong bases are harsh (corrosive) and unsustainable. Research into heterogeneous catalysts for biodiesel synthesis is dominated by acid catalysts,<sup>256</sup> but we hoped to show that our series of heterogeneous basic polymers can prove competitive.

## Synthesis

We wanted to test our best performing polymers from this work, but we also wanted to be able to compare to similar acid catalysts. We have recently published the synthesis and characterisation of a series of novel post-polymerisation functionalised hyper-crosslinked polymers of intrinsic microporosity (HCP-PIMs), which have been applied for carbon capture and storage, and for the efficient separation of CO<sub>2</sub> from N<sub>2</sub> and CH<sub>4</sub>.<sup>257</sup>

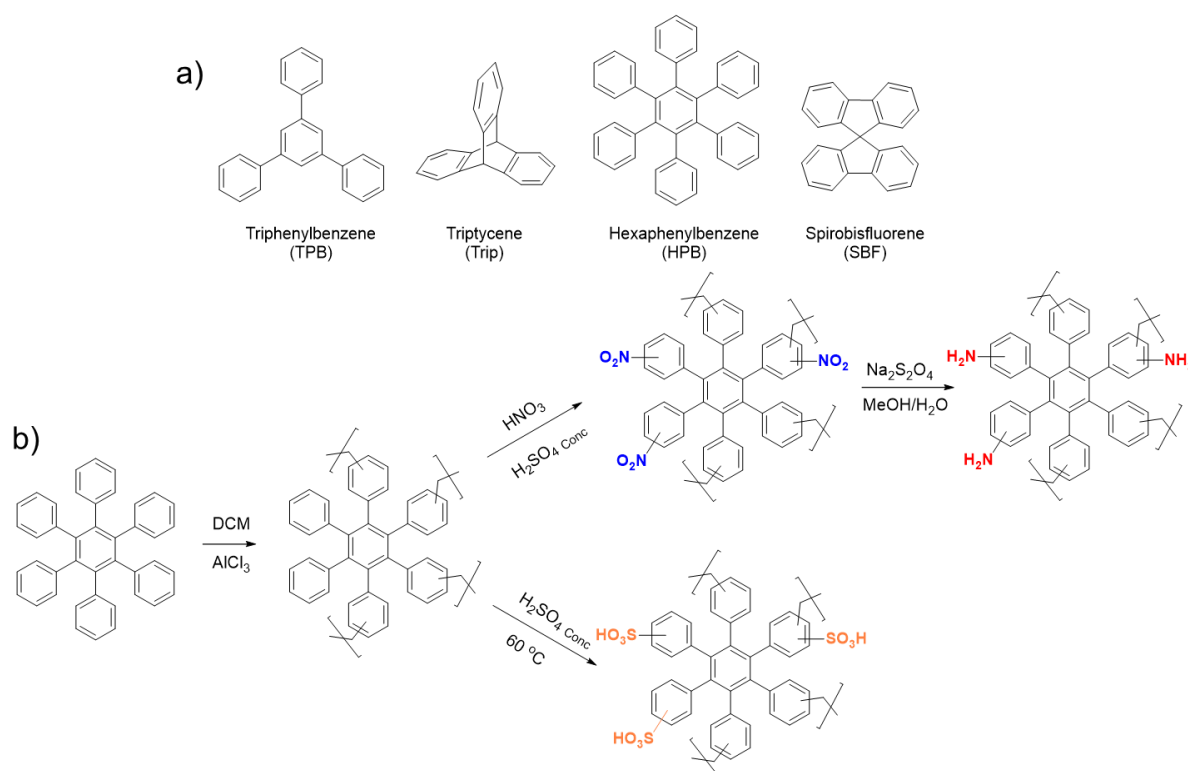


**Figure 6.1:** a) Core units of the functionalised polymers used in chapter 6; b) example of functionalisation.<sup>257</sup>

In this series we decorated the initial hydrocarbon-based PIMs with nitro-, amino- and sulfonated- functionalities, which enhanced the properties of the final materials because of the inclusion of groups with diverse nature and polarity. In view of these modifications, and the high porosity of the materials, we decided to test how the functional groups would help the catalysis towards the synthesis of biodiesels. The sulfonated polymers provide an excellent starting point for our catalysis, as they can be directly compared to similar materials in the literature. The aminated polymers then can offer a comparison between acid and base catalysis, though we must point out that the aminated polymers are much weaker bases than the sulfonated polymers are acidic. Considering this latter point, the TB polymers used in this work will also make an interesting comparison with the sulfonated polymers. The series of hydrocarbon-based HCP-PIMs were synthesised starting from their corresponding hydrocarbon monomers via a Friedel-Crafts polymerisation (**Figure 6.1 a**). DCM was used as both a solvent and as the source of the cross-linking ligands between the monomers, and  $\text{AlCl}_3$  is used as a Lewis acid catalyst. The resulting polymers were then modified to introduce the aforementioned functionalities. To add  $-\text{SO}_3\text{H}$  groups, polymers were stirred in concentrated sulfuric acid at  $60\text{ }^\circ\text{C}$ . To add  $-\text{NO}_2$  groups, instead, polymers were stirred in the typical sulfonitric mixture (nitric acid and a catalytic amount of sulfuric acid). These nitrated polymers can then be reduced using  $\text{Na}_2\text{S}_2\text{O}_4$  in ethanol and water, giving  $-\text{NH}_2$  functionalities (**Figure 6.1 b**). We decided to use monomers which typically produced high performing PIMs in other works<sup>258-260</sup> and we noticed that, although the structures are relatively similar to one to another, the purely hydrocarbon PIMs provide much higher BET surface areas, with PIM-Trip-HC and PIM-TPB-HC bearing the highest porosity, compared to the functionalised polymers and to their TB counterparts (**Table 6.1**). As discussed in chapter 4, basic nitrogen centres can cause polymer chain compression due to strong intramolecular attraction between nitrogen and hydrogen atoms, which leads to a decrease in surface area. This is noticeable in the aminated and TB polymers in comparison to the hydrocarbon counterparts. There is also a decrease in surface area for the sulfonated polymers, but this is mainly because of the functional groups blocking the pores.<sup>261, 262</sup>

**Table 6.1:** Surface areas of polymers used throughout chapter 6

Entry	Monomer Core	Polymer	Surface Area
1	Triptycene	PIM-Trip-TB	950
2		PIM-Trip-HC	1880
3		PIM-Trip-SO <sub>3</sub> H	1145
4		PIM-Trip-NH <sub>2</sub>	610
5	Triphenylbenzene	PIM-TAPB-TB	500
6		PIM-TPB-HC	2540
7		PIM-TPB-SO <sub>3</sub> H	1585
8		PIM-TPB-NH <sub>2</sub>	710
9	Hexaphenylbenzene	PIM-HPB-HC	1933
10		PIM-HPB-SO <sub>3</sub> H	1390
11		PIM-HPB-NH <sub>2</sub>	997
12	Spirobisfluorene	PIM-SBF-HC	1604
13		PIM-SBF-SO <sub>3</sub> H	1063
14		PIM-SBF-NH <sub>2</sub>	669

## Results and Discussion

### Esterification of Acids

It is commonplace to assess the suitability of catalysts for biodiesel synthesis, by testing them in simple Fischer esterification reactions between long chained fatty acids and alcohols (**Figure 6.2**).<sup>263</sup>

**Figure 6.2:** Esterification of a carboxylic acid

A good example is provided by Tantisriyanurak *et al.*, who used conjugated microporous polymers with sulfonic acid functionalities as catalysts for this reaction.<sup>147</sup> Considering that the structure of their materials is somewhat similar to our own, we decided to use their testing procedure as a benchmark. As a typical reaction, 1 mmol of lauric acid was stirred in 2 mL of methanol, and 10 mg of catalyst was added to the vessel. The reaction was then heated to 60 °C for 4 hours.

**Table 6.2:** Esterification of lauric acid and methanol with various catalysts

Catalyst (10 mg)	Time (hours)			
	1	2	3	4
<i>Blank</i>				5
<i>PIM-TPB-SO<sub>3</sub>H</i>	67	83	90	94
<i>PIM-TPB-NH<sub>2</sub></i>				4
<i>PIM-TAPB-TB</i>				5
<i>PIM-TPB-HC</i>				3
<i>Activated Carbon</i>				<5

The series of polymers featuring triphenylbenzene cores were the first ones tested (**Table 6.2**). PIM-TPB-SO<sub>3</sub>H gave the best performance, giving a 94% conversion in just 4 hours. This is already remarkable, given that in the work by Tantisriyanurak that we used as a comparison, the best sulfonated polymers took 24 hours to reach this same conversion, under the same conditions. Additionally, this is also a competitive result also compared to similar studies in the literature.<sup>254, 264</sup> Much to our surprise, PIM-TPB-NH<sub>2</sub> only gave a 4% conversion in 4 hours that. We considered that this was due to the fact that, as anticipated, the sulfonated groups are more acidic than the amino groups are basic, and therefore give a stronger catalytic performance.<sup>265</sup> It was therefore decided to try the reaction with the structurally similar PIM-TAPB-TB, to see if these more basic sites would improve the results. However, this catalyst also only gave a 5% conversion, basically the same as the reaction with no catalyst. This was initially very surprising, given that the literature describes base catalysis as more favourable than acid catalysis for transesterification reactions.<sup>256</sup> But this is not a *transesterification* reaction, and we then found that actually basic conditions are unfavourable for carboxylic acids undergoing substitution reactions, such as Fischer esterifications.<sup>266</sup> The reason lies in the simple assessment of the chemistry of the reaction. At first the base deprotonates the -OH group of the carboxylic acid creating the carboxylate salt, which is not reactive towards esterification unless the reaction is heated for a long time and to much higher temperatures. The mechanism for the acid catalysed transesterification is very similar to the mechanism for the acid catalysed esterification of carboxylic acids, and therefore this is a good reaction to

test acid catalysts with. However, it clearly is not appropriate for testing base catalysts (**Figure 6.3**).

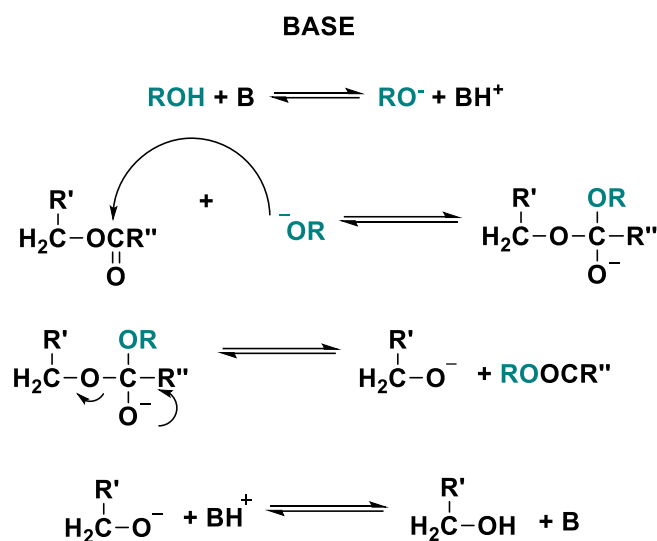


**Figure 6.3:** Base catalysed transesterification

It was considered that the confinement effect of the reagents into the small pores of the polymers alone could play a crucial role. This theory initially seemed to be confirmed by the catalysis conducted with PIM-TPB-HC, as this gave a conversion of 55% in 4 hours despite having no functional groups. However, a thorough search of the literature could find no such examples of the reaction occurring only in the presence of a porous framework, most of the time the polymer must bear acidic functions.<sup>267</sup> We repeated the reaction using commercially available activated carbon, which did not give any catalytic performance. PIM-TPB-HC is synthesised using an aluminium-based catalyst, and it was thought that there could have been trace amounts left in the pores. The polymer was stirred in ammonia, and then thoroughly washed in varying solvents and then drying under pressure for 24 hours. A sample of this polymer was then used in the reaction, and there was no conversion found. Our current theory, therefore, is the initial findings are attributable to residual aluminium in the pores, which would be quite remarkable. The polymers were thoroughly cleaned prior to testing, and so the number of catalytic sites actually present in the reaction must have been very low, and yet the reaction achieved a 55% conversion. If this theory is correct, then it would mean that the porous structure must have played a big part in the activity, and it is unfortunate that we cannot



quantify just how little metal was present, as this would be a very impressive result. Clearly further work is needed here and will be a priority research area for the group in the near future.

### Transesterification of Esters with PIMs

Before testing the catalysts with oils, which are large structures that may hinder the ability to monitor the reaction by  $^1\text{H}$  NMR due the large number of proton environments, we wanted to test the catalysts in a reaction that would occur through the same mechanism. It was decided therefore to test the catalysts in a transesterification reaction using a simpler ester. This is not commonly done in the literature, because the catalysts can also catalyse the reverse reaction, as it will occur through the same mechanism, and we know it is reversible. We therefore tried to use starting materials that would produce products that would not favourably take part in the reverse reaction.  $^t\text{Bu}$  acetate and methanol were chosen for this task, as it was thought that the *tert*-butanol product would be unlikely to react (**Figure 6.4**).



**Figure 6.4:** Transesterification of  $^t\text{Bu}$  acetate

10 mg of PIM-HPB-SO<sub>3</sub>H was added to 1 mmol of  $^t\text{Bu}$  acetate in 2 ml of methanol, and the reaction was stirred at 50 °C for 4 hours. However, we found issues with the  $^1\text{H}$  NMR sampling. When preparing the samples, it is essential to make sure that excess methanol is eliminated, as the peaks relating to the reagents and products overlap, making it difficult to quantify conversions. However, the product formed in this reaction (methyl acetate) has a low boiling point, and therefore when the sample was dried on a rotary evaporator, any product formed will have also evaporated.  $^1\text{H}$  NMR spectra were recorded without the removal of methanol, but it was not possible to isolate product peaks from reactants. Alternative reagents were considered, but it was found difficult to use ones that would fulfil the two requirements, of having thermally stable products but also that would not favour the reverse reaction. It was therefore decided to try the transesterification of oils, and carefully compare to literature studies.

## Transesterification of Oils

The transesterification of oils is a process whereby triglycerides present in the oil undergo esterification reactions with methanol to create long chain esters, known as fatty acid methyl esters (FAMES), and glycerol as a by-product (**Figure 6.5**).

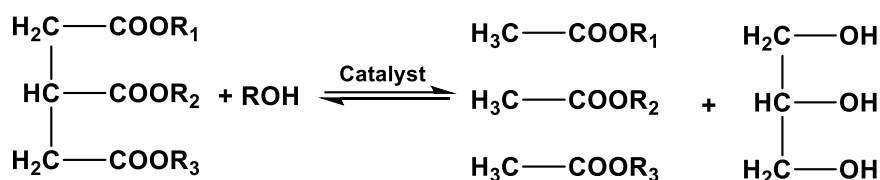


**Figure 6.5:** Transesterification of triglycerides

The relative simplicity of this reaction, combined with the abundant and sustainable feedstock, makes it a highly desirable reaction for fuel production in the near future. For this work, the range of oils used were purposely commercial products purchased from supermarkets and were not purified prior to use. There is some debate about the ethics of biodiesel production from such sources, mainly because it is argued that the crops produced for biodiesel production should instead be used to combat global hunger. This is a viable argument for first generation biofuels, but new methods use waste biomass or farmed algae, which only need a relatively small amount of space to grow.<sup>254</sup> For the purposes of our small scale tests in the lab, it was far more practical to use these commercial oils that would still give a good indication of catalytic activity in this mechanism. PIM-HPB-SO<sub>3</sub>H was the first polymer used to catalyse a range of oils' transformation (**Table 6.3**).

**Table 6.3:** Transesterification of varying oils with methanol (5 ml), using 10 mg of PIM-HPB-SO<sub>3</sub>H catalyst, at 60°C for 24 hours

Entry	Oil	Conversion (%)
1	Coconut Oil	28
2	Olive Oil	19
3	Sesame Oil	38
4	Sunflower Oil	17
5	Vegetable Oil	22
6	Used Vegetable Oil	24

$^1\text{H}$  NMR spectra of the resulting polymers prove to be not as challenging to analyse as initially thought – whilst there are a significant number of peaks associated with the oil, the peaks are relatively well defined. Furthermore, the majority of the ester product peaks overlap with their corresponding starting material peak, as the electronic nature of most of the proton sites does not change much during the reaction.<sup>268, 269</sup> The reaction can be monitored by comparing the methylene peaks of the original oil (**Figure 6.6**), which appears at around 4.15 ppm (circled green), with the peak that is formed after the reaction, which is found around 3.6 ppm (circled purple) and associated with the methyl groups on the glycerol by-product. These peaks are chosen as they are in unique environments that do not overlap with the large peaks associated with the long hydrocarbon chains of the oils. It is essential, as seen previously, that methanol is removed before running the samples, as this can cause a shift in the peaks and lead to the product peak overlapping with the solvent peak. In this case this proved not to be an issue.

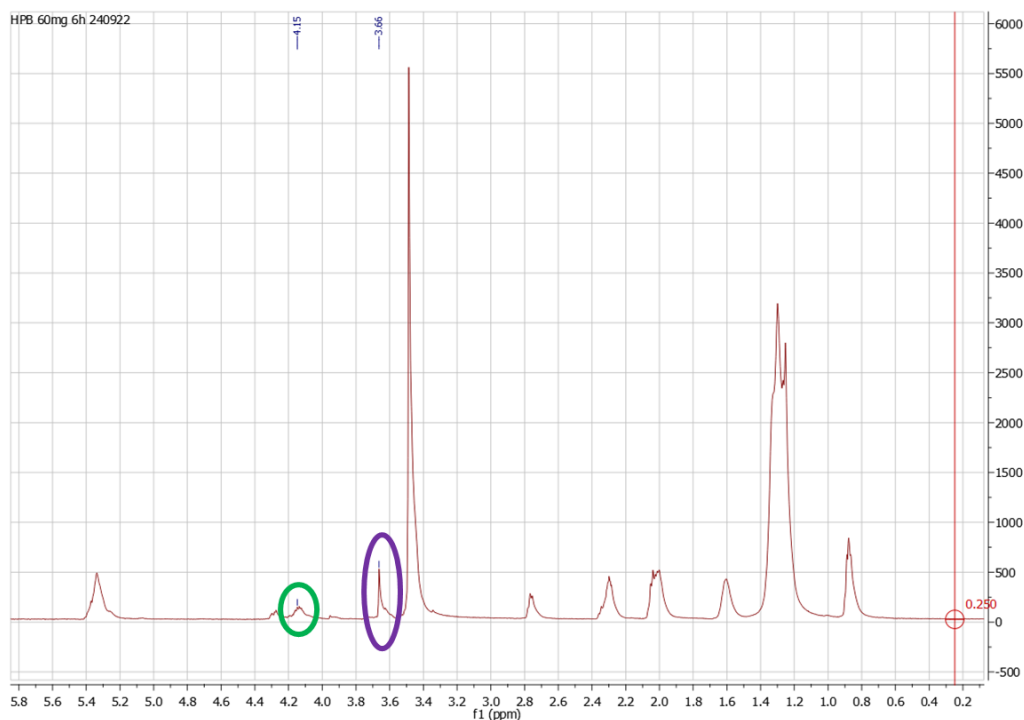


**Figure 6.6:** Example of an NMR spectra for biodiesel reaction

The PIM-HPB- $\text{SO}_3\text{H}$  catalyst proved successful across with all oils tested, with the best performance coming from the transesterification of sesame oil. Entries 5 and 6 show the

conversions of vegetable oils – 5 being straight from the bottle, and 6 had been used in cooking and collected after use (so that we could compare wasted oil too). There was very little difference in performance between these two oils, showing that PIM catalysts could be used in the transesterification of waste oils, which is a more sustainable option for this type of reaction as it gives value to otherwise waste product, rather than using food-quality materials. Compared to literature these results prove to be very competitive, especially considering only 10 mg of catalyst was used, whereas Tantisriyanurak *et al.* used 30 mg to achieve similar results. We repeated the reactions with increasing quantities of catalyst to see if we could reach a complete conversion in 24 hours (**Figure 6.7**). There is a positive correlation between the amount of catalyst and the conversion time, but the difference between each is very small, with only about a 2-3% difference between each increase. All polymers achieved a 50-60% conversion in a 48-hour period, which is less competitive in comparison to the literature.

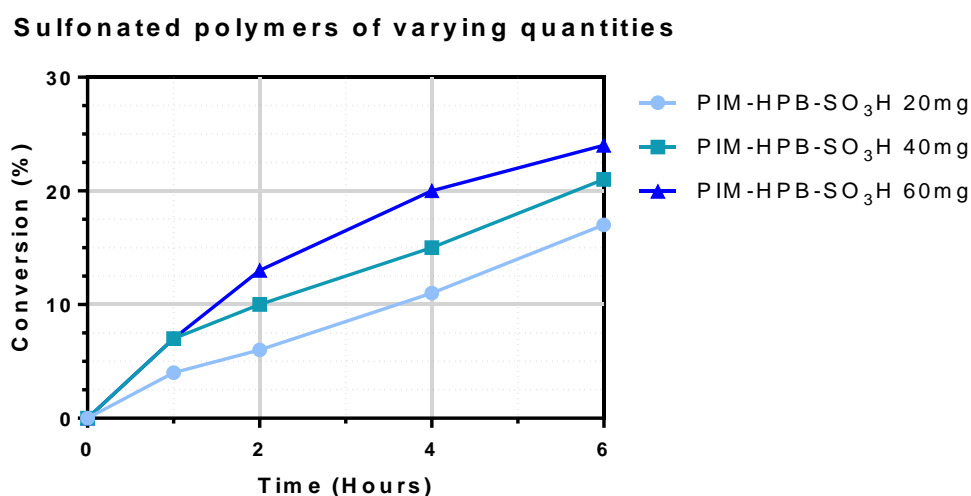


**Figure 6.7:** Conversion of PIM-HPB-SO<sub>3</sub>H in increasing quantities in the transesterification of sesame oil with methanol

The other sulfonated polymers in this series featuring alternative cores were tested in the transesterification of sesame oil, and whilst they all successfully catalysed the reaction, the conversion was much lower than with PIM-HPB-SO<sub>3</sub>H (**Table 6.4**).

**Table 6.4:** Conversions in the transesterification of sesame oil with methanol in the presence of varying catalysts

Entry	Catalyst (10 wt%)	Conversion after x time		
		4h	24h	48h
1	PIM-HPB-SO <sub>3</sub> H	8	38	52
2	PIM-TPB-SO <sub>3</sub> H		13	23
3	PIM-SBF-SO <sub>3</sub> H		10	17
4	PIM-Trip-SO <sub>3</sub> H	10	12	20
5	PIM-HPB-NH <sub>2</sub>		0	0
6	PIM-Trip-NH <sub>2</sub>		0	0
7	PIM-TAPAT+TB-TB		0	0
8	TB-homogeneous		0	0
9	NaOH	100	-	-
10	Blank		0	0

Aminated polymers PIM-HPB-NH<sub>2</sub> and PIM-Trip-NH<sub>2</sub> were tested under the same conditions, but were unable to catalyse the reaction, with a 0% conversion after 48 hours. The more basic PIM-TAPAT+TB-TB was also tested, but also demonstrated a 0% conversion in 48 hours. Homogeneous TB was also tested, but this was also unsuccessful, which suggested that the TB site was not catalytically active enough in this reaction. These results were disappointing as there was much hope that this series of basic catalysts would show great promise in this area. It is known that base catalysts struggle to catalyse the transesterification reaction if there is too high a concentration of free fatty acids present (>0.5 wt%) as these free acids neutralise the basic sites.<sup>270</sup> It is likely that this is the case in the commercial oils tested. It is also possible that our catalysts simply were not basic enough to catalyse the reaction – the reaction ease reached completion using sodium hydroxide under similar conditions. As mentioned in chapter 4, we have sent a selection of polymers to test their basicity, and this will give a better understanding moving forward.

## Conclusion

In this chapter, we have further explored the potential range of applications of PIM catalysts. Although in this instance the base catalysts tested proved unsuccessful for the transesterification of biodiesel, we have still demonstrated the versatility of PIMs as catalyst by introducing acidic sites through post-functionalisation reactions, thus showing that PIMs

can be fine-tuned for many different reactions, not just base catalysed reactions. We hope that a better understanding of the basicity of the TB PIMs will help to further understand why they were unsuccessful in this reaction, and we will certainly return to this reaction in the future.

# Chapter 7 – Future Work and Conclusions

During this project, we have only just begun to scratch the surface of potential work into PIM catalysts. We have demonstrated the unique properties that polymers of intrinsic microporosity can provide which can enhance catalytic performance.

Firstly, in chapters 2 and 3, we explored the concept of flexibility and swellability – studying the effects of introducing more flexible components into otherwise rigid PIM structures. We were able to demonstrate through both extensive lab tests and through computational studies that increasing the degree of flexibility in the polymer chains promoted a swelling effect in the polymers. This “swellability” leads to an increase in catalytic performance, particularly when reactions take place in a solvent. The “swellability” also allows for a more diverse range of reagents to be used, as the polymer catalysts are able to host larger substrates. The results we achieved were very impressive – our catalysts outperform those in the literature when it comes to the Knoevenagel reaction, in particular when using larger substrates.<sup>271</sup> However, we were not able to establish an upper bound of flexibility – our best performing polymer in this series was the most flexible. One of the benefits of the swellable polymers is that they induce a confinement effect within the pore space, which leads to increased collisions with the active sites and therefore increases the activity. With this in mind, there is presumably a level of flexibility that will prevent this confinement effect, and therefore would lead to a decrease in catalytic activity. This would be a very interesting area for future research – further exploring the effects of flexibility and trying to establish an upper bound by synthesising new, more flexible polymer catalysts.

In chapter 4 we looked at the effects of introducing various nitrogen sites into the polymer structure, in order to increase the number of active sites in the structure from only the TB linkers used in the first series. This series of polymers did perform very well and includes the best performing catalysts for the Knoevenagel reaction between <sup>t</sup>Bu-benzaldehyde and malononitrile in this study. They did also prove successful in catalysing numerous reactions with substituted methylene species, which is significant as this is considered to be the reagent that interacts directly with the catalytic site. In this respect, success using less favourable reagents is an indication of a good base catalyst. However, we also recorded a variety of unsuccessful reactions between benzaldehydes and methylene species that were thought to be highly acidic (and therefore more susceptible to base catalysis), such as acetylacetone and diethyl malonate. It is noteworthy that all the successful reactions featured a methylene species with an adjacent cyano- group, and this is a trend that has been noted in the literature before. We were unable to ascertain the pKa values of the polymers in the timespan of this project, but we hope that this information will aid future understanding into these results. That being said, we have still shown how easy it is to introduce new functionalities into polymer catalysts. The simple TB polymerisation method proved successful with all monomers used in this study, demonstrating how wide the scope for future catalysts is. It is anticipated that future research will consider introducing even more functionalities into PIM catalysts and expanding the potential range of applications for them.

In chapter 5, we began to explore some of these potential applications, with a particular ambition to test the sustainable and environmentally beneficial CO<sub>2</sub> utilisation reaction. We found that a simple post-polymerisation quaternisation reaction could create a series of polymers that were capable of catalysing the cycloaddition of CO<sub>2</sub> into epoxides without the need of a cocatalyst. The results obtained in our lab were very promising, and we greatly look forward to seeing how they perform under more controlled and consistent conditions with our collaborators. We expect that they will obtain results even better than those we found in the



lab, which will make these materials highly competitive in comparison to the literature and will open up a whole new avenue of future work for PIMs in that field.

In chapter 6, we tested our polymers as catalysts in the synthesis of biodiesel, a technology anticipated to have great global importance in the coming years. Literature studies suggested that base catalysis was particularly efficient at this type of reaction, and so we strongly believed that our basic catalysts would perform well, and that they would outperform their acidic counterparts. The acidic sulfonated polymers tested were all high performing, but unfortunately none of the basic polymers tested proved to be successful. We hope to better understand these findings when we know the pKa values of the polymers, it may be that the polymers are not basic enough for these reactions. Regardless, the positive results from the sulfonated polymers should not be ignored, in fact it further demonstrates the ease with which new functionalities can be introduced in order to tune PIM catalysts for specific applications.

We believe that this study is just the tip of the iceberg in terms of research into PIM catalysts. We have demonstrated the unique properties of PIMs that make them highly desirable as catalysts on an industrial scale, and we hope that this work inspires others to pursue research into broader applications.

Last but not least, the work produced in this thesis allowed us to publish three articles in important journals:

1. **Polymers of intrinsic microporosity (PIMs) for catalysis: a perspective.** A.R. Antonangelo, N. Hawkins, M. Carta. *Current Opinion in Chemical Engineering* **2022**, 35, 100766

A mini-review perspective that shows the “under-utilisation” of PIMs in catalysis.

2. **Tröger’s Base Network Polymers of Intrinsic Microporosity (TB-PIMs) with Tunable Pore Size for Heterogeneous Catalysis** A.R. Antonangelo, N. Hawkins, E. Tocci, C. Muzzi, A. Fuoco, M. Carta. *Journal of the American Chemical Society*, **2022**, 144 (34), 15581-15594

Which includes the main results of chapter 2 and 3, in this paper we reported the first example of “swellable” PIMs for heterogeneous catalysis.

3. **Adjustable Functionalization of Hyper-Cross-Linked Polymers of Intrinsic Microporosity for Enhanced CO<sub>2</sub> Adsorption and Selectivity over N<sub>2</sub> and CH<sub>4</sub>.** H. Zhou, C. Rayer, A.R. Antonangelo, N. Hawkins, M Carta. *ACS Applied Materials & Interfaces*. **2022**, 14 (18), 20997–21006

In this paper we reported the synthesis and characterisation of novel hypercrosslinked PIMs that, eventually, were used in chapter 6 for esterification and transesterification reactions, and the production of biodiesel.

# Chapter 8 – Experimental Section

The commercially available reagents, solvents and gases were used without further purification. Reagents were bought from Merck, Fisher Scientific, or Fluorochem. Any reaction that required sensitive materials, such as air or moisture sensitive reagents, were performed in oven-dried apparatus, and under a nitrogen atmosphere.

During synthesis, thin layer chromatography (TLC) analysis was used to monitor reactions. Aluminium-backed plates coated with Merck Kieselgel 60 GF254 were used in this analysis. The TLC plates were viewed under UV fluorescence, and in some cases by staining using a solution of cerium sulfate in dilute sulfuric acid.

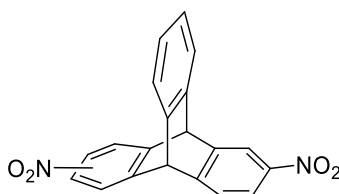
The following apparatus was used to analyse the compounds synthesised in this project.

- Melting Points were recorded using a Cole-Parmer Stuart™ Digital Melting Point Apparatus and are uncorrected.
- Infrared spectra were recorded using a PerkinElmer Spectrum Two FT-IR Spectrometer.
- $^1\text{H}$  NMR spectra were recorded in deuterated solvent, as stated, using an Avance Bruker DPX 500 instrument at 500 MHz.
- $^{13}\text{C}$  NMR spectra were recorded in deuterated solvent, as stated, using an Avance Bruker DPX 500 instrument at 125 MHz.
- Solid-state  $^{13}\text{C}$  NMR spectra were recorded using a Bruker Avance III spectrometer equipped with a wide-bore 9.4 T magnet (Larmor frequencies of 100.9 MHz for  $^{13}\text{C}$ ). This analysis was performed at the University of St. Andrews.

- Gas Chromatography mass spectra were recorded using an Advion Expression equipped with APCI (flow injection or ASAP) and ESI (flow injection) ion sources, with a mass range of 10-2000 Da, and a nominal mass accuracy of 0.1 Da.
- BET Surface Area data were collected using N<sub>2</sub> (77 K) or CO<sub>2</sub> (273 K) adsorption/desorption measurements with a Quantachrome Nova-e. In each case, samples were degassed for 800 min at 80 °C under high vacuum prior to analysis. The data were analysed with the software provided with the instrument. Further analyses, such as pore size distribution and total pore volume were calculated by performing NLDFT and H-K analysis respectively, considering a carbon equilibrium transition kernel at 273 K based on a slit-pore model; the kernel is based on a common, one centre, Lennard-Jones model.
- Thermogravimetric analyses were performed using a Thermal Analysis SDT Q600 at a heating rate of 10 °C/min from 30 to 995 °C.
- SEM images were recorded with a Hitachi S-4800 field emission (~1 nm resolution).

## Monomer Synthesis

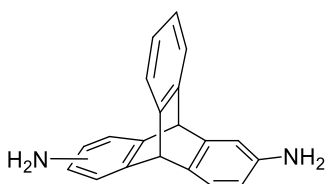
### Dinitrotritycene (DNT)<sup>200</sup>



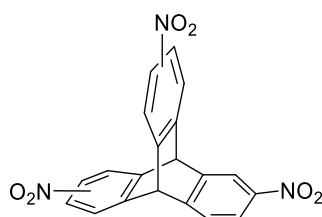
Triptycene (4.00 g, 15.74 mmol) was added to a mixture of potassium nitrate (3.34 g, 33.1 mmol) and acetonitrile (80 mL). Trifluoroacetic acid anhydride (15 mL, 109 mmol) was added dropwise, and the reaction was left to stir at room temperature for 16 hours. The reaction was crashed out in water and neutralised with sodium bicarbonate. The crude product was extracted with dichloromethane and washed with water (3 x 50 mL). The mixture was dried with magnesium sulfate, filtered, and rotary evaporated. The crude product was purified via

column chromatography with a 2:1 DCM : petroleum ether eluent to afford off white crystals. (4.52 g, 83%) MP: 240 °C; IR:  $\nu_{\max}$  ( $\text{cm}^{-1}$ ) 1592, 1514, 1457, 1338, 1192, 1165, 1070, 892, 827, 738, 633, 616, 529, 483;  $^1\text{H}$  NMR: (500 MHz,  $\text{CDCl}_3$ )  $\delta$  ppm 8.27-8.24 (m, 2H, ArH), 8.01-7.98 (m, 2H, ArH), 7.58-7.55 (m, 2H, ArH), 7.50-7.46 (m, 2H, ArH), 7.12-7.10 (m, 2H, ArH), 5.68 (m, 2H,  $\text{R}_3\text{CH}$ );  $^{13}\text{C}$  NMR: (125 MHz,  $\text{CDCl}_3$ )  $\delta$  ppm 151.0, 150.5, 145.7, 145.3, 142.8, 142.3, 141.8, 126.5, 124.5, 121.9, 119.1, 53.7, 53.6, 53.4; MS: calculated  $\text{C}_{20}\text{H}_{12}\text{N}_2\text{O}_4$  344.08 found 345.0 [ $\text{M}^+$ ].

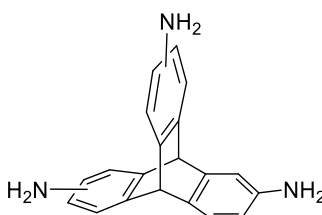
### Diaminotriptycene (DAT)<sup>200</sup>



Under a nitrogen atmosphere, dinitrotriptycene (5.5 g, 16.00 mmol) was stirred in tetrahydrofuran (180 mL). A spatula tip of Raney<sup>®</sup> Nickel was placed in the flask. Hydrazine monohydrate (15.6 mL, 319 mmol) was added dropwise, and the reaction was refluxed for 16 hours. The mixture was filtered through a layer of ceelite to collect the nickel, washed with THF, and then rotary evaporated to remove most of the THF. The mixture was then crashed out in water, and then was extracted with chloroform. The mixture was dried with  $\text{MgSO}_4$ , filtered, and rotary evaporated to afford yellow crystals. (4.78 g, 95%) MP: 230 °C; IR:  $\nu_{\max}$  ( $\text{cm}^{-1}$ ) 3441, 3372, 3000, 2956, 1621, 1521, 1479, 1327, 1296, 1267, 1185, 1150, 1136, 1115, 1091, 1020, 940, 864, 847, 830, 807, 777, 745;  $^1\text{H}$  NMR: (500 MHz,  $\text{CDCl}_3$ )  $\delta$  ppm 7.33-7.28 (m, 2H, ArH), 7.12-7.08 (m, 2H, ArH), 6.99-6.92 (m, 2H, ArH), 6.77-6.73 (m, 2H, ArH), 6.29-6.22 (m, 2H, ArH), 5.20-5.12 (t, 2H,  $\text{R}_3\text{CH}$ ) 3.49 (br s, 4H, NH);  $^{13}\text{C}$  NMR: (125 MHz,  $\text{DMSO-d}_6$ )  $\delta$  ppm 147.7, 147.3, 146.9, 146.5, 146.3, 146.2, 146.0, 134.3, 133.3, 125.0, 124.7, 124.5, 124.0, 123.6, 123.6, 123.2, 122.9, 111.0, 110.6, 109.2, 109.0, 53.7, 52.6, 51.4; MS: calculated  $\text{C}_{20}\text{H}_{16}\text{N}_2$  284.1 found 284.7 [ $\text{M}^+$ ].

**Trinitrotriptycene (TNT)**<sup>199</sup>

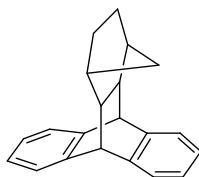
Triptycene (4.50 g, 17.71 mmol) was added to a mixture of concentrated HNO<sub>3</sub> (70%, 180 mL) and concentrated H<sub>2</sub>SO<sub>4</sub> (95%, 15 mL), and refluxed at 80 °C for 16 hours. The temperature was increased to 100 °C for 3 hours, until the solution became clear. The reaction mixture was quenched in water and neutralised using aqueous sodium hydroxide. The crude product was extracted with chloroform (3 x 150 ml), dried using magnesium sulfate, and the chloroform then removed on a rotavap. A plug was performed in DCM, giving a product as a light-yellow powder. (5.24 g, 76%) MP: 173 °C; IR:  $\nu_{\max}$  (cm<sup>-1</sup>) 3092, 1591, 1521, 1460, 1346, 1198, 795, 736 cm<sup>-1</sup>; <sup>1</sup>H NMR: (500 MHz, CDCl<sub>3</sub>)  $\delta$  ppm 8.38-8.33 (m, 3H, ArH), 8.10-8.05 (m, 3H, ArH), 7.69-7.63 (m, 3H, ArH) 5.89-5.82 (q, 2H, R<sub>3</sub>CH); <sup>13</sup>C NMR: (125 MHz, CDCl<sub>3</sub>)  $\delta$  ppm 149.6, 149.2, 148.8, 146.2 144.7, 144.3, 143.9, 125.0, 122.6, 122.5, 121.0, 119.6, 53.5, 53.4, 53.2, 53.1; MS: calculated C<sub>20</sub>H<sub>11</sub>N<sub>3</sub>O<sub>6</sub> 389.06 found 389.5 [M<sup>+</sup>].

**Triaminotriptycene (TAT)**<sup>199</sup>

Dinitrotriptycene (5 g, 1.29 x 10<sup>-2</sup> mol) was stirred in tetrahydrofuran (185 ml) with a spatula tip of Raney<sup>®</sup> Nickel. Hydrazine monohydrate (6 ml) was added dropwise, and the mixture was refluxed at 60 °C for 16 hours. The mixture was filtered through ceelite and washed with hot THF. The filtrate was rotavapped to remove most of the solvent, and then crashed out in water. The product was extracted with DCM, dried with magnesium sulfate, and rotavapped to give the product as an off-white crystal. (4.13 g, 93%). MP: 160 °C; IR:  $\nu_{\max}$  (cm<sup>-1</sup>) 3461, 3378, 3320, 3210, 3030, 1633, 1605, 1576, 1492, 1430, 1364, 1294, 1178, 1148, 955, 851, 810,

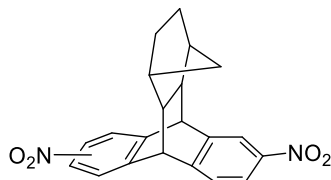
642, 589, 512;  $^1\text{H NMR}$ : (500 MHz,  $\text{CDCl}_3$ )  $\delta$  ppm 7.09-7.04 (m, 3H, ArH), 6.74-6.69 (m, 3H, ArH), 6.28-6.22 (m, 3H, ArH), 5.09-4.99 (m, 2H,  $\text{R}_3\text{CH}$ ), 3.49 (br s, 6H, NH);  $^{13}\text{C NMR}$ : (125 MHz,  $\text{CDCl}_3$ )  $\delta$  ppm 147.8, 147.1, 146.3, 143.8, 143.6, 143.4, 137.3, 136.4, 135.6, 125.5, 123.8, 123.6, 123.4, 111.7, 111.5, 111.3, 110.9, 110.7, 110.4, 54.4, 53.4, 52.4, 51.4; MS: calculated  $\text{C}_{20}\text{H}_{17}\text{N}_3$  299.14 found 300.1 [ $\text{M}^+$ ].

### **Benzomethanoanthracene (BMA)**<sup>272</sup>



Anthracene (2.00 g, 11.2 mmol) and norbornene (1.2 g, 12.8 mmol) and a few drops of water were placed in a microwave and was heated at 250 °C for 1 hour. The resulting dark brown mixture was stirred in THF and maleic anhydride were added and refluxed overnight. The reaction mixture was poured into water and stirred until an off-white solid formed. The solid was filtered and then stirred in methanol for 1 hour. The solid was filtered again to giving the product as an off-white powder. (3.05 g, 88%). MP: 153 °C; IR  $\nu_{\text{max}}$  ( $\text{cm}^{-1}$ ): 3000, 2938, 2875, 1457, 1293, 1171, 1018, 933, 764, 740, 629, 587, 462, 437;  $^1\text{H NMR}$  (500 MHz,  $\text{CDCl}_3$ ):  $\delta$  7.30 (2H, m, ArH), 7.24 (2H, m, ArH), 7.17 (2H, m, ArH), 7.13 (2H, m, ArH), 4.30 (2H, d,  $\text{R}_3\text{CH}$ ), 2.05 (2H, d,  $\text{R}_3\text{CH}$ ), 1.94 (2H, d,  $\text{R}_3\text{CH}$ ), 1.44 (2H, m,  $\text{R}_3\text{CH}$ ), 1.09 (2H, m,  $\text{R}_3\text{CH}$ ), 0.43 (1H, d,  $\text{R}_2\text{CH}_2$ ), -0.32 (1H, d,  $\text{R}_2\text{CH}_2$ );  $^{13}\text{C NMR}$  (125 MHz,  $\text{CDCl}_3$ ): 144.8, 142.2, 125.9, 125.5, 124.3, 123.2, 49.3, 48.7, 39.7, 33.1, 31.0; MS: calculated  $\text{C}_{21}\text{H}_{20}$  272.16 found 272.4 [ $\text{M}^+$ ].

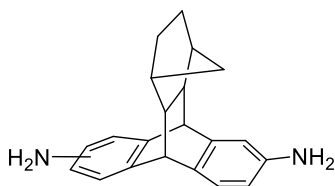
### **Dinitrobenzomethanoanthracene (DNBMA)**<sup>272</sup>



Benzomethanoanthracene (10.00 g, 36.8 mmol) and potassium nitrate (8.17 g, 80.9 mmol) was stirred in degassed acetonitrile (180 mL). Trifluoroacetic anhydride (18 ml, 128.75 mmol)

was added dropwise, and the mixture was left to stir for 16 hours. The reaction mixture was poured into water and neutralised with aqueous sodium hydroxide. The mixture was extracted with chloroform (3 x 150 ml), dried with magnesium sulfate, and rotavapped to a brown powder. The crude product was purified by a silica plug using chloroform to give the product as off-white crystals. (9.50 g, 73%). MP: 106 °C; IR  $\nu_{\max}$  (cm<sup>-1</sup>): 3094, 2947, 2909, 1591, 1513, 1341, 1175, 1126, 1078, 1013, 901, 860, 808, 739, 619, 591, 508; <sup>1</sup>H NMR (500 MHz, CDCl<sub>3</sub>)  $\delta$  8.13 (m, 1H, ArH), 8.09 (m, 1H, ArH), 8.04 (m, 1H, ArH), 7.40 (2H, m, ArH), 4.53 (2H, s, R<sub>3</sub>CH), 2.11 (2H, s, R<sub>3</sub>CH), 1.96 (2H, m, R<sub>3</sub>CH), 1.44 (m, 2H, R<sub>3</sub>CH), 1.06 (2H, m, R<sub>3</sub>CH), 0.46 (1H, d, R<sub>2</sub>CH<sub>2</sub>), -0.38 (1H, d, R<sub>2</sub>CH<sub>2</sub>); <sup>13</sup>C NMR: (125 MHz, CDCl<sub>3</sub>) 150.6, 150.1, 148.9, 148.4, 146.9, 146.5, 144.9, 144.5, 142.9, 142.4, 125.4, 125.3, 124.3, 124.3, 122.6, 122.2, 119.7, 119.6, 118.9, 118.9, 49.0, 49.0, 48.9, 48.8, 48.8, 48.7, 48.6, 48.4, 40.0, 39.8, 39.8, 39.7, 33.7, 31.0; MS: calculated C<sub>21</sub>H<sub>20</sub>N<sub>2</sub>O<sub>4</sub> 362.13 found 363.7 [M<sup>+</sup>].

### Diaminobenzomethanoanthracene (DABMA)<sup>272</sup>

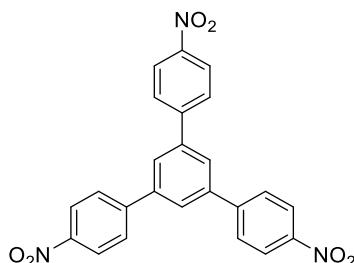


Dinitrobenzomethanoanthracene (4.00 g, 11.0 mmol) was stirred in diethyl ether (120 ml) with a spatula tip of Raney<sup>®</sup> Nickel. Hydrazine monohydrate (5 ml, 101.2 mmol) was added dropwise, and the mixture was refluxed at 45 °C for 16 hours. The mixture was filtered through ceelite and washed with hot diethyl ether. The reaction was neutralised with aqueous sodium hydroxide, dried with magnesium sulfate and rotavapped to give the product as an off-white crystal. (3.27 g, 98%). MP: 119 °C; IR:  $\nu_{\max}$  (cm<sup>-1</sup>) 3430, 3337, 3207, 2925, 1619, 1478, 1352, 1293, 1265, 1219, 1141, 1120, 862, 797, 690, 586, 441; <sup>1</sup>H NMR: (500 MHz, CDCl<sub>3</sub>)  $\delta$  6.98-6.87 (m, 2H, ArH), 6.63-6.55 (m, 2H, ArH), 6.44-6.35 (m, 2H, ArH), 4.02-3.91 (m, 2H, R<sub>3</sub>CH), 3.36 (br s, 4H, NH), 1.94 (m, 2H, R<sub>3</sub>CH), 1.81 (m, 2H, R<sub>3</sub>CH), 1.35 (d, 2H, R<sub>3</sub>CH), 1.01 (d, 2H, R<sub>3</sub>CH), 0.37 (d, 1H, R<sub>2</sub>CH<sub>2</sub>), -0.15 (d, 1H, R<sub>2</sub>CH<sub>2</sub>); <sup>13</sup>C NMR: (125 MHz, CDCl<sub>3</sub>) 146.6, 145.8, 144.4, 144.3, 143.9, 143.8, 143.1, 136.3, 135.4, 133.5, 132.5, 124.6, 124.3, 123.5, 123.3,



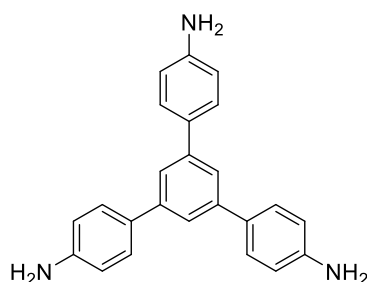
112.4, 112.2, 112.1, 111.9, 111.6, 111.4, 111.2, 111.0, 50.0, 49.9, 49.3, 49.2, 49.0, 47.9, 47.9, 46.8, 39.7, 39.6, 39.6, 33.1, 31.0, 30.9; MS: calculated  $C_{21}H_{22}N_2$  302.18 found 302.4  $[M^+]$ .

### Trinitrophenylbenzene (TNPB)<sup>203</sup>



4'-nitroacetophenone (10.00 g, 60.6 mmol) was stirred in ethanol (18 ml). Thionyl chloride (7.4 ml, 102 mmol) was added dropwise over ice. The reaction was then refluxed for 4 hours giving a bright orange precipitate. The mixture was crashed out in water and neutralised with  $NaHCO_3$ . The mixture was filtered and the solid was washed with water, ethanol, and diethyl ether. The crude product was recrystallised in DMF to afford a pale-yellow powder. (4.60 g, 52%). MP: 326 °C; IR:  $\nu_{max}$  ( $cm^{-1}$ ) 1593, 1509, 1449, 1393, 1344, 1251, 1106, 1011, 862, 842, 817, 749, 689, 495, 460;  $^1H$  NMR: (500 MHz,  $CDCl_3$ )  $\delta$  not soluble in any deuterated solvent;  $^{13}C$  NMR: not soluble in any deuterated solvent; MS: calculated  $C_{24}H_{15}N_3O_6$  441.10 found 441.5  $[M^+]$ .

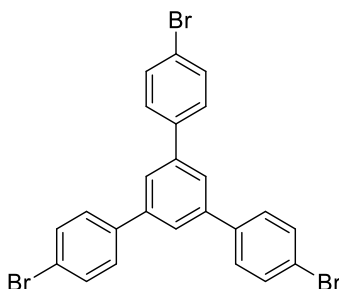
### Triaminophenylbenzene (TAPB)<sup>204</sup>



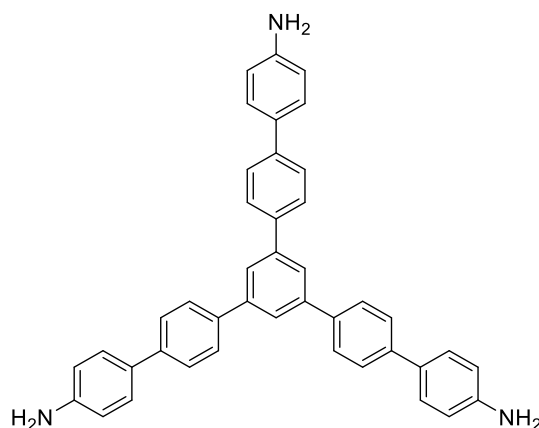
Trinitrophenylbenzene (2.00 g, 4.45 mmol) and Pd/C (0.44 g) were stirred in ethanol (50 ml) under a nitrogen atmosphere for 10 minutes. Hydrazine monohydrate (9.1 ml, 184.2 mmol) was added dropwise over a 10-minute period, and then the reaction was then refluxed at 80 °C, for 16 hours. The reaction was hot filtered to remove the catalyst, washing with hot ethanol. The crude product was recrystallised in ethanol and cooled at -20 °C for 4 hours. The solid

product was then separated by filtration to afford a yellow powder. (1.17 g, 75% yield). MP: 263 °C; IR:  $\nu_{\text{max}}$  ( $\text{cm}^{-1}$ ) 3422, 3345, 3020, 1616, 1514, 1451, 1404, 1277, 1184, 1129, 1088, 823, 710, 647, 607, 558, 500;  $^1\text{H}$  NMR: (500 MHz,  $\text{CDCl}_3$ ):  $\delta$  = 7.6 (s, 3H, ArH), 7.53-7.49 (d, 6H, ArH), 6.79-6.77 (d, 6H, ArH), 6.17 (s, 6H, NH).  $^{13}\text{C}$  NMR: (125 MHz,  $\text{CDCl}_3$ )  $\delta$  = 145.9, 141.9, 131.9, 128.2, 122.9, 115.4; MS: calculated  $\text{C}_{24}\text{H}_{21}\text{N}_3$  351.17 found 351.1 [ $\text{M}^+$ ].

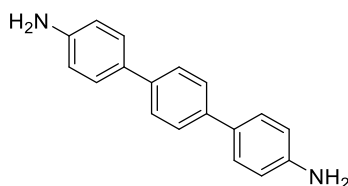
### **Tribromophenylbenzene (TBPB)**<sup>204</sup>



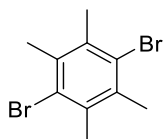
4-Bromoacetophenone (10.00 g, 50.2 mmol) was stirred in ethanol (30 mL), and thionyl chloride (7 mL, 96 mmol) was added dropwise. The solution was left to warm gradually to room temperature, before increasing the heat to 60 °C and stirred for 16 hours. The suspension was then cooled in an ice bath, and a saturated solution of  $\text{NaHCO}_3$  was added slowly. The precipitate was collected and washed three times in hot ethanol, and dried under reduced pressure to afford 1,3,5-tris(4-bromophenyl) benzene as pale-yellow solid (5.50 g, 60%). MP: 267 °C;  $^1\text{H}$  NMR: (500 MHz,  $\text{CDCl}_3$ )  $\delta$  = 7.70 (s, 3H, ArH), 7.62-7.60 (d, 6H, ArH), 7.55-7.53 (s, 6H, ArH).  $^{13}\text{C}$  NMR: (125 MHz,  $\text{CDCl}_3$ )  $\delta$  = 141.5, 139.6, 132.1, 129.0, 125.0, 122.1; MS: calculated  $\text{C}_{24}\text{H}_{15}\text{Br}_3$  541.87 found 542.00 [ $\text{M}^+$ ].

**Triaminobiphenylbenzene (TAPBext)<sup>217</sup>**

1,3,5-Tris(4-bromo)benzene (2.50 g, 4.60 mmol) and 4-aminophenylboronic pinacolate (3.22 g, 14.7 mmol) were dissolved in a mixture of THF: toluene (50:50 mL), followed by addition of NaOH (2.80 g, 69 mmol). The resulting mixture was degassed with nitrogen for 15 minutes, and then Pd(PPh<sub>3</sub>)<sub>2</sub>Cl<sub>2</sub> (0.32 g, 0.46 mmol) was added. The solution was degassed for a further 10 minutes and was heated to 90 °C for 20 h under nitrogen atmosphere. The reaction mixture was cooled to room temperature and the solvents were removed via a rotary evaporator. The remaining crude product was solubilized in hot ethyl acetate and the mixture was hot filtrated over celite, which was washed with hot ethyl acetate several times, and the solvent was rotary evaporated. Finally, the obtained dark yellow solid was washed using hot methanol and filtered. This process was repeated two times to yield a pale-yellow powder. (2.00 g, 75% yield). MP: 281 °C; IR:  $\nu_{\max}$  (cm<sup>-1</sup>) 3660, 3438, 3348, 2997, 2987, 2904, 1618, 1499, 1446, 1391, 1280, 1180, 1067, 1000, 814, 695, 540, 511; <sup>1</sup>H NMR: (500 MHz, DMSO-d<sub>6</sub>)  $\delta$  = 7.92 (s, 3H, ArH), 7.91 – 7.87 (d, 6H, ArH), 7.70 – 7.68 (d, 6H, ArH), 7.47-7.45 (d, 6H, ArH), 6.69-6.68 (d, 6H, ArH), 5.28 (s, 6H, NH); <sup>13</sup>C NMR: (125 MHz, DMSO-d<sub>6</sub>):  $\delta$  = 148.9, 141.8, 140.4, 137.8, 127.9, 127.6, 127.2, 126.2, 123.9, 114.7; MS: calculated C<sub>42</sub>H<sub>33</sub>N<sub>3</sub> 579.27 found 579.7 [M<sup>+</sup>].

**Extended Aniline 1 (A1)**<sup>214</sup>

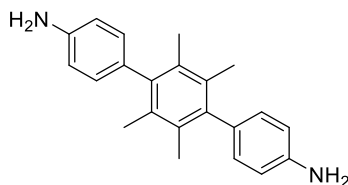
1,4-dibromobenzene (5.00 g, 21.2 mmol) and 4-aminophenylboronic pinacolate (10.20 g, 46.6 mmol) were stirred in a mixture of toluene and water (50:50 mL), followed by addition of potassium carbonate (44.00 g, 318 mmol). The resulting mixture was degassed with nitrogen for 15 minutes, and Pd(PPh<sub>3</sub>)<sub>2</sub>Cl<sub>2</sub> (0.73 g, 1 mmol) was added. The solution was degassed for a further 10 minutes before heating to 120 °C for 20 hours under a nitrogen atmosphere. The reaction mixture was cooled to room temperature, extracted with EtOAc (3 × 50 mL) and the combined organic extracts were dried over anhydrous MgSO<sub>4</sub>. The solution was filtered, and the solvent was removed under vacuum. The remaining crude product was purified by flash column chromatography on silica gel (40 to 60% EtOAc in hexanes) to yield a light brown solid A1 (2.76 g, 50%). MP: 190 °C; <sup>1</sup>H NMR: (500 MHz, DMSO-d<sub>6</sub>) δ = 7.59 (s, 4H, ArH), 7.44 – 7.43 (d, 4H, ArH), 6.71 – 6.69 (d, 4H, ArH), 5.26 (s, 4H, NH). <sup>13</sup>C NMR: (125 MHz, DMSO-d<sub>6</sub>) δ = 148.6, 138.4, 127.6, 127.3, 126.0, 114.7; MS: calculated C<sub>18</sub>H<sub>16</sub>N<sub>2</sub> 260.13 found 260.7 [M<sup>+</sup>].

**1,4-dibromo-tetramethylbenzene (pre-A2)**<sup>215</sup>

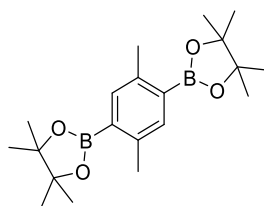
1,2,4,5-tetramethylbenzene (2.50 g, 18.6 mmol) was dissolved in DCM (25 mL). Iodine was added (0.1 g, 0.4 mmol), followed by a solution of Br<sub>2</sub> (2.4 mL, 47 mmol) in DCM (20 mL) added dropwise. The resulting mixture was heated under reflux for 1.5 hours, and after cooling down, 10% NaOH aqueous solution (30 mL) was added. The crude product was collected by filtration and washed with cold DCM, giving the desired product as a white solid (3.50 g, 65%).

$^1\text{H}$  NMR: (500 MHz,  $\text{CDCl}_3$ )  $\delta$  = 2.51 (s, 12H,  $\text{CH}_3$ ).  $^{13}\text{C}$  NMR: (125 MHz,  $\text{CDCl}_3$ ) 135.0, 128.0, 22.2; MS: calculated  $\text{C}_8\text{H}_8\text{Br}_2$  293.90 found 296.6 [ $\text{M}^+$ ].

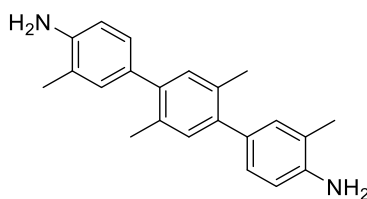
### Extended Aniline 2 (A2)<sup>215</sup>



1,4- dibromo-2,3,5,6-tetramethylbenzene (2.20 g, 7.50 mmol) and 4-aminophenylboronic pinacolate (3.63 g, 16.6 mmol) were dissolved in a mixture of THF and toluene (50:50 mL), followed by the addition of NaOH (4.52 g, 113 mmol). The resulting mixture was degassed with nitrogen for 15 minutes, and  $\text{Pd}(\text{PPh}_3)_2\text{Cl}_2$  (0.30 g, 0.43 mmol) was added. The solution was degassed for a further 10 minutes, and then the mixture was heated to 90 °C for 20 hours under a nitrogen atmosphere. The reaction mixture was cooled to room temperature and the solvent was removed under reduced pressure. The crude product was purified by flash column chromatography on silica gel (20 to 100% EtOAc in hexanes) and the dark brown solid obtained was recrystallized from DCM/methanol (1:4) to give a light brown solid (0.90 g, 42% yield). MP: 198 °C; IR:  $\nu_{\text{max}}$  ( $\text{cm}^{-1}$ ) 3660, 3445, 3364, 3202, 2987, 2904, 1731, 1620, 1518, 1410, 1273, 1178, 987, 825, 815, 573, 537;  $^1\text{H}$  NMR: (500MHz,  $\text{DMSO-d}_6$ )  $\delta$  = 6.75 – 6.73 (d, 4H, ArH), 6.64 – 6.62 (d, 4H, ArH), 5.02 (s, 4H, NH), 1.88 (s, 12H,  $\text{CH}_3$ ).  $^{13}\text{C}$  NMR: (125 MHz,  $\text{DMSO-d}_6$ )  $\delta$  = 145.8, 140.2, 132.1, 131.8, 131.0, 129.3, 127.5, 121.1, 114.0, 20.4, 17.9; MS: calculated  $\text{C}_{22}\text{H}_{24}\text{N}_2$  316.19 found 317.1 [ $\text{M}^+$ ].

**1,4-bis(pinacolatoboronyl)-2,5-dimethylbenzene (pre-A3)**<sup>216</sup>

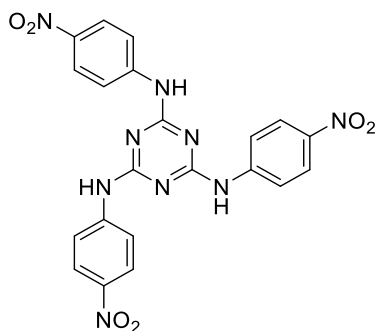
1,4-dibromo-2,5-dimethylbenzene (2.00 g, 1 equiv., 7.6 mmol) and bis(pinacolato)diboron (5.80 g, 3 equiv., 22.8 mmol), potassium acetate (4.50 g, 6 equiv., 45.6 mmol) and dimethylformamide, DMF (80 mL). The resulting mixture was degassed for 15 min by a flow of nitrogen, and Pd(PPh<sub>3</sub>)<sub>4</sub> (0.56 g, 0.06 equiv., 0.5 mmol) was added. The resulting mixture was degassed again for 10 min by a flow of nitrogen and was heated to 85 °C for 24 under nitrogen atmosphere. The reaction mixture was cooled down to room temperature, then added to water before being extracted with dichloromethane. Combined organic layers were washed with water and brine, then dried with magnesium sulfate and evaporated under reduced pressure. The crude product was purified by column chromatography (50 to 70 % dichloromethane in n-hexane) to give a white solid (2.15 g, 80%); <sup>1</sup>H NMR: (500 MHz, CDCl<sub>3</sub>) δ = 7.58 (s, 2H, ArH), 2.53 (s, 6H, CH<sub>3</sub>), 1.38 (s, 24H, CH<sub>3</sub>); <sup>13</sup>C NMR: (125 MHz, CDCl<sub>3</sub>) δ = 140.5, 136.9, 88.4, 24.9, 21.5; MS: calculated C<sub>20</sub>H<sub>32</sub>B<sub>2</sub>O<sub>4</sub> 358.25 found 262.7 [M<sup>+</sup>].

**Extended Aniline 3 (A3)**<sup>216</sup>

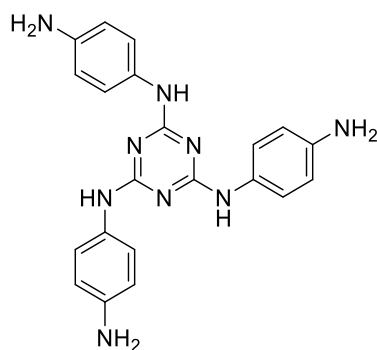
A two-necked round bottom flask (250 mL) was equipped with a reflux condenser, magnetic stirrer bar, septum, and was charged with 1,4-bis(pinacolatoboronyl)-2,5-dimethylbenzene (2.00 g, 5.6 mmol), 4-bromo-2methyl aniline (2.80 g, 15 mmol), NaOH (3.36 g, 84 mmol), toluene (50 mL) and THF (50 mL). The resulting mixture was degassed with nitrogen for 15 minutes and Pd(PPh<sub>3</sub>)<sub>4</sub> (0.55 g, 0.48 mmol) was added. The resulting mixture was degassed for a further 10 minutes, before it was heated to 90 °C for 18 hours under a nitrogen

atmosphere. The reaction mixture was cooled to room temperature and the solvent was removed under reduced pressure. The crude product was purified by column chromatography on silica gel (20 to 100% ethyl acetate in hexanes) and the obtained dark brown solid was washed with methanol (20 mL) to give a light brown solid (1.20 g, 71% yield); MP: 200 °C; IR:  $\nu_{\max}$  ( $\text{cm}^{-1}$ ) 3674, 3431, 3358, 2959, 1615, 1490, 1440, 1273, 1155, 1039, 885, 824, 732, 635, 576, 572, 545, 470, 439;  $^1\text{H}$  NMR: (500 MHz,  $\text{DMSO-d}_6$ )  $\delta$ = 6.98 (s, 2H, ArH), 6.92 (s, 2H, ArH), 6.90 – 6.89 (d, 2H, ArH), 6.66 – 6.65 (d, 2H, ArH), 4.86 (s, 4H, NH), 2.20 (s, 6H,  $\text{CH}_3$ ), 2.10 (s, 6H,  $\text{CH}_3$ ).  $^{13}\text{C}$  NMR: (125 MHz,  $\text{DMSO-d}_6$ )  $\delta$ = 145.8, 140.2, 132.1, 131.8, 131.0, 129.3, 127.5, 121.1, 114.0, 20.4, 17.9; MS: calculated  $\text{C}_{22}\text{H}_{24}\text{N}_2$  316.19 found 316.2 [ $\text{M}^+$ ].

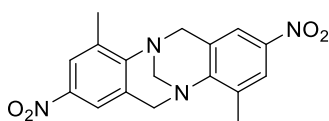
### **Trinitrophenylaminotriazine (TNPAT)**<sup>222</sup>



Cyanuric chloride (2.00 g, 10.8 mmol) was stirred to 1,4-dioxane (120 mL), followed by *p*-nitroaniline (7.47 g, 54.2 mmol) and  $\text{K}_2\text{CO}_3$  (9.00 g, 65.1 mmol). The mixture was then refluxed at 100 °C for 24 hours. The crude product was filtered, washing with portions of cold water and methanol. The product was dried under vacuum to produce a pale-yellow solid. (4.28 g, 81%). MP: >300 °C; IR:  $\nu_{\max}$  ( $\text{cm}^{-1}$ ) 3334, 3085, 1624, 1589, 1518, 1481, 1420, 1295, 1244, 1186, 1108, 1010, 846, 796, 749, 686, 493, 456;  $^1\text{H}$  NMR: (500 MHz;  $\text{DMSO-d}_6$ )  $\delta$  10.25 (s, 3H, NH), 8.20 (d, 6H, ArH), 8.07 (d, 6H, ArH) ppm;  $^{13}\text{C}$  NMR: (125 MHz;  $\text{DMSO-d}_6$ )  $\delta$  147, 125, 124, 120, 119; MS: calculated  $\text{C}_{21}\text{H}_{15}\text{N}_9\text{O}_6$  489.11 found 489.5 [ $\text{M}^+$ ].

**Triaminophenylaminotriazine (TAPAT)<sup>224, 225</sup>**

2,4,6-Tris(*p*-nitrophenylamino)-1,3,5-triazine (2.80 g, 5.72 mmol) was stirred in a mixture of ethanol (50 mL) and hydrochloric acid (50 mL). Tin (6.15 g) was added, and the mixture was refluxed at 80 °C for 48 hours. The resulting reaction mixture was filtered to remove the solvent, and the crude solid product was dissolved in hot water. The mixture was filtered, and the filtrate was basified using NaOH solution to a pH of 11. The solid product was collected washed with water and methanol, to give a pale-yellow powder. (1.05 g, 46%). MP: 285 °C; IR:  $\nu_{\max}$  (cm<sup>-1</sup>) 3446, 3363, 2807, 2571, 2106, 1620, 1556, 1494, 1418, 1340, 1249, 1178, 1113, 1067, 1014, 886, 826, 748, 511; <sup>1</sup>H NMR: (500 MHz; DMSO-d<sub>6</sub>)  $\delta$  8.48 (s, 3H, NH), 7.33 (s, 6H, ArH), 6.50 (s, 6H, ArH) 4.74 (s, 6H, NH), 3.73 (s, 6H) ppm; <sup>13</sup>C NMR: (125 MHz; CDCl<sub>3</sub>)  $\delta$  162.0, 145.0, 137.0, 118.0, 114.0; MS: calculated C<sub>21</sub>H<sub>21</sub>N<sub>9</sub> 399.19 found 399.2 [M<sup>+</sup>].

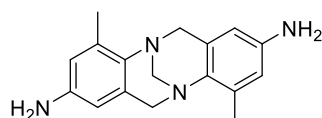
**4,10-dimethyl-2,8-dinitro-6H,12H-5,11-methanodibenzo[b,f][1,5] diazocine (TB-NO<sub>2</sub>)<sup>226</sup>**

To a mixture of 2-methyl-4-nitroaniline (10.00 g, 65.8 mmol) TFA (80 mL) in an ice bath, paraformaldehyde (4.77 g, 160 mmol) was gradually added. The ice bath was removed, and the reaction was left to stir at room temperature for 14 days. The reaction mixture was poured into water and basified to pH 9 with NaOH. The crude product was collected by filtration and resuspended in hot acetone for 20 minutes. The solution was cooled, and then placed in the freezer at -20 °C for 16 hours. The solid product was collected and dried to give a yellow solid. (10.18 g, 91%). MP: >300 °C; IR:  $\nu_{\max}$  (cm<sup>-1</sup>) 3393, 1677, 1586, 1508, 1436, 1329, 1290, 1206,



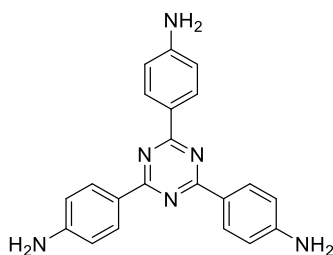
1140, 1098, 1067, 974, 950, 894, 794, 760, 746, 650, 522, 494;  $^1\text{H}$  NMR: (500 MHz; DMSO- $d_6$ )  $\delta$  7.97 (s, 2H, ), 7.82 (s, 2H, ), 4.68 (d, 2H, ), 4.36 (s, 2H, ), 4.33 (d, 2H, ), 2.48 (s, 6H,  $\text{CH}_3$ ) ppm;  $^{13}\text{C}$  NMR: (125 MHz; DMSO- $d_6$ )  $\delta$  153.1, 143.5, 135.3, 129.8, 124.0, 121.3, 67.6, 55.5, 17.1; MS: calculated  $\text{C}_{17}\text{H}_{16}\text{N}_4\text{O}_4$  340.12 found 339.9 [ $\text{M}^+$ ].

**4,10-dimethyl-6H,12H-5,11-methanodibenzo[b,f][1,5]diazocine-2,8-diamine (TB-NH<sub>2</sub>)<sup>226</sup>**



4,10-dimethyl-2,8-dinitro-6H,12H-5,11-methanodibenzo[b,f][1,5] diazocine (4.50 g, 13.2 mmol) was stirred in a mixture of ethanol (100 mL) and hydrochloric acid (100 mL). Tin (15.77 g) was added, and the reaction was refluxed at 80 °C for 24 hours. The reaction was filtered, and the filtrate was neutralised with NaOH. Then crude product was collected and washed in DCM. The product was then filtered and dried to give an off-white solid. (3.5 g, 94%). MP: >300 °C; IR:  $\nu_{\text{max}}$  ( $\text{cm}^{-1}$ ) 3316, 2951, 2335, 2098, 1914, 1613, 1478, 1323, 1214, 1012, 918, 846, 513;  $^1\text{H}$  NMR: (500 MHz;  $\text{CDCl}_3$ )  $\delta$  6.82 (s, 2H, ArH), 6.53 (s, 2H, ArH), 5.33 (s, 2H,  $\text{NCH}_2$ ), 4.28 (s, 4H,  $\text{NCH}_2$ ), 3.45 (br s, 4H, NH), 2.36 (s, 6H,  $\text{CH}_3$ );  $^{13}\text{C}$ : NMR (125 MHz;  $\text{CDCl}_3$ )  $\delta$  142.2, 138.6, 134.5, 129.9, 116.5, 110.7, 68.6, 55.9, 17.5; MS: calculated  $\text{C}_{17}\text{H}_{20}\text{N}_4$  280.17 found 280.8 [ $\text{M}^+$ ].

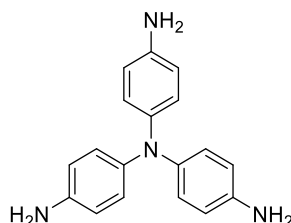
**Triaminophenyltriazine (TAPT)<sup>220</sup>**



4-aminobenzonitrile (3.00 g, 25.4 mmol) was stirred in trifluoromethanesulfonic acid (7.76 mL, 85.7 mmol) under a nitrogen atmosphere for 24 hours at room temperature. The reaction was poured into water (50 mL) and neutralised with NaOH. The crude product was filtered and washed with portions of water. The product was then dried to give a bright yellow solid. (2.58

g, 86 %). MP: >300 °C; IR:  $\nu_{\max}$  (cm<sup>-1</sup>) 3461, 3378, 3320, 3210, 3030, 1633, 1605, 1576, 1492, 1430, 1364, 1294, 1178, 1148, 955, 851, 810, 642, 589, 512; <sup>1</sup>H NMR: (500 MHz; DMSO-d<sub>6</sub>)  $\delta$  8.34 (d, 6H, ArH), 6.68 (d, 6H, ArH), 5.9 (s, 6H, NH); <sup>13</sup>C NMR: (125 MHz; DMSO-d<sub>6</sub>)  $\delta$  167.6, 153.5, 130.6, 122.3, 113.8; MS: calculated C<sub>21</sub>H<sub>18</sub>N<sub>6</sub> 356.17 found 354.9 [M<sup>+</sup>].

### **Triaminophenylamine (TAPA)**<sup>221</sup>



Tris(nitrophenyl)amine (3.04 g, 8.0 mmol) was stirred in a mixture of Pd/C (0.20 g) and ethanol (150 mL). Hydrazine monohydrate (16 mL, 323.9 mmol) was added dropwise over a 30-minute period. The reaction was then heated to 80 °C and refluxed overnight. The reaction was then hot filtered and washed with hot ethanol. The solvent was removed by rotary evaporation and then the crude product was recrystallised in ethanol. The mixture was placed in the freezer at -20 °C overnight, and then the product was collected and dried to give fine silver crystals. (1.68 g, 72%) MP: 240 °C; IR:  $\nu_{\max}$  (cm<sup>-1</sup>) ; <sup>1</sup>H NMR: (500 MHz; DMSO-d<sub>6</sub>) 6.6 (d, 6H, ArH), 6.46-6.43 (d, 6H, ArH), 4.70 (br s, 6H, NH); <sup>13</sup>C NMR: (125 MHz; DMSO-d<sub>6</sub>) 143.5, 139.5, 124.6, 115.3 MS: calculated 290.15 C<sub>18</sub>H<sub>18</sub>N<sub>4</sub> found 291.1 [M<sup>+</sup>].

## **Polymer Synthesis**

### **General Procedure A of Ladder Homopolymer Synthesis**

All polymers were prepared according to literature procedures of TB-PIM synthesis,<sup>188</sup> with some modifications where necessary. A chosen di-substituted monomer (1 molar equivalent) was reacted with dimethoxymethane (DMM) (5 equivalents) in DCM (approximately 6-12 mL), followed by dropwise addition of trifluoroacetic acid (TFA) (37 equivalents). The reaction was left to stir at room temperature until the mixture was viscous, when it was crashed out in a

mixture of ammonia and ice and stirred overnight. The product was then filtered, washed with plenty of water, and refluxed in acetone. The polymer was then dissolved in a minimal amount of chloroform, and methanol was added dropwise until the solution became cloudy. The product was then filtered off, and this step was repeated a further two times. The polymer was then dissolved in minimal chloroform and then pipetted into hexane. The solid was collected, and refluxed in THF, acetone and methanol for 1h each, and then refluxed in methanol one further time overnight. The polymer was then dried in a vacuum oven at 85 °C for 24 hours.

### General Procedure B of Network Homopolymer Synthesis

All polymers were prepared according to literature procedures of PIM synthesis,<sup>199</sup> with some modifications where necessary. A chosen tri-substituted monomer (1 molar equivalent) was reacted with dimethoxymethane (DMM) (7-8 equivalents) in DCM (approximately 6-12 mL), followed by dropwise addition of trifluoroacetic acid (TFA) (37 equivalents). The reaction was left to stir at room temperature until the mixture was viscous, where it was crashed out in a mixture of ammonia and ice and stirred overnight. The product was then filtered, washed with plenty of water, and refluxed in acetone, THF, DCM and methanol for 1h each, and then refluxed in methanol one further time overnight. The polymer was then dried in a vacuum oven at 85 °C for 24 hours.

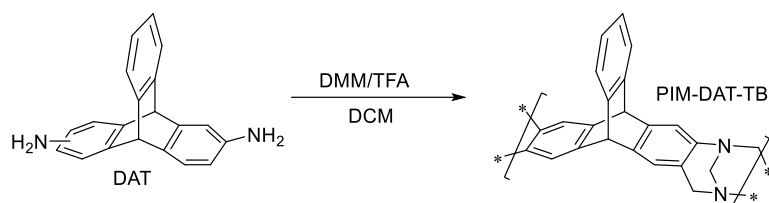
### General Procedure C of Copolymer Synthesis

All polymers were prepared according to literature procedures of PIM synthesis with modifications.<sup>199</sup> Two chosen monomers (in varying molar ratios depending on number of polymerisation sites\*) was reacted with dimethoxymethane (DMM) (7-8 equivalents) in DCM (approximately 6-12 mL), followed by dropwise addition of trifluoroacetic acid (TFA) (37 equivalents). The reaction was left to stir at room temperature until the mixture was viscous or jelly-like, typically 16 hours. The resulting reaction was ground down into fine parts, and then poured into a mixture of ammonia and ice and stirred overnight. The product was then filtered, washed with plenty of water, and refluxed in acetone, THF, DCM and methanol for 1h each,

and then refluxed in methanol one further time overnight. The polymer was then dried in a vacuum oven at 85 °C for 24 hours.

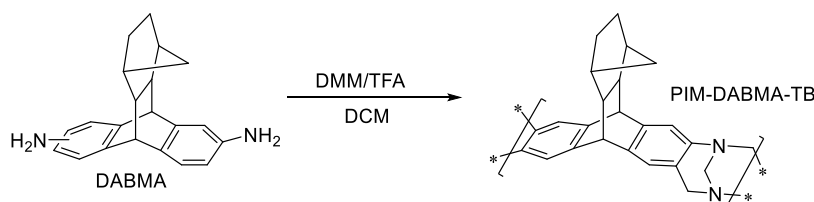
\* For a combination of two di-substituted monomers, or two tri-substituted monomers, they are combined in a 1:1 molar ratio. For a combination of one di- and one tri-substituted monomers, they are combined in a 3:2 molar ratio, to ensure complete polymerisation at all sites.

### DAT homopolymer

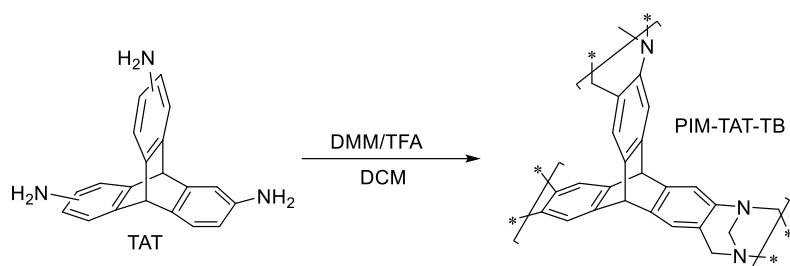


General procedure A was followed using diaminotriptycene (DAT) (0.70 g,  $2.46 \times 10^{-3}$  mol) and DMM (0.9 mL,  $1.39 \times 10^{-2}$  mol) were stirred in 9 mL of DCM. TFA (4.5 mL, 58.8 mmol) was added dropwise, and the reaction was left to stir for 72 hours, to yield a yellow solid. (0.67 g, 85%) BET: ( $N_2$ , 77 K) =  $1024 \text{ m}^2 \text{ g}^{-1}$ ; Total pore volume = 0.71 (at  $P/P_0 \sim 0.98$ ); FT-IR:  $\nu_{\text{max}}$  ( $\text{cm}^{-1}$ ) 2920, 2850, 1737, 1630, 1569, 1463, 1419, 1338, 1293, 1076, 1026, 928, 798, 742.

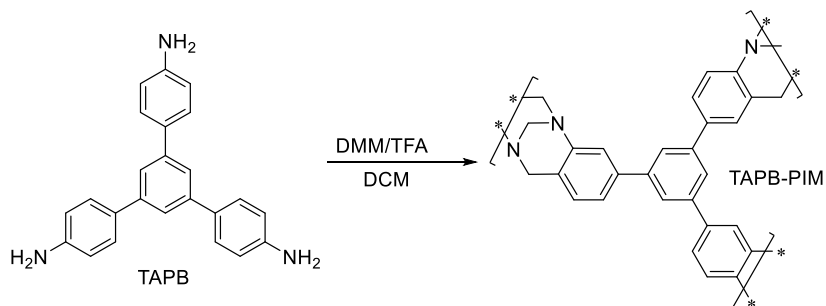
### DABMA homopolymer



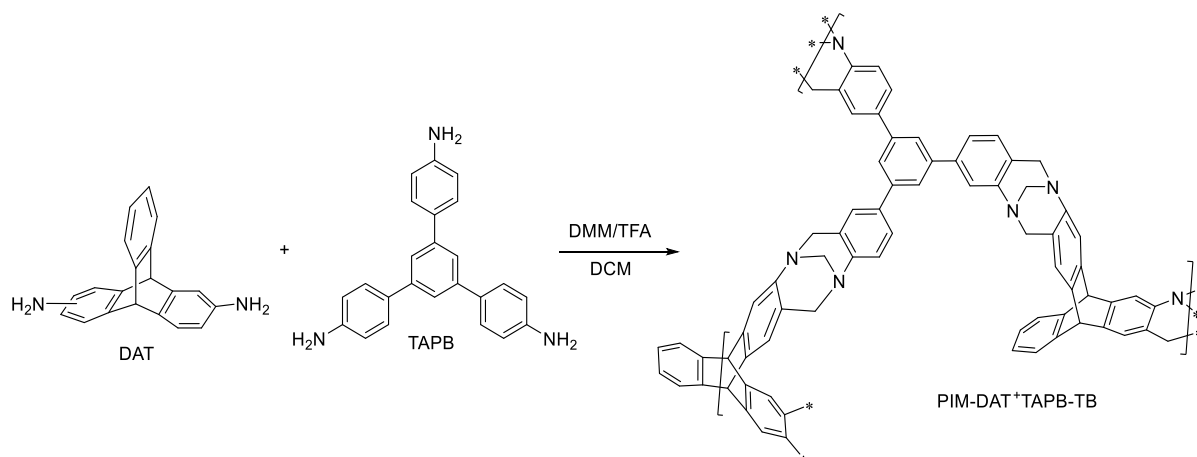
General procedure A was followed using diaminobenzomethanoanthracene (DABMA) (1.5 g, 4.97 mmol) and DMM (2.48 mL, 28.0 mmol) were stirred in 9 mL of DCM. TFA (14.1 mL, 183.9 mmol) was added dropwise, and the reaction was left to stir for 72 hours, to yield a yellow solid. (1.55 g, 88%) BET: ( $N_2$ , 77 K) =  $562 \text{ m}^2 \text{ g}^{-1}$ ; Total pore volume = 0.42 (at  $P/P_0 \sim 0.98$ ); TGA: initial mass loss at 320 °C; FT-IR:  $\nu_{\text{max}}$  ( $\text{cm}^{-1}$ ) 2937, 2870, 1681, 1624, 1569, 1469, 1420, 1354, 1298, 1211, 1155, 1111, 1078, 1082, 1032, 958, 935, 887, 841, 801, 747.

**TAT homopolymer**

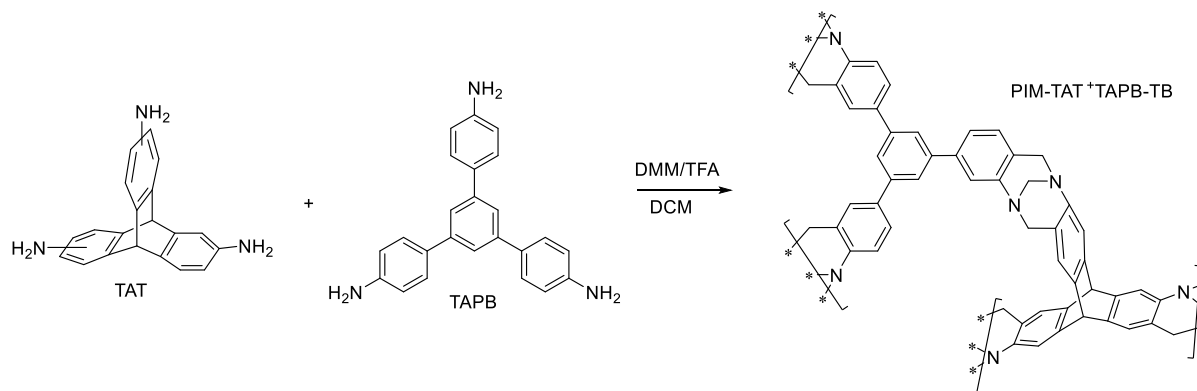
General procedure B was followed using triaminotriptycene (TAT) (0.50 g, 1.67 mmol) and DMM (1.033 mL, 11.7 mmol) were stirred in 10 mL of DCM. TFA (5.88 mL, 76.7 mmol) was added dropwise, and the reaction was left to stir for 3 hours, to yield a yellow solid. (0.55 g, 93%) BET: ( $N_2$ , 77 K) =  $900 \text{ m}^2 \text{ g}^{-1}$ ; Total pore volume = 0.58 (at  $P/P_0 \sim 0.99$ ); TGA: initial mass loss at 400 °C; FT-IR:  $\nu_{\text{max}}$  ( $\text{cm}^{-1}$ ) 3776, 3662, 3333, 2972, 2902, 2324, 1615, 1464, 1418, 1335, 1264, 1209, 1204, 1075, 925, 890, 837, 747, 600, 547, 461.

**TAPB homopolymer**

General procedure B was followed using tris(4-aminophenyl)benzene (TAPB) (0.70 g, 2 mmol) and dimethoxymethane (1.4 mL, 15.8 mmol) were stirred in DCM (14 mL), followed by dropwise addition of TFA (5.7 mL, 74.5 mmol) to yield a pale-yellow solid. (0.76 g, 95% yield) BET: ( $\text{CO}_2$ , 273 K) =  $500 \text{ m}^2 \text{ g}^{-1}$ ; Total pore volume = 0.13 (at  $P/P_0 \sim 0.98$ ); TGA: initial mass loss at 440 °C. FT-IR:  $\nu_{\text{max}}$  ( $\text{cm}^{-1}$ ) 2900, 1610, 1593, 1513, 1205, 950, 825;  $^{13}\text{C}$  NMR SS: (101 MHz)  $\delta$  161.6, 147.1, 141.9, 127.3, 66.8, 59.7, 49.4, 29.3, 16.2, 1.9.

**PIM-DAT+TAPB-TB**

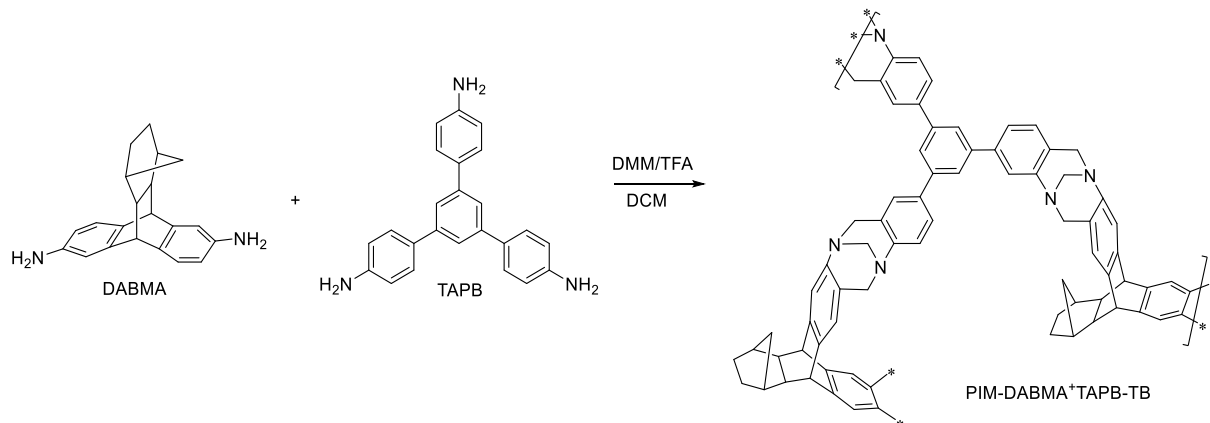
General procedure C was followed using diaminotriptycene (DAT) (0.50 g, 1.77 mmol), tris(4-aminophenyl)benzene (TAPB) (0.41 g, 11.7 mmol), and dimethoxymethane (0.78 ml, 8.83 mmol) were stirred in DCM (10 mL), followed by dropwise addition of TFA (3.5 mL, 45 mmol) to yield a brown solid. (1.10 g, 63%) BET: (CO<sub>2</sub>, 273 K) = 385 m<sup>2</sup> g<sup>-1</sup>; Total pore volume = 0.05 (at P/P<sub>0</sub> ~ 0.99); TGA: initial mass loss at 400 °C; FT-IR: ν max (cm<sup>-1</sup>) 3632, 3356, 2924, 2050, 1665, 1593, 1497, 1460, 1292, 1183, 1072, 935, 826, 747, 595, 521, 475.

**PIM-TAT+TAPB-TB**

General procedure C was followed using tris(4-aminophenyl)benzene (TAPB) (0.47 g, 1.34 mmol), triaminotriptycene (TAT) (0.40 g, 1.34 mmol) and dimethoxymethane (0.83 ml, 9.38 mmol) were stirred in DCM (10 mL), followed by dropwise addition of TFA (3.5 mL, 45 mmol). The reaction was left to stir for 16 hours, to yield a brown solid. (0.70 g, 78%) BET: (CO<sub>2</sub>, 273 K) = 545 m<sup>2</sup> g<sup>-1</sup>; Total pore volume = 0.08 (at P/P<sub>0</sub> ~ 0.99); TGA: initial mass loss at 420 °C;

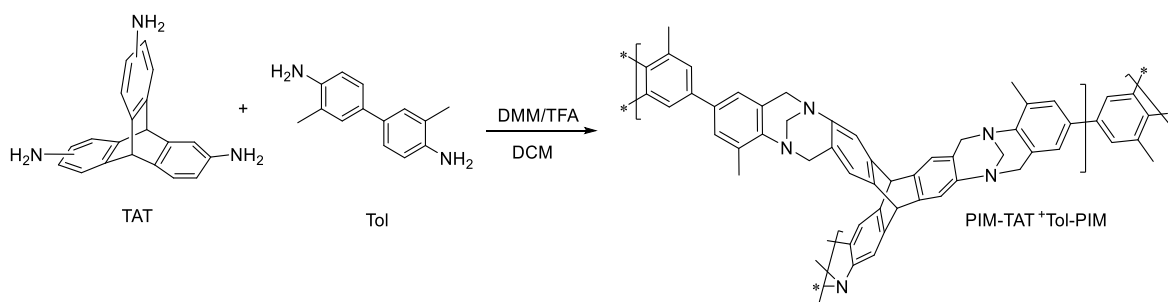
FT-IR:  $\nu$  max ( $\text{cm}^{-1}$ ) 3566, 2199, 1608, 1508, 822;  $^{13}\text{C}$  NMR SS: (101 MHz)  $\delta$  160.5, 144.3, 124.6, 66.8, 58.9, 53.0, 28.3, 20.3, 2.2.

### PIM-DABMA+TAPB-TB



General procedure C was followed using diaminobenzomethanoanthracene (DABMA) (0.50 g, 1.65 mmol), tris(4-aminophenyl)benzene (TAPB) (0.39 g, 1.10 mmol), and dimethoxymethane (0.75 mL, 8.26 mmol) were stirred in DCM (8 mL), followed by dropwise addition of TFA (3.19 mL, 41 mmol). The reaction was left to stir for 16 hours, to yield a brown solid. (0.73 g, 77%) BET: ( $\text{CO}_2$ , 273 K) =  $321 \text{ m}^2 \text{ g}^{-1}$ ; total pore volume = 0.06 (at  $P/P_0 \sim 0.99$ ); TGA: initial mass loss at 330 °C; FT-IR:  $\nu$  max ( $\text{cm}^{-1}$ ) 3664, 3361, 2930, 1669, 1594, 1515, 1212, 1208, 1079, 936, 823, 707, 528.

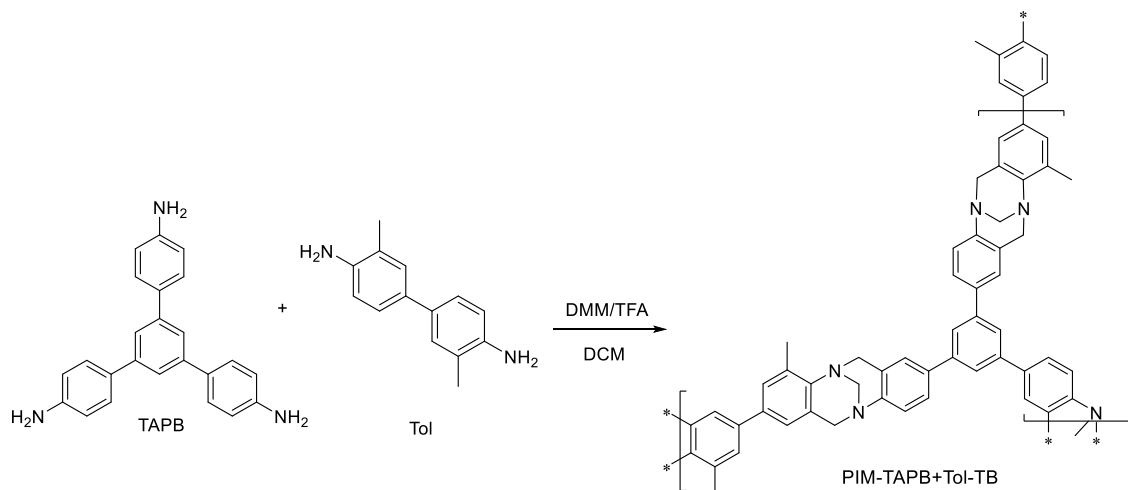
### PIM-TAT+Tol-TB



General procedure C was followed using triaminotriptycene (TAT) (0.53 g, 1.77 mmol), tolidine (Tol) (0.56 g, 2.66 mmol) and dimethoxymethane (1.09 ml, 12.3 mmol) were stirred in DCM (8 mL), followed by dropwise addition of TFA (4 mL, 52.3 mmol). The reaction was left to stir for 16 hours, to yield a brown solid. (0.89 g, 74%) BET: ( $\text{CO}_2$ , 273 K) =  $430 \text{ m}^2 \text{ g}^{-1}$ ; Total pore

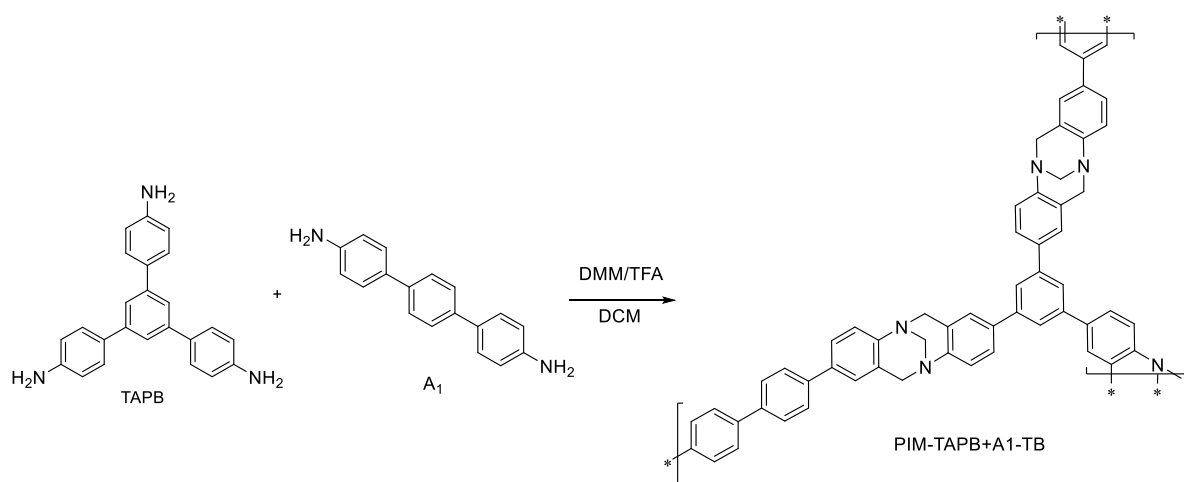
volume = 0.09 (at  $P/P_0 \sim 0.99$ ); TGA: initial mass loss at 440 °C; FT-IR:  $\nu$  max ( $\text{cm}^{-1}$ ) 3676, 2988, 2902, 1409, 1251, 1066, 892.  $^{13}\text{C}$  NMR SS: (101 MHz)  $\delta$  161.9, 144.8, 132.1, 127.7, 123.7, 111.6, 67.5, 53.9, 33.3, 16.6, 2.1.

### PIM-TAPB+Tol-TB

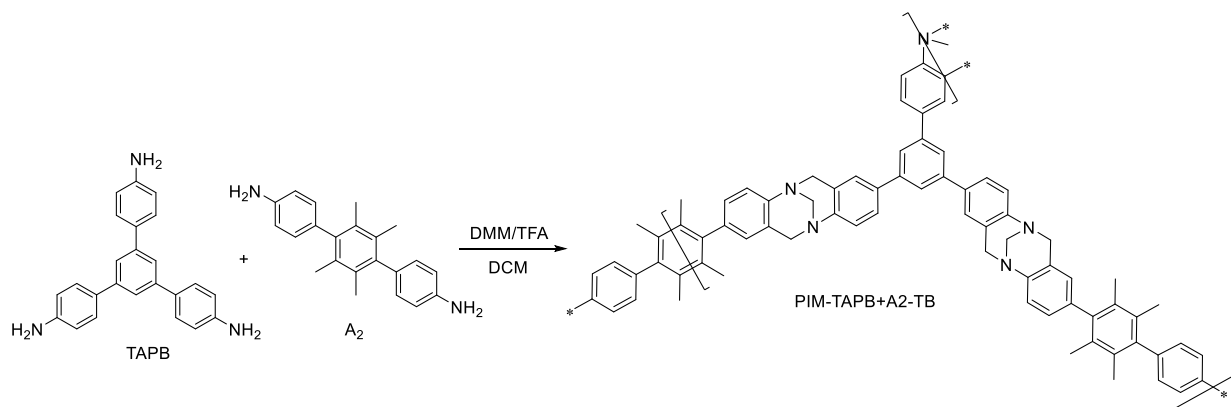


General procedure C was followed using tris(4-aminophenyl)benzene (TAPB) (0.47 g, 1.34 mmol), tolidine (Tol) (0.42 g, 2.01 mmol) and dimethoxymethane (0.83 mL, 9.4 mmol) were stirred in DCM (8 mL), followed by dropwise addition of TFA (3.5 mL, 45.8 mmol). The reaction was left to stir for 16 hours, to yield an orange-brown solid. (0.75 g, 78%) BET: ( $\text{CO}_2$ , 273 K) =  $360 \text{ m}^2 \text{ g}^{-1}$ ; Total pore volume = 0.06 (at  $P/P_0 \sim 0.98$ ); TGA: initial mass loss at 440 °C; FT-IR:  $\nu$  max ( $\text{cm}^{-1}$ ) 2893, 1667, 1199, 825;  $^{13}\text{C}$  NMR SS: (101 MHz)  $\delta$  162.0, 147.6, 144.4, 138.4, 127.4, 80.9, 67.4, 55.7, 27.3, 16.1, 3.2.



**PIM-TAPB+A1-TB**

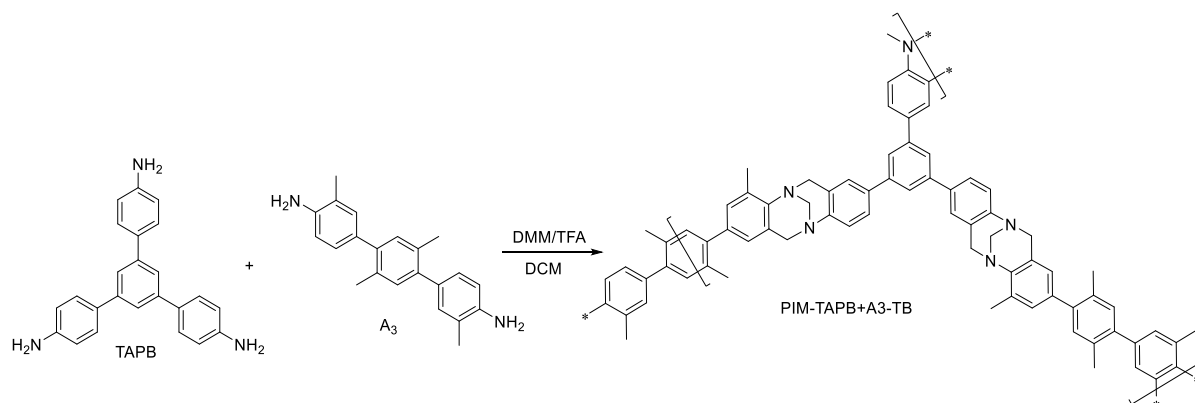
General procedure C was followed using tris(4-aminophenyl)benzene (TAPB) (0.50 g, 1.42 mmol), A1 (0.56 g, 2.13 mmol) and dimethoxymethane (1.0 mL, 11.3 mmol) were stirred in DCM (10 mL), followed by dropwise addition of TFA (4.2 mL, 55 mmol). The reaction was left to stir for 16 hours, to yield a pale-yellow solid. (0.9 g, 78% yield) BET: (CO<sub>2</sub>, 273 K) = 330 m<sup>2</sup> g<sup>-1</sup>; Total pore volume = 0.08 (at P/P<sub>0</sub> ~ 0.98); TGA: initial mass loss at 440 °C; FT-IR: ν max (cm<sup>-1</sup>) 1670, 1606, 1480, 1200, 944, 818; <sup>13</sup>C NMR SS: (101 MHz) δ 157.5, 147.3, 139, 126.7, 67.0, 59.6, 50.7, 42.3, 15.8, 2.7.

**PIM-TAPB+A2-TB**

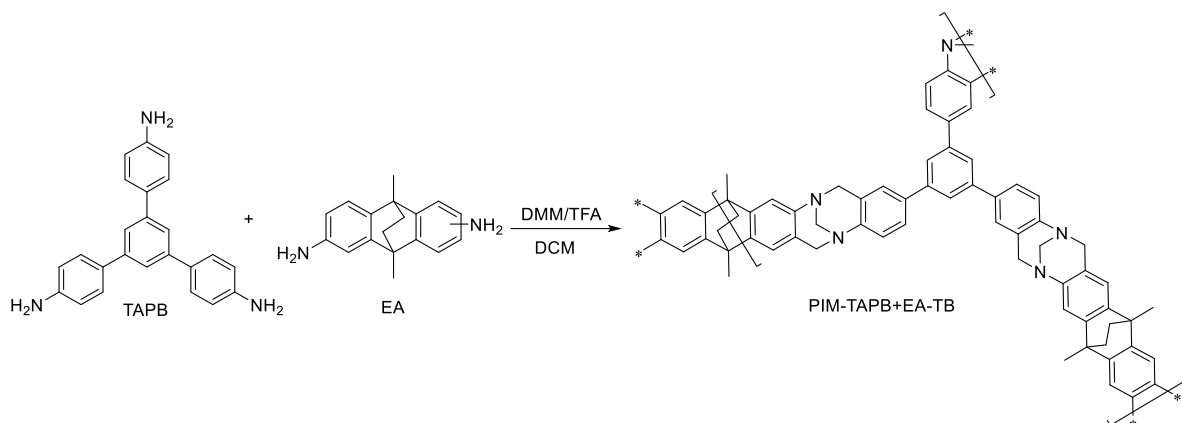
General procedure C was followed using tris(4-aminophenyl)benzene (TAPB) (0.46 g, 1.31 mmol), A2 (0.62 g, 1.96 mmol) and dimethoxymethane (1.0 mL, 11.3 mmol) were stirred in DCM (10 mL), followed by dropwise addition of TFA (4.0 mL, 52 mmol). The reaction was left to stir for 16 hours, to yield a pale-yellow solid. (0.86 g, 75% yield) BET: (CO<sub>2</sub>, 273 K) = 370

$\text{m}^2 \text{g}^{-1}$ ; Total pore volume = 0.08 (at  $P/P_0 \sim 0.98$ ); TGA: initial mass loss at 440 °C; FT-IR:  $\nu_{\text{max}} (\text{cm}^{-1})$  2900, 1660, 1600, 1515, 1207, 950, 830;  $^{13}\text{C}$  NMR SS: (101 MHz)  $\delta$  157.0, 146.9, 140.4, 130.4, 128.0, 67.3, 59.6, 50.2, 32.0, 17.1, 3.7.

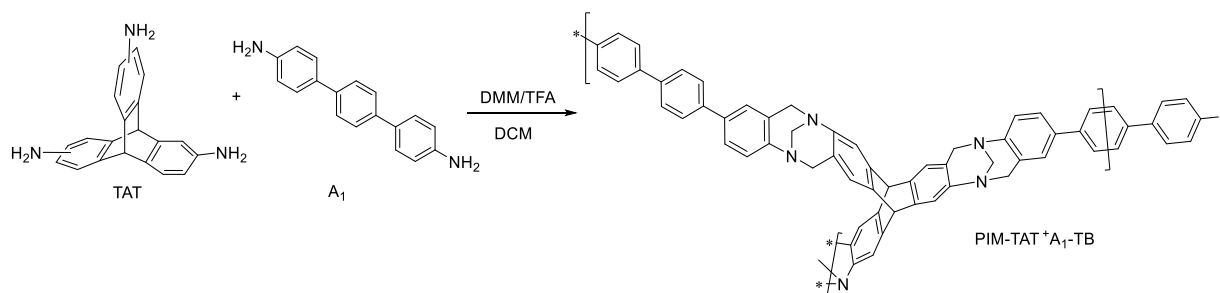
### PIM-TAPB+A3-TB



General procedure C was followed using tris(4-aminophenyl)benzene (TAPB) (0.5 g, 1.42 mmol), A2 (0.67 g, 2.13 mmol) and dimethoxymethane (1.0 mL, 11.3 mmol) were stirred in DCM (10 mL), followed by dropwise addition of TFA (4.2 mL, 52 mmol). The reaction was left to stir for 16 hours, to yield a pale-yellow solid. (0.86 g, 69% yield) BET: ( $\text{CO}_2$ , 273 K) = 350  $\text{m}^2 \text{g}^{-1}$ ; Total pore volume = 0.07 (at  $P/P_0 \sim 0.98$ ); TGA: initial mass loss at 440 °C; FT-IR:  $\nu_{\text{max}} (\text{cm}^{-1})$  2960, 1670, 1590, 1470, 1210, 1060, 940, 865, 830;  $^{13}\text{C}$  NMR SS: (101 MHz)  $\delta$  158.0, 147.3, 143.9, 138.1, 128.0, 67.5, 55.7, 46.2, 25.7, 17.5, 3.4.

**PIM-TAPB+EA-TB**

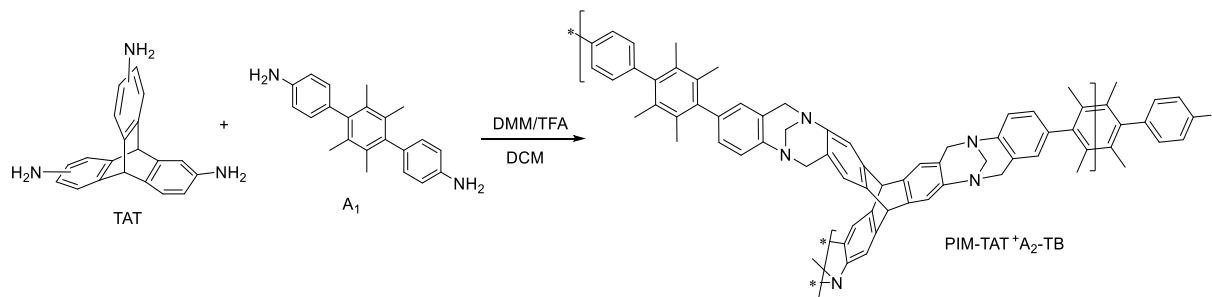
General procedure C was followed using tris(4-aminophenyl)benzene (TAPB) (0.40 g, 1.14 mmol), EA (0.45 g, 1.70 mmol) and dimethoxymethane (1.0 mL, 11.3 mmol) were stirred in DCM (10 mL), followed by dropwise addition of TFA (4.0 mL, 52 mmol). The reaction was left to stir for 16 hours, to yield a pale-yellow solid (0.75 g, 83% yield). BET: (CO<sub>2</sub>, 273 K) = 530 m<sup>2</sup> g<sup>-1</sup>; Total pore volume = 0.14 (at P/P<sub>0</sub> ~ 0.98); TGA: initial mass loss at 440 °C; FT-IR: ν max (cm<sup>-1</sup>) 2930, 1670, 1590, 1495, 1454, 1320, 1203, 1070, 990, 833; <sup>13</sup>C NMR SS: (101 MHz) δ 159.2, 145.3, 124.6, 117.4, 67.2, 59.2, 40.7, 35.9, 17.4, 2.1.

**PIM-TAT+A1-TB**

General procedure C was followed using triaminotriptycene (TAT) (0.50 g, 1.67 mmol), A1 (0.65 g, 2.50 mmol) and dimethoxymethane (1.2 mL, 13.6 mmol) were stirred in DCM (10 mL), followed by dropwise addition of TFA (4.5 mL, 58.8 mmol). The reaction was left to stir for 16 hours, to yield a red-brown solid. (0.85 g, 69% yield) BET: (CO<sub>2</sub>, 273 K) = 520 m<sup>2</sup> g<sup>-1</sup>; Total pore volume = 0.12 (at P/P<sub>0</sub> ~ 0.98); TGA: initial mass loss at 440 °C; FT-IR: ν max (cm<sup>-1</sup>)

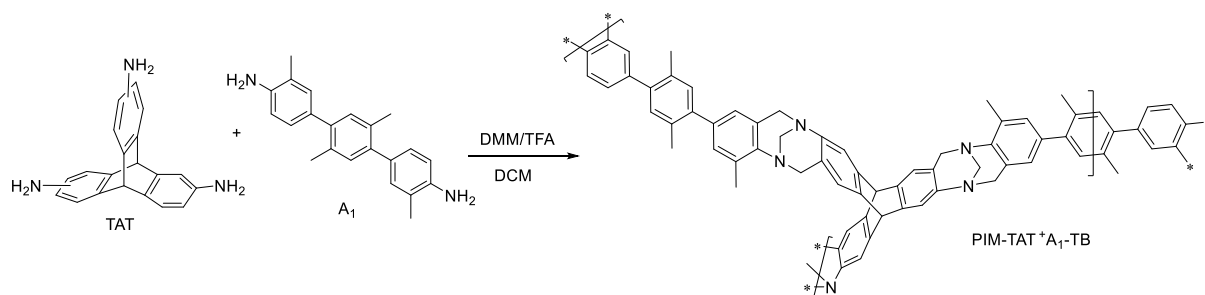
2925, 1664, 1610, 1480, 1205, 1070, 930, 820;  $^{13}\text{C}$  NMR SS: (101 MHz)  $\delta$  156.7, 144.9, 140.7, 125.6, 67.0, 58.9, 52.9, 29.8, 23.5, 1.1.

### PIM-TAT+A2-TB



General procedure C was followed using triaminotriptycene (TAT) (0.32 g, 1.07 mmol), A2 (0.51 g, 1.6 mmol) and dimethoxymethane (0.8 mL, 9.00 mmol) were stirred in DCM (10 mL), followed by dropwise addition of TFA (3.0 mL, 39.2 mmol). The reaction was left to stir for 16 hours, to yield a pale orange solid (0.6 g, 68% yield). BET: ( $\text{CO}_2$ , 273 K) =  $600 \text{ m}^2 \text{ g}^{-1}$ , total pore volume = 0.15 (at  $P/P_0 \sim 0.98$ ); TGA: initial mass loss at 440 °C; FT-IR:  $\nu$  max ( $\text{cm}^{-1}$ ) 2960, 1613, 1460, 1208, 1080, 925, 825;  $^{13}\text{C}$  NMR SS: (101 MHz)  $\delta$  158.5, 145.4, 140.9, 131.3, 123.2, 67.3, 59.3, 53.5, 25.5, 17.1, 1.7.

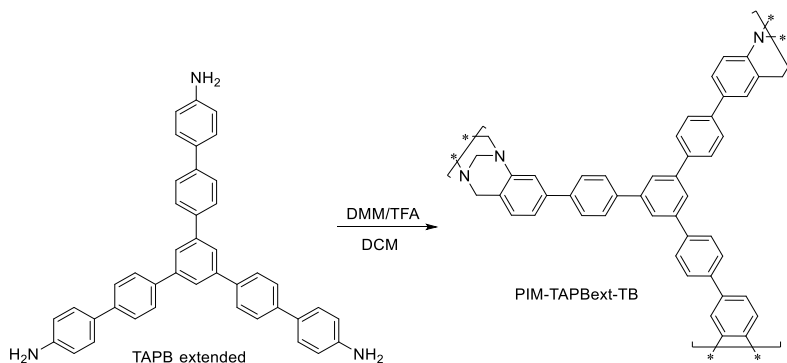
### PIM-TAT+A3-TB



General procedure C was followed using triaminotriptycene (TAT) (0.36 g, 1.20 mmol), A3 (0.57 g, 1.8 mmol) and dimethoxymethane (0.8 mL, 9 mmol) were stirred in DCM (10 mL), followed by dropwise addition of TFA (3.5 mL, 46 mmol). The reaction was left to stir for 16 hours, to yield a brown solid. (0.7 g, 73% yield). BET: ( $\text{CO}_2$ , 273 K) =  $500 \text{ m}^2 \text{ g}^{-1}$ ; Total pore volume = 0.12 (at  $P/P_0 \sim 0.98$ ); TGA: initial mass loss at 440 °C; FT-IR:  $\nu$  max ( $\text{cm}^{-1}$ ) 2970,

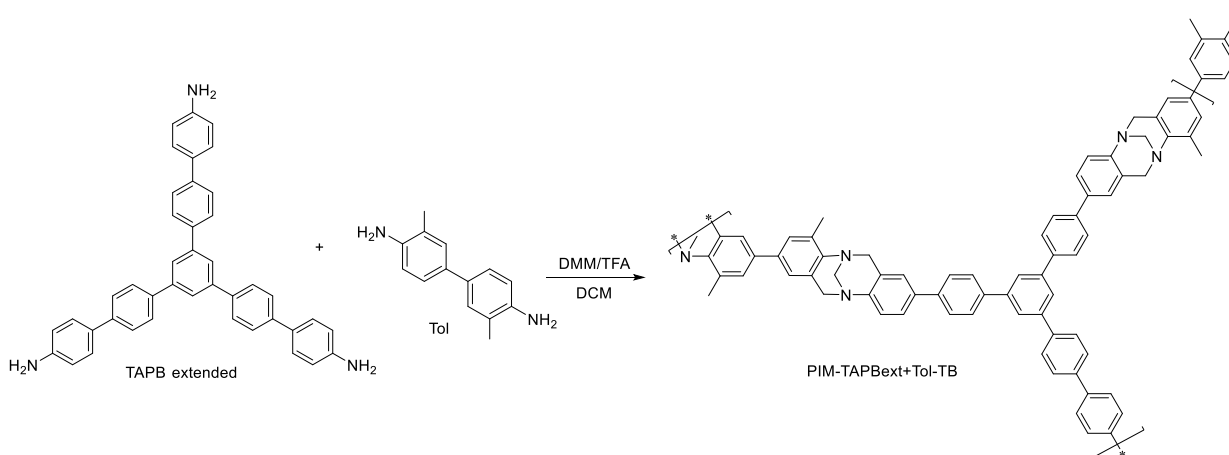
1613, 1465, 1210, 1070, 930, 870;  $^{13}\text{C}$  NMR SS: (101 MHz)  $\delta$  162.1, 144.7, 141.0, 131.6, 124.0, 67.5, 53.7, 39.3, 17.6, 7.4, 3.1.

### PIM-TAPBext-TB



General procedure B was followed using extended tris(4-aminophenyl)benzene (TAPB ext) (0.50 g, 0.86 mmol) and dimethoxymethane (0.6 mL, 6.8 mmol) were stirred in DCM (10 mL), followed by dropwise addition of TFA (2.5 mL, 32.7 mmol). The reaction was left to stir for 16 hours, to yield a pale-yellow solid. (0.38 g, 70% yield) BET: ( $\text{CO}_2$ , 273 K) =  $350 \text{ m}^2 \text{ g}^{-1}$ ; Total pore volume = 0.07 (at  $P/P_0 \sim 0.98$ ); TGA: initial mass loss at 495 °C; FT-IR:  $\nu$  max ( $\text{cm}^{-1}$ ) 1590, 1490, 81;  $^{13}\text{C}$  NMR SS: (101 MHz)  $\delta$  158.0, 147.4, 140.4, 126.9, 67.3, 59.8, 49.5, 39.0, 16.1, 2.4.

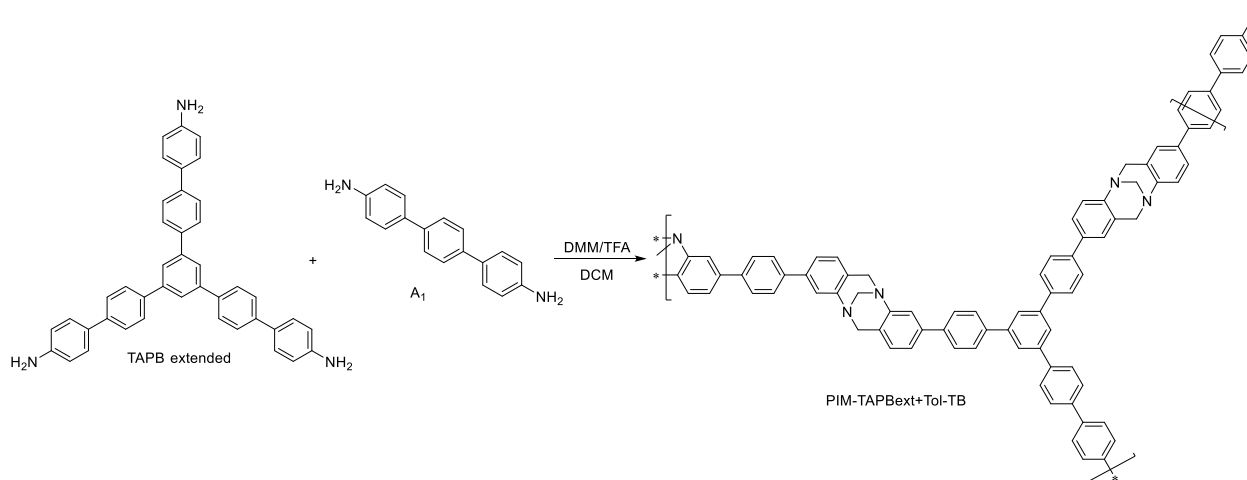
### TAPBext + Tol



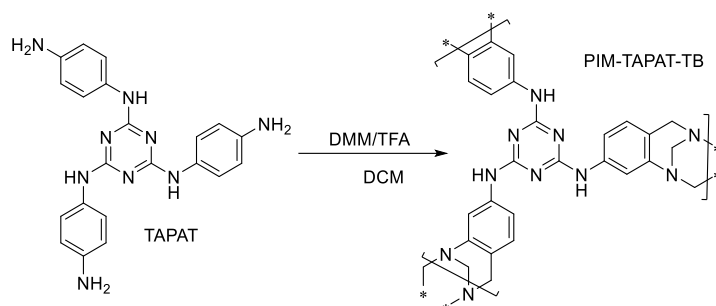
General procedure C was followed using extended Tris(4-aminophenyl)benzene (TAPB ext) (0.5 g, 0.86 mmol), tolidine (Tol) (0.27 g, 1.29 mmol) and dimethoxymethane (0.72 mL, 8 mmol) were stirred in DCM (8 mL), followed by dropwise addition of TFA (3.9 mL, 51 mmol).

The reaction was left to stir for 16 hours, to yield a pale-yellow solid (0.66 g, 80% yield). BET: (CO<sub>2</sub>, 273 K) = 395 m<sup>2</sup> g<sup>-1</sup>; Total pore volume = 0.07 (at P/P<sub>0</sub> ~ 0.98); TGA: initial mass loss at 420 °C; FT-IR:  $\nu$  max (cm<sup>-1</sup>) 3000, 1669, 1596, 1487, 1206, 937, 818, 520; <sup>13</sup>C NMR SS: (101 MHz)  $\delta$  159.9, 147.5, 139.4, 127.2, 67.6, 55.8, 42.0, 26.0, 16.2, 3.0.

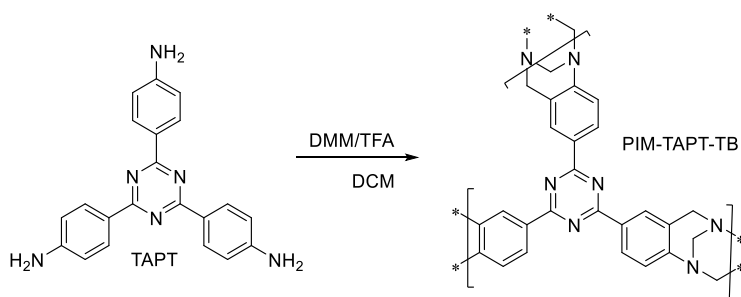
### TAPBext + A1



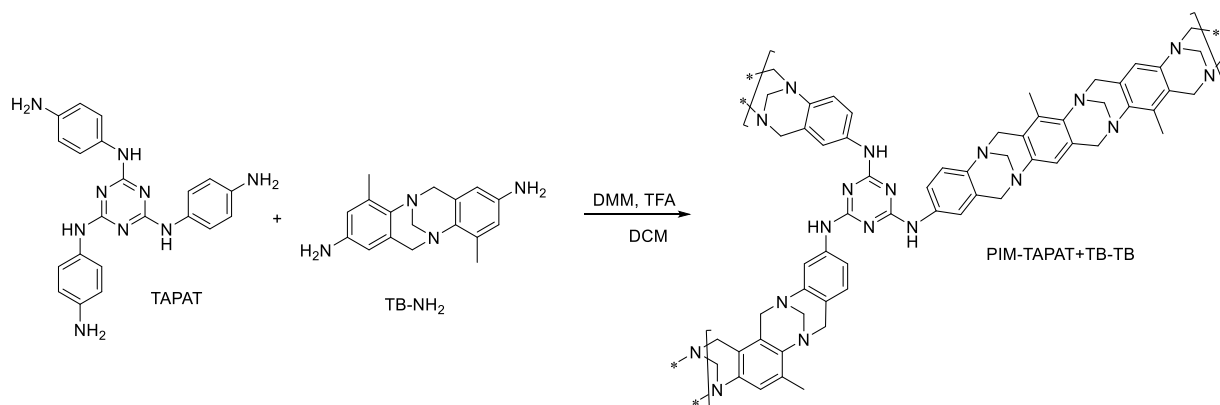
General procedure C was followed using extended tris(4-aminophenyl)benzene (TAPB ext) (0.80 g, 1.38 mmol), A1 (0.54 g, 2.07 mmol) and dimethoxymethane (1.0 mL, 11.3 mmol) were stirred in DCM (10 mL), followed by dropwise addition of TFA (4.0 mL, 52.3 mmol). The reaction was left to stir for 16 hours, to yield a pale-yellow solid (1.00 g, 71% yield). BET: (CO<sub>2</sub>, 273 K) = 250 m<sup>2</sup> g<sup>-1</sup>; Total pore volume = 0.06 (at P/P<sub>0</sub> ~ 0.98); TGA: initial mass loss at 430 °C; FT-IR:  $\nu$  max (cm<sup>-1</sup>) 2980, 1680, 1600, 1490, 1203, 1070, 940, 812; <sup>13</sup>C NMR SS: (101 MHz)  $\delta$  162.1, 144.7, 141.0, 131.6, 124.0, 67.5, 53.7, 39.3, 17.6, 7.4, 3.1.

**TAPAT homopolymer**

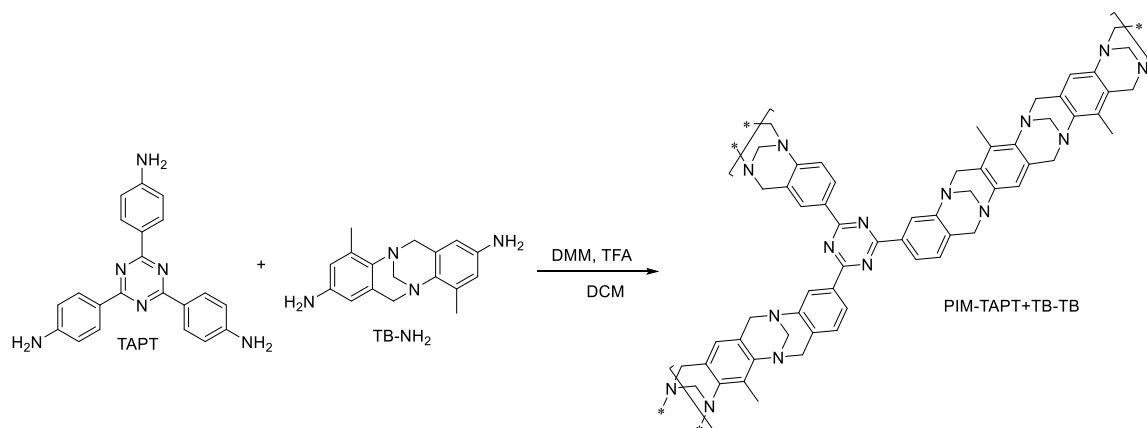
General procedure B was followed using extended tris(aminophenyl)aminotriazine (TAPAT) (1.00 g, 2.50 mmol) and dimethoxymethane (0.6 mL, 17.6 mmol) were stirred in DCM (10 mL), followed by dropwise addition of TFA (7.08 mL, 92.6 mmol). The reaction was left to stir for 18 hours, to yield a brown solid. (1.13 g, 84% yield) BET: (CO<sub>2</sub>, 273 K) = 160 m<sup>2</sup> g<sup>-1</sup>; Total pore volume = 0.03 (at P/P<sub>0</sub> ~ 0.98); TGA: initial mass loss at 495 °C; FT-IR: ν max (cm<sup>-1</sup>) 3370, 2105, 1567, 1481, 1403, 1225, 1198, 1061, 962, 922, 803, 512.

**TAPT homopolymer**

General procedure B was followed using extended tris(aminophenyl)triazine (TAPT) (0.50 g, 1.41 mmol) and dimethoxymethane (0.4 mL, 11.3 mmol) were stirred in DCM (8 mL), followed by dropwise addition of TFA (4.9 mL, 64.1 mmol). The reaction was left to stir for 16 hours, to yield a yellow solid. (0.58 g, 86% yield) BET: (CO<sub>2</sub>, 273 K) = 312 m<sup>2</sup> g<sup>-1</sup>; Total pore volume = 0.05 (at P/P<sub>0</sub> ~ 0.98); TGA: initial mass loss at 460 °C; FT-IR: ν max (cm<sup>-1</sup>) 3660, 2973, 2883, 1676, 1603, 1497, 1357, 1183, 944, 815, 578.

**TAPAT + TB**

General procedure C was followed using tri(aminophenyl)aminotriazine (TAPAT) (0.65 g, 1.63 mmol), TB-NH<sub>2</sub> (0.68 g, 2.44 mmol) and dimethoxymethane (1.01 mL, 11.41 mmol) were stirred in DCM (12 mL), followed by dropwise addition of TFA (5.0 mL, 62.8 mmol). The reaction was left to stir for 16 hours, to yield a pale-yellow solid. (1.12 g, 77% yield) BET: (CO<sub>2</sub>, 273 K) = 285 m<sup>2</sup> g<sup>-1</sup>; Total pore volume = 0.04 (at P/P<sub>0</sub> ~ 0.98); TGA: initial mass loss at 440 °C; FT-IR: v max (cm<sup>-1</sup>) 3663, 2922, 1981, 1708, 1610, 1486, 1265, 1207, 1065, 925, 829, 826, 720, 608, 529, 436.

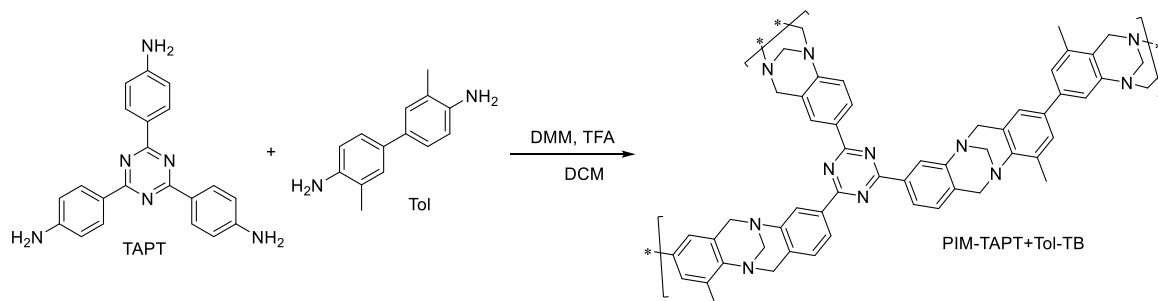
**TAPT + TB**

General procedure C was followed using tri(aminophenyl)triazine (TAPT) (0.50 g, 1.41 mmol), TB-NH<sub>2</sub> (0.59 g, 2.12 mmol) and dimethoxymethane (0.9 mL, 10.2 mmol) were stirred in DCM (12 mL), followed by dropwise addition of TFA (4.0 mL, 52.3 mmol). The reaction was left to stir for 16 hours, to yield a pale-yellow solid. (0.95 g, 69% yield) BET: (CO<sub>2</sub>, 273 K) = 150 m<sup>2</sup>



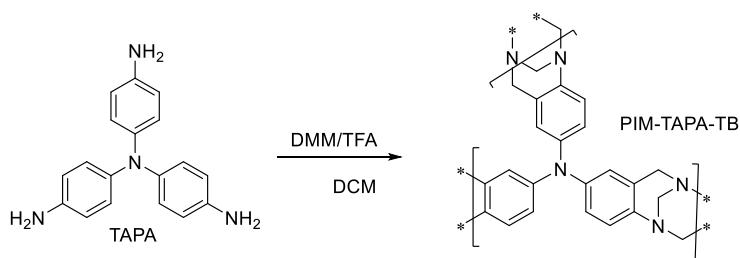
$\text{g}^{-1}$ ; Total pore volume = 0.04 (at  $P/P_0 \sim 0.98$ ); TGA: initial mass loss at 460 °C; FT-IR:  $\nu_{\text{max}}$  ( $\text{cm}^{-1}$ ) 3399, 2900, 1672, 1605, 1502, 1416, 1358, 1285, 1181, 1144, 813, 534.

### TAPT + Tol

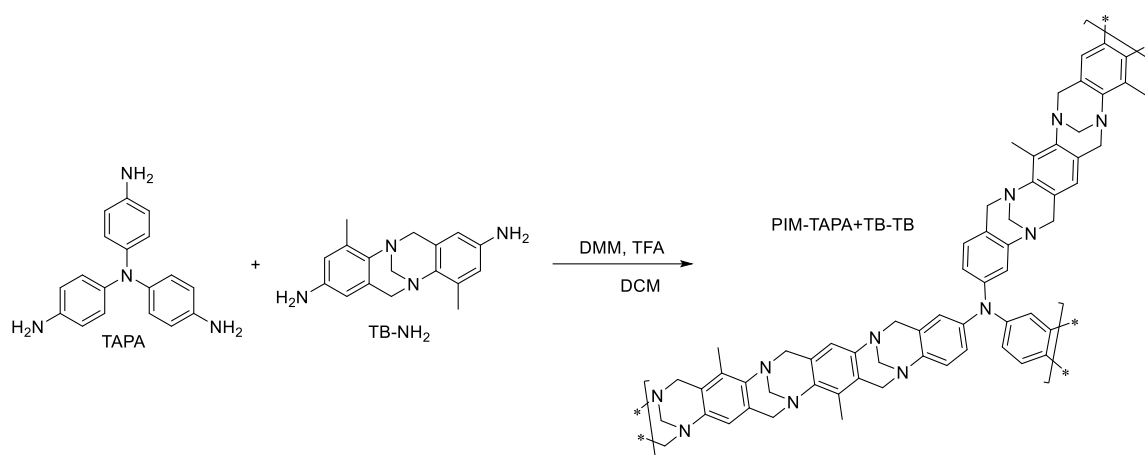


General procedure C was followed using tri(aminophenyl)triazine (TAPT) (0.61 g, 1.72 mmol), tolidine (Tol) (0.55 g, 2.58 mmol) and dimethoxymethane (1.22 mL, 13.77 mmol) were stirred in DCM (10 mL), followed by dropwise addition of TFA (5.93 mL, 77.4 mmol). The reaction was left to stir for 16 hours, to yield a pale-yellow solid. (1.04 g, 71%) BET: ( $\text{CO}_2$ , 273 K) = 220  $\text{m}^2 \text{g}^{-1}$ ; Total pore volume = 0.03 (at  $P/P_0 \sim 0.98$ ); TGA: initial mass loss at 440 °C; FT-IR:  $\nu_{\text{max}}$  ( $\text{cm}^{-1}$ ) 2920, 2109, 2019, 1667, 1604, 1503, 1351, 1177, 810, 510, 416.

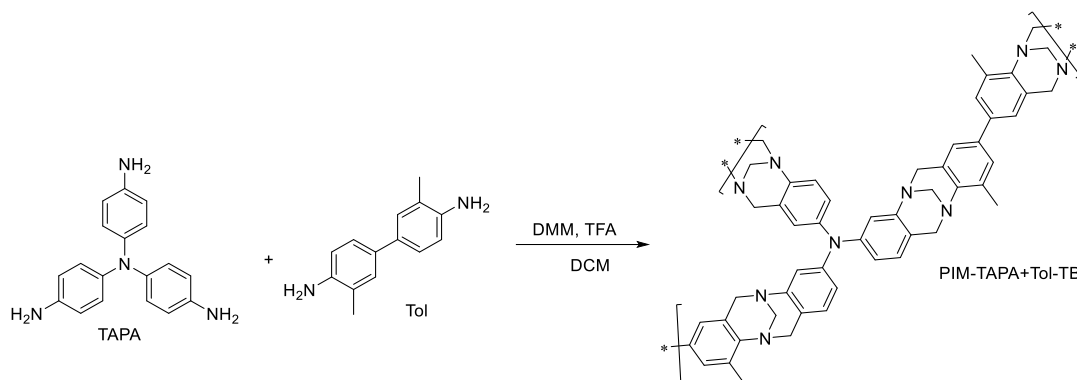
### TAPA homopolymer



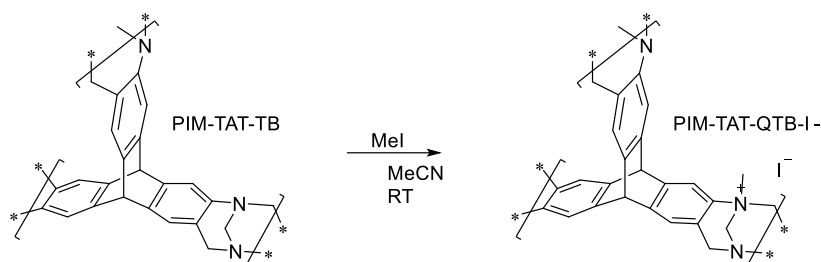
General procedure B was followed using extended tris(aminophenyl)amine (TAPA) (0.50 g, 1.72 mmol) and dimethoxymethane (0.6 mL, 17.6 mmol) were stirred in DCM (10 mL), followed by dropwise addition of TFA (4.9 mL, 64.1 mmol). The reaction was left to stir for 16 hours, to yield a yellow solid. (0.5 g, 84% yield) BET: ( $\text{CO}_2$ , 273 K) = 420  $\text{m}^2 \text{g}^{-1}$ ; Total pore volume = 0.04 (at  $P/P_0 \sim 0.98$ ); TGA: initial mass loss at 440 °C; FT-IR:  $\nu_{\text{max}}$  ( $\text{cm}^{-1}$ ) 3662, 2988, 2902, 1982, 1655, 1605, 1485, 1407, 1230, 1066, 929, 824, 719, 530.

**TAPA + TB**

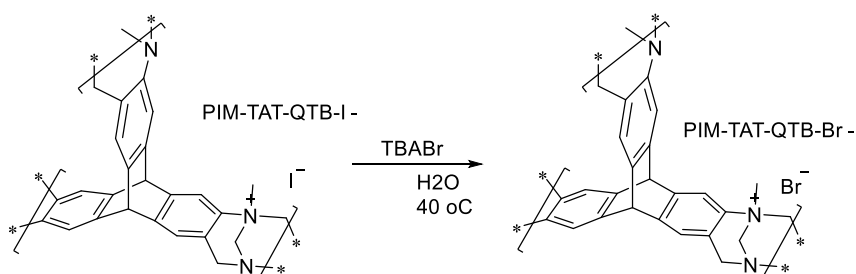
General procedure C was followed using tri(aminophenyl)amine (TAPA) (0.50 g, 1.72 mmol), TB-NH<sub>2</sub> (0.72 g, 2.58 mmol) and dimethoxymethane (1.22 mL, 13.77 mmol) were stirred in DCM (8 mL), followed by dropwise addition of TFA (5.93 mL, 77.4 mmol). The reaction was left to stir for 16 hours, to yield a pale-yellow solid. (1.20 g, 74%) BET: (CO<sub>2</sub>, 273 K) = 170 m<sup>2</sup> g<sup>-1</sup>; Total pore volume = 0.03 (at P/P<sub>0</sub> ~ 0.98); TGA: initial mass loss at 440 °C; FT-IR:  $\nu$  max (cm<sup>-1</sup>) 3663, 2924, 1669, 1606, 1505, 1200, 1066, 929, 826, 530.

**TAPA + Tol**

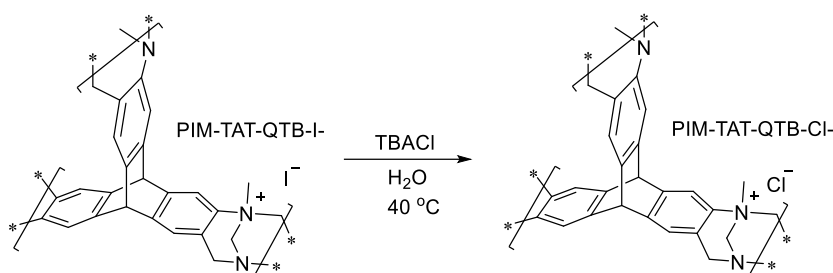
General procedure C was followed using tri(aminophenyl)amine (TAPA) (0.50 g, 1.72 mmol), tolidine (Tol) (0.55 g, 2.58 mmol) and dimethoxymethane (1.22 mL, 13.77 mmol) were stirred in DCM (6 mL), followed by dropwise addition of TFA (5.93 mL, 77.4 mmol). The reaction was left to stir for 16 hours, to yield a pale-yellow solid. (1.06 g, 78%) BET: (CO<sub>2</sub>, 273 K) = 260 m<sup>2</sup> g<sup>-1</sup>; Total pore volume = 0.01 (at P/P<sub>0</sub> ~ 0.98); TGA: initial mass loss at 420 °C; FT-IR:  $\nu$  max (cm<sup>-1</sup>) 3361, 1668, 1517, 1480, 1405, 1218, 804, 510.

**PIM-TAT-QTB-I<sup>-</sup>**

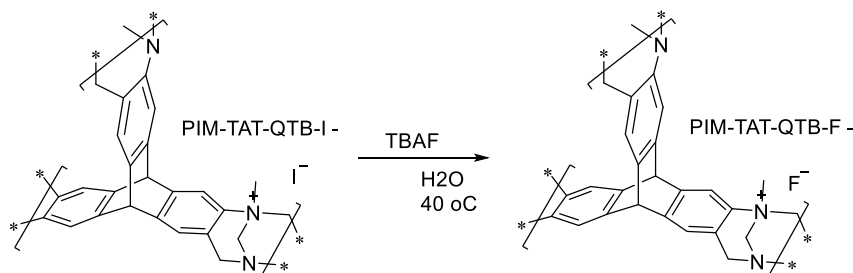
PIM-TAT-TB (0.50 g, 1.38 mmol) was added to a mixture of acetonitrile (10 ml) and methyl iodide (1.3 ml), and the reaction was left to stir at room temperature for 7 days. The reaction was filtered through an oven dry sinter and washed with plenty of deionised water (~ 300 ml) into a solution of NaOH to neutralise the excess methyl iodide. The reaction was then washed with 100 ml portions of ethanol and methanol, and then refluxed in methanol for 48 hours. The powder was then filtered and dried in a vacuum oven at a low temperature overnight to give the product as a light brown powder (0.7 g, 100%). BET: (N<sub>2</sub>, 77 K) = 40 m<sup>2</sup> g<sup>-1</sup>; Total pore volume = 0.17 (at P/P<sub>0</sub> ~ 0.98); TGA: initial mass loss at 150 °C, then 500 °C.

**PIM-TAT-QTB-Br<sup>-</sup>**

PIM-TAT-QTB-I<sup>-</sup> (0.70 g, 1.38 mmol) was added to a mixture of deionised water (20 ml) and tetrabutylammonium bromide (6.5 g), and then stirred at 40 °C for 7 days. The mixture was filtered through an oven dry sinter funnel and washed with plenty of deionised water (~300 ml), followed by methanol. The solid was then refluxed twice in methanol, before filtering and dry it at a low temperature in a pressure oven, to give the product as a pale brown powder (0.63 g, 100%). BET: (N<sub>2</sub>, 77 K) = 165 m<sup>2</sup> g<sup>-1</sup>; Total pore volume = 0.17 (at P/P<sub>0</sub> ~ 0.98); TGA: initial mass loss at 170 °C, then 440 °C.

**PIM-TAT-QTB-Cl<sup>-</sup>**

PIM-TAT-QTB-I<sup>-</sup> (0.70 g, 1.38 mmol) was added to a mixture of deionised water (20 ml) and tetrabutylammonium chloride (5.6 g), and then stirred at 40 °C for 7 days. The mixture was filtered through an oven dry sinter funnel and washed with plenty of deionised water (~300 ml), followed by methanol. The solid was then refluxed twice in methanol, before filtering and dry it at a low temperature in a pressure oven, to give the product as a pale brown powder (0.57 g, 100%). BET: (N<sub>2</sub>, 77 K) = 397 m<sup>2</sup> g<sup>-1</sup>; Total pore volume = 0.22 (at P/P<sub>0</sub> ~ 0.98); TGA: initial mass loss at 170 °C, then 460 °C.

**PIM-TAT-QTB-F<sup>-</sup>**

PIM-TAT-QTB-I<sup>-</sup> (0.70 g, 1.38 mmol) was added to a mixture of deionised water (20 ml) and tetrabutylammonium fluoride (5.27 g), and then stirred at 40 °C for 7 days. The mixture was filtered through an oven dry sinter funnel and washed with plenty of deionised water (~300 ml), followed by methanol. The solid was then refluxed twice in methanol, before filtering and dry it at a low temperature in a pressure oven, to give the product as a pale brown powder (0.55 g, 100%). BET: (N<sub>2</sub>, 77 K) = 560 m<sup>2</sup> g<sup>-1</sup>; Total pore volume = 0.29 (at P/P<sub>0</sub> ~ 0.98); TGA: initial mass loss at 200 °C, then 400 °C.

# Chapter 9 – References

1. C. Le Quéré, R. M. Andrew, P. Friedlingstein, S. Sitch, J. Hauck, J. Pongratz, P. A. Pickers, J. I. Korsbakken, G. P. Peters and J. G. Canadell, *Earth System Science Data*, 2018, **10**, 2141-2194.
2. P. Anastas and N. Eghbali, *Chemical Society Reviews*, 2010, **39**, 301-312.
3. E. Harrison, H. Smith and I. Dekker.
4. J. Clayden, N. Greeves and S. Warren, *Organic Chemistry*, Oxford University Press, Oxford, 2nd edn., 2012.
5. P. Flowers, K. Theopold and R. Langley, Chemistry, <https://opentextbc.ca/chemistry/chapter/12-7-catalysis/>, (accessed June 2019).
6. M. F. Rayner-Canham, M. Rayner-Canham and G. Rayner-Canham, *Women in Chemistry: Their Changing Roles from Alchemical Times to the Mid-twentieth Century*, Chemical Heritage Foundation, 2001.
7. A. U. Czaja, N. Trukhan and U. Müller, *Chemical Society Reviews*, 2009, **38**, 1284-1293.
8. P. H. Pfromm, *Journal of Renewable and Sustainable Energy*, 2017, **9**.
9. V. Smil, *Enriching the Earth: Fritz Haber, Carl Bosch, and the Transformation of World Food Production*, MIT Press, 2004.
10. M. D. Fryzuk, *Nature*, 2004, **427**, 498-499.
11. E. Farnetti, R. Di Monte and J. Kašpar, *Inorganic and Bio-Inorganic Chemistry*, 2009, **2**, 50-86.
12. M. Bowker, *Oxford Chemistry Primers*, 1998, **53**, ALL-ALL.
13. M. Bowker, *THE BASIS AND APPLICATIONS OF HETEROGENEOUS CATALYSIS. Edition en anglais*, Oxford University Press, Incorporated, 1998.
14. M. A. van Spronsen, J. W. M. Frenken and I. M. N. Groot, *Nature Communications*, 2017, **8**.
15. R. Whyman, *Oxford Chemistry Primers*, 2001, **96**, ALL-ALL.
16. C. Costentin, S. Drouet, M. Robert and J.-M. Savéant, *Journal of the American Chemical Society*, 2012, **134**, 11235-11242.
17. M. Boudart, *Chemical reviews*, 1995, **95**, 661-666.
18. S. Kozuch and J. M. Martin, *Journal*, 2012.
19. D. Shriver and P. Atkins, *Inorganic Chemistry*, W. H. Freeman, 2009.
20. J. Rouquerol, D. Avnir, C. W. Fairbridge, D. H. Everett, J. H. Haynes, N. Pernicone, J. D. F. Ramsay, K. S. W. Sing and K. K. Unger, *Pure and Applied Chemistry*, 1994, **66**, 1739-1758.
21. S. Brunauer, P. H. Emmett and E. Teller, *Journal of the American chemical society*, 1938, **60**, 309-319.
22. J. Su and J.-S. Chen, *Microporous and Mesoporous Materials*, 2017, **237**, 246-259.
23. E. M. Flanigen, in *Studies in surface science and catalysis*, Elsevier, 1991, vol. 58, pp. 13-34.
24. C. Baerlocher and L. B. McCusker, Database of Zeolite Structures, <http://www.iza-structure.org/databases/>, (2020).
25. C. S. Cundy and P. A. Cox, *Chemical reviews*, 2003, **103**, 663-702.
26. Y. Li, L. Li and J. Yu, *Chem*, 2017, **3**, 928-949.

27. R. Millini, X. Zou, K. Strohmaier, W. Schwieger, P. Eliasova, R. E. Morris, B. Weckhuysen, W. Zhou, S. Abdo and A. Martinez, *Zeolites in catalysis: properties and applications*, Royal Society of Chemistry, 2017.
28. S. Bhatia, *Zeolite catalysts: principles and applications*, CRC press, 1989.
29. J. Liang, Z. Liang, R. Zou and Y. Zhao, *Advanced Materials*, 2017, **29**, 1701139.
30. U. Olsbye, S. Svelle, M. Bjørgen, P. Beato, T. V. Janssens, F. Joensen, S. Bordiga and K. P. Lillerud, *Angewandte Chemie International Edition*, 2012, **51**, 5810-5831.
31. J. Li, H. Chang, L. Ma, J. Hao and R. T. Yang, *Catalysis today*, 2011, **175**, 147-156.
32. B. Yilmaz, N. Trukhan and U. MÜLLER, *Chinese Journal of Catalysis*, 2012, **33**, 3-10.
33. J. Cejka, A. Corma and S. Zones, *Zeolites and catalysis: synthesis, reactions and applications*, John Wiley & Sons, 2010.
34. J. Weitkamp, *Solid state ionics*, 2000, **131**, 175-188.
35. A. Corma, M. J. Díaz-Cabañas, J. Martínez-Triguero, F. Rey and J. Rius, *Nature*, 2002, **418**, 514-517.
36. A. Dhakshinamoorthy, M. Alvaro, A. Corma and H. Garcia, *Dalton Transactions*, 2011, **40**, 6344-6360.
37. Y. Murakami, A. Iijima and J. W. Ward, *New developments in zeolite science and technology*, Elsevier, 1986.
38. T. F. Degnan Jr, C. M. Smith and C. R. Venkat, *Applied catalysis A: general*, 2001, **221**, 283-294.
39. K. Tanabe and W. F. Hölderich, *Applied Catalysis A: General*, 1999, **181**, 399-434.
40. L. Kurfířtová, Y.-K. Seo, Y. K. Hwang, J.-S. Chang and J. Čejka, *Catalysis today*, 2012, **179**, 85-90.
41. M. Bejblova, D. Prochazkova and J. Čejka, *ChemSusChem: Chemistry & Sustainability Energy & Materials*, 2009, **2**, 486-499.
42. B. I. Roman, N. D. Kimpe and C. V. Stevens, *Chemical reviews*, 2010, **110**, 5914-5988.
43. C. Guignard, V. Pédrón, F. Richard, R. Jacquot, M. Spagnol, J. Coustard and G. Pérot, *Applied Catalysis A: General*, 2002, **234**, 79-90.
44. H. Owen, S. K. Marsh and B. S. Wright, *Journal*, 1984.
45. C. S. H. Chen and R. F. Bridger, *Journal of Catalysis*, 1996, **161**, 687-693.
46. R. J. Quann, L. A. Green, S. A. Tabak and F. J. Krambeck, *Industrial & engineering chemistry research*, 1988, **27**, 565-570.
47. R. I. Kureshy, S. Singh, N.-u. H. Khan, S. H. R. Abdi, E. Suresh and R. V. Jasra, *Journal of Molecular Catalysis A: Chemical*, 2007, **264**, 162-169.
48. R. I. Kureshy, S. Agrawal, M. Kumar, H. K. Noor-ul, S. H. Abdi and H. C. Bajaj, *Catalysis letters*, 2010, **134**, 318-323.
49. B. Tang, W. Dai, G. Wu, N. Guan, L. Li and M. Hunger, *ACS Catalysis*, 2014, **4**, 2801-2810.
50. M. S. Holm, E. Taarning, K. Egeblad and C. H. Christensen, *Catalysis Today*, 2011, **168**, 3-16.
51. M. Bjørgen, S. Svelle, F. Joensen, J. Nerlov, S. Kolboe, F. Bonino, L. Palumbo, S. Bordiga and U. Olsbye, *Journal of Catalysis*, 2007, **249**, 195-207.
52. H. Kim, H.-G. Jang, E. Jang, S. J. Park, T. Lee, Y. Jeong, H. Baik, S. J. Cho and J. Choi, *Catalysis Today*, 2018, **303**, 150-158.
53. J. Kim, M. Choi and R. Ryoo, *Journal of Catalysis*, 2010, **269**, 219-228.

54. T. Ennaert, J. Van Aelst, J. Dijkmans, R. De Clercq, W. Schutyser, M. Dusselier, D. Verboekend and B. F. Sels, *Chemical Society Reviews*, 2016, **45**, 584-611.
55. D. Verboekend, S. Mitchell and J. Pérez-Ramírez, *CHIMIA International Journal for Chemistry*, 2013, **67**, 327-332.
56. A. Feliczak-Guzik, *Microporous and Mesoporous Materials*, 2018, **259**, 33-45.
57. M. I. Besson, P. Gallezot and C. Pinel, *Chemical reviews*, 2014, **114**, 1827-1870.
58. T. Ennaert, J. Geboers, E. Gobechiya, C. M. Courtin, M. Kurttepel, K. Houthoofd, C. E. Kirschhock, P. C. Magusin, S. Bals and P. A. Jacobs, *ACS catalysis*, 2015, **5**, 754-768.
59. A. Galadima and O. Muraza, *Energy Conversion and Management*, 2015, **105**, 338-354.
60. J. Jae, G. A. Tompsett, A. J. Foster, K. D. Hammond, S. M. Auerbach, R. F. Lobo and G. W. Huber, *Journal of Catalysis*, 2011, **279**, 257-268.
61. D. Verboekend, N. Nuttens, R. Locus, J. Van Aelst, P. Verolme, J. Groen, J. Pérez-Ramírez and B. Sels, *Chemical Society Reviews*, 2016, **45**, 3331-3352.
62. M. Moliner, C. Martínez and A. Corma, *Angewandte Chemie International Edition*, 2015, **54**, 3560-3579.
63. C. Perego and R. Millini, *Chemical Society Reviews*, 2013, **42**, 3956-3976.
64. Y. Zhou, S. Hu, X. Ma, S. Liang, T. Jiang and B. Han, *Journal of Molecular Catalysis A: Chemical*, 2008, **284**, 52-57.
65. J. N. Appaturi and F. Adam, *Applied Catalysis B: Environmental*, 2013, **136**, 150-159.
66. X.-B. Lu and D. J. Darensbourg, *Chemical Society Reviews*, 2012, **41**, 1462-1484.
67. E. J. Doskocil, S. V. Bordawekar, B. G. Kaye and R. J. Davis, *The Journal of Physical Chemistry B*, 1999, **103**, 6277-6282.
68. C.-G. Li, L. Xu, P. Wu, H. Wu and M. He, *Chemical Communications*, 2014, **50**, 15764-15767.
69. A. Corma, V. Fornes, R. Martin-Aranda, H. Garcia and J. Primo, *Applied catalysis*, 1990, **59**, 237-248.
70. S. Saravanamurugan, M. Palanichamy, M. Hartmann and V. Murugesan, *Applied Catalysis A: General*, 2006, **298**, 8-15.
71. M. Opanasenko, A. Dhakshinamoorthy, M. Shamzhy, P. Nachtigall, M. Horáček, H. Garcia and J. Čejka, *Catalysis Science & Technology*, 2013, **3**, 500-507.
72. J. Weitkamp, M. Hunger and U. Ryma, *Microporous and Mesoporous Materials*, 2001, **48**, 255-270.
73. D. J. Tranchemontagne, J. L. Mendoza-Cortés, M. O'Keeffe and O. M. Yaghi, *Chemical Society Reviews*, 2009, **38**, 1257-1283.
74. G. Chen, X. Leng, J. Luo, L. You, C. Qu, X. Dong, H. Huang, X. Yin and J. Ni, *Molecules*, 2019, **24**, 1211.
75. J. Gascon and F. Kapteijn, *Angewandte Chemie International Edition*, 2010, **49**, 1530-1532.
76. Y. Li and J. Yu, *Chemical reviews*, 2014, **114**, 7268-7316.
77. D. Farrusseng, S. Aguado and C. Pinel, *Angewandte Chemie International Edition*, 2009, **48**, 7502-7513.
78. T. C. Wang, W. Bury, D. A. Gómez-Gualdrón, N. A. Vermeulen, J. E. Mondloch, P. Deria, K. Zhang, P. Z. Moghadam, A. A. Sarjeant and R. Q. Snurr, *Journal of the American Chemical Society*, 2015, **137**, 3585-3591.

79. A. H. Chughtai, N. Ahmad, H. A. Younus, A. Laypkov and F. Verpoort, *Chemical Society Reviews*, 2015, **44**, 6804-6849.
80. A. Corma, H. García and F. Lladrés i Xamena, *Chemical reviews*, 2010, **110**, 4606-4655.
81. M. H. Alkordi, Y. Liu, R. W. Larsen, J. F. Eubank and M. Eddaoudi, *Journal of the American Chemical Society*, 2008, **130**, 12639-12641.
82. J. Perles, M. Iglesias, M.-Á. Martín-Luengo, M. Á. Monge, C. Ruiz-Valero and N. Snejko, *Chemistry of materials*, 2005, **17**, 5837-5842.
83. C. Di Nicola, Y. Y. Karabach, A. M. Kirillov, M. Monari, L. Pandolfo, C. Pettinari and A. J. Pombeiro, *Inorganic chemistry*, 2007, **46**, 221-230.
84. R. Q. Zou, H. Sakurai and Q. Xu, *Angewandte Chemie International Edition*, 2006, **45**, 2542-2546.
85. C. J. Chuck, M. G. Davidson, M. D. Jones, G. Kociok-Köhn, M. D. Lunn and S. Wu, *Inorganic chemistry*, 2006, **45**, 6595-6597.
86. S. Yuan, L. Feng, K. Wang, J. Pang, M. Bosch, C. Lollar, Y. Sun, J. Qin, X. Yang and P. Zhang, *Advanced Materials*, 2018, **30**, 1704303.
87. C. Janiak and J. K. Vieth, *New Journal of Chemistry*, 2010, **34**, 2366-2388.
88. P. Horcajada, S. Surblé, C. Serre, D.-Y. Hong, Y.-K. Seo, J.-S. Chang, J.-M. Grenèche, I. Margiolaki and G. Férey, *Chemical Communications*, 2007, 2820-2822.
89. A. Dhakshinamoorthy, M. Alvaro and H. Garcia, *Advanced Synthesis & Catalysis*, 2010, **352**, 711-717.
90. A. Dhakshinamoorthy, M. Alvaro and H. Garcia, *Chemistry—A European Journal*, 2010, **16**, 8530-8536.
91. L. Mitchell, B. Gonzalez-Santiago, J. P. Mowat, M. E. Gunn, P. Williamson, N. Acerbi, M. L. Clarke and P. A. Wright, *Catalysis Science & Technology*, 2013, **3**, 606-617.
92. Y. X. Zhou, Y. Z. Chen, Y. Hu, G. Huang, S. H. Yu and H. L. Jiang, *Chemistry—A European Journal*, 2014, **20**, 14976-14980.
93. O. V. Zalomaeva, A. M. Chibiryayev, K. A. Kovalenko, O. A. Kholdeeva, B. S. Balzhinimaev and V. P. Fedin, *Journal of catalysis*, 2013, **298**, 179-185.
94. O. V. Zalomaeva, N. V. Maksimchuk, A. M. Chibiryayev, K. A. Kovalenko, V. P. Fedin and B. S. Balzhinimaev, *Journal of energy chemistry*, 2013, **22**, 130-135.
95. M. G. Goesten, J. Juan-Alcañiz, E. V. Ramos-Fernandez, K. S. S. Gupta, E. Stavitski, H. van Bekkum, J. Gascon and F. Kapteijn, *Journal of catalysis*, 2011, **281**, 177-187.
96. P.-Z. Li, X.-J. Wang, J. Liu, J. S. Lim, R. Zou and Y. Zhao, *Journal of the American Chemical Society*, 2016, **138**, 2142-2145.
97. A. Henschel, K. Gedrich, R. Kraehnert and S. Kaskel, *Chemical Communications*, 2008, 4192-4194.
98. L. Bromberg, Y. Diao, H. Wu, S. A. Speakman and T. A. Hatton, *Chemistry of Materials*, 2012, **24**, 1664-1675.
99. F. Vermoortele, R. Ameloot, A. Vimont, C. Serre and D. De Vos, *Chemical communications*, 2011, **47**, 1521-1523.
100. F. Vermoortele, B. Bueken, G. I. Le Bars, B. Van de Voorde, M. Vandichel, K. Houthoofd, A. Vimont, M. Daturi, M. Waroquier and V. Van Speybroeck, *Journal of the American Chemical Society*, 2013, **135**, 11465-11468.
101. F. Vermoortele, M. Vandichel, B. Van de Voorde, R. Ameloot, M. Waroquier, V. Van Speybroeck and D. E. De Vos, *Angewandte Chemie International Edition*, 2012, **51**, 4887-4890.



102. D. Feng, Z.-Y. Gu, Y.-P. Chen, J. Park, Z. Wei, Y. Sun, M. Bosch, S. Yuan and H.-C. Zhou, *Journal of the American Chemical Society*, 2014, **136**, 17714-17717.
103. C. H. Hendon and A. Walsh, *Chemical science*, 2015, **6**, 3674-3683.
104. K. Schlichte, T. Kratzke and S. Kaskel, *Microporous and Mesoporous Materials*, 2004, **73**, 81-88.
105. W. Y. Gao, Y. Chen, Y. Niu, K. Williams, L. Cash, P. J. Perez, L. Wojtas, J. Cai, Y. S. Chen and S. Ma, *Angewandte Chemie International Edition*, 2014, **53**, 2615-2619.
106. L. Alaerts, E. Séguin, H. Poelman, F. Thibault-Starzyk, P. A. Jacobs and D. E. De Vos, *Chemistry—A European Journal*, 2006, **12**, 7353-7363.
107. X. Zhang, F. L. i Xamena and A. Corma, *Journal of Catalysis*, 2009, **265**, 155-160.
108. C. M. Miralda, E. E. Macias, M. Zhu, P. Ratnasamy and M. A. Carreon, *Acs Catalysis*, 2012, **2**, 180-183.
109. A. Munyentwali, H. Li and Q. Yang, *Applied Catalysis A: General*, 2022, 118525.
110. J. Gascon, U. Aktay, M. D. Hernandez-Alonso, G. P. van Klink and F. Kapteijn, *Journal of Catalysis*, 2009, **261**, 75-87.
111. Z. Wang and S. M. Cohen, *Journal of the American Chemical Society*, 2007, **129**, 12368-12369.
112. S. S. Kaye, A. Dailly, O. M. Yaghi and J. R. Long, *Journal of the American Chemical Society*, 2007, **129**, 14176-14177.
113. S. Hausdorf, J. r. Wagler, R. Moßig and F. O. Mertens, *The Journal of Physical Chemistry A*, 2008, **112**, 7567-7576.
114. Y. K. Hwang, D. Y. Hong, J. S. Chang, S. H. Jhung, Y. K. Seo, J. Kim, A. Vimont, M. Daturi, C. Serre and G. Férey, *Angewandte Chemie International Edition*, 2008, **47**, 4144-4148.
115. M. Savonnet, S. Aguado, U. Ravon, D. Bazer-Bachi, V. Lecocq, N. Bats, C. Pinel and D. Farrusseng, *Green Chemistry*, 2009, **11**, 1729-1732.
116. P. Ejikeme, I. Anyaogu, C. Ejikeme, N. Nwafor, C. Egbuonu, K. Ukogu and J. Ibemesi, *Journal of Chemistry*, 2010, **7**, 1120-1132.
117. K. Tan, N. Nijem, Y. Gao, S. Zuluaga, J. Li, T. Thonhauser and Y. J. Chabal, *CrystEngComm*, 2015, **17**, 247-260.
118. N. Pal and A. Bhaumik, *RSC Advances*, 2015, **5**, 24363-24391.
119. J. Gascon, A. Corma, F. Kapteijn and F. X. Llabres i Xamena, *Acs Catalysis*, 2014, **4**, 361-378.
120. P. Kaur, J. T. Hupp and S. T. Nguyen, *ACS Catalysis*, 2011, **1**, 819-835.
121. Y. Zhang and S. N. Riduan, *Chemical Society Reviews*, 2012, **41**, 2083-2094.
122. A. Trewin and A. I. Cooper, *Angewandte Chemie International Edition*, 2010, **49**, 1533-1535.
123. Q. Sun, Z. Dai, X. Meng, L. Wang and F.-S. Xiao, *ACS Catalysis*, 2015, **5**, 4556-4567.
124. S. Xu, Y. Luo and B. Tan, *Macromolecular rapid communications*, 2013, **34**, 471-484.
125. N. B. McKeown and P. M. Budd, *Macromolecules*, 2010, **43**, 5163-5176.
126. L. Tan and B. Tan, *Chemical Society Reviews*, 2017, **46**, 3322-3356.
127. K. Wang, Z. Jia, X. Yang, L. Wang, Y. Gu and B. Tan, *Journal of catalysis*, 2017, **348**, 168-176.

128. Y. Gu, S. U. Son, T. Li and B. Tan, *Advanced Functional Materials*, 2021, **31**, 2008265.
129. J. Li, X. Wang, G. Chen, D. Li, Y. Zhou, X. Yang and J. Wang, *Applied Catalysis B: Environmental*, 2015, **176**, 718-730.
130. L. Sekerová, P. Březinová, T. T. Do, E. Vyskočilová, J. Krupka, L. Červený, L. Havelková, B. Bashta and J. Sedláček, *ChemCatChem*, 2019.
131. E. Andrijanto, E. Dawson and D. Brown, *Applied Catalysis B: Environmental*, 2012, **115**, 261-268.
132. R. M. N. Kalla, S. S. Reddy and I. Kim, *Catalysis Letters*, 2019, **149**, 2696-2705.
133. W. Zhang, F. Ma, L. Ma, Y. Zhou and J. Wang, *ChemSusChem*, 2020, **13**, 341-350.
134. L.-J. Feng, M. Wang, Z.-Y. Sun, Y. Hu and Z.-T. Deng, *Designed monomers and polymers*, 2017, **20**, 344-350.
135. Y. B. Zhou and Z. P. Zhan, *Chemistry—An Asian Journal*, 2018, **13**, 9-19.
136. J.-S. M. Lee and A. I. Cooper, *Chemical reviews*, 2020, **120**, 2171-2214.
137. R. Dawson, A. Laybourn, R. Clowes, Y. Z. Khimyak, D. J. Adams and A. I. Cooper, *Macromolecules*, 2009, **42**, 8809-8816.
138. J. H. Ko, S. M. Lee, H. J. Kim, Y.-J. Ko and S. U. Son, *ACS Macro Letters*, 2018, **7**, 1353-1358.
139. Y. He, D. Gehrig, F. Zhang, C. Lu, C. Zhang, M. Cai, Y. Wang, F. Laquai, X. Zhuang and X. Feng, *Advanced Functional Materials*, 2016, **26**, 8255-8265.
140. W. Zhao, Y. Jiao, J. Li, L. Wu, A. Xie and W. Dong, *Journal of Catalysis*, 2019, **378**, 42-50.
141. S. Bhattacharyya, D. Samanta, S. Roy, V. P. Haveri Radhakantha and T. K. Maji, *ACS applied materials & interfaces*, 2019, **11**, 5455-5461.
142. J. X. Jiang, C. Wang, A. Laybourn, T. Hasell, R. Clowes, Y. Z. Khimyak, J. Xiao, S. J. Higgins, D. J. Adams and A. I. Cooper, *Angewandte Chemie International Edition*, 2011, **50**, 1072-1075.
143. L. Chen, Y. Yang and D. Jiang, *Journal of the American Chemical Society*, 2010, **132**, 9138-9143.
144. Y. Xie, T.-T. Wang, X.-H. Liu, K. Zou and W.-Q. Deng, *Nature communications*, 2013, **4**, 1-7.
145. D. S. Kundu, J. Schmidt, C. Bleschke, A. Thomas and S. Blechert, *Angewandte Chemie International Edition*, 2012, **51**, 5456-5459.
146. Y. Zhang, Y. Zhang, Y. L. Sun, X. Du, J. Y. Shi, W. D. Wang and W. Wang, *Chemistry—A European Journal*, 2012, **18**, 6328-6334.
147. S. Tantisriyanurak, H. N. Duguid, L. Peattie and R. Dawson, *ACS Applied Polymer Materials*, 2020, **2**, 3908-3915.
148. R. Gao, G. Zhang, F. Lu, L. Chen and Y. Li, *Frontiers in chemistry*, 2021, **9**, 687183.
149. S. Ren, R. Dawson, A. Laybourn, J.-x. Jiang, Y. Khimyak, D. J. Adams and A. I. Cooper, *Polymer Chemistry*, 2012, **3**, 928-934.
150. Y. Liao, Z. Cheng, W. Zuo, A. Thomas and C. F. Faul, *ACS applied materials & interfaces*, 2017, **9**, 38390-38400.
151. M. Y. Liu, L. P. Guo, S. B. Jin and B. E. Tan, *Journal of Materials Chemistry A*, 2019, **7**, 5153-5172.
152. C. Krishnaraj, H. S. Jena, K. Leus and P. Van der Voort, *Green Chemistry*, 2020, **22**, 1038-1071.
153. P. Puthiaraj, Y.-R. Lee, S. Zhang and W.-S. Ahn, *Journal of Materials Chemistry A*, 2016, **4**, 16288-16311.

154. K. Wang, L. M. Yang, X. Wang, L. Guo, G. Cheng, C. Zhang, S. Jin, B. Tan and A. Cooper, *Angewandte Chemie International Edition*, 2017, **56**, 14149-14153.
155. P. Kuhn, M. Antonietti and A. Thomas, *Angewandte Chemie International Edition*, 2008, **47**, 3450-3453.
156. S. Ren, M. J. Bojdys, R. Dawson, A. Laybourn, Y. Z. Khimyak, D. J. Adams and A. I. Cooper, *Advanced Materials*, 2012, **24**, 2357-2361.
157. Y. Zhang and S. B. Jin, *Polymers*, 2019, **11**.
158. N. Tahir, C. Krishnaraj, K. Leus and P. Van der Voort, *Polymers*, 2019, **11**.
159. J. Artz and R. Palkovits, *ChemSusChem*, 2015, **8**, 3832-3838.
160. C. E. Chan-Thaw, A. Villa, P. Katekomol, D. Su, A. Thomas and L. Prati, *Nano letters*, 2010, **10**, 537-541.
161. M. Pilaski, J. Artz, H.-U. Islam, A. M. Beale and R. Palkovits, *Microporous and Mesoporous Materials*, 2016, **227**, 219-227.
162. T. He, L. Liu, G. Wu and P. Chen, *Journal of Materials Chemistry A*, 2015, **3**, 16235-16241.
163. A. V. Bavykina, M. G. Goesten, F. Kapteijn, M. Makkee and J. Gascon, *Chemsuschem*, 2015, **8**, 809-812.
164. A. V. Bavykina, A. I. Olivos-Suarez, D. Osadchii, R. Valecha, R. Franz, M. Makkee, F. Kapteijn and J. Gascon, *ACS applied materials & interfaces*, 2017, **9**, 26060-26065.
165. T. T. Liu, R. Xu, J. D. Yi, J. Liang, X. S. Wang, P. C. Shi, Y. B. Huang and R. Cao, *Chemcatchem*, 2018, **10**, 2036-2040.
166. A. H. Liu, J. J. Zhang and X. B. Lv, *Chinese Journal of Catalysis*, 2018, **39**, 1320-1328.
167. J. Roeser, K. Kailasam and A. Thomas, *Chemsuschem*, 2012, **5**, 1793-1799.
168. G. Tuci, M. Pilaski, H. Ba, A. Rossin, L. Luconi, S. Caporali, C. Pham-Huu, R. Palkovits and G. Giambastiani, *Advanced Functional Materials*, 2017, **27**.
169. G. Tuci, A. Iemhoff, H. Ba, L. Luconi, A. Rossin, V. Papaefthimiou, R. Palkovits, J. Artz, C. Pham-Huu and G. Giambastiani, *Beilstein Journal of Nanotechnology*, 2019, **10**, 1217-1227.
170. H. S. Jena, C. Krishnaraj, J. Schmidt, K. Leus, K. Van Hecke and P. Van der Voort, *Chemistry-a European Journal*, 2020, **26**, 1548-1557.
171. Y. Zhao, H. Huang, H. Zhu and C. Zhong, *Microporous and Mesoporous Materials*, 2022, **329**, 111526.
172. Y. Yuan and G. S. Zhu, *Acs Central Science*, 2019, **5**, 409-418.
173. U. Diaz and A. Corma, *Coordination Chemistry Reviews*, 2016, **311**, 85-124.
174. T. Ben and S. Qiu, *CrystEngComm*, 2013, **15**, 17-26.
175. E. Rangel-Rangel, E. Verde-Sesto, A. M. Rasero-Almansa, M. Iglesias and F. Sanchez, *Catalysis Science & Technology*, 2016, **6**, 6037-6045.
176. L. Y. Li, Z. L. Chen, H. Zhong and R. H. Wang, *Chemistry-a European Journal*, 2014, **20**, 3050-3060.
177. E. Verde-Sesto, M. Pintado-Sierra, A. Corma, E. M. Maya, J. G. de la Campa, M. Iglesias and F. Sanchez, *Chemistry-a European Journal*, 2014, **20**, 5111-5120.
178. C. Monterde, R. Navarro, M. Iglesias and F. Sanchez, *Journal of Catalysis*, 2019, **377**, 609-618.
179. E. Verde-Sesto, E. Merino, E. Rangel-Rangel, A. Corma, M. Iglesias and F. Sanchez, *Acs Sustainable Chemistry & Engineering*, 2016, **4**, 1078-1084.
180. E. Karakhanov, Y. Kardasheva, L. Kulikov, A. Maximov, A. Zolotukhina, M. Vinnikova and A. Ivanov, *Catalysts*, 2016, **6**.

181. L.-P. Jing, J.-S. Sun, F. Sun, P. Chen and G. Zhu, *Chemical science*, 2018, **9**, 3523-3530.
182. Y. J. Yang, X. Q. Zou, P. Cui, Y. X. Zhou, S. Zhao, L. L. Wang, Y. Yuan and G. S. Zhu, *Acs Applied Materials & Interfaces*, 2017, **9**, 30958-30963.
183. E. Merino, E. Verde-Sesto, E. M. Maya, M. Iglesias, F. Sanchez and A. Corma, *Chemistry of Materials*, 2013, **25**, 981-988.
184. P. M. Budd, B. S. Ghanem, S. Makhseed, N. B. McKeown, K. J. Msayib and C. E. Tattershall, *Chemical communications*, 2004, 230-231.
185. S. Das, P. Heasman, T. Ben and S. Qiu, *Chemical reviews*, 2017, **117**, 1515-1563.
186. T. M. Long and T. M. Swager, *Advanced Materials*, 2001, **13**, 601-+.
187. L. Friedman and F. M. Logullo, *Journal of the American Chemical Society*, 1963, **85**, 1549-1549.
188. B. S. Ghanem, K. J. Msayib, N. B. McKeown, K. D. M. Harris, Z. Pan, P. M. Budd, A. Butler, J. Selbie, D. Book and A. Walton, *Chemical Communications*, 2007, DOI: 10.1039/b614214a, 67-69.
189. J. Tröger, *Journal für Praktische Chemie*, 1887, **36**, 225-245.
190. M. Spielman, *Journal of the American Chemical Society*, 1935, **57**, 583-585.
191. B. Wepster, *Recueil des Travaux Chimiques des Pays-Bas*, 1953, **72**, 661-672.
192. E. Marquis, J. Graton, M. Berthelot, A. Planchat and C. Laurence, *Canadian journal of chemistry*, 2004, **82**, 1413-1422.
193. M. Carta, R. Malpass-Evans, M. Croad, Y. Rogan, J. C. Jansen, P. Bernardo, F. Bazzarelli and N. B. McKeown, *Science*, 2013, **339**, 303-307.
194. C. Ma and J. J. Urban, *Proc. Nat. Res. Soc*, 2018, **2**, 2002.
195. N. B. McKeown, *Polymer*, 2020, **202**, 122736.
196. P. M. Budd, B. Ghanem, K. Msayib, N. B. McKeown and C. Tattershall, *Journal of Materials Chemistry*, 2003, **13**, 2721-2726.
197. H. J. Mackintosh, P. M. Budd and N. B. McKeown, *Journal of Materials Chemistry*, 2008, **18**, 573-578.
198. N. Sehlotho and T. Nyokong, *Journal of Molecular Catalysis A: Chemical*, 2004, **209**, 51-57.
199. M. Carta, M. Croad, K. Bugler, K. J. Msayib and N. B. McKeown, *Polymer Chemistry*, 2014, **5**, 5262-5266.
200. M. Carta, M. Croad, R. Malpass-Evans, J. C. Jansen, P. Bernardo, G. Clarizia, K. Friess, M. Lanč and N. B. McKeown, *Advanced Materials*, 2014, **26**, 3526-3531.
201. D. Butler, A. Barrette and R. Snow, *Synthetic Communications*, 1975, **5**, 101-106.
202. A. Galanti, V. Diez-Cabanes, J. Santoro, M. Valášek, A. Minoia, M. Mayor, J. Cornil and P. Samorì, *Journal of the American Chemical Society*, 2018, **140**, 16062-16070.
203. G. Li, B. Zhang, J. Yan and Z. Wang, *Journal of Materials Chemistry A*, 2014, **2**, 18881-18888.
204. W. Q. Xu, Y. Z. Fan, H. P. Wang, J. Teng, Y. H. Li, C. X. Chen, D. Fenske, J. J. Jiang and C. Y. Su, *Chemistry—A European Journal*, 2017, **23**, 3542-3547.
205. G. Gattuso, G. Grasso, N. Marino, A. Notti, A. Pappalardo, S. Pappalardo and M. F. Parisi, *European Journal of Organic Chemistry*, 2011, **2011**, 5696-5703.
206. M. Carta, R. Malpass-Evans, M. Croad, Y. Rogan, M. Lee, I. Rose and N. B. McKeown, *Polymer Chemistry*, 2014, **5**, 5267-5272.

207. A. H. Alahmed, M. E. Briggs, A. I. Cooper and D. J. Adams, *Journal of Materials Chemistry A*, 2019, **7**, 549-557.
208. M. Carta, K. J. Msayib, P. M. Budd and N. B. McKeown, *Organic letters*, 2008, **10**, 2641-2643.
209. J. Jeromenok and J. Weber, *Langmuir*, 2013, **29**, 12982-12989.
210. X. Du, Y. Sun, B. Tan, Q. Teng, X. Yao, C. Su and W. Wang, *Chemical Communications*, 2010, **46**, 970-972.
211. E. Tocci, L. De Lorenzo, P. Bernardo, G. Clarizia, F. Bazzarelli, N. B. Mckeown, M. Carta, R. Malpass-Evans, K. Friess and K. t. Pilnáček, *Macromolecules*, 2014, **47**, 7900-7916.
212. I. Rodriguez, G. Sastre, A. Corma and S. Iborra, *Journal of Catalysis*, 1999, **183**, 14-23.
213. Z. Benzekri, H. El Aaadad, S. Sibous, H. Serrar, S. Boukhris, A. Chahine and A. Souizi, *Heliyon*, 2020, **6**, e05293.
214. D. A. Vazquez-Molina, G. M. Pope, A. A. Ezazi, J. L. Mendoza-Cortes, J. K. Harper and F. J. Uribe-Romo, *Chemical Communications*, 2018, **54**, 6947-6950.
215. W. Meng, J. K. Clegg, J. D. Thoburn and J. R. Nitschke, *Journal of the American Chemical Society*, 2011, **133**, 13652-13660.
216. S. Grosjean, Z. Hassan, C. Wöll and S. Bräse, *European Journal of Organic Chemistry*, 2019, **2019**, 1446-1460.
217. R. Z. Lange, G. Hofer, T. Weber and A. D. Schlüter, *Journal of the American Chemical Society*, 2017, **139**, 2053-2059.
218. D. Lozano-Castelló, D. Cazorla-Amorós and A. Linares-Solano, *Carbon*, 2004, **42**, 1233-1242.
219. I. del Hierro, Y. Pérez and M. Fajardo, *Microporous and Mesoporous Materials*, 2018, **263**, 173-180.
220. Y. Zhi, Z. Li, X. Feng, H. Xia, Y. Zhang, Z. Shi, Y. Mu and X. Liu, *Journal of Materials Chemistry A*, 2017, **5**, 22933-22938.
221. G. Gattuso, G. Grasso, N. Marino, A. Notti, A. Pappalardo, S. Pappalardo and M. F. Parisi, *Journal*, 2011.
222. J. Feng, B. Liang, D. Wang, H. Wu, L. Xue and X. Li, *Langmuir*, 2008, **24**, 11209-11215.
223. H. Wu, R. Hu, B. Zeng, L. Yang, T. Chen, W. Zheng, X. Liu, W. Luo and L. Dai, *RSC advances*, 2018, **8**, 37631-37642.
224. C. López-Lira, R. A. Tapia, A. Herrera, M. Lapier, J. D. Maya, J. Soto-Delgado, A. G. Oliver, A. G. Lappin and E. Uriarte, *Bioorganic Chemistry*, 2021, **111**, 104823.
225. P. Sun, Y. Chen, B. Sun, H. Zhang, K. Chen, H. Miao, Q. Fan and W. Huang, *ACS Applied Bio Materials*, 2021, **4**, 4542-4548.
226. L. Trupp, A. C. Bruttomesso and B. C. Barja, *New Journal of Chemistry*, 2020, **44**, 10973-10981.
227. R.-B. Lin, Y. He, P. Li, H. Wang, W. Zhou and B. Chen, *Chemical Society Reviews*, 2019, **48**, 1362-1389.
228. J. N. Appaturi, R. Ratti, B. L. Phoon, S. M. Batagarawa, I. U. Din, M. Selvaraj and R. J. Ramalingam, *Dalton Transactions*, 2021, **50**, 4445-4469.
229. M. Guerrini, E. Delgado Aznar and C. Cocchi, *The Journal of Physical Chemistry C*, 2020, **124**, 27801-27810.
230. S. A. A. Razavi and A. Morsali, *Inorganic Chemistry*, 2019, **58**, 14429-14439.

231. N. V. Belova, H. Oberhammer, N. H. Trang and G. V. Girichev, *The Journal of organic chemistry*, 2014, **79**, 5412-5419.
232. N. V. Belova, H. Oberhammer and G. V. Girichev, *Journal of molecular structure*, 2004, **689**, 255-260.
233. J. Spencer, E. S. Holmboe, M. R. Kirshenbaum, D. W. Firth and P. B. Pinto, *Canadian Journal of Chemistry*, 1982, **60**, 1178-1182.
234. P. O. Sandusky, *Journal of Chemical Education*, 2014, **91**, 739-742.
235. H. Liu, H. Wu, Z. Luo, J. Shen, G. Kang, B. Liu, Z. Wan and J. Jiang, *Chemistry–A European Journal*, 2012, **18**, 11899-11903.
236. E. Madrid, Y. Rong, M. Carta, N. B. McKeown, R. Malpass-Evans, G. A. Attard, T. J. Clarke, S. H. Taylor, Y.-T. Long and F. Marken, *Angew. Chem., Int. Ed.*, 2014, **53**, 10751-10754.
237. E. Madrid, P. Cottis, Y. Rong, A. T. Rogers, J. M. Stone, R. Malpass-Evans, M. Carta, N. B. McKeown and F. Marken, *Journal of Materials Chemistry A*, 2015, **3**, 15849-15853.
238. M. H. Abdellattif and H. M. Mohamed, *Green and Sustainable Chemistry*, 2018, **8**, 139-155.
239. F. G. Cirujano, R. Luque and A. Dhakshinamoorthy, *Molecules*, 2021, **26**, 1445.
240. N. Anbu, R. Maheswari, V. Elamathi, P. Varalakshmi and A. Dhakshinamoorthy, *Catalysis Communications*, 2020, **138**, 105954.
241. B. Tamami and A. Fadavi, 2006.
242. T. He, R. Shi, Y. Gong, G. Jiang, M. Liu, S. Qian and Z. Wang, *Synlett*, 2016, **27**, 1864-1869.
243. J. S. Yadav, B. V. S. Reddy, A. K. Basak, B. Visali, A. V. Narsaiah and K. Nagaiah, *European Journal of Organic Chemistry*, 2004, **2004**, 546-551.
244. K. van Beurden, S. de Koning, D. Molendijk and J. van Schijndel, *Green Chemistry Letters and Reviews*, 2020, **13**, 349-364.
245. J. G. Clayden, N Warren, S, in *Organic Chemistry*, ed. O. U. Press, 2012, ch. 26, pp. 629-630.
246. BEIS, *Net Zero Strategy: Build Back Greener*, 2021.
247. K. Kiatkittipong, M. A. A. Mohamad Shukri, W. Kiatkittipong, J. W. Lim, P. L. Show, M. K. Lam and S. Assabumrungrat, *Processes*, 2020, **8**, 548.
248. M. Sinchow, N. Semakul, T. Konno and A. Rujiwatra, *ACS Sustainable Chemistry & Engineering*, 2021, **9**, 8581-8591.
249. R. K. Tak, P. Patel, S. Subramanian, R. I. Kureshy and N.-u. H. Khan, *ACS Sustainable Chemistry & Engineering*, 2018, **6**, 11200-11205.
250. A. Rehman, F. Saleem, F. Javed, A. Ikhlq, S. W. Ahmad and A. Harvey, *Journal of Environmental Chemical Engineering*, 2021, **9**, 105113.
251. J. Sun, W. Cheng, W. Fan, Y. Wang, Z. Meng and S. Zhang, *Catalysis Today*, 2009, **148**, 361-367.
252. S. Senthilkumar, M. S. Maru, R. Somani, H. Bajaj and S. Neogi, *Dalton Transactions*, 2018, **47**, 418-428.
253. M. Frondel and J. Peters, *Energy policy*, 2007, **35**, 1675-1684.
254. I. Rizwanul Fattah, H. Ong, T. Mahlia, M. Mofijur, A. Silitonga, S. A. Rahman and A. Ahmad, *Frontiers in Energy Research*, 2020, **8**, 101.
255. S. Pathak, *Journal of Chemical and Pharmaceutical Research*, 2015, **7**, 1780-1786.
256. D.-W. Lee, Y.-M. Park and K.-Y. Lee, *Catalysis surveys from Asia*, 2009, **13**, 63-77.

257. H. Zhou, C. Rayer, A. R. Antonangelo, N. Hawkins and M. Carta, *ACS Applied Materials & Interfaces*, 2022.
258. K. J. Msayib and N. B. McKeown, *Journal of Materials Chemistry A*, 2016, **4**, 10110-10113.
259. C. G. Bezzu, M. Carta, M.-C. Ferrari, J. C. Jansen, M. Monteleone, E. Esposito, A. Fuoco, K. Hart, T. P. Liyana-Arachchi, C. M. Colina and N. B. McKeown, *Journal of Materials Chemistry A*, 2018, **6**, 10507-10514.
260. M. Carta, P. Bernardo, G. Clarizia, J. C. Jansen and N. B. McKeown, *Macromolecules (Washington, DC, U. S.)*, 2014, **47**, 8320-8327.
261. Y. Liu, S. Wu, G. Wang, G. Yu, J. Guan, C. Pan and Z. Wang, *Journal of Materials Chemistry A*, 2014, **2**, 7795-7801.
262. G. G. Stavropoulos, P. Samaras and G. P. Sakellariopoulos, *Journal of Hazardous Materials*, 2008, **151**, 414-421.
263. M. Adamczak, U. T. Bornscheuer and W. Bednarski, *European Journal of Lipid Science and Technology*, 2009, **111**, 800-813.
264. R. Nayab, M. Imran, M. Ramzan, M. Tariq, M. B. Taj, M. N. Akhtar and H. M. Iqbal, *Fuel*, 2022, **328**, 125254.
265. O. Braissant, A. W. Decho, C. Dupraz, C. Glunk, K. M. Przekop and P. T. Visscher, *Geobiology*, 2007, **5**, 401-411.
266. G. Clayden, N. Greeves and S. Warren, in *Organic Chemistry*, ed. O. U. Press, 2012, ch. 10, p. 207.
267. R. M. N. Kalla, M.-R. Kim and I. Kim, *Industrial & Engineering Chemistry Research*, 2018, **57**, 11583-11591.
268. F. Faraguna, M. Racar, Z. Glasovac and A. Jukic, *Energy & Fuels*, 2017, **31**, 3943-3948.
269. G. Gelbard, O. Bres, R. Vargas, F. Vielfaure and U. Schuchardt, *Journal of the American Oil Chemists' Society*, 1995, **72**, 1239-1241.
270. A. L. de Lima, C. M. Ronconi and C. J. Mota, *Catalysis Science & Technology*, 2016, **6**, 2877-2891.
271. A. R. Antonangelo, N. Hawkins, E. Tocci, C. Muzzi, A. Fuoco and M. Carta, *Journal of the American Chemical Society*, 2022, **144**, 15581-15594.
272. R. J. Williams, University of Edinburgh, 2017.